Université de Montréal

Novel Methods to Evaluate Blindsight and Develop Rehabilitation Strategies for Patients with Cortical Blindness

Par

Vanessa Hadid

Faculté de Médecine

Thèse présentée en vue de l'obtention du grade de Philosophiæ Doctor (Ph.D.)

en Sciences Biomédicales, option Médecine Expérimentale

Septembre, 2021

Université de Montréal

Faculté de Médecine

Cette thèse intitulée

Novel Methods to Evaluate Blindsight and Develop Rehabilitation Strategies for Patients with Cortical Blindness

Présentée par

Vanessa Hadid

A été évalué(e) par un jury composé des personnes suivantes

Dr Christian Casanova

Président-rapporteur

Dr Franco Lepore

Directeur de recherche

Dr Karim Jerbi

Codirecteur de recherche

Dr Guillaume Dumas

Membre du jury

Dr Melvyn A.Goodale

Examinateur externe

Dr Stéphane Molotchnikoff

Représentant du doyen

Résumé

20 à 57 % des victimes d'un accident vasculaire cérébral (AVC) sont diagnostiqués aves des déficits visuels qui réduisent considérablement leur qualité de vie. Parmi les cas extrêmes de déficits visuels, nous retrouvons les cécités corticales (CC) qui se manifestent lorsque la région visuelle primaire (V1) est atteinte. Jusqu'à présent, il n'existe aucune approche permettant d'induire la restauration visuelle des fonctions et, dans la plupart des cas, la plasticité est insuffisante pour permettre une récupération spontanée. Par conséquent, alors que la perte de la vue est considérée comme permanente, des fonctions inconscientes mais importantes, connues sous le nom de vision aveugle (blindsight), pourraient être utiles pour les stratégies de réhabilitation visuelle, ce qui suscite un vif intérêt dans le domaine des neurosciences cognitives. La vision aveugle est un phénomène rare qui dépeint une dissociation entre la performance et la conscience, principalement étudiée dans des études de cas.

Dans le premier chapitre de cette thèse, nous avons abordé plusieurs questions concernant notre compréhension de la vision aveugle. Comme nous le soutenons, une telle compréhension pourrait avoir une influence significative sur la réhabilitation clinique des patients souffrant de CC. Par conséquent, nous proposons une stratégie unique pour la réhabilitation visuelle qui utilise les principes du jeu vidéo pour cibler et potentialiser les mécanismes neuronaux dans le cadre de l'espace de travail neuronal global, qui est expliqué théoriquement dans l'étude 1 et décrit méthodologiquement dans l'étude 5. En d'autres termes, nous proposons que les études de cas, en conjonction avec des critères méthodologiques améliorés, puissent identifier les substrats neuronaux qui soutiennent la vision aveugle et inconsciente.

Ainsi, le travail de cette thèse a fourni trois expériences empiriques (études 2, 3 et 4) en utilisant de nouveaux standards dans l'analyse électrophysiologique qui décrivent les cas de patients SJ présentant une cécité pour les scènes complexes naturelles affectives et ML présentant une cécité pour les stimuli de mouvement. Dans les études 2 et 3, nous avons donc sondé les substrats neuronaux sous-corticaux et corticaux soutenant la cécité affective de SJ en utilisant la MEG et nous avons comparé ces corrélats à sa perception consciente. L'étude 4 nous a permis de caractériser les substrats de la détection automatique des changements en l'absence de conscience

visuelle, mesurée par la négativité de discordance (en anglais visual mismatch negativity : vMMN) chez ML et dans un groupe neurotypique. Nous concluons en proposant la vMMN comme biomarqueur neuronal du traitement inconscient dans la vision normale et altérée indépendante des évaluations comportementales. Grâce à ces procédures, nous avons pu aborder certains débats ouverts dans la littérature sur la vision aveugle et sonder l'existence de voies neurales secondaires soutenant le comportement inconscient.

En conclusion, cette thèse propose de combiner les perspectives empiriques et cliniques en utilisant des avancées méthodologiques et de nouvelles méthodes pour comprendre et cibler les substrats neurophysiologiques sous-jacents à la vision aveugle. Il est important de noter que le cadre offert par cette thèse de doctorat pourrait aider les études futures à construire des outils thérapeutiques ciblés efficaces et des stratégies de réhabilitation multimodale.

Mots-clés : Cécité corticale, vision aveugle, vision aveugle affective, perception consciente, perception inconsciente, espace de travail neuronal global, électrophysiologie, voies visuelles, voies sous-corticales, négativité de discordance, réhabilitation visuelle.

Abstract

20 to 57% of victims of a cerebrovascular accident (CVA) develop visual deficits that considerably reduce their quality of life. Among the extreme cases of visual deficits, we find cortical blindness (CC) which manifests when the primary visual region (V1) is affected. Until now, there is no approach that induces restoration of visual function and in most cases, plasticity is insufficient to allow spontaneous recovery. Therefore, while sight loss is considered permanent, unconscious yet important functions, known as blindsight, could be of use for visual rehabilitation strategies raising strong interest in cognitive neurosciences. Blindsight is a rare phenomenon that portrays a dissociation between performance and consciousness mainly investigated in case reports.

In the first chapter of this thesis, we've addressed multiple issues about our comprehension of blindsight and conscious perception. As we argue, such understanding might have a significant influence on clinical rehabilitation patients suffering from CB. Therefore, we propose a unique strategy for visual rehabilitation that uses video game principles to target and potentiate neural mechanisms within the global neuronal workspace framework, which is theoretically explained in study 1 and methodologically described in study 5. In other words, we propose that case reports, in conjunction with improved methodological criteria, might identify the neural substrates that support blindsight and unconscious processing.

Thus, the work in this Ph.D. work provided three empirical experiments (studies 2, 3, and 4) that used new standards in electrophysiological analyses as they describe the cases of patients SJ presenting blindsight for affective natural complex scenes and ML presenting blindsight for motion stimuli. In studies 2 and 3, we probed the subcortical and cortical neural substrates supporting SJ's affective blindsight using MEG as we compared these unconscious correlates to his conscious perception. Study 4 characterizes the substrates of automatic detection of changes in the absence of visual awareness as measured by the visual mismatch negativity (vMMN) in ML and a neurotypical group. We conclude by proposing the vMMN as a neural biomarker of unconscious processing in normal and altered vision independent of behavioral assessments. As a

result of these procedures, we were able to address certain open debates in the blindsight literature and probe the existence of secondary neural pathways supporting unconscious behavior.

In conclusion, this thesis proposes to combine empirical and clinical perspectives by using methodological advances and novel methods to understand and target the neurophysiological substrates underlying blindsight. Importantly, the framework offered by this doctoral dissertation might help future studies build efficient targeted therapeutic tools and multimodal rehabilitation training.

Keywords: Cortical blindness, blindsight, affective blindsight, conscious perception, unconscious perception, global neuronal workspace, electrophysiology, visual pathways, subcortical pathways, visual mismatch negativity, visual rehabilitation.

Table des Matières

Liste des Tableaux

Liste des Figures

Chapter 3

Chapter 4

Chapter 5

Chapter 6

Liste des Sigles et Abréviations

AUC: area under the curve

BEM: Boundary Element Method

CB: cortical blindness

DA: decoding accuracy

DOI: difference of influence

EEG: electroencephalography

EOG: electrooculography

ERF: event-related field

ERP: event-related potential

Frites: FRamework for Information Theoretical analysis of Electrophysiological data and statistics

FC: functional connectivity

fMRI: functional magnetic resonance imaging

GC: Granger causality

HFO: high gamma oscillations

HH: homonymous hemianopia

IAPS: International Affective Picture System

ISI: inter-stimulus-interval

LPP: late positive potential

LGN: lateral geniculate nucleus

mLPP: magnetic late positive potential

MRI: magnetic resonance imaging

MEG: magnetoencephalography

MT or V5/MT: medio-temporal area

MNE: Minimum Norm Estimate

NCC: neural correlates of consciousness

PAS: perceptual awareness scale

PT: perceptual training

V1: primary visual cortex

RT: reaction time

ROI: region on interest

SC: superior colliculus

STS: superior temporal sulcus

TF: time-frequency

VG: video game

VRT: vision restitution therapy

VER: visual evoked responses

vMMN: visual mismatch negativity

wpli: weighted phase lag index

À Abbas, Nour et Zayn qui ont pleinement vécu cette thèse avec moi.

Abbas, tu as été ma fondation durant ce cheminement.

Nour, tu es ma source de lumière et d'amour.

Zayn, j'ai hâte de te rencontrer.

Remerciements

Pour réaliser une thèse, il ne faut pas qu'un cerveau. Il faut plusieurs amygdales, insulas et lobes frontaux qui renforcent ensemble le système de récompense. En d'autres termes, on ne fait pas 6 ans de thèse seule.

Mes premiers remerciements vont à mon directeur de thèse, Dr. Franco Lepore. On se connaît depuis longtemps maintenant et je tiens à t'exprimer ma plus grande et sincère reconnaissance, et ce, pour toutes les opportunités que tu m'as données. Tu as été une source d'inspiration, d'idées et de motivations qui ont permis à ce projet doctoral d'avoir autant d'ambition, mais c'est surtout par ton support, ta disponibilité, ta compréhension et ta confiance indéniable que tu as marqué chaque instant de mon doctorat. C'est donc avec tout mon respect et admiration que je tiens à te dire que je n'oublierais jamais la chance que j'ai eu de t'avoir comme directeur de thèse.

Mes seconds remerciements vont à mon codirecteur de thèse, Dr. Karim Jerbi. Lorsque j'ai décidé d'entreprendre mon doctorat c'était par soif de connaissances, mais sans ton expertise, ta perspicacité et chaque petit conseil que tu m'as donné je n'aurais jamais autant appris. Si cette thèse a la dimension qu'elle a aujourd'hui c'est grâce à ton investissement et toutes les ressources que tu m'as offertes. Ces années de doctorat dans le CoCo lab sous ta codirection ont eu un réel impact sur mes perspectives et ambitions futures, et c'est pour cela que je te remercie sincèrement d'avoir été un mentor hors pair.

J'aimerais également prendre le temps de remercier tous les membres du jury d'avoir accepté de lire et d'évaluer ma thèse.

Un remerciement spécial pour ceux qui ont contribué de manière significative aux études de ce projet, Annalisa et Tarek. Sans votre aide, la méthodologie retrouvée dans cette thèse n'aurait pas eu la même rigueur, car c'est grâce à votre expertise en analyses, en programmation et en machine learning que j'ai réussi à me mouvoir dans une avenue qui me passionne maintenant et à laquelle j'aspire. Je vous remercie aussi ainsi que toutes les personnes du CoCo lab avec qui j'ai développé un lien solide d'avoir rendu ce parcours non seulement stimulant au niveau intellectuel mais aussi au niveau personnel. Merci pour tous les moments passés ensemble qui ont fait de ce

doctorat une expérience inoubliable. Michèle, merci pour toutes nos discussions portant sur le projet et pour ta motivation, ton aide et l'effort que tu as donné. Marie celle qui a partagé mon bureau depuis le début, merci de m'avoir supporté et de m'avoir tenue si belle compagnie durant toutes ses années. Stéphane, mon voisin de bureau avec qui j'ai eu le plaisir d'échanger à tous les jours, un gros merci pour ta présence et ton soutien. Je tiens également à remercier toutes les personnes qui ont participé aux différentes études de cette thèse.

Si j'ai réussi à accomplir ce doctorat, c'est parce que j'ai réellement les meilleurs amis et famille qui soient et malgré cette dernière année de pandémie je ne vous ai jamais senti aussi proche. Votre support émotionnel, votre présence, nos nuits à travailler ou à faire la fête, ont fait en sorte que ces dernières années ont été les plus belles de ma vie. Merci Zorina, Christine et Simona, pour tous nos moments de complicités et nos soirées jusqu'au lever du soleil; Ghina pour les nuits dans les cafés qui finissaient au gym à 2 heures du matin; Loubna pour tous les moments à faire des pomodoros à distance ou en présentiel, et qui se terminaient on ne sait trop où; Aya pour toutes nos soirées de gossip et ton encouragement, Stéphanie pour tous nos moments partagés; Madeleine pour tout ton soutien, et ce, depuis biomed; Camille pour tes messages de support et toutes nos soirées de folies, Séverine, ma sœur de cœur, ma complice, sans toi, sans ton amitié, il y a bien des moments où je me serais sentie prise au dépourvue et d'autres qui auraient été bien moins party animal, merci d'être dans ma vie. À tous les amis que je n'ai pas nommés, mais qui ont contribués à la création de souvenirs inoubliables ou presque, j'ai hâte qu'on puisse fêter ensemble!

Le fait que j'ai réussi à faire ce doctorat tient beaucoup au support de ma belle-sœur, mon neveu, mon beau-frère et ma belle-mère. Je vous suis éternellement reconnaissante, et ce, d'avoir été présent pour Nour durant toutes ses années. Votre support et votre amour n'a pas de prix et je suis extrêmement chanceuse de vous avoir. Belle-maman, je tiens à te dire à quel point je suis reconnaissante pour toutes les nuits que tu as passé avec Nour et tous les repas que tu m'as envoyés dans les moments difficiles. Merci infiniment.

À mes frères et ma sœur, ceux avec qui je partage les souvenirs oubliés, les souvenirs à venir, ceux qui sont toujours là pour moi, vous avez chacun à votre façon eu un impact sur ce doctorat. Hani, tu es une inspiration pour moi, un modèle de rigueur et de travail et aussi mon meilleur ami depuis qu'on a 1 an. Ce que tu as accompli dans ta vie, ta persévérance et tes sacrifices

m'ont montré l'exemple à suivre pour terminer cette thèse. Laura, je suis tellement chanceuse de t'avoir comme sœur, comme amie et comme confidente. Ton soutien, ton amitié et ton amour ont été une source de réconfort pour moi tout au long de ce doctorat. Danny, merci pour ta spontanéité, tes messages hilarants, tes actions toujours imprévisibles, ma vie aurait été bien plus plate sans toi.

Après toutes ses années d'éducation, il y a deux personnes en particulier à qui j'aimerais exprimer mon amour profond. Papa et maman, merci de m'avoir supporté, soutenu, poussé, cru en moi, d'avoir été des parents fiers et toujours présents. Papa, merci de m'avoir inculqué ta passion de l'éducation et ta soif de connaissance. Maman, merci de m'avoir appris à toujours dépasser mes propres limites pour atteindre mes objectifs. Je me souviens, enfant, vous me disiez toujours : 'fait ce que tu veux dans ta vie mais éduque-toi', je pense que ces mots m'ont réellement marqué et je vous remercie de m'avoir donné le rationnel et l'amour qui ont mené à la réalisation de cette thèse.

Cette thèse, qui n'aurait pas été possible sans toi, Abbas. Je ne pourrais jamais assez te remercier pour ces 6 dernières années. Tu as donné tout ce que tu pouvais pour que je puisse réaliser cet objectif tout en me permettant d'être épanouie dans toutes les autres sphères de ma vie, et tu l'as fait en m'aimant, en m'encourageant, en me poussant, mais surtout en me donnant toute la confiance du monde que j'allais y arriver. Je te remercie d'avoir été un père exceptionnel à notre fille durant des périodes où tout ce que je pouvais faire c'est travailler et d'avoir été d'un soutien indispensable durant cette dernière année où tu as su t'occuper de tout pour que je puisse terminer cette étape avant notre prochaine grande aventure. Cette thèse est aussi la tienne mon amour.

Un petit mot pour ma Nour. Malgré tes 7 ans, tu as su démontrer tellement de maturité au regard du travail que maman avait à faire, le support affectif que tu m'as offert durant toutes tes petites années n'ont aucun prix, je t'aime et sache que ta compréhension et ton amour ont fait toute la différence. Zayn, tes petits coups m'ont donné la force de me rendre à la ligne d'arrivée, merci d'avoir été patient avec moi.

Chapter 1: Theoretical Background

1.1. Blindsight

1.1.1. Cortical Blindness

Strokes and disorders affecting the primary visual cortex (V1) in one hemisphere cause cortical blindness (CB) in the contralateral hemifield (Goodwin, 2014; Sand et al., 2013). Depending on the size of the lesion and hemisphere affected, CB can extend to a few degrees within one hemifield, as observed in delimited scotomas, it can cover a quarter of a hemifield, i.e. quadranopsia, it can affect the entire hemifield, which is known as homonymous hemianopia (HH) or it can even affect the entirety of the visual field caused by bilateral V1-lesions within both hemispheres (Swienton and Thomas, 2014). Unfortunately, approximately 50 % of stroke victims live with CB (Rowe et al., 2019). This condition significantly reduces the quality of life (Perez and Chokron, 2014) and prognosis linked to comorbidity, leading to a decrease in recovery of other functions (Patel et al., 2000).

When V1 is altered due to post-chiasmatic lesions, neuronal plasticity with various degrees of structural and physiological adaptations and major changes in brain circuitry emerge such as 1) loss of function in the impacted region, 2) reinforcement of spared pathways or formation of new ones to strengthen the original connections, and 3) emergence of new or modified functions (Ajina and Bridge, 2017; Bridge et al., 2008; Stoerig and Cowey, 1995). Although occipital cortical connectivity is subject to changes following a lesion, this plasticity is seldom associated with a retake of visual function unless it occurs within the first months following the lesion (Duquette & Barrel, 2009). In fact, within the subacute phase, i.e. 6 months after a stroke affecting the visual cortex, visual consciousness is preserved but disappears after a period (Saionz et al., 2020). Therefore, to date, there is no systematic approach that induces recovery of function. Nonetheless, while sight loss is often considered permanent, unconscious yet important functions referred to as blindsight (Weiskrantz et al., 1974), provide a unique opportunity to study the behavioral and neural mechanisms of conscious and unconscious processing and probe new methods to assess residual abilities after a V1-lesion raising strong interests in cognitive neurosciences. These residual abilities once apprehended in terms of neural mechanisms could be exploited in the development of restoration therapies.

1.1.2. Blindsight and Behavior

Blindsight portrays a rare case of dissociation between performance and consciousness, more specifically between what is reported, for example, the subject states not seeing anything, and what is measured objectively, i.e. a performance that is above chance-level. Weiskrantz first tokened the term blindsight by reporting the case of D.B. and by using multiple behavioral approaches to show that blindsight can be associated with a wide variety of manifestations, ranging from locating random targets by reaching or pointing at them, to determining the presence or absence of visual targets especially when these targets are of low spatial frequencies or in motion (Weiskrantz, 1986). With these findings reforming the field of unconscious visual perception, subsequent research showed different abilities in blindsight patients as the ability to recognize colors (Brent et al., 1994), detect global movement, and distinguish between coherence (Alexander and Cowey, 2009; Pavan et al., 2011), to recognize facial expressions (de Gelder et al., 1999; Striemer et al., 2019; Tamietto et al., 2009) or to perform an action based on an unseen target (Brown et al., 2008; Danckert et al., 2003). As we will go further into the discussion of conscious and unconscious processing, it is important to define what we refer to as consciousness. For clarity, the work in this thesis refers to content consciousness and will not discuss philosophical differences between theories of consciousness as we will mainly take an empirical point of view on the question (Doerig et al., 2020). In other terms, we refer to ″consciousness″, ″conscious processing″, ″visual consciousness″, and ″visual awareness″ as the ability to report a percept and we define ″unconsciousness″, ″unconscious processing″, ″absence of visual consciousness″ and ″absence of visual awareness″ as the lack of reported perceptual experience. Though theoretical neural frameworks will be presented to better comprehend the neural substrates supporting blindsight, they will not be viewed from a philosophical perspective.

Blindsight can be observed in the absence of visual awareness which refers to Type I blindsight or can be associated with a form of awareness that is described as something happening in the blind hemifield which is known as Type II blindsight (Lau and Passingham, 2006; Leopold, 2012). **In chapter 3**, we discuss different hypotheses regarding the nature of blindsight and the lack of understanding revolving around its neurological processes, leading to inefficient visual rehabilitation training. We thus propose a new perspective on residual visual abilities. The reason

why some patients may not present residual vision or awareness could include an inability to allocate sufficient resources to the information presented in the blind hemifield and to access their state of consciousness which could derive from a lack of neuronal synchrony between inefficient networks/workspaces of attention, perception, and consciousness (Melloni et al., 2007; Silvanto, 2015). This unavailability may be caused by structural and functional changes following cerebral lesions. Some authors refute the theory of unconscious vision by stating that blindsight is only a sort of degraded near-threshold normal vision (Mazzi et al., 2016; Overgaard and Grünbaum, 2011). While arguments that support both theories can be given, we propose in **chapter 3** to describe residual abilities depending on the pathways that support residual abilities after a V1-lesion, and in **chapter 6** we provide some insights into the difference between the neural mechanisms underlying lack of visual awareness in neurotypical and blindsight individuals.

1.2. The Neurophysiological Correlates Supporting Blindsight

1.2.1. The Neural Substrates Involved in Visual Consciousness

Visual inputs presented in the visual field stimulate specific retinal ganglion cells causing the activity to propagate to the optic chiasma through the optic nerve. Specifically, activity driven by the stimulation of the one hemifield will first be projected into the contralateral hemisphere before recruiting the ipsilateral hemisphere through inter-hemispheric transfer (Urbanski et al., 2014). The decussation via the optic chiasma leads to projections to contralateral subcortical structures, mainly to the lateral geniculate nucleus (LGN) found within the thalamus. Therefore, stimulus-driven information is received by the thalamus and is then sent to the striate cortex via the geniculo-striate pathway (McFadyen et al., 2020). V1 will then project its activity to higher-order visual regions within the ventral parvocellular and dorsal magnocellular pathways involved in conscious and unconscious perception (Breitmeyer, 2014). A stimulus either remains unconscious or is accessed by consciousness depending on bottom-up, e.g. strength of the stimulus, and top-down modulations, e.g. visuospatial attention (Dehaene et al., 2006). Hence, information from the bottom-up and top-down systems is continually updated through reciprocal influences contributing to both unconscious and conscious processing which can involve higher-order cognitive mechanisms such as expectation, knowledge, attention, prediction, feedback, and learning

(Mashour and Hudetz, 2018). Henceforward, investigating the neural correlates of consciousness (NCC) and isolating them from substrates of higher-order cognitive mechanisms is challenging. The role of V1 in consciousness is still up to debate, mainly due to opposing theories, the first suggesting the necessity and sufficiency of recurrent activity in V1 (Koch et al., 2016a; Lamme, 2018; Tong, 2003; Tononi et al., 2016) and the second of higher-order regions (Baars, 2002; Dehaene and Changeux, 2011; Dehaene et al., 1998). We can tackle this problem by understanding the temporal dynamics of conscious and unconscious processing through electrophysiological studies. Such dynamics can be assessed by (1) the changes in the event-related potentials (ERPs) or the visual evoked responses (VER) (Förster et al., 2020; Kranczioch et al., 2007; Rutiku et al., 2016) which will be examined in **chapters 5** and **6** and by (2) the modulations of the properties of brain rhythms mediated by neural synchronization mechanisms, (Aru and Bachmann, 2009; Baars et al., 2013; Doesburg et al., 2009; Engel and Singer, 2001) which will be addressed in **chapters 4** and **6**, as both neural substrates can be inherently linked and can be considered to be potential electrophysiological markers of conscious processing.

(1) The assessment of VER is fundamental in our understanding of cognitive processing and its underlying brain mechanisms. For instance, we can measure the presence of an early visual component referred to as C1 that originates within V1 and that characterizes the early processing of visual information as soon as 90 ms (Di Russo et al., 2002) while subsequent P1 and N1 components around 100 ms emerge from extra-striate higher-order regions (Hillyard and Anllo-Vento, 1998; Klimesch, 2011; Di Russo et al., 2002). These VER are thought to reflect early sensory information that is processed before visual consciousness even though some have shown modulations of P1 in visual awareness (Aru and Bachmann, 2009). The earliest component that seems to be associated with visual awareness and feedback processing emerges around 200 ms and is characterized by a negative deflection (Koivisto and Grassini, 2016; Pins and Ffytche, 2003; Railo et al., 2015). This negativity referred to as N2 has been demonstrated to fluctuate through stages of visual consciousness in numerous studies (Förster et al., 2020).

On the other hand, a negative component in the N2 time range referred to as the visual mismatch negativity (vMMN) was found to be independent of visual awareness. The vMMN can be elicited using an oddball sequence that is ignored by the participant and where the presence of a rare stimulus, i.e. deviant stimulus, alters a sequence of frequent stimuli, i.e. standard stimuli

(Pazo-Alvarez et al., 2003; Qian et al., 2014; Stefanics et al., 2014). The presentation of the deviant stimulus causes predictions errors (Oxner et al., 2019; Rowe et al., 2020; Stefanics et al., 2016) due to a violation of regularities (Fitzgerald and Todd, 2020; Yeark et al., 2021) which can notably be measured by the vMMN when comparing the VER of the deviant and standard stimulus, where the bottom-up information contradicts top-down expectations. Nonetheless, it is still up to debate whether this component can be triggered in the absence of visual awareness which assessment could lead to a new tool for measuring unconsciousness in blindsight patients independent of behavior, an idea that will be supported by empirical evidence in **chapter 6**. Such conclusions on the use of the vMMN could also serve in other dysfunctions of consciousness as is the case for the auditory MMN (Höller et al., 2011; Solís-Vivanco et al., 2021).

Moreover, another line of research suggests that visual awareness is only modulated at a late time frame measured by a positive component emerging around 300 ms usually termed the P3 (Dehaene et al., 2003a; Salti et al., 2012), however, this late positivity can also be modulated by other higher-order cognitive processes (Patel and Azzam, 2005; Railo et al., 2011; Rutiku et al., 2015) raising the question about whether P3 accompanies visual awareness or if it supports it (Förster et al., 2020). Studies in neurotypical individuals have debated the difference between early and late processing involving the dynamic processes of bottom-up, recurrent, and top-down activity (Förster et al., 2020; Koivisto et al., 2010; Mashour et al., 2020; Moratti et al., 2011; Rutiku et al., 2016). This discussion on when the earliest component of visual awareness emerges can be further discussed through the literature on brain rhythms where the cleavage between early and late stage processing in the involvement of the NCC is also argued, with early theories mainly supporting the role of N2 and recurrent activity in V1, and late theories supporting the role of P3 and ignition of the global workspace. Let us nonetheless bear in mind that this clear separation between both theories is not set in stone as it will be discussed further in **chapters 5** and **6**.

(2) The rhythmic activity involved in visual perception has been driving recent research on visual consciousness to allow for a better understanding of the NCC (Bourdillon et al., 2020; Dehaene and Changeux, 2005; Gallotto et al., 2017; Pal et al., 2020). Once visual information is received by V1, it distributes the information to higher-order regions within 100 ms through gamma (>30Hz) feedforward sweeps and almost instantly extra-striate feedback propagations carried by alpha (8-13 Hz) and beta (13-30 Hz) rhythms are sent to V1 (Michalareas et al., 2016). Thus, even

before the involvement of prefrontal areas, V1 is reactivated by recurrent processes driven by extra-striate regions which have been proposed to induce visual consciousness (Lamme and Roelfsema, 2000). Consistent with this view, evidence suggests that visual consciousness can sufficiently arise from the communication between the striate and extra-striate cortex without the subsequent involvement of higher order regions, thus suggesting that consciousness arises in an early time window (Hurme et al., 2017, 2019; Koch et al., 2016a).

Nonetheless, a parallel stream of research that provides a different view has shown that alpha feedforward and feedback pathways and gamma feedforward propagation between the macaque thalamus and frontoparietal regions modulate global state consciousness (Redinbaugh et al., 2020). These results corroborate with the workspace model proposal that the NCC are driven by the subsequent ignition of higher-order regions (Baars, 2002; Dehaene et al., 2003a; King et al., 2016; van Vugt et al., 2018). In fact, studies have found that prefrontal regions (Knotts et al., 2018; Liu et al., 2019; Panagiotaropoulos et al., 2012) and the parieto-frontal network are modulated by beta oscillations (Quentin et al., 2015a; Vernet et al., 2019a) and gamma power (Dehaene and Changeux, 2005; Panagiotaropoulos et al., 2012) play important roles in visual consciousness. Even so, these changes could be confounded with higher-order cognitive processes (Tsuchiya et al., 2015). In fact, gamma modulations in higher-order regions have been shown to enhance global neural potentiation to improve attention (Fiebelkorn et al., 2018), subjective reports (Lau and Passingham, 2006), self-awareness (Lou et al., 2017), qualia (Babiloni et al., 2016), rather than induce visual consciousness, per se.

Taken together the debates that animate the VER and oscillatory literature, it is fair to say that identifying the NCC is a multidimensional complex challenge even though promising integrative views are now proposed (Mashour et al., 2020; Melloni et al., 2021). For this reason, the study of blindsight provides a unique opportunity in understanding the neural correlates of conscious and unconscious perception as an alteration to the primary visual pathway has a direct impact on conscious perception (Boly et al., 2017), while unconscious processing can be preserved (Silvanto, 2015a). Moreover, higher-order cognitive processes emerging from unconscious perception as the detection of deviant changes associated with prediction errors are yet to be addressed in the blindsight literature which could provide insights into the early-late and local-global debates providing a new framework for blindsight. Therefore, we can contribute to the NCC

problem and clinical problem associated with CB by probing the neural mechanisms supporting blindsight and enhancing them through visual training. Investigating these notions which drive this thesis work starts with understanding the implication of the thalamo-extrastriate pathway in blindsight (Danckert and Goodale, 2000; Danckert and Rossetti, 2005; Fox et al., 2020).

1.2.2. The Subcortical-Extrastriate Pathways: A Window into Blindsight

After a V1-lesion, primary visual pathways as described in the previous section are altered which suggests that blindsight emerges from subcortical secondary pathways recruiting extrastriate regions (Ajina et al., 2015a; Bridge et al., 2016; Kinoshita et al., 2019; Persaud et al., 2011; Tamietto and Morrone, 2016). The cortical modulations that occur after the blind field of blindsight patients are stimulated are mainly influenced by the thalamus (Min, 2010; Vakalopoulos, 2005a) and include the LGN (Ajina et al., 2014, 2015) and the pulvinar (Bourne and Morrone, 2017; Maior et al., 2010; Villeneuve et al., 2005) which receives inputs from the superior colliculus (SC) (Leh et al., 2006; Lyon et al., 2010; Tamietto et al., 2010). The thalamus more specifically drives koniocellular and magnocellular-like projections that bypass V1 through a dorsal stream in order to reach extra-striate regions (Ajina et al., 2015a; Lyon et al., 2010; Vakalopoulos, 2005b). The projections are thought to directly discharge their activity to V2-V4 and more importantly the medio-temporal area (MT) without the input of V1 (Fox et al., 2020). Once the extra-striate regions of the lesioned hemisphere are recruited, higher order regions can be involved (Tipura et al., 2017), as well as the intact hemisphere through interhemispheric transfer (Celeghin et al., 2015; Chaumillon et al., 2018; Georgy et al., 2020; Goebel et al., 2001; Tamietto and de Gelder, 2008).

The LGN – While lesions to V1 directly impact the geniculo-striate pathway and visual consciousness, it does not lead to complete degeneration of the LGN where koniocellular projections can still send information via the dorsal pathway to secondary extrastriate regions, such as V5/MT, a region specialized in motion processing (Warner et al., 2010). Moreover, a causal link between the responsiveness of the LGN and blindsight has been established in macaques (Schmid et al., 2010). In humans, connections between the LGN and V5/MT, have also shown a correlation with blindsight (Ajina and Bridge, 2019; Ajina et al., 2015; Bridge et al., 2008).

Therefore, the koniocellular pathway (Sincich et al., 2004; Warner et al., 2010, 2015) and extra-striate regions as V5/MT (Hervais-Adelman et al., 2015; Silvanto et al., 2009) may play a crucial role in processing information from the blind hemifield.

The SC – The superior colliculus may play a crucial role in multisensory integration and saccadic movements (Bell et al., 2005; Corneil et al., 2002; Gingras et al., 2009) when visual awareness is altered which can be targeted in audio-visual training requiring saccades towards the target (Bolognini et al., 2005; Passamonti et al., 2009). This pathway can be triggered by stimulating the blind hemifield using specific stimulations that recruit the magnocellular pathway. Neuroimaging studies of blindsight case reports have shown the functional role of the SC in processing motion stimuli along with area V5/MT (Leh et al., 2006; Tran et al., 2019) through a dorsal magnocellular pathway (Lyon, Nasi, & Callaway, 2010). Nonetheless, these collicular responses mostly send their projections to the pulvinar which is involved in large neural networks essential to perception (Schmid and Maier, 2015). The anatomical and functional role of the pulvinar will further be dissected as the empirical thalamic neurophysiological dynamics provided by **chapters 4** and **5** are mainly interpreted with regard to the function of the pulvinar.

The pulvinar – From an anatomical point of view, the pulvinar receives a lot of inputs from the SC and connections directly from the retina. The medial pulvinar projects its activity via the dorsal pathway to MT, the medial superior temporal area, and the superior temporal sulcus (STS), while the lateral pulvinar is connected to the ventral pathway (Warner et al., 2010, 2015). In fact, MT receives considerable direct inputs from the medial pulvinar that does not pass through V1 which allows MT to achieve specificity early in the brain development of newborns in order to perceive motion stimuli (Warner et al., 2015). The anatomy and connectivity of the pulvinar have been primarily reported in animals, specifically, in the marmoset monkey, but advances in functional imaging (fMRI) have allowed for some cross-species extrapolations regarding the dorsal and ventral contributions (Arcaro et al., 2015). Therefore, the pulvinar has a critical role in the maturation of the visual pathways from the retina to the pulvinar to MT which makes him an ideal candidate for processing information when V1 is lesioned. Nonetheless, gradually, the pulvinar loses come of its influence input and gives way to the geniculo-striate pathway (Bourne and Morrone, 2017).

From a functional point of view, an association between the extrastriate colliculo-pulvinar pathway and blindsight has been found in a hemispherectomized patient (Leh et al., 2006). For instance, Lyon et al. (2010) demonstrated projections from the SC to areas V3 and V5/MT via the pulvinar in the macaque demonstrating the possibility that blindsight may be mediated by a dorsal pathway from the retina, to the pulvinar, through the SC, similar to the magnocellular pathway involved in eye movements and orientations (Lyon et al., 2010). The pulvinar also responds to high-level visual information, such as motion selectivity (Villeneuve et al., 2005) and affective processing (Maior et al., 2010). In fact, emotional processing could be mediated by activations and projections of the pulvinar and SC going to the amygdala for non-consciously perceived fearful visual stimuli (Koller et al., 2019).

1.3. The Neural Substrates of Affective Blindsight

1.3.1. A Thalamo-Amygdala Pathway

As we move through the external world, the saliency of a visual stimulus allows us to select relevant information more quickly, and in an adaptive manner, to process only unconsciously what the brain receives as input that it deems nonessential to the analysis of its environment (Kentridge et al., 2004). By exploiting this principle, it is possible to ask healthy participants to pay attention to a target stimulus and simultaneously present a non-consciously perceived stimulus in the opposite hemifield which interferes with the target stimulus response either by playing on duration (Song and Keil, 2013), eccentricity (Bayle et al., 2011), masks (Wiens, 2006), or low spatial frequency filters (Rohr and Wentura, 2014). We notably respond almost automatically to fearful stimuli even in the absence of visual awareness (Troiani et al., 2014). In fact, fMRI studies have demonstrated that the colliculo-thalamo-amygdala pathway constitutes a functional network in response to implicit fearful facial expressions (Anderson et al., 2003; Striemer et al., 2019; Vuilleumier et al., 2001). Thus, human perception seems to utilize, when needed, a neural network where relevant visual information is not processed via the striate cortex, V1, and that privileges certain emotions or features. This could be the result of an evolutionary process where 'risky' information has an advantage. Therefore, any information that is processed unconsciously should also be processed

rapidly, hence the importance of studying the temporal dynamics underlying implicit emotional processing.

There are clear behavioral, anatomical, and functional indications of a human functional fast thalamo-amygdala pathway that bypasses the striate cortex (Fox et al., 2020; LeDoux, 2000; McFadyen et al., 2020). To provide evidence for a fast alternative subcortical pathway, Kiebel and colleagues (2009) used dynamic causal modeling based on electroencephalography (EEG) and magnetoencephalography (MEG) data, which consists of comparing two functional models to each other, in this case, the subcortical pathway and the cortical pathway and determining which of the two is more likely. They found that the subcortical model was able to explain greater variability in early activity found in the amygdala (Kiebel et al., 2009). Moreover, temporo-spectral dynamics of the thalamus and amygdala have been reported in neurotypical individuals using MEG and source reconstruction showing very early gamma synchronization in the thalamus and the amygdala in response to fearful stimuli prior to activity in the visual cortex (Luo et al., 2007) with the attentional load of the task affecting the activity of the amygdala only at longer latencies (Luo et al., 2010). Furthermore, this processing seems to be mediated by early gamma connectivity from the thalamus to the amygdala specific to negative emotional stimuli (Liu et al., 2015). Corroborating these results, numerous studies have driven their interpretations toward this unconscious 'risky' specific evolutionary pathway (Bayle et al., 2009; Dumas et al., 2013; Hung et al., 2010; Koller et al., 2019; McFadyen et al., 2019; Méndez-Bértolo et al., 2016; Rigoulot et al., 2011; Ward et al., 2005), while others show that this pathway is also involved irrespective of one specific emotion (Garrido et al., 2012; McFadyen et al., 2017), which distinction will be discussed in **chapters 4** and **5**.

1.3.2. Affective Blindsight and Case-Reports

The reported previous studies on neurotypical individuals suggest that there might be a fast pathway for processing non-consciously perceived visual and emotional information in the normal brain. This idea was tested using the inactivation of V1 in neurotypical individuals during an emotional congruence task between two stimuli each presented within one hemifield (Cecere et al., 2013). The results of this study showed an acceleration of the response induced by the masked

emotion of fear that generated a facilitating effect on conscious emotional processing further suggesting a 'low road' involved in affective-blindsight after a V1-lesion. Further studies extrapolated these results to patients with V1-lesions. Affective-blindsight was therefore tested in these patients via indirect tasks, i.e., where the behavior is oriented towards the intact hemifield but is influenced by the presentation of a stimulus presented in the blind hemifield. These researches showed a congruence effect where the presentation of the same emotion in the blind hemifield influenced the reaction times reported for the intact hemifield and a reinforcing effect when presenting fear stimuli in the blind hemifield which results were interpreted by the interhemispheric neural summation hypothesis (Bertini et al., 2013, 2017; Cecere et al., 2014; Tamietto and de Gelder, 2008). The reason why affective-blindsight within the blind hemifields of these patients was not directly tested is since only a few individuals with CB have been documented as having the ability to discriminate emotional expression presented in the blind hemifield on direct tasks.

Case reports of patients with unique abilities in their blind hemifield are of critical importance in probing the neural substrates of blindsight and, more extensively, of affective unconscious processing (Andino et al., 2009; Burra et al., 2019; de Gelder et al., 1999; Morris et al., 2001; Pegna et al., 2005; Striemer et al., 2019; Del Zotto et al., 2013). Specifically, affective-blindsight was discovered in 1999 in well-known and studied patient G.Y. presenting residual visual abilities in his blind hemifield (de Gelder et al., 1999) and was later assessed in patient TN who suffered from bilateral V1-lesions, thus exhibiting complete cortical blindness (Del Zotto et al., 2013a). TN was tested in a functional magnetic resonance imaging (fMRI) paradigm using neutral and fearful emotional faces that were either unfiltered or filtered in low or high spatial frequencies. Unfiltered and low spatial frequency filtered emotional fearful faces activated the amygdala, which was not the case for high frequency filtered faces (Burra et al., 2014). Functional evidence showed that affective-blindsight might be caused by greater activation of the amygdala and subcortical structures, including the superior colliculus and pulvinar, in response to non-consciously perceived facial expressions without prior influence from V1 (de Gelder et al., 1999; Morris et al., 2001a). On the other hand, an EEG study on blindsight patient TN revealed significant differences in the frontal alpha band (7-13 Hz) between emotional and neutral faces in a time interval ranging from 100-400ms following the presentation of the visual stimulus (Del Zotto et

al., 2013a). Therefore, it seems that a whole literature is missing regarding the subcortical temporal dynamics existing between the thalamus and amygdala in affective-blindsight assessed by case-reports which was the main focus of **chapters 4** and **5.**

1.4. Improving Visual Awareness in Cortical Blindness

1.4.1. Multisensory Training

Multisensory training has been developed to target bottom-up mechanisms through non-specific perceptual learning and allow the generalization of learning to several cognitive processes, such as motion processing and visual-spatial orientation (Kim et al., 2008; Seitz et al., 2006). Multisensory stimulations, e.g. presenting a sound and a visual stimulus simultaneously, mainly target the bimodal neurons of the SC that responds to audio-visual stimuli by fortifying functionality within the extra-striate pathways (Calvert et al., 2001). Moreover, the SC has a crucial role in ocular movements which become faster and more accurate with repetitive multisensory stimulations (Kato et al., 2011; Lee et al., 1988). Importantly, multisensory stimuli can induce facilitation in learning and improvement in performance allowing to considerably decrease the number of training sessions needed, which could solve an important problem in the feasibility of rehabilitation interventions (Alvarado et al., 2008; Doubell et al., 2003; Perrault et al., 2011). In CB, multisensory training combined with saccades can be used as a compensation strategy to allocate greater attentional resources towards the blind hemifield resulting in more optimal saccades (Kerkhoff et al., 1992). In fact, it has been shown in HH patients that visual performance is greater for bimodal coincident stimuli (congruent) compared to unimodal stimuli and bimodal stimuli presented at different locations (incongruent) (Leo et al., 2008). Furthermore, after multisensory training, an amelioration of the global oculomotor pattern was reported (Passamonti et al., 2009) and an increase in visual responsiveness in the ipsilesional SC of cats was correlated with recovery of visual exploratory behavior (Jiang et al., 2015). Moreover, by targeting the colliculo-pulvinar extrastriate pathway such training could increase attentional processes in the blind hemifield (Dundon et al., 2015). Indeed, following extensive audio-visual training, patients with HH showed a reduction in the P3

amplitude known for reflecting attentional allocation for the intact hemifield. These results demonstrate a decrease in attentional bias towards the intact hemifield that can be attributed to an increase in attentional capacities within the blind hemifield generated by neuronal reorganization (Dundon et al., 2015). Increasing attentional allocation towards the blind hemifield could increase residual abilities within the blind hemifield (Kentridge et al., 2004; Vernet et al., 2019b) which justifies why rehabilitation strategies should include multisensory training (Grasso et al., 2016). Moreover, such training has been associated with improved visual detection and exploration (Bolognini et al., 2005; Leo et al., 2008; Passamonti et al., 2009) and quality of life (Roth et al., 2009). Although compensatory therapies have been shown to be effective for more than two decades now (Kerkhoff et al., 1992), they are still underestimated due to the little clinical impact and specificity associated with them (Pollock et al., 2011). For this reason, the use of bottom-up multisensory training in combination with top-down training, e.g. the visual restitution training, could lead to greater improvement in visual detection, localization and recognition which will be discussed in **chapters 3** and **7**.

1.4.2. Visual Restitution Training Using Motion Stimuli

Visual restitution techniques aim to reduce the size of the scotoma or blind hemifield by measuring the performance within one training area or multiple training areas depending on how much of the visual field is trained (Bouwmeester et al., 2007; Saionz et al., 2021). In order to do so, restitution training needs to target and reinforce the residual extra-striate pathways involved in blindsight (Huxlin et al., 2009). One way that could lead to the enhancement of secondary pathways following a V1 lesion, is the use of high contrast visual stimulations, high temporal frequencies, low spatial frequencies, and motion stimuli (Sahraie et al., 2013). Training patients with these stimuli can increase detection (Sahraie et al., 2006), identification, recognition, pointing, and localization (Chokron et al., 2008) or discriminations abilities (Kavcic et al., 2015a). Notably, these studies showed the importance of using double stimulations including complex motion and static stimuli presented in different positions in the blind field (Das et al., 2014), increasing the difficulty of visual detection and discrimination as the performance gets better (Kasten et al., 2008), using spatial and temporal cues (Kentridge et al., 1999) and using feature-based attentional cues (Cavanaugh et al., 2019). Moreover, this perceptual enhancement was transferred to other types

of stimuli and experiments (Huxlin et al., 2009). Thus, there is important evidence regarding the beneficial role of perceptual relearning using visual restitution training in patients with CB, however, this learning is still limited in terms of transfer learning and size recovery of the blind areas. In fact, current training does not sufficiently target multiple cognitive processes to ensure conscious vision restoration, which is why in **chapter 7** we propose a new training combining multisensory and specific visual stimuli inspired by compensatory and restitution strategies.

Chapter 2: Aims and Research Hypotheses

2. General Aims

Blindsight studies bring new perspectives to different areas of research in neuroscience as they provide unique opportunities to probe the existence of secondary neural pathways supporting unconscious behavior. Specifically, the study of individuals with exceptional abilities as described by case reports allows to (1) achieve a new understanding of unconscious behavior, (2) assess the functional role of neural pathways involved in unconscious processing that are hard to identify in neurotypical individuals, (3) compare the neural substrates of conscious and unconscious processing and (4) exploit the neural mechanisms underlying blindsight with adequate rehabilitation strategies to restore vision in patients with CB.

While this literature is rich and captivating, there are gaps concerning the nature and mechanisms of blindsight as described in chapter 1. Therefore, the aims of this thesis were threefold: (1) to offer an integrative perspective on blindsight and residual abilities based on previous theories, (2) to investigate the neural substrates of blindsight and affective-blindsight by utilizing methodological advances in electrophysiology, and (3) to propose new methods in probing and enhancing unconscious perception.

2.1. Aims of the First Study

The first study is a theoretical paper proposing a new interpretation of the nature of blindsight and how its understanding can lead to optimized rehabilitation strategies (**chapter 3**). Blindsight is often characterized as unconscious perception (Weiskrantz, 1986), however, some authors refute this claim by referring to blindsight as normal degraded vision (Brogaard, 2011; Phillips, 2020). Their rationale is mainly driven by the fact that some blindsight patients preserve extraordinary abilities comparable to what is observed in normal degraded vision, but yet that the majority of people affected with CB do not demonstrate residual abilities. We, therefore, make a point about why and how behavioral assessment is important to understand discrepancies between patients. Thus, the first aim of this paper was to suggest a new way to assess behavior in blindsight patients. Our second aim was to propose an integrative way to understand residual visual abilities in terms of their subjective nature and to make a fair point about inter-individual differences that can support the unconscious and degraded vision hypotheses. As the paper was mainly inspired by the global

workspace theory first proposed by Bernard Baars (Baars, 1988) and later broadened by Stanislas Dehaene (Dehaene et al., 1998), our third aim was to better frame the nature and mechanisms of blindsight within an altered unsynchronized neuronal framework of global workspace following a V1-lesion. Finally, the last aim of this paper was to suggest a new consolidative rehabilitation strategy to improve vision in CB that combines multisensory compensation training with restitution training where the rationale was incorporated into our theoretical altered neuronal framework.

2.2. Aims and Hypotheses of the Second Study

The second study is a case report that aimed to investigate the subcortical gamma connectivity involved in affective blindsight as no empirical evidence of fast thalamo-amygdala dynamics has been evidenced in patients following a V1-lesion (**chapter 4**). To do so, we reported the case of a patient with HH not yet described in the literature that we referred to as SJ. Interestingly, SJ preserved residual abilities for discriminating affective natural complex scenes which is a unique characteristic not yet investigated in the blindsight literature. Based on the theory of an unconscious evolutionary subcortical pathway (Fox et al., 2020; McFadyen et al., 2020) and studies of brain rhythms in neurotypical individuals (Liu et al., 2015; Luo et al., 2007), we hypothesized that the thalamus exerts a causal influence on the amygdala and extrastriate regions through high-frequency oscillations in order to process unconscious affective information presented in the blind hemifield. To test our hypothesis, we used MEG, cortical and subcortical source reconstruction, spectral, Granger causality analysis, and linear regression.

2.3. Aims and Hypotheses of the Third Study

The third study also report the case of SJ as the aim was to decode the subcortical and striate temporal signal associated with conscious and unconscious experiences for affective natural scenes using MEG and source reconstruction (**chapter 5**). With respect to the early-late debate on when the earliest component associated with conscious perception emerges (Förster et al., 2020; Mashour et al., 2020), we hypothesized that conscious and unconscious percept can be decoded in late time windows through maintained and recurrent activity, while differences in conditions within the blind hemifield could be assessed at very early stages. To validate our hypothesis, we used MEG, cortical and subcortical source reconstruction, evoked analysis, decoding, temporal decoding, temporal generalization, and Granger causality analysis.

2.4. Aims and Hypotheses of the Fourth Study

The fourth study aimed to assess the vMMN and its spectral connectivity to address the debate on evaluating unconscious processing independent of subjective bias and behavior. To do so, we tested neurotypical individuals and blindsight patient ML (chapter 6). Patient ML has been reported in our previous study where we showed that her blindsight for motion stimuli involved subcortical structures and extra-striate regions (Tran et al., 2019). The rationale to test the vMMN in blindsight patients is twofold: (1) it is still unknown whether the vMMN reflects true detection of changes in the absence of visual awareness which could be determined in blindsight patients and (2) measuring unconscious processing depends on multiple factors including the subjective bias and dependency on the protocol thus an objective measure with no report that is independent of behavior is needed. Therefore, our hypothesis states that the vMMN can reflect a reliable index of unconscious processing which would be assessed in both the neurotypical group and blindsight patient. To verify our hypothesis, we used EEG, evoked, spectral and connectivity analyses.

2.5. Aims of the Fifth Study

The fifth study aimed to propose a combined strategy for visual rehabilitation of patients with CB (**chapter 7**). Therefore, we developed a dynamic and motivating environment using the beneficial approaches of video games. In order to stimulate alternative visual pathways thought to support blindsight, we used (1) multisensory stimulations to enhance visual exploration and saccadic performances towards the blind hemifield (Leo et al., 2008) and (2) motion stimuli, high temporal frequencies, and low spectral frequencies presented at multiple locations of the blind hemifield (Huxlin et al., 2009). The proposed training combining a multisensory compensation approach and a visual restitution approach involves attentional engagement and positive reinforcement.

Chapter 3

Article 1. From Cortical Blindness to Conscious Visual Perception: Theories on Neuronal Networks and Visual Training Strategies

Article 1. From Cortical Blindness to Conscious Visual Perception: Theories on Neuronal Networks and Visual Training Strategies

Vanessa Hadid[1], Franco Lepore[2, 3]

[1]Département de sciences biomédicales, Université de Montréal

[2]Centre de recherche en neuropsychologie et cognition (CERNEC), Université de Montréal

[3]Département de psychologie, Université de Montréal.

Abstract

Homonymous hemianopia (HH) is the most common cortical visual impairment leading to blindness in the contralateral hemifield. It is associated with many inconveniences and daily restrictions such as exploration and visual orientation difficulties. However, patients with HH can preserve the remarkable ability to unconsciously perceive visual stimuli presented in their blindfield, a phenomenon known as blindsight. Unfortunately, the nature of this captivating residual ability is still misunderstood and the rehabilitation strategies in terms of visual training have been insufficiently exploited. This paper discusses type I and type II blindsight in a neuronal framework of altered global workspace, resulting from inefficient perception, attention, and conscious networks. To enhance synchronization and create global availability for residual abilities to reach visual consciousness, rehabilitation tools need to stimulate subcortical extrastriate pathways through V5/MT. Multisensory bottom-up compensation combined with top-down restitution training could target pre-existing and new neuronal mechanisms to recreate a framework for potential functionality.

Cortical blindness

Normal vision in humans is primarily mediated by the geniculo-striate pathway where the visual information is processed in a hierarchical order via the retina, the lateral geniculate nucleus (LGN), and the striate cortex. Once the primary characteristics of visual information are processed, visual connections are sent to the parietal cortex involved in spatial attention and action (dorsal pathway) and to the temporal cortex involved in recognition and identification (ventral pathway). Following post-chiasmatic lesions inducing an alteration in the geniculo-striate pathway, contralateral cortical blindness (CB) occurs, either as a result of a neurophysiologic disorder requiring surgical interventions of V1 or mainly subsequent to a stroke affecting the posterior visual cortex (Sand et al., 2013, for review, see Goodwin, 2014). Depending on the extent of the lesioned cortex, the visual field deficit may correspond to a CB of a few degrees (scotoma), a quarter of a hemifield (quadranopsia), or an entire hemifield (hemianopsia) (for review, see Swienton & Thomas, 2014). The homonymous hemianopsia (HH) is the most common visual cortical deficit representing 10% of stroke cases, with little more than 70 000 new cases per year in the US (Writing Group Members et al., 2016; Zhang et al., 2006). Moreover, more than 500,000 Americans live with a HH and this deficit reduces significantly their quality of life, for example preventing them from driving and, decreasing their reading, orientation, and exploration visuospatial abilities (Perez and Chokron, 2014). In addition, due to comorbidity, HH significantly reduces the prognosis and the possibility of recovery from other damaged functions after stroke, including motor skills (Patel et al., 2000). As only a small minority experiences spontaneous recovery, possible within the first 6 months (Duquette & Barrel, 2009), it is crucial to rehabilitate these individuals during this time. Unfortunately, except for vision restitution therapy (VRT) which, while being approved by the FDA due to its therapeutic potential (Kasten et al., 2006; Sabel et al., 2005), remains controversial regarding its benefits in terms of pure visual restitution (Bouwmeester et al., 2007; Horton, 2005a, 2005b; Melnick et al., 2016), there are very few available resources for clinical interventions. This may be due to a lack of consensus in the literature caused by inconsistent results across the target population, differences between protocols used in research, and an inefficient vision recovery (Pollock et al., 2011; for reviews, see Pouget et al., 2012; Riggs, Andrews, Roberts, & Gilewski, 2007). Furthermore, there is so much inter-individual variability in the origin and extent of lesions that most probably plasticity in the visual system is heterogeneous throughout the population. This leads us to the question: is the visual recovery in cortically blind individuals possible with strategic

rehabilitation? In theory, it would be conceivable, in the light of a well-documented preserved visual ability in CB referred to as blindsight, where visual information is processed in the blindfield without the knowledge of visual awareness (Weiskrantz, Warrington, Sanders, & Marshall, 1974). From a behavioral perspective, blindsight is the dissociation between what is reported subjectively, for example, the subject states not seeing anything in the usual scale of the binary report (seen, not seen), and what is measured objectively, i.e. the rate of correct answers in the two-alternative forced-choice paradigm is above the chance level. The first extended precepts of the phenomenon are described from the results obtained on GY who had a trauma affecting the striate cortex at a young age (Barbur et al., 1980; de Gelder et al., 1999; Kentridge et al., 2004) and DB who required removal of V1 at an adult age (Tamietto et al., 2009; Weiskrantz, 1987). Blindsight includes the unconscious ability to be able to locate random targets by reaching or pointing at them, to determine the presence or absence of visual targets, to have considerable visual acuity mainly for low spatial frequencies, to discriminate directions (Weiskrantz, 1986), to recognize colors (Brent et al., 1994), to detect global movement, to distinguish between coherence (Alexander and Cowey, 2009; Pavan et al., 2011) and to recognize facial expressions (De Gelder, Vroomen, Pourtois, & Weiskrantz, 1999). However, it has been found that high contrast and fast movement stimuli could induce sensations described as something elusive that happened in the blind hemifield. Accordingly, a distinction has been made between type I blindsight, i.e. absolute blindness without conscious awareness, and type II blindsight, i.e. blindness with awareness but no visual qualia (Lau and Passingham, 2006). In fact, attempting to understand the intrinsic process governing this unconscious vision has been the foundation of many theories (Kanemoto, 2004; Smythies, 1999; Zeman, 2004).

Fine Line between Type I and Type II Blindsight

It was in 1917 that the first evidence of a residual visual ability in the blind field emerged when a patient reported visual sensation specifically to motion. This non absolute blindness sustained a form of visual qualia called the Riddoch Syndrome (Riddoch, 1917). Keeping this in mind, the notion of visual qualia is quite important to consider in blindsight studies, especially when considering blindsight type II because even if some kind of awareness remains it has to be dissociated from visual awareness (Ko and Lau, 2012) which we will discuss further on. Subsequently, the characterization and understanding of the dissociation between type I blindsight

and type II is controversial, due to the fact that only a few studies have been able to demonstrate a correlation between the loss of the striate cortex, the takeover of secondary visual pathways and the state of visual consciousness (for review, see Leopold, 2012). The problem that arises with respect to blindsight is to figure out which hypothesis could best explain the phenomenon: (1) A degraded normal vision (2) An unconscious vision (3) A degraded abnormal vision.

(1) Degraded normal vision occurs when visual stimuli are processed through the primary visual pathway, but do not reach the threshold of full visual awareness. In fact, in some cases, spared islands of the striate cortex explain the residual visual capabilities found in HH (Fendrich et al., 1992, 2001). However, several patients may present blindsight in the absence of a functional striate cortex (Ajina et al., 2015; Mazzi et al., 2016; Morland et al., 2004), regardless of the state of awareness (Ffytche and Zeki, 2011). Though we should not overlook the importance of targeting vestiges of V1 in rehabilitation strategies, we must be able to stimulate the secondary visual pathways bypassing V1 potentially responsible for type I and II blindsight. Therefore, we need to understand the mechanisms governing the two forms of this phenomenon.

(2) Unconscious vision has been showcased by proving that residual abilities in HH do not follow the same rules as it is qualitatively different from that of the conscious normal vision (Weiskrantz, 2009). In fact, for certain visual stimulations, the performance in the blind side is better than the one in the normal side (Trevethan et al., 2007). For example, unlike normal vision, performance in a task of exclusion is inversely correlated to the stimuli's contrasts (Persaud and Cowey, 2008), there is a clear abnormal distinction between choice-forced and detection performances (Azzopardi and Cowey, 1997) and some physical attributes are processed in the blind hemifield, while others are not (Kentridge et al., 2007; Morland et al., 1999). Taken together, these studies provide robust evidences to the hypothesis that blindsight is different from normal vision and is not simply a form of degraded normal vision. However, they have assumed that this abnormal vision is unconscious, whereas an abnormal degraded vision could also explain the behavioral results. In fact, unconscious and degraded abnormal vision can both refer to a vision qualitatively different from normal vision mediated by secondary neurophysiological correlates, but that differ in terms of conscious subjectivity and the nature of the sensation.

(3) Some authors refute the theory of unconscious vision by stating that the residual visual capabilities are due to a degraded abnormal vision that does not reach the threshold of detection (Mazzi et al., 2016; Overgaard and Grünbaum, 2011). In GR and SL case studies, with complete

lesion to the striate cortex, the perceptual awareness scale (PAS) was used to allow a subjective finer report based on four indices, instead of the usual scale of binary report (seen, not seen). This showed that patients tend to have a higher threshold to acknowledge that something is conscious if the criterions are not based on a scale of consciousness. In fact, after using the PAS, awareness was better than what the theory of unconsciousness would have predicted (Mazzi et al., 2016; Overgaard et al., 2008). They concluded that type I blindsight can be wrongly considered as unconscious; instead, it seems that above chance level performance comes with conscious perception. Therefore, GR and SL do not have blindsight, rather they have conscious vision. Their results agree with the continuum perception theory, where there is a correlation between increased visual sensitivity and higher brain activity. In the normal population, results are contradictory depending on the paradigm used. For example, when using masked stimuli, results tend to suggest that performance can't exist without awareness and that if the reverse is often inferred, it is due to visual bias induced by inappropriate methodological tools measuring awareness. Moreover, even among the ideal model, performance is greater than awareness in a non-linear relationship where the threshold for perception is inferior to the one for awareness which could explain why in altered perception, the state of consciousness decreases more rapidly than the performance. Thus, even if performance is accompanied by awareness, the latter can be wrongly underestimated without the appropriate tools, since thresholds for explicit visual consciousness is not reached (Peters and Lau, 2015). Therefore, is it possible that blindsight consists of an abnormal conscious degraded vision mediated by secondary visual pathways? If this extrapolation is accurate, we nevertheless disagree with the conclusion of Mazzi and colleagues (2016) that SL's residual abilities are due to conscious vison inducing visual qualia, thus inferring that in such case there is no such thing as blindsight. First, blindsight was employed to explain an ability which was phenomenologically different from blindness and sight and can be referred to as the loss of visual function that is accompanied by altered 'sight'. Secondly, SL had the feeling that something happened in her blindfield; however she couldn't visually describe what she saw. Can we say that she showed a form of consciousness? Yes. Can we conclude that the nature of the feeling is visual? Not so much. The scale evaluated the following perceptual judgments as: "(1) no experience of the stimulus, (2) brief glimpse, (3) almost clear experience, and (4) clear experience" (Mazzi et al., 2016). There was never a reference to the nature of the visual stimuli, or even to what was seen, contrarily to the Riddoch phenomenon where visual qualia of motion were described (Riddoch, 1917). While we agree that the use of the

PAS allows patients to 'pay more attention', subsequently giving more insight on residual abilities and potential tools to rehabilitation, it's nevertheless insufficient to conclude on the nature of the awareness and the continuum scale of perception. In fact, others have also used a continuous scale to assess visual awareness and showed that either the visual stimuli presented in the attentional blink was completely perceived or not detected at all independently of stimuli visibility (Sergent and Dehaene, 2004a). The non-perceived stimuli in the attentional blink were correlated with suppression of the P300 wave, and a dynamic change in brain oscillations indicating that perception without consciousness has distributed neuronal correlates (Kranczioch et al., 2007). Unfortunately, the neuronal correlates underlying theses controversial residual abilities has yet to be explained.

An unsynchronised framework for blindsight

This paper supports the global neuronal workspace framework as a model for conscious and unconscious vision (Sergent and Dehaene, 2004b). Thus, in alignment with promising views on 'local' and 'global' visual functions in blindsight (Silvanto, 2015), blindsight can be understood as a lack of synchronisation in neuronal activity (Melloni et al., 2007) and rapid globalization for specific visual properties between altered perception processors (neuronal networks implicated in bottom-up activity and visual performances), attention processors (systems of complex neuronal association that allow perceptual information to access consciousness) and conscious processors (workspace neurons for awareness via top-down activity). Moreover, because the attention network can interact with the perception network without creating any kind of visual awareness, it is most probable that the perception workspace can send projections to the attention workspace without creating any attentional awareness. This phenomenon recently called attentional unawareness was hypothesized in blindsight patient for emotional stimuli, subsequent to studies in normal vision (for review, see Diano, Celeghin, Bagnis, & Tamietto, 2016). In this context, it would be conceivable to induce learning effect resulting in awareness, and moreover visual consciousness, if attentional and perceptual feedforward and feedback connections were simultaneously stimulated. This would lead to synchronization enhancement and would allow cascading amplification resulting in long-distance reciprocal connections and global availability (Dehaene et al., 1998). Indeed, attention is necessary to visual consciousness even if not sufficient (Kentridge et al., 2004; Schurger et al., 2008; Yoshida et al., 2012). Visual consciousness would be mediated by top-down activity through connections between higher and lower perception processors, as well as between perception,

attention and conscious processors creating a global workspace. As a result, the inability of cortically blind people to describe what is presented in their blind field could be linked to a lack of global availability of the global workspace due to inefficient looping among the altered perception and attention processors and interaction with the conscious network. Hence, according to the global workspace, blindsight could be mediated by secondary visual pathways that activate the neuronal perception and attention networks insufficiently and only locally, without sending long ranging connections to other networks in the brain therefore suppressing visual qualia which could explain the above-chance visual performances in choice-forced paradigms. Consequently, in type I blindsight, the neuronal network generates sufficient activity to process the stimulus, however the neuronal pattern required for phenomenal consciousness is insufficient. In type II blindsight, activity is sufficient to create a sense of awareness, perhaps due to the activation of local conscious processors, but it doesn't reach the threshold for global availability (see Figure 1).

Nonetheless, all residual visual abilities found in CB are not necessarily due to blindsight, in the contrary it could be linked to degraded normal or abnormal vision, as we discussed previously. In reality multiple networks can co-exist, vary in function of the lesions and express themselves depending on the stimulation or given paradigm. In literature, the term blindsight lacks clarity because it refers to several types of visions, mechanisms and correlates all at once. Residual visual abilities are found only in a few individuals with CB. However, it is more than possible that co-existent residual secondary pathways arise together (Tamietto and Morrone, 2016), but when cortical alterations are too diffuse residual pathways aren’t activated strongly enough to induce residual vision. Therefore, a same individual could have multiple types of residual visual abilities or the potential to develop them with training. Thus, we propose the following terminology:

(1) Degraded visual abilities consist of a degraded normal vision caused by vestiges of the striate cortex. It is linked to reduced performances and/or visual awareness that are qualitatively similar to normal vision but quantitatively poorer.

(2) Blindsight consists of an unconscious vision mediated by secondary visual pathways bypassing V1 independent of visual awareness. It could be explained by inexistent (blindsight type I) or not optimal synchronization (blindsight type II) between the perception, attention and conscious networks.

(3) Alternative visual abilities consist of an abnormal degraded vision which is qualitatively different from normal vision but is associated with visual awareness mediated by secondary visual pathways that can't be explained by the activity of the striate cortex.

The idea is to understand how we can pass from blindsight type I, to blindsight type II to an alternative visual ability. In other terms how can we pass from a state of no awareness to a state of awareness and finally to visual awareness by stimulating secondary visual pathways?

Neuronal substrates underlying the framework of blindsight

Geniculo-extrastriate pathway: a door to perception

The geniculo-extrastriate pathway is a perfect candidate to our altered perception workspace. Its existence implies that V1 lesions do not lead to a complete degeneration of the LGN, and that koniocellular projections are sent to the secondary extrastriate regions, such as MT (Warner et al., 2010). In macaques with no striate cortex (eliminating the possibility of V1 islands) there is a causal link between the LGN and blindsight (Schmid et al., 2010). In fact, by presenting high contrasts stimuli in the blindfield, the authors have observed visual processing corresponding to blindsight, correlated with fMRI activations in several areas including extrastriate region MT. By inactivating the LGN, the neuronal activations and the residual detection skills were abolished (Schmid et al., 2010). Also in macaques, direct koniocellular projections were found between the LGN and MT corroborated by a retrograde technique of tracing and histological sections. In addition, a new neuronal population, not belonging to the koniocellular system, has been discovered in the intercalated layers of the LGN (Sincich et al., 2004). Interestingly, in humans MT (hMT+) acts similarly to V1 when presented with global motion (Ajina et al., 2014). This highlights the role of existing subcortical visual pathways in blindsight, which was specifically and exclusively correlated with the presence of the geniculo-extrastriate pathway (Ajina et al., 2015). However, in this study, blindsight was assessed with a motion task; it is possible that the correlation existed just for the geniculo hMT+ pathway because the psychophysical measure was specific to this pathway. Blindsight negative individuals were categorized as such using the same task, nonetheless they could have exhibited blindsight using saccadic localization of a brief visual flash or using indirect methods where reaction time to stimuli presented in the normal field are enhanced by stimuli

presented in the blind field. We extrapolate a possible correlation between blindsight positive individuals derived from such paradigms and the colliculo-extrastriate pathway or interhemispheric connections between hMT+, respectively.

Colliculo-pulvinar-extrastriate pathway: a door to integration and attention

The implication of the superior colliculus (SC) in blindsight is strongly corroborated with behavioral data. More specifically, the physical parameters of stimuli inducing blindsight correspond specifically to the inherent characteristics of the SC neurons (Leh et al., 2010; Tamietto et al., 2010). For example, the lack of projections from the short-wavelength sensitive cones of the retina towards SC neurons is associated with blindness to blue (Leh, Ptito, Schönwiesner, Chakravarty, & Mullen, 2010; Tamietto & De Gelder, 2010). Consequently, when the color blue is used instead of red or an achromatic visual stimulation, then blindsight and activations of the SC disappears. From a functional point of view, an association between the collicular pathway and type I blindsight was found in a hemispherectomized patient, as well as interhemispheric connections extending from the SC to the visual, parietal and prefrontal, areas (Leh et al., 2006). Even if the SC could relay to the extrastriate cortex via colliculo-geniculate projections (Harting et al., 1991), Lyon and colleagues, have demonstrated projections from the SC to V3 and V5/MT throughout the pulvinar in macaques assessing the possibility that blindsight could be mediated by relays ranging from the SC to the pulvinar and the dorsal pathway similar to the magnocellular pathway involved in movement and ocular orientations (Lyon, Nasi, & Callaway, 2010). We postulate that the subcortical extrastriate pathway passing by the SC and the pulvinar serves attentional workspaces and can be enhanced with multisensory stimulations. In fact, bimodal neurons of the SC respond to audio-visual stimuli by fortifying extrastriate pathways (Paraskevopoulos et al., 2012; Stein and Rowland, 2011). Moreover, the SC is responsible for ocular movements in the centers of attention becoming faster and more accurate with repetitive multisensory stimulations (Bell et al., 2005; Corneil et al., 2002; Gingras et al., 2009). Training of the oculomotor track could allow a potential increase in allocation of attention in the blind hemifield, which is necessary to perception and visual consciousness. On another note, it seems that the pulvinar can perform higher order visual processing, as motion-selectivity and emotional processing for the former (Maior et al., 2010; Villeneuve et al., 2005) so can the SC, as Gestalt like analysis associated with faster responses for stimuli with specific configuration and numerosity

(Celeghin et al., 2015a; Georgy et al., 2016). Other studies demonstrated activations, projections and connections from the SC and the pulvinar to the amygdala when unconscious visual emotional stimuli occurred in hemispherectomized patients (Celeghin et al., 2015b; de Gelder et al., 1999; Morris et al., 2001; Tamietto et al., 2012). Therefore, specific perceptual training could directly target these structures and reinforce subcortical pathways bypassing V1, hence the idea of combining different types of visual training.

Multiple workspaces of consciousness

We hypothesize that consciousness and moreover visual consciousness is mediated by multiple workspaces interacting together. Conscious processors can be mediated by interactions of the fronto-parietal and prefrontal network (Persaud et al., 2011; Zeman, 2004) with higher visual areas (Dehaene and Changeux, 2011), and visual conscious processors by the thalamic reticular network (Min, 2010). Consciousness, and more specifically visual consciousness can be achieved with feedforward and feedback connections from higher to lower visual areas (for review, see Urbanski, Coubard, & Bourlon, 2014). An alteration in feedback loops and synchronisation between high cognitive areas and visual areas could lead to a lack of awareness (blindsight type I). Between higher and lower visual areas inefficient long ranging connections could lead to the lack of visual awareness found in type II blindsight. This blindsight model is subsequently the result of altered local workspaces that take over when a normal global network degenerates (Silvanto, 2015). Therefore, connectivity between new workspaces of perception and abnormal workspace of consciousness are weak and non-specific, due to a lack of visual learning reflected by a lack of appropriate synchronisation. This unsynchronized framework between posterior and more anterior areas diminishes the visual sensitivity for motion stimuli in healthy subjects demonstrating precisely the effects of synchronization on V5/MT (Romei et al., 2016). Hence, the idea is to employ neurorehabilitation to target residual pathways passing by V5/MT, induce new connectivity between interhemispheric V5/MT areas (Bridge et al., 2008; Silvanto et al., 2009) and functional interactions within the lesioned hemisphere (Huxlin, 2008).

A model of combined interventions reinforcing the global framework of blindsight

Importance of the subacute period

This section reports the estimated tools to promote plasticity following a CB and increase potential recovery of functional vision. First, future research should emphasize the importance of stimulating visual pathways in the subacute period following the lesion (Alber et al., 2017) to notably reduce the degenerations of subcortical tracks (Nijboer et al., 2013) and increase the chances of visual improvement (Keller and Lefin-Rank, 2010). In fact, spontaneous restoration in the subacute phase is associated with a reactivation of V1, a restoration of the ipsilateral optical radiations and a progressive recovery of visual functions (for review, see Matteo, Viganò, Cerri, & Perin, 2016). An increase in spontaneous restoration could be induced with reinforcement of the residual tracks and recruitment of new ones by activating interhemispheric connections.

The value of interhemispheric connections

It has been demonstrated that subsequent to a striate lesion, reorganization of the cerebral cortex in favor of the intact hemisphere induces V5/MT of the ipsilateral hemifield to project to V5/MT of the contralateral hemifield after stimulation of the blind field (Bridge et al., 2008). Moreover, in the lesioned hemisphere, there are areas that respond to stimulations presented in the normal hemifield, but not to stimulations in the blind hemifield (Kavcic et al., 2015). Simultaneous stimulation of the two hemifields could produce an effect of learning, allow for ipsilesional reorganization (Celeghin et al., 2015c), and would be essential to regain visual perception (Silvanto et al., 2007). Contralesional V5/MT activation induced by repetitive stimulation of the normal hemifield would allow reorganization and potentiation of the ipsilesional V5/MT via interhemispheric connections, and therefore gain new normal functionality instead of the "V1 like functions". In fact, we postulate that connections from the contralesional to the ipsilesional V5/MT could lower the threshold to induce global availability within the lesioned hemisphere by activating new processors in the lesioned hemisphere and/or by interhemispheric synchronisation between workspaces. These results added to the proposed neuronal substrates of the global workspace seem to lead to the notion that V5/MT could be considered as the crossroad of residual abilities and should therefore be the central key to rehabilitation. Multisensory bottom-up activations mediated

by the colliculo-extrastriate pathway could lead to V5/MT enhancement without the need of attentional processes.

Enhancing attention with audio-visual training

Reorganization following audio-visual stimulations allows a decrease of the ipsilesional attentional bias showed by a reduction in P300 amplitude (Dundon et al., 2015a), potentially moving the attentional capacities towards the blind hemifield. The role of the SC in this attentional process is particularly important, since such an effect is obtained by the intermediary of saccadic movements. This enhancement of attentional capacities, without prior visual attention needed, is exactly why rehabilitation tools should include audio-visual stimulation training (for review, see Grasso, Làdavas, & Bertini, 2016) which has been associated with an improvement in visual detection and exploration (Bolognini et al., 2005; Leo et al., 2008; Passamonti et al., 2009), and in life quality (Roth et al., 2009). Although compensation therapies proved their reliability over more than two decades (Kerkhoff et al., 1992), they are still underestimated, due to very little clinical evidence of their impact (Pollock et al., 2011). For this reason, the use of multisensory bottom-up training in association with top-down training could lead to a higher chance of improving visual detection, localization and recognition.

Re-establishing perception with restitution training

Restitution techniques are effective if they aim typical visual attributes training specific to blindsight to expand over a large spectrum of visual characteristics and functions. For example, a transfer of information can be achieved by presenting simultaneous and diversified stimulations in the blind field accompanied by temporal and spatial cues (Kentridge et al., 1999). As well, it would be possible to improve conscious visual detection performances with training of residual visual abilities (Chokron et al., 2008), to improve visual functions that are initially outside of the spatiotemporal band of blindsight by using double stimulations including complex motion and static stimuli presented in different positions in the blind field (Das et al., 2014). This improvement in perception is obtained when a transfer of information processing happens between different stimuli and experimental conditions (Huxlin et al., 2009), implying that the perception workspace is capable of great plasticity when it is targeted via different mechanisms. Restitution tools must therefore target multiple functions used in perception, that is to say: detection, localization,

identification and discrimination, as well as functions used in consciousness, that is to say: a judgment on the nature and the level of visual consciousness (Sahraie et al., 2013). Moreover, it is possible with repeated stimulation to increase visual sensitivity (Sahraie et al., 2006, 2010; Trevethan, Urquhart, Ward, Gentleman & Sahraie, 2012). This change in subjective awareness linked to the performance, highlights the possibility of a transfer from an unconscious vision (type I blindsight), to a state of awareness (type II blindsight), hence to a potential visual qualia (vision), which is encouraging in regards of rehabilitation tools (Sahraie, Trevethan, Macleod, Weiskrantz, & Hunt, 2013). Taken together, these results imply that to gain vision, we have to trigger long-term plasticity by targeting multiple pathways and mechanisms together creating a synchronous activity through multiple processors of the blindsight framework. Thus, we endorse a combined strategy using multisensory compensation and restitution.

Potential effects of a combined-training within a global subcortical framework of blindsight

Audio-Visual Scanning Training could allow feedforward interactions between the SC and V5/MT (Dundon et al., 2015b), causing V5/MT to increase its functional activity and potential to make stronger connections in the attentional workspace. When applied with restitution training, the increase in functionality could optimally reinforce the tracks between the LGN and V5/MT in the perception workspace (Ajina et al., 2015), leading to more efficient interactions with lower and higher visual areas resulting in long-distance reciprocal connections and cascading amplification in the conscious workspace (see Figure 2). Therefore, a stimulation of the altered blindsight framework would allow attention and perception to enhance each other leading to a better access to consciousness by a decrease in the threshold of visual attention and discrimination. Lowering these thresholds implicates that the visual properties of a stimulus are prompt to be accessible to different areas of the brain making them more easily perceived and processed permitting awareness. This will be reflected by higher synchronisation of neural activity in visual and higher cognitive areas which will induce global availability and possibly lead to conscious visual perception (Melloni et al., 2007). Finally, although the main focus of this review covered visual training, we can't omit the potential benefit of pharmacological interventions (Gratton et al., 2017) and novel tools for neuromodulation used alone (Gall et al., 2015) or combined with vision restauration strategies, e.g. VRT with dtCS (Alber et al., 2017; Plow et al., 2011), that could target in different ways the global workspace. However, let's keep in mind that prior to using any kind

of neurostimulation it would be essential to use an efficient visual training that could facilitate rehabilitation at home.

Conclusion

The problematic is to know how visual therapies can target residual visual abilities when neurophysiological correlates are so divergent between patients. Can we really use what we know of blindsight to develop rehabilitation tools? Our review explains how combined rehabilitation tools using visual training can enhance blindsight by targeting an inefficient global framework. Blindsight, defined as an unconscious residual visual ability, can come with or without awareness, but except in rare cases, doesn't elicit visual awareness (Balsdon and Azzopardi, 2014). The reason why some patients may not present residual vision or awareness could include an inability to allocate sufficient attention to the information presented in the blind hemifield and to access their own state of consciousness. By understanding blindsight within the global workspace theory (Sergent and Dehaene, 2004b), we can define the lack of visual awareness as a lack of neuronal synchrony and global availability between inefficient workspaces of attention, perception and consciousness that we can target and optimize with rehabilitation tools. Therefore, it would be possible to pass from a state of no awareness (type I blindsight) to a state of awareness (type II blindsight) to a state of visual awareness (alternative visual abilities) by moving the thresholds of attention, perception and consciousness via stimulation of the colliculo and geniculo-extrastriate pathways and creating connections between different processors. By doing so, we could target higher visual areas as V5/MT, induce loops with higher cognitive areas, synchronization of neuronal activity and global availability, and potentially it would lead to visual consciousness. These mechanisms can be targeted optimally in the subacute phase, using interhemispheric stimulations, Audio-Visual Scanning Training and combined restitution strategies, where several processes are enhanced at the same time inducing learning transfer and promoting the brain reorganization. The establishment of new guidelines in rehabilitation tools targeting the global framework of blindsight can lead to clinical intervention tools applicable to the majority of CB patients.

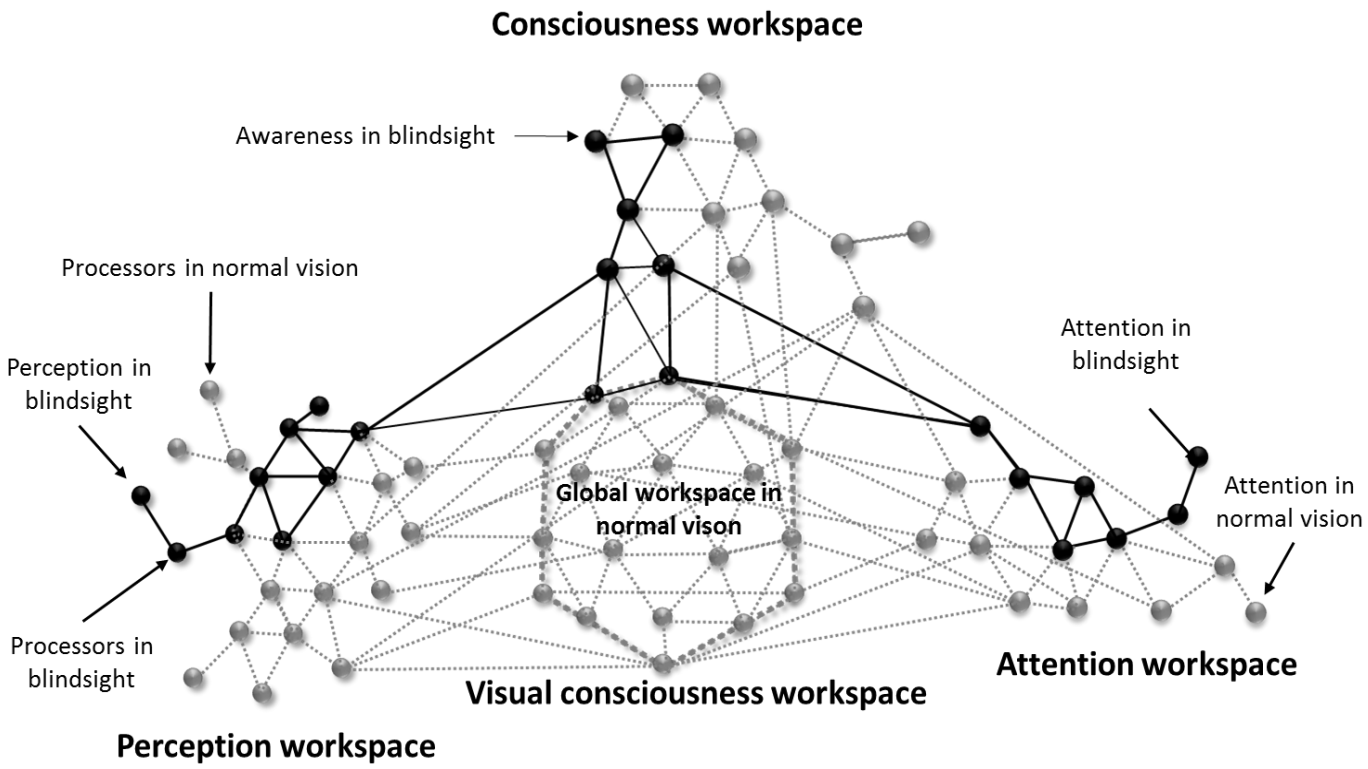

Figure 1. – An illustrative schematic of the proposed model for unsynchronized framework for blindsight

An illustrative schematic of the proposed model for unsynchronized framework for blindsight (inspired from S Dehaene, Kerszberg, & Changeux, 1998). The grey circles represent neuronal processors that are activated in normal vision and the grey lines their respective connections. The black circles illustrate the neuronal processors that underlie blindsight and the black lines their respective connections. Blindsight can be understood as an alteration in the perception and attentional systems, therefore inactivating the long-range workspace connectivity, global availability and conscious visual perception. The lack of visual awareness is due to a non-efficient global workspace. Awareness found in blindsight type II, could be linked to some long-range connectivity between the perception, attention and consciousness workspaces without activating the global workspace. – Figure 1

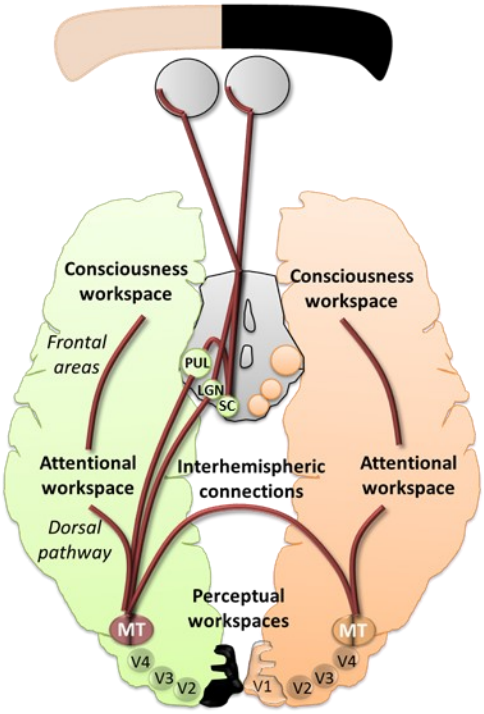

Figure 2. – An illustrative schematic of the proposed hypothesis of the pathways involved in blindsight within the model of global workspace.

An illustrative schematic of the proposed hypothesis of the pathways involved in blindsight within the model of global workspace. In peach and green are represented the normal and lesioned hemispheres and subcortical areas projecting towards their respective hemispheres. The brown lines represent feedforward and feedback projections between workspaces. Enhancing the projections from the superior colliculus (SC)/pulvinar and the Lateral Geniculate Nucleus (LGN) to V5/MT and interhemispheric connections between V5/MT could allow synchronisation between different areas, including the extrastriate regions, the dorsal pathways and the frontal areas, thus leading to more efficient interactions between lower and higher visual areas resulting in long-distance reciprocal connections and cascading amplification in the conscious workspace. – Figure 2

References

Fendrich, R., Wessinger, C.M., and Gazzaniga, M.S. (2001). Speculations on the neural basis of islands of blindsight. Prog. Brain Res. 134, 353–366.

Ffytche, D.H., and Zeki, S. (2011). The primary visual cortex, and feedback to it, are not necessary for conscious vision. Brain 134, 247–257.

Gall, C., Silvennoinen, K., Granata, G., de Rossi, F., Vecchio, F., Brösel, D., Bola, M., Sailer, M., Waleszczyk, W.J., Rossini, P.M., et al. (2015). Non-invasive electric current stimulation for restoration of vision after unilateral occipital stroke. Contemp. Clin. Trials 43, 231–236.

de Gelder, B., Vroomen, J., Pourtois, G., and Weiskrantz, L. (1999). Non-conscious recognition of affect in the absence of striate cortex. Neuroreport 10, 3759–3763.

Georgy, L., Celeghin, A., Marzi, C.A., Tamietto, M., and Ptito, A. (2016). The superior colliculus is sensitive to gestalt-like stimulus configuration in hemispherectomy patients. Cortex. 81, 151–161.

Gingras, G., Rowland, B.A., and Stein, B.E. (2009). The differing impact of multisensory and unisensory integration on behavior. J. Neurosci. 29, 4897–4902.

Goodwin, D. (2014). Homonymous hemianopia: Challenges and solutions. Clin. Ophthalmol. 8, 1919–1927.

Grasso, P.A., Làdavas, E., and Bertini, C. (2016). Compensatory Recovery after Multisensory Stimulation in Hemianopic Patients: Behavioral and Neurophysiological Components. Front. Syst. Neurosci. 10, 45.

Gratton, C., Yousef, S., Aarts, E., Wallace, D.L., D'Esposito, M., and Silver, M.A. (2017). Cholinergic, But Not Dopaminergic or Noradrenergic, Enhancement Sharpens Visual Spatial Perception in Humans. J. Neurosci. 37, 4405–4415.

Harting, J.K., Huerta, M.F., Hashikawa, T., and van Lieshout, D.P. (1991). Projection of the mammalian superior colliculus upon the dorsal lateral geniculate nucleus: organization of tectogeniculate pathways in nineteen species. J. Comp. Neurol. 304, 275–306.

Horton, J.C. (2005a). Disappointing results from Nova Vision's visual restoration therapy. Br. J. Ophthalmol. 89, 1–2.

Horton, J.C. (2005b). Vision restoration therapy: confounded by eye movements. Br. J. Ophthalmol. 89, 792–794.

Huxlin, K.R. (2008). Perceptual plasticity in damaged adult visual systems. Vision Res. 48, 2154–2166.

Huxlin, K.R., Martin, T., Kelly, K., Riley, M., Friedman, D.I., Burgin, W.S., and Hayhoe, M. (2009). Perceptual relearning of complex visual motion after V1 damage in humans. J. Neurosci. 29, 3981–3991.

Kanemoto, K. (2004). [What is impaired consciousness? Revisiting impaired consciousness as psychiatric concept]. Seishin Shinkeigaku Zasshi 106, 1083–1109.

Kasten, E., Bunzenthal, U., and Sabel, B.A. (2006). Visual field recovery after vision restoration therapy (VRT) is independent of eye movements: An eye tracker study. Behav. Brain Res. 175, 18–26.

Kavcic, V., Triplett, R.L., Das, A., Martin, T., and Huxlin, K.R. (2015). Role of inter-hemispheric transfer in generating visual evoked potentials in V1-damaged brain hemispheres. Neuropsychologia 68, 82–93.

Keller, I., and Lefin-Rank, G. (2010). Improvement of visual search after audiovisual exploration training in hemianopic patients. Neurorehabil. Neural Repair 24, 666–673.

Kentridge, R.W., Heywood, C.A., and Weiskrantz, L. (1999). Effects of temporal cueing on residual visual discrimination in blindsight. Neuropsychologia 37, 479–483.

Kentridge, R.W., Heywood, C.A., and Weiskrantz, L. (2004). Spatial attention speeds discrimination without awareness in blindsight. Neuropsychologia 42, 831–835.

Kentridge, R.W., Heywood, C.A., and Weiskrantz, L. (2007). Color contrast processing in human striate cortex. Proc. Natl. Acad. Sci. U. S. A. 104, 15129–15131.

Kerkhoff, G., Münßinger, U., Haaf, E., Eberle-Strauss, G., and Stögerer, E. (1992). Rehabilitation of homonymous scotomata in patients with postgeniculate damage of the visual system: saccadic compensation training. Restor. Neurol. Neurosci. 4, 245–254.

Ko, Y., and Lau, H. (2012). A detection theoretic explanation of blindsight suggests a link between conscious perception and metacognition. Philos. Trans. R. Soc. Lond. B. Biol. Sci. 367, 1401–1411.

Kranczioch, C., Debener, S., Maye, A., and Engel, A.K. (2007). Temporal dynamics of access to consciousness in the attentional blink. Neuroimage 37, 947–955.

Lau, H.C., and Passingham, R.E. (2006). Relative blindsight in normal observers and the neural correlate of visual consciousness. Proc. Natl. Acad. Sci. U. S. A. 103, 18763–18768.

Leh, S.E., Johansen-Berg, H., and Ptito, A. (2006). Unconscious vision: new insights into the neuronal correlate of blindsight using diffusion tractography. Brain 129, 1822–1832.

Leh, S.E., Ptito, A., Schönwiesner, M., Chakravarty, M.M., and Mullen, K.T. (2010). Blindsight mediated by an S-cone-independent collicular pathway: an fMRI study in hemispherectomized subjects. J. Cogn. Neurosci. 22, 670–682.

Leo, F., Bolognini, N., Passamonti, C., Stein, B.E., and Làdavas, E. (2008). Cross-modal localization in hemianopia: new insights on multisensory integration. Brain 131, 855–865.

Leopold, D.A. (2012). Primary visual cortex: awareness and blindsight. Annu. Rev. Neurosci. 35, 91–109.

Lyon, D.C., Nassi, J.J., and Callaway, E.M. (2010). A disynaptic relay from superior colliculus to dorsal stream visual cortex in macaque monkey. Neuron 65, 270–279.

Maior, R.S., Hori, E., Tomaz, C., Ono, T., and Nishijo, H. (2010). The monkey pulvinar neurons differentially respond to emotional expressions of human faces. Behav. Brain Res. 215, 129–135.

Matteo, B.M., Viganò, B., Cerri, C.G., and Perin, C. (2016). Visual field restorative rehabilitation after brain injury. J. Vis. 16, 11.

Mazzi, C., Bagattini, C., and Savazzi, S. (2016). Blind-Sight vs. Degraded-Sight: Different Measures Tell a Different Story. Front. Psychol. 7, 901.

Melloni, L., Molina, C., Pena, M., Torres, D., Singer, W., and Rodriguez, E. (2007). Synchronization of neural activity across cortical areas correlates with conscious perception. J. Neurosci. 27, 2858–2865.

Melnick, M.D., Tadin, D., and Huxlin, K.R. (2016). Relearning to See in Cortical Blindness. Neurosci. 22, 199–212.

Min, B.-K. (2010). A thalamic reticular networking model of consciousness. Theor. Biol. Med. Model. 7, 10.

Morland, A.B., Jones, S.R., Finlay, A.L., Deyzac, E., Lê, S., and Kemp, S. (1999). Visual perception of motion, luminance and colour in a human hemianope. Brain 122 (Pt 6, 1183–1198.

Morland, A.B., Lê, S., Carroll, E., Hoffmann, M.B., and Pambakian, A. (2004). The role of spared calcarine cortex and lateral occipital cortex in the responses of human hemianopes to visual motion. J. Cogn. Neurosci. 16, 204–218.

Morris, J.S., DeGelder, B., Weiskrantz, L., and Dolan, R.J. (2001). Differential extrageniculostriate and amygdala responses to presentation of emotional faces in a cortically blind field. Brain 124, 1241–1252.

Nijboer, T., van de Port, I., Schepers, V., Post, M., and Visser-Meily, A. (2013). Predicting functional outcome after stroke: the influence of neglect on basic activities in daily living. Front. Hum. Neurosci. 7, 182.

Overgaard, M., and Grünbaum, T. (2011). Consciousness and modality: on the possible preserved visual consciousness in blindsight subjects. Conscious. Cogn. 20, 1855–1859.

Overgaard, M., Fehl, K., Mouridsen, K., Bergholt, B., and Cleeremans, A. (2008). Seeing without Seeing? Degraded Conscious Vision in a Blindsight Patient. PLoS One 3, e3028.

Paraskevopoulos, E., Kuchenbuch, A., Herholz, S.C., and Pantev, C. (2012). Evidence for training-induced plasticity in multisensory brain structures: an MEG study. PLoS One 7, e36534.

Passamonti, C., Bertini, C., and Làdavas, E. (2009). Audio-visual stimulation improves oculomotor patterns in patients with hemianopia. Neuropsychologia 47, 546–555.

Patel, A.T., Duncan, P.W., Lai, S.-M., and Studenski, S. (2000). The relation between impairments and functional outcomes poststroke. Arch. Phys. Med. Rehabil. 81, 1357–1363.

Pavan, A., Alexander, I., Campana, G., and Cowey, A. (2011). Detection of first- and second-order coherent motion in blindsight. Exp. Brain Res. 214, 261–271.

Perez, C., and Chokron, S. (2014). Rehabilitation of homonymous hemianopia: insight into blindsight. Front. Integr. Neurosci. 8, 82.

Persaud, N., and Cowey, A. (2008). Blindsight is unlike normal conscious vision: evidence from an exclusion task. Conscious. Cogn. 17, 1050–1055.

Persaud, N., Davidson, M., Maniscalco, B., Mobbs, D., Passingham, R.E., Cowey, A., and Lau, H. (2011). Awareness-related activity in prefrontal and parietal cortices in blindsight reflects more than superior visual performance. Neuroimage 58, 605–611.

Peters, M.A.K., and Lau, H. (2015). Human observers have optimal introspective access to perceptual processes even for visually masked stimuli. Elife 4, e09651.

Plow, E.B., Obretenova, S.N., Halko, M.A., Kenkel, S., Jackson, M. Lou, Pascual-Leone, A., and Merabet, L.B. (2011). Combining visual rehabilitative training and noninvasive brain stimulation to enhance visual function in patients with hemianopia: a comparative case study. PM R 3, 825–835.

Pollock, A., Hazelton, C., Henderson, C.A., Angilley, J., Dhillon, B., Langhorne, P., Livingstone, K., Munro, F.A., Orr, H., Rowe, F.J., et al. (2011). Interventions for visual field defects in patients with stroke. Cochrane Database Syst. Rev. CD008388.

Pouget, M.-C., Lévy-Bencheton, D., Prost, M., Tilikete, C., Husain, M., and Jacquin-Courtois, S. (2012). Acquired visual field defects rehabilitation: critical review and perspectives. Ann. Phys. Rehabil. Med. 55, 53–74.

Riddoch, G. (1917). On the Relative Perceptions of Movement and a Stationary Object in Certain Visual Disturbances due to Occipital Injuries. Proc. R. Soc. Med. 10, 13–34.

Riggs, R. V, Andrews, K., Roberts, P., and Gilewski, M. (2007). Visual deficit interventions in adult stroke and brain injury: a systematic review. Am. J. Phys. Med. Rehabil. 86, 853–860.

Romei, V., Chiappini, E., Hibbard, P.B., and Avenanti, A. (2016). Empowering Reentrant Projections from V5 to V1 Boosts Sensitivity to Motion. Curr. Biol. 26, 2155–2160.

Roth, T., Sokolov, A.N., Messias, A., Roth, P., Weller, M., and Trauzettel-Klosinski, S. (2009). Comparing explorative saccade and flicker training in hemianopia: A randomized controlled study. Neurology 72, 324–331.

Sabel, B.A., Kenkel, S., and Kasten, E. (2005). Vision restoration therapy. Br. J. Ophthalmol. 89, 522–524.

Sahraie, A., Trevethan, C.T., MacLeod, M.J., Murray, A.D., Olson, J.A., and Weiskrantz, L. (2006). Increased sensitivity after repeated stimulation of residual spatial channels in blindsight. Proc. Natl. Acad. Sci. U. S. A. 103, 14971–14976.

Sahraie, A., Macleod, M.-J., Trevethan, C.T., Robson, S.E., Olson, J.A., Callaghan, P., and Yip, B. (2010). Improved detection following Neuro-Eye Therapy in patients with post-geniculate brain damage. Exp. Brain Res. 206, 25–34.

Sahraie, A., Trevethan, C.T., Macleod, M.-J., Weiskrantz, L., and Hunt, A.R. (2013). The continuum of detection and awareness of visual stimuli within the blindfield: from blindsight to the sighted-sight. Invest. Ophthalmol. Vis. Sci. 54, 3579–3585.

Schmid, M.C., Mrowka, S.W., Turchi, J., Saunders, R.C., Wilke, M., Peters, A.J., Ye, F.Q., and Leopold, D.A. (2010). Blindsight depends on the lateral geniculate nucleus. Nature 466, 373–377.

Schurger, A., Cowey, A., Cohen, J.D., Treisman, A., and Tallon-Baudry, C. (2008). Distinct and independent correlates of attention and awareness in a hemianopic patient. Neuropsychologia 46, 2189–2197.

Sergent, C., and Dehaene, S. (2004a). Is consciousness a gradual phenomenon? Evidence for an all-or-none bifurcation during the attentional blink. Psychol. Sci. 15, 720–728.

Sergent, C., and Dehaene, S. (2004b). Neural processes underlying conscious perception: experimental findings and a global neuronal workspace framework. J. Physiol. Paris 98, 374–384.

Silvanto, J. (2015). Why is "blindsight" blind? A new perspective on primary visual cortex, recurrent activity and visual awareness. Conscious. Cogn. 32, 15–32.

Silvanto, J., Cowey, A., Lavie, N., and Walsh, V. (2007). Making the blindsighted see. Neuropsychologia 45, 3346–3350.

Silvanto, J., Walsh, V., and Cowey, A. (2009). Abnormal functional connectivity between ipsilesional V5/MT+ and contralesional striate cortex (V1) in blindsight. Exp. Brain Res. 193, 645–650.

Sincich, L.C., Park, K.F., Wohlgemuth, M.J., and Horton, J.C. (2004). Bypassing V1: a direct geniculate input to area MT. Nat. Neurosci. 7, 1123–1128.

Smythies, J. (1999). Consciousness: some basic issues--A neurophilosophical perspective. Conscious. Cogn. 8, 164–172.

Stein, B.E., and Rowland, B.A. (2011). Organization and plasticity in multisensory integration: early and late experience affects its governing principles. Prog. Brain Res. 191, 145–163.

Swienton, D.J., and Thomas, A.G. (2014). The visual pathway--functional anatomy and pathology. Semin. Ultrasound. CT. MR 35, 487–503.

Tamietto, M., and de Gelder, B. (2010). Neural bases of the non-conscious perception of emotional signals. Nat. Rev. Neurosci. 11, 697–709.

Tamietto, M., and Morrone, M.C. (2016). Visual Plasticity: Blindsight Bridges Anatomy and Function in the Visual System. Curr. Biol. 26, R70-3.

Tamietto, M., Castelli, L., Vighetti, S., Perozzo, P., Geminiani, G., Weiskrantz, L., and de Gelder, B. (2009). Unseen facial and bodily expressions trigger fast emotional reactions. Proc. Natl. Acad. Sci. U. S. A. 106, 17661–17666.

Tamietto, M., Cauda, F., Corazzini, L.L., Savazzi, S., Marzi, C.A., Goebel, R., Weiskrantz, L., and de Gelder, B. (2010). Collicular vision guides nonconscious behavior. J. Cogn. Neurosci. 22, 888–902.

Tamietto, M., Pullens, P., de Gelder, B., Weiskrantz, L., and Goebel, R. (2012). Subcortical connections to human amygdala and changes following destruction of the visual cortex. Curr. Biol. 22, 1449–1455.

Trevethan, C.T., Sahraie, A., and Weiskrantz, L. (2007). Can blindsight be superior to "sighted-sight"? Cognition 103, 491–501.

Trevethan, C.T., Urquhart, J., Ward, R., Gentleman, D., and Sahraie, A. (2012). Evidence for perceptual learning with repeated stimulation after partial and total cortical blindness. Adv. Cogn. Psychol. 8, 29–37.

Urbanski, M., Coubard, O.A., and Bourlon, C. (2014). Visualizing the blind brain: brain imaging of visual field defects from early recovery to rehabilitation techniques. Front. Integr. Neurosci. 8, 74.

Villeneuve, M.Y., Kupers, R., Gjedde, A., Ptito, M., and Casanova, C. (2005). Pattern-motion selectivity in the human pulvinar. Neuroimage 28, 474–480.

Warner, C.E., Goldshmit, Y., and Bourne, J.A. (2010). Retinal afferents synapse with relay cells targeting the middle temporal area in the pulvinar and lateral geniculate nuclei. Front. Neuroanat. 4, 8.

Weiskrantz, L. (1986). Blindsight : A Case Study and Implications: A Case Study and Implications (Clarendon Press).

Weiskrantz, L. (1987). Residual vision in a scotoma. A follow-up study of "form" discrimination. Brain 110 (Pt 1, 77–92.

Weiskrantz, L. (2009). Is blindsight just degraded normal vision? Exp. Brain Res. 192, 413–416.

Weiskrantz, L., Warrington, E.K., Sanders, M.D., and Marshall, J. (1974). Visual capacity in the hemianopic field following a restricted occipital ablation. Brain 97, 709–728.

Writing Group Members, Mozaffarian, D., Benjamin, E.J., Go, A.S., Arnett, D.K., Blaha, M.J., Cushman, M., Das, S.R., de Ferranti, S., Després, J.-P., et al. (2016). Heart Disease and Stroke Statistics-2016 Update: A Report From the American Heart Association. Circulation 133, e38-360.

Yoshida, M., Itti, L., Berg, D.J., Ikeda, T., Kato, R., Takaura, K., White, B.J., Munoz, D.P., and Isa, T. (2012). Residual attention guidance in blindsight monkeys watching complex natural scenes. Curr. Biol. 22, 1429–1434.

Zeman, A. (2004). Theories of visual awareness. Prog. Brain Res. 144, 321–329.

Zhang, X., Kedar, S., Lynn, M.J., Newman, N.J., and Biousse, V. (2006). Homonymous hemianopia in stroke. J. Neuroophthalmol. 26, 180–183.

Chapter 4

Article 2: High Gamma Oscillations Guide Subcortical Connectivity in Affective Conscious and Unconscious Perception

Article 2. High Gamma Oscillations Guide Subcortical Connectivity in Affective Conscious and Unconscious Perception

Vanessa Hadid[1,3,8], Annalisa Pascarella[3,4,6], Tarek Lajnef[3,6], Sophie Vinet[2], Dang Khoa Nguyen[5], Franco Lepore[2,7], Karim Jerbi[2,3,7]

1Département de Sciences Biomédicales, Université de Montréal,
2Département de Psychologie, Université de Montréal
3Computational and Cognitive Neuroscience Lab (CoCo Lab)
4Italian National Research Council, Rome, Italy
5Service de neurologie, Centre Hospitalier de l'Université de Montréal
6Co-second author
7Co-last author
8Lead contact

Abstract

Gamma rhythms have been hypothesized to guide subcortical communication that bypasses the primary visual cortex (V1) in unconscious perception. However, evidence that such functional connectivity can explain affective unconscious human behavior is needed. Here, we recorded, using magnetoencephalography, the neurophysiological activity of a patient with left homonymous hemianopia following epilepsy surgery of the right V1. He had a unique form of affective-blindsight revealed by his ability to unconsciously discriminate between affective natural scenes presented to his left blind hemifield. Our results showed that fast thalamo-amygdala and thalamo-extra-striate pathways guided through high gamma oscillations (HFOs: 90–120 Hz) could support SJ's blindsight abilities. Moreover, we found that affective specific differences were coded by the direction of connectivity between the thalamus and amygdala for both seen and unseen pictures. The role of subcortical gamma connectivity was furthermore emphasized as they were predictive of SJ's reaction times. In conclusion, this study establishes the role of causal functional subcortical communications guided by high-frequency oscillations in patient SJ with unique unconscious abilities for affective natural complex scenes.

Introduction

A unique opportunity to probe unconscious neural correlates is to study individuals with acquired homonymous hemianopia (HH) subsequent to a V1-lesion who are able to unconsciously process visual stimuli despite being cortically blind in one hemifield (Goodwin, 2014; Hadid and Lepore, 2017; LeDoux et al., 2020). This phenomenon tokened as blindsight (Weiskrantz, 2004; Weiskrantz et al., 1995) can also be revealed using emotional stimuli and is known as affective blindsight (de Gelder et al., 1999; Heywood and Kentridge, 2000). These unconscious abilities have been shown to be mediated by subcortical-extrastriate pathways (Danckert and Rossetti, 2005; Leopold, 2012; Tran et al., 2019; Urbanski et al., 2014) and by connectivity between the thalamus and amygdala (Ajina et al., 2020; Bertini et al., 2018; Morris et al., 1999, 2001; Tamietto et al., 2012). However, the spectral and temporal features that guide these communications have yet to be characterized in unconscious processing. In other words, how do thalamic pathways that bypass the primary visual cortex (V1) support affective unconscious processing?

Nonetheless, in electrophysiological studies where participants were perceptually aware of the stimuli, results show very early gamma (>30Hz) synchronization in the thalamus (10-20 ms) and amygdala (20-30 ms) in response to fearful stimuli prior to activity in the visual cortex (Luo et al., 2007) with attentional load affecting the activity of the amygdala only at longer latencies (Luo et al., 2010). Negative emotional processing has also been found to induce early gamma connectivity from the thalamus to the right amygdala (Liu et al., 2015). Thus, the dominant view postulates the involvement of a human functional fast thalamo-amygdala pathway that bypasses the striate cortex (Fox et al., 2020; LeDoux, 2000; McFadyen et al., 2020). Some studies suggest that this pathway is specific to threatening-fearful-unpleasant pictures (Bayle et al., 2009; Dumas et al., 2013; Hung et al., 2010; Koller et al., 2019; McFadyen et al., 2019; Méndez-Bértolo et al., 2016; Rigoulot et al., 2011; Ward et al., 2005), while others show that it is irrespective of a specific emotion (Garrido et al., 2012; McFadyen et al., 2017). The advantage found for negative stimuli could have been influenced by the psychophysical properties mainly used to discriminate between emotional faces (Kokinous et al., 2017; Prete et al., 2016; Rohr and Wentura, 2014). In affective-blindsight, behavioral demonstrations have also found an advantage for fearful faces (Bertini et al., 2013, 2019), though electrophysiological studies showed activation in the amygdala that is not restricted to negative emotions (Andino et al., 2009; Pegna et al., 2005). Therefore, the behavioral

bias found towards negative stimuli may be due to saliency rather than affective-specific differences (Garrido, 2012) or psychophysical differences between fearful-angry and happy faces which stimulate the magnocellular pathway involved in blindsight and the parvocellular pathway altered in blindsight, respectively (Burra et al., 2019; Mu and Crewther, 2020). To bypass this issue, unpleasant and pleasant natural complex scenes instead of emotional faces known to also stimulate the limbic system (Colibazzi et al., 2010; D'Hondt et al., 2013; Frank and Sabatinelli, 2014) can be used to investigate the spectral dynamics and directed connectivity within the subcortical affective pathway in blindsight patients to address the pathways of unconsciousness.

Thus, the purpose of this investigation was to demonstrate that gamma rhythms guide fast communication within subcortical routes in order to process unseen positive and negative affective natural scenes. In fact, gamma oscillations have been shown to exert multiple roles in visual cognition (Tallon-Baudry, 2009), visual (un)consciousness (Mashour et al., 2020), and affective processing (Headley and Pare, 2013). Though no report of patients able to discriminate between affective scenes has been yet described in the literature, we had the chance to test a patient (SJ) suffering from a left HH who exhibited a unique form of affective-blindsight for complex natural scenes. Hence, to understand how and when the thalamus communicates with the amygdala and other regions in the absence of visual awareness, we applied new standards in electrophysiology (Meunier et al., 2020). In fact, we combined magnetoencephalography (MEG) and source reconstruction, and Granger causality (GC) to assess the gamma connectivity in the thalamo-striate (within the intact hemisphere) and thalamo-amygdala pathways focusing the analysis on the connectome formed by both thalami, amygdalae and the left intact V1. An exploratory GC analysis was also performed to assess any other thalamocortical pathways involved in unconscious processing.

Experimental Procedures

Case study

SJ was 22 years old at the time of this study. He developed epilepsy at the age of 10 years. Seizures were characterized by luminous phosphenes in the left visual hemifield followed by nausea, a feeling of déjà vu, impaired awareness, panting, and occasionally, bilateral tonic-clonic movements. A comprehensive non-invasive presurgical evaluation followed by an invasive intracranial EEG study identified right occipital epilepsy (superior occipital gyrus, cuneus, lingual

gyrus. A first limited resection (hoping to spare his vision) was performed at age 15 years without success; a more extensive resection was then performed at age 16 years which led to seizure-freedom but resulted in a left HH with no macular sparing.

SJ demonstrated unconscious abilities to discriminate between unseen natural scenes with performance above chance-level and reaction times (RTs) modulated by non-specific to affective conditions (i.e. performance and eccentricity) and by affective specific conditions (i.e. affective valence). Thus, SJ presented preserved blindsight Type I abilities (Sahraie et al., 2010), i.e. behavior modulated by the presentation of stimuli with no conscious visual awareness in his left blind hemifield, as well as affective-blindsight, i.e. specific to the affective condition. To our knowledge, SJ is the first reported patient with such capability which allowed us to use an experimental paradigm that exploits natural scenes instead of faces that are less prone to psychophysical bias as mentioned previously. Therefore, the complete resection of V1 and SJ's neurological condition provides a unique opportunity to study the neurophysiological correlates of unconscious processing specific and non-specific to affective stimuli that bypass V1.

Procedure

Experimental design

A 3-alternative forced-choice affective discrimination paradigm was assessed during the scanning session. We presented 300 pictures of unpleasant, neutral, and pleasant natural scenes selected from the International Affective Picture System (IAPS) for which we controlled for arousal and salience as described in (D'Hondt et al., 2013). The pictures of size 9 x 12° were randomly projected on a screen to the intact right visual field (RVF) or the blind left visual field (LVF) for 1000 ms (150 stimuli per hemifield). On the center of the screen, a fixation cross was visible at all times. Stimuli were presented briefly either within the paracentral or near peripheral visual regions, i.e. at 6° or 12° of eccentricity from the fixation cross, respectively, to assess any differences in central and peripheral perception, known to stimulate the parvocellular and magnocellular pathway (Baizer et al., 1991; Dacey and Petersen, 1992).

Simultaneous to the picture presentation, a white noise of 100 ms presented to both ears using earphones signaled that a response was needed as fast as possible. After the picture presentation, an inter-stimulus interval (ISI) varied randomly between 2000 and 2500 ms (Figure

1). Fixation of the cross was required at all times and trials with ocular movements (>1°) to the left or right were identified automatically from the electrooculogram (EOG) and then removed (17/300 removed trials). Involuntary microsaccades were not removed due to the difficulty to inhibit them when presenting a salient stimulus at the border of each hemifield, notably for the seen paracentral condition. These microsaccades did not influence the performance in the blind hemifield, i.e. did not help in discriminating between affective conditions, considering the size of the stimulus and the absence of macular sparing in SJ. This is corroborated by the fact that unseen paracentral pictures were not more discriminable than the unseen near periphery pictures which right edge, i.e. nearest to the cross, was presented at 6° of eccentricity (performance for unseen paracentral = 41% and for unseen near periphery = 46%). However, subsequent interpretations of power results account for the presence of microsaccades (Yuval-Greenberg et al., 2008).

SJ was instructed to orient his attention to both hemifields pre-stimulus considering that the timing and location of the stimulus were unpredictable. This type of paradigm using reflexive attentional processes limits top-down modulation prior to stimulus presentation and rapidly triggers the magnocellular pathway for fast reorienting (Chica et al., 2013; Corbetta and Shulman, 2002; Corbetta et al., 2008; LeDoux, 2000; Ries and Hopfinger, 2011). In fact, SJ knew where to orient his attention post-stimulus, i.e. if after the noise the stimulus was seen, he oriented his visuospatial attention to the right hemifield and if not, he oriented his attention to his left hemifield. Thus, when a visual stimulus was presented to the blind hemifield, SJ had to guess the 'correct' answer even if it was not perceived. The experiment was designed to perform statistical analysis between four main comparisons: between (1) hemifields, (2) eccentricities, (3) performances, and (4) affective conditions across all trials. Trials were categorized into (1) seen and unseen, i.e. right intact hemifield and left blind hemifield, respectively, (2) paracentral and near periphery, i.e. 6° and 12° of eccentricity for seen and unseen pictures, respectively, (3) correct and incorrect responses for seen and unseen pictures and (3) unpleasant, neutral, and pleasant pictures for seen and unseen pictures. This paradigm was adapted from (D'Hondt et al., 2013).

MEG data acquisition

MEG data were acquired during the affective discrimination task using a 275-channel whole-head MEG system (CTF MEG Int, British Columbia, Canada). Continuous data were recorded with a sampling rate of 1200 Hz, an antialiasing filter with a 600 Hz cut-off, and third-order spatial

gradient noise cancellation. Horizontal and vertical electrooculograms and an electrocardiogram were acquired with bipolar montages. The head position inside the MEG sensor helmet was determined with coils positioned at the nasion and the preauricular points (fiducial points). For anatomical registration with the anatomical MRI data, the spatial positions of the fiducial coils and of about 300 scalp points were obtained using a 3D digitizer system (Polhemus Isotrack, Polhemus, Colchester, VT, USA). Participants were seated in an upright position in a sound-attenuated, magnetically shielded recording room.

Behavioral analyses

Performance

The number of correct answers was calculated for each affective condition and seen and unseen stimuli presented in the intact and blind hemifield, respectively. A trial was considered correct if the provided response matched the expected valence of a specific natural scene (unpleasant, neutral, and pleasant) (Figure 2). To assess the statistical significance of correct responses for stimuli presented in each hemifield, we conducted a Chi-square (X2) test comparing the number of correct responses to a 33.33% chance level (since three response options were available).

Reaction times (RTs) analysis

Single-trial RTs were estimated as the time taken to press the button and categorize the stimulation into an unpleasant, neutral, or pleasant picture. RTs were compared by grouping them into our four main comparisons (Figure 2). Consequently, a factorial ANOVA between trials was conducted to compare the main effects of the four independent variables on the RTs: hemifield (2 levels), eccentricity (2 levels), performance (2 levels), affective valence (3 levels), as well as the interaction effect between them. Levene's test indicated that the assumption of normality had not been violated ($F = 1.50$, $p =. 292$). A Bonferroni post hoc test was performed to assess differences between affective conditions. The F-ratio (F), p-value (p), and effect size (r) are reported in the results. Effect sizes around 0.01, 0.06, and 0.14 were respectively considered small, moderate, and large effects. These results were obtained using IBM SPSS Statistics.

MEG preprocessing and source reconstruction

MEG data preprocessing and source construction were conducted using standard pipelines implemented in the open-source NeuroPycon toolbox (Meunier et al., 2020), and tools from MNE python (Gramfort et al., 2013). The data were filtered offline using a finite impulse response filtering (FIR1, order = 3) between 0.1 Hz and 600 Hz and a notch filter at the power frequency (60 Hz) to eliminate line noise artifacts. Eye and heart-related artifacts were identified from the data using independent components analysis and visual inspection. Independent components related to eye blinks, lateral eye movements, and cardiac activity were removed from the dataset. Accordingly, 5.66% of the trials (17/300 trials) were rejected from further analysis. A trial consisted of a baseline period of 200 ms pre-stimulus (-200 to 0 ms) and 800 ms post-stimulus (0 to 800 ms), for a total duration of 1000 ms. The subsequent inverse method was applied to the 283 trials.

Cortical and subcortical parcellation and structural segmentation of the patient's T1-weighted MRI images were automatically obtained using Freesurfer (Fischl et al., 2002). Structural coregistration to the data segmentation was performed by means of the digitized head points and used for the lead field matrix. The anatomical mixed source space resulted in 7328 cortical and subcortical nodes for both hemispheres, including 7279 nodes for the cortical surface (4098 nodes in the left intact hemisphere and 3181 nodes in the right lesioned hemisphere) and 149 nodes for the subcortical structures, i.e. deep regions modeled as volume source spaces, (both thalami and the amygdalae with 123 and 26 nodes, respectively).

Source reconstruction was estimated across all trials and performed using the inverse pipeline implemented in NeuroPycon (Meunier et al., 2020). First, the lead field matrix was computed by using the Boundary Element Method (BEM) from the MNE-python package (Gramfort et al., 2013). The extracted BEM surfaces were inspected to ensure adequate quality of structural segmentation, more specifically around the lesion. Moreover, the noise covariance matrix was assessed from a 5-minute-empty-room-recording. Lastly, we selected the weighted Minimum Norm Estimate (wMNE) (Hämäläinen and Ilmoniemi, 1994) available in the MNE-python package (Gramfort et al., 2013) to solve the inverse problem. Consequently, for cortical nodes, the dipole orientation was constrained to be normal to the cortical surface. However, to assess the activity in deep structures, 3 dipoles with free orientation were computed for each

subcortical node (Meunier et al., 2020). Hence, the subsequent source reconstruction matrix contained the estimated time series of all mixed source space dipoles for every epoch (7328 nodes * 1200 time points * 283 epochs) providing fine spatio-temporal event-related precision.

Subsequent MEG analyses were performed on nodes that were identified using the Destrieux atlas (Fischl et al., 2004) as part of five specific regions on interest (ROIs), i.e. the left calcarine sulcus with 58 nodes (referred to as the intact V1), the left thalamus averaged across 67 nodes, the right thalamus averaged across 56 nodes, the left amygdala averaged across 11 nodes and the right amygdala averaged across 15 nodes. All MEG analyses and statistical assessments were computed to compare (1) seen against unseen, (2) paracentral against near periphery, i.e. 6° and 12° of eccentricity for seen and unseen pictures, (3) correct against incorrect for seen and unseen pictures and (4) the three contrasts resulting from the comparisons between unpleasant, neutral and pleasant pictures for seen and unseen pictures. The cortical and subcortical MEG activities projected on the brain were visualized using the open-source Visbrain package (Combrisson et al., 2019).

Note that while MEG reconstruction of neuromagnetic activity in subcortical areas was long considered to be questionable, there is now substantial evidence for the feasibility of assessing activity from deep structures with MEG, including the cerebellum (Andersen et al., 2020), the hippocampus (Dalal et al., 2013; Hanlon et al., 2003; Pizzo et al., 2019; Quraan et al., 2011), the amygdala (Balderston et al., 2013; Bayle et al., 2009; Cornwell et al., 2008; Dumas et al., 2013; Luo et al., 2010; Pizzo et al., 2019) and the thalamus (Lithari et al., 2015; Liu et al., 2015; Luo et al., 2007; Roux et al., 2013).

Spectral power analysis

Time-frequency analysis was assessed for frequencies between 7 and 120 Hz and a temporal window ranging between 200 ms pre-stimulus to 800 ms post-stimulus. The relative power signal for each ROI was averaged across nodes and estimated using a Hilbert transform over 50 ms time windows implemented in Brainpipe, a python-based toolbox. Specifically, baseline normalization was applied by subtracting the power value by the baseline average and further dividing this difference by the baseline average, i.e. relative power = (power – baseline average) / baseline average. For oscillations under 50 Hz, a sustained desynchronization after 200 ms and an increase in power before 200 ms were observed. The short period synchronization was most probably

influenced by a P1 peak driven by the trial-by-trial time event-related field (ERF) response which we investigated in another study (Hadid et al. 2021 in preparation). Power for high gamma oscillations (50–120 Hz), which was the focus of this study, showed significant synchronization over time. Thus, we will be referring to the 50–90 Hz range as the high gamma band and the 90–120 Hz range as high-frequency oscillations (HFOs). Therefore, the single-trial power over time was computed for the high gamma band and the HFOs for all nodes. The power was averaged across all nodes within an ROI and cluster-based permutation analysis estimated the significant differences over time between conditions (Figure 3). The single-trial gamma activity over time was used to perform the functional connectivity (FC) measures between ROIs and was averaged over time for the regression analysis.

Directed and undirected single-trial FC analysis between ROIs

Directed FC, and more specifically conditional covariance-based Granger causality (GC) measures, based on single-trial power estimations, is central in studying the temporal causal relation between two regions, X and Y, where X exerts a causal influence on Y, in a specific frequency band. Without making any assumption whatsoever about structural connectivity, we were able to statistically predict how gamma activity in one ROI will be modulated in the future based on the past activity modulation of another ROI, given the cognitive processes involved. This was possible by computing total Granger interdependence, which informs us about the undirected connectivity between ROIs, and the relations between two ROIs' mutual information and conditional entropies using the directed connectivity based on Brovelli et al., paper (Brovelli et al., 2015) implemented in the python toolbox FRamework for Information Theoretical analysis of Electrophysiological data and statistics (Frites). The covariance-based GC measures were assessed among ROI pairs of single-trial gamma activity over time. The time windows duration (T) used for the calculation of the covariance matrices was optimal at 200 times points for seen stimuli and 300 times points for unseen stimuli and the lag was 20 and 30 time points, respectively (i.e., 10 % of T). Due to the difference between the time windows duration used, activity for seen stimuli started at 33 ms pre-stimulus, and activity for seen stimuli started at 50 ms post-stimulus.

Before concluding causality between two ROIs, measures of undirected connectivity were tested. For each pair of ROIs, we first ensured that total Granger interdependence over time was superior to zero and that linear correlation was statistically significant using Pearson's correlation

for each pair of trials, i.e. Th-lh ↔ Am-lh; Th-lh ↔ left V1; Am-lh ↔ V1-lh; Th-rh ↔ Am-rh; Th-rh ↔ left V1; Am-rh ↔ V1-lh. The correlation was compared across conditions for both gamma frequency bands (Figure 4)

Subsequently, directed GC measures were computed for each time point and all combinations of ROI pairs, i.e. Th-lh → Am-lh; Th-lh → left V1; Am-lh → V1-lh; Th-rh → Am-rh; Th-rh → left V1; Am-rh → V1-lh; Th-lh ← Am-lh; Th-lh ← left V1; Am-lh ← V1-lh; Th-rh ← Am-rh; Th-rh ← left V1; Am-rh ← V1-lh. To comprehend the dominant directionality in GC between pairs of ROIs and conditions, we computed the difference of influence (DOI) by assessing the net difference between GC measured from ROI 1 to the ROI 2 and the GC measured from ROI 2 to ROI 1 (Bastin et al., 2017). Significant differences over time between conditions in DOI among ROI pairs were assessed using cluster-based permutation analysis. Linear correlation values and directed GC values averaged across time for all combinations of ROI pairs and conditions were given to the linear regression analysis (Figures 5 and 6). Finally, we estimated the GC DOIs (direction of influence) between each pair of ROIs listed in the Destrieux Atlas until all connectomes were formed which included the thalamus, amygdala, and one cortical area. This additional exploratory analysis allowed us to address all subcortico-cortical connectivity involved in the comparison between our conditions, i.e. seen vs unseen, paracentral vs near periphery, correct vs incorrect, and unpleasant vs neutral vs pleasant (Figure 5).

Linear regression analysis

A linear regression analysis was conducted separately to predict single-trial RTs based on the single-trial gamma activity. In other words, we aimed to assess whether the gamma power and directed and undirected connectivity features were of significant importance in predicting behavior and, if so, contingent on what predictor(s). In the complete regression model, 46 independent continuous variables were given to the model considering that for both gamma bands, we extracted the power values averaged over time for all five ROIs the correlation values averaged over time for all 6 undirected correlations between ROIs, the GC values averaged over time for all 12 directed connectivity measures between ROIs. Moreover, increases in predictive performance, for both regression models, were achieved by fitting three independent categorical variables into the regression model, i.e. eccentricity (paracentral and near periphery), performance (correct and incorrect), and affective conditions (pleasant, neutral, and unpleasant). The F-ratio (F), the

correlation coefficient (R2), and the adjusted correlation coefficient (R2 (adj)) representing the portion of the explained variance were computed to assess the predictive power of the regression model (Figure 7). The significant Pearson coefficients between the independent variable and RTs were presented as well as the significant standardized beta coefficient (β), t-value, p-value and partial correlation which were used to identify each significant predictor and the direction of the effect for the complete regression model (Table 1). The analysis was performed using IBM SPSS Statistics.

Cluster-based permutation over time

Statistical differences between conditions were obtained by computing cluster-based permutation tests over time corrected for multiple comparisons developed in MNE-python (Gramfort et al., 2013). Clusters were first identified based on the temporal adjacency of independent t-tests exceeding an uncorrected p-value of .05. Each cluster was therefore associated with its maximum t-value which was then compared to the largest cluster t-value for each permutation under a null distribution of 1000 permutations using shuffled labels to address the multiple-comparison problem. If the maximum t-value exceeded the maximum cluster-level statistics using a threshold of p-value = .05 corrected for multiple comparisons then we concluded that the corresponding cluster showed significant differences between conditions (Maris and Oostenveld, 2007). Using cluster-based permutation over time, we assessed power and GC DOI differences between conditions over time.

Results

Behavior Is Modulated by Awareness, Performance, Eccentricity, and Affective Conditions

We first aimed to validate the presence of affective-blindsight in SJ's blind hemifield who performed a 3-alternative forced-choice affective discrimination paradigm. To validate unconscious abilities, we reported the performance and RTs in response to the presentation of affective natural scenes in the paracentral (6° of eccentricity) or near peripheral (12° of eccentricity) visual areas of the intact and blind hemifields. Hence, we determined the accuracy in both hemifields by measuring the number of correct responses between the intact hemifield (108 correct / 149 = 72.67%) and the blind hemifield (66 correct / 150 = 44%) which revealed better performance for seen stimuli. Nonetheless, a Chi-square analysis was performed to evaluate

whether the number of correct answers was above the chance level of 33% and revealed that SJ was able to significantly dissociate between affective conditions in both the intact ($X2=108.93$, $p < .001$) and blind hemifields ($X2=10.47$, $p = .005$) (Figure 3A). Therefore, when we consider the non-specific performances by confounding all conditions, we conclude that the expected valence was adequately evaluated in the intact hemifield and that SJ demonstrated blindsight abilities that were non-specific to one affective condition.

Further investigating the differences between conditions, we found that seen stimuli generated above chance-level performances for the paracentral ($X2=66.68$, $p < .001$), near periphery ($X2=31.32$, $p < .001$) (Figure 3B), unpleasant (82.46%, $X2=65.23$, $p < .001$), neutral (76.08%, $X2=42.37$, $p < .001$) and pleasant (57.44%, $X2=15.53$, $p < .001$) conditions (Figure 3C). However, unseen stimuli induced performance above chance-level only for the near periphery (45.95%, $X2=7.76$, $p = .02$) (Figure 3B) and pleasant conditions (47.17%, $X2=7.51$, $p = .02$) (Figure 3C). While the advantage in the near periphery was expected in unconscious perception, the higher performance for pleasant compared to unpleasant pictures was surprising since we were expecting an advantage of the negative affect. Also, the best performances in conscious perception were achieved by the paracentral and unpleasant conditions, which suggest different mechanisms involved in both types of processing. Thus, to further understand these results, we wanted to investigate how performance, eccentricity as well as affective valence influenced RTs for seen and unseen stimuli. We sought to understand how RTs were influenced by the type of visual stimulus in the absence of visual awareness and how to do these changes compare to RTs in the presence of visual awareness.

Significant large effects of hemifield, $F(1, 281) = 7.015$, $p = .009$, $r = .026$, of performance, $F(1, 281) = 4.414$, $p = .037$, $r = .017$, and of eccentricity, $F(1, 281) = 5.963$, $p = .015$, $r = .023$, were observed. As expected, we found that seen pictures triggered faster RTs compared to unseen pictures (seen: 914.772 ± 16.125 ms, unseen: 969.672 ± 13.024 ms) (Figures 3D-F). However, interestingly directions of effects were similar in the intact and blind hemifields for differences in performance, eccentricity, and affective valence. In fact, correct responses (seen: 880.635 ± 15.577 ms, unseen: 960.262 ± 19.644 ms) were associated with significant faster RTs compared to incorrect responses (seen: 948.909 ± 28.238 ms, unseen: 979.082 ± 17.107 ms) for both hemifields (Figure 3D). Moreover, pictures presented in paracentral vision (seen: 940.059 ± 21.490 ms,

unseen: 995.002 ± 18.436 ms) triggered significant slower RTs compared to near periphery pictures (seen: 889.486 ± 24.045 ms, unseen: 944.341 ± 18.403 ms) for both hemifields (Figure 3E). While no significant main effect was found for affective conditions, the posthoc analysis with Bonferroni adjustment ($p = 0.04$) showed significant faster RTs for unpleasant stimuli (seen: 898.200 ± 31.996 ms, unseen: 941.591 ± 23.792 ms) compared to pleasant stimuli (seen: 938.916 ± 23.854 ms, unseen: 1006.043 ± 21.859 ms) for both hemifields (Figure 3F). Therefore, if we compare the RTs to the performance, we can conclude that unpleasant pictures triggered imprecise but faster responses compared to pleasant pictures, which suggests that unpleasant and pleasant conditions are mediated by two different neural mechanisms, which we identify in the MEG results and address in the discussion.

Moreover, seen pleasant pictures were more rapidly processed in the paracentral vision compared to the near periphery (6° pleasant: 922.869 ± 37.307 ms, 12° pleasant: 954.962 ± 29.737 ms), while a faster response for near peripheral stimuli was observed for unpleasant and neutral pictures in the intact hemifield (6° unpleasant: 956.643 ± 31.622 ms, 12° unpleasant: 839.758 ± 55.633 ms; 6° neutral: 940.666 ± 42.007 ms, 12° neutral: 873.736 ± 34.991 ms) (Figure 3G) and was independent of the affective valence in the blind hemifield (6° unpleasant: 957.067 ± 33.028 ms, 12° unpleasant: 924.114 ± 34.255 ms; 6° neutral: 999.879 ± 31.871 ms, 12° neutral: 922.883 ± 30.260 ms; 6° pleasant: 1026.060 ± 30.859 ms, 12° pleasant: 986.027 ± 30.967 ms) (Figure 3H). These results suggest that for seen stimuli, processing pleasant pictures is facilitated in paracentral vision, i.e. parvocellular pathway compared to the near periphery, contrarily to unpleasant stimuli supporting previous reports (Bayle et al., 2011). However, facilitation in the absence of conscious perception is increased for the peripheral unpleasant system implying a specific fast pathway which underlying neurophysiological correlates we address in another paper (Hadid et al., 2021 in preparation). Nevertheless, these last behavioral results are marginal since no significant interaction effect (hemifield x eccentricity x affective condition) was observed and will not be further discussed.

High Gamma Power (> 50Hz) Differs between Seen and Unseen stimuli

To assess the role of the gamma band (30-120 Hz) in conscious and unconscious affective processing we sought to verify the impact of awareness on gamma power and gamma functional connectivity. Therefore, we first computed the spectral activity over time for the sighted and blind

hemifields in each ROI which was illustrated using time-frequency (TF) maps (Figure 3A). Values in the TF maps representing relative power across time points (-200 to 800 ms) and frequencies (4 to 120 Hz) showed that the presentation of a stimulus induced increases and decreases of power in distinct frequency bands in the intact V1 and subcortical structures confirming synchronization in the gamma range between 50 and 120 Hz following stimulus presentation and enduring over time.

To investigate the high range frequency activity, we estimated the relative power over time for two gamma bands, i.e. the high gamma band (50–90 Hz) and HFOs (90–120 Hz). In the high gamma band, 10 ms post-stimulus, an increase in V1 gamma power was observed for both seen and unseen pictures. Nonetheless, presentation of seen and unseen pictures resulted in gamma synchronization post-stimulus compared to baseline and later significant desynchronized gamma activity in the unseen condition (seen: maximum peak at 518 ms and relative power of 0.20 ± 0.08 in z-score, unseen: maximum peak at 503 ms and relative power of -0.29 ± 0.07 in z-score, seen vs unseen: cluster between 478 and 528 ms, $p < .05$ corrected; Figure 3B). We observe the same HFOs pattern of activity in both conditions in the left amygdala (seen: peak at 434 ms and relative power of 0.18 ± 0.08 in z-score, unseen: peak at 425 ms and relative power of -0.17 ± 0.07 in z-score, seen vs unseen: cluster between 411 and 468 ms, $p < .05$ corrected; Figure 3B).

In the intact V1, we observe an increase in HFO power from 200 to 410 ms for both seen and unseen pictures. After 250 ms, seen stimuli induced higher power compared to unseen stimuli (seen: maximum peak at 316 ms and relative power of 0.77 ± 0.11 in z-score, unseen: maximum peak at 251 ms and relative power of 0.43 ± 0.10 in z-score, seen vs unseen: cluster between 275 and 395 ms, $p < .05$ corrected; Figure 3B). Significantly, the increase in V1 HFOs was stronger for paracentral stimuli compared to the near periphery for both seen (seen paracentral: maximum peak at 317 ms and relative power of 0.94 ± 0.14 in z-score, seen near periphery: maximum peak at 251 ms and relative power of 0.61 ± 0.17 in z-score, seen paracentral vs near periphery: clusters between 250 and 306 ms and between 330 and 411 ms, $p < .05$ corrected; Figure 3B) and unseen stimuli (unseen paracentral: maximum peak at 252 ms and relative power of 0.49 ± 0.14 in z-score, unseen near periphery: maximum peak at 251 ms and relative power of 0.39 ± 0.13 in z-score, unseen paracentral vs near periphery: cluster between 346 and 427 ms, $p < .05$ corrected; Figure 3B). A longer HFOs desynchronization for seen paracentral stimuli compared to near periphery stimuli was also observed at early latencies (seen paracentral: peak at 57 ms and relative power of

-0.36 ± 0.10 in z-score, seen near periphery: peak at 49 ms and relative power of 0.09 ± 0.15 in z-score, seen paracentral vs near periphery: cluster between 0 and 78 ms, $p < .05$ corrected; Figure 3B).

At the thalamic level, differences were also observed in the left thalamus where the presentation of a contralateral seen stimuli induced desynchronization at stimulus onset that was significantly different from 0 in the high gamma band (between -60 to 34 ms, $p < .05$ corrected; Figure 3B) and significantly different from the unseen condition for HFOs (seen: peak at 0 ms and relative power of -0.41 ± 0.06 in z-score, unseen: no peak at 0 ms and relative power of -0.05 ± 0.08 in z-score, seen vs unseen: cluster between -64 and 20 ms, $p < .05$ corrected; Figure 3B). No significant differences were observed between seen and unseen pictures in the right thalamus and amygdala. Thus, solely reporting gamma power does not provide a clear indication of the neural mechanisms supporting affective perception in the presence and absence of visual consciousness as distinct mechanisms. Consequently, we aimed a better understanding of the pathways involved in both processing using functional undirected and directed connectivity mediated through gamma oscillations by computing the correlation and GC between for each pair of ROIs, respectively.

Conscious Perception Relies on Gamma Connectivity between the Thalamus and Intact V1

Correlational activity between ROIs for seen and unseen stimuli showed significant correlation between the left thalamus and the left amygdala for HFOs (seen (90-120Hz): $r(139) = .19$, $p = .022$, unseen (90-120Hz): $r(140) = .22$, $p = .007$; Figure 4), between the left amygdala and the intact left V1 in the high gamma band (Am-lh ↔ V1-lh: seen (50-90Hz): $r(139) = .27$, $p = .001$, unseen (50-90Hz): $r(140) = .32$, $p < .001$; Figure 4) and for both gamma bands between the right thalamus and the right amygdala (Th-rh ↔ Am-rh: seen (50-90Hz): $r(139) = .49$, $p < .001$, unseen (50-90Hz): $r(140) = .56$, $p < .001$, seen (90-120Hz): $r(139) = .41$, $p < .001$, unseen (90-120Hz): $r(140) = .44$, $p < .001$; Figure 4). Seen stimuli also triggered significant correlation between the left thalamus and the intact left V1 in both gamma bands (Th-lh ↔ V1-lh: seen (50-90Hz): $r(139) = .20$, $p = .018$, seen (90-120Hz): $r(139) = .18$, $p = .03$; Figure 4) and additionally between the left amygdala and the intact left V1 for HFOs (seen (90-120Hz): $r(139) = .21$, $p = .012$; Figure 4). The correlational coefficients, therefore, confirmed that the left thalamus and left intact V1 were significant only for seen stimuli. In order to address the directionality and causality of these correlations in the temporal domain, GC DOI between ROIs for each time point was performed to

assess specific differences between conditions. Subsequent results show that significant differences were obtained between performance and affective conditions for HFOs.

Thalamic Connectivity Guided by HFOs Influences Performance in Conscious and Unconscious Processing

Causal-directed FC driven by HFOs showed differences in directionality in influence between subcortical structures when comparing correct and incorrect responses. First, correct responses for seen pictures induced an increase in the GC DOI from the thalamus to the amygdala around 200 ms, while incorrect responses were rather mediated by the amygdala influencing the thalamus (Figure 5A). More precisely, seen correct and incorrect responses were driven by inverse FC between the right thalamus and the right amygdala (correct: Th-rh → Am-rh, GC DOI > 0 between 191 and 261 ms and values between 0.02 ± 0.01 and 0.04 ± 0.01, incorrect: Th-rh ← Am-rh, GC DOI < 0 between 191 and 285 ms and values between -0.03 ± 0.02 and -0.06 ± 0.03, correct vs incorrect: cluster between 191 and 267 ms, $p < .05$ corrected; Figure 5B).

Based on the HFOs causal directed FC in the absence of visual consciousness, we were also able to dissociate between a correct and an incorrect response, with the right thalamus exerting a direct influence on the right amygdala for the former and the right amygdala exerting a direct influence on the right thalamus for the latter. However, these differences happen as soon as 50 ms post-stimulus (Figure 5C) suggesting that correct answers for unseen stimuli were triggered by a faster mechanism than the one found for consciously perceived stimuli. We also sought a better understanding of the thalamocortical mechanisms involved by performing the GC DOI exploratory analysis between the subcortical areas and all the other cortical areas. We specifically found that the right thalamus and the right superior temporal sulcus (STS) were causally modulating each other with correct and incorrect answers driven by thalamo-STS and STS-thalamic influences, respectively (Figure 5C). Thus, non-affective specific blindsight is driven by a thalamo-amygdala pathway (correct: Th-rh → Am-rh, GC DOI > 0 between 50 and 100 ms and values between 0.02 ± 0.02 and 0.03 ± 0.02, incorrect: Th-rh ← Am-rh, GC DOI < 0 between 90 and 274 ms and values between -0.03 ± 0.01 and -0.05 ± 0.01, correct vs incorrect: cluster between 50 and 227 ms, $p < .05$ corrected; Figure 5D) and a thalamo-STS pathway (correct: Th-rh → STS-rh, GC DOI > 0 between 138 and 225 ms and values between 0.03 ± 0.02 and 0.04 ± 0.02, incorrect: Th-rh ← STS-

rh, GC DOI < 0 between 79 and 177 ms and values between -0.02 ± 0.01 and -0.04 ± 0.01, correct vs incorrect: cluster between 108 and 227 ms, $p < .05$ corrected; Figure 5D).

Late Contralateral Interactions Between the Thalamus and Amygdala Are Specific to Affective Conscious and Unconscious Processing

Affective specific differences in GC DOI between the thalamus and amygdala driven by HFOs were also observed in the intact (Figure 6A) and blind hemifields (Figure 6B). In fact, for unpleasant seen stimuli, the left contralateral thalamus exerted a causal influence on the left contralateral amygdala, through HFOs around 500 ms, and the DOI was inversed for pleasant stimuli (unpleasant: Th-lh → Am-lh, GC DOI > 0 between 501 and 518 ms and values between 0.02 ± 0.02 and 0.06 ± 0.02, pleasant: Th-lh ← Am-lh, GC DOI < 0 between 482 and 577 ms and values between -0.03 ± 0.02 and -0.06 ± 0.02, unpleasant vs neutral: cluster between 482 and 544 ms, $p < .05$ corrected; Figure 6C). In the same manner, pleasant stimuli induced a greater GC DOI from the amygdala to the thalamus compared to neutral stimuli via HFOs around 510 ms (pleasant: Th-lh ← Am-lh, GC DOI < 0 between 482 and 577 ms and values between -0.03 ± 0.02 and -0.06 ± 0.02, neutral: Th-lh → Am-lh, GC DOI > 0 between 467 and 484 ms and values between 0.04 ± 0.02 and 0.05 ± 0.03, pleasant vs neutral: cluster between 467 and 567 ms, $p < .05$ corrected; Figure 6C).

In the blind hemifield, unpleasant unseen stimuli triggered the right contralateral thalamus to exert a direct influence on the right contralateral amygdala at around 350 ms through HFOs compared to neutral pictures (unpleasant: Th-rh → Am-rh, GC DOI > 0 between 360 and 460 ms and values between 0.04 ± 0.01 and 0.07 ± 0.02, neutral: no sig GC DOI ≠ 0, unpleasant vs neutral: cluster between 360 and 450 ms, $p < .05$ corrected; Figure 6D) and pleasant pictures (unpleasant: Th-rh → Am-rh, GC DOI > 0 between 360 and 460 ms and values between 0.04 ± 0.01 and 0.07 ± 0.02, pleasant: Th-rh ← Am-rh, GC DOI < 0 between 360 and 400 ms and values between -0.02 ± 0.01 and -0.03 ± 0.01, unpleasant vs pleasant: cluster between 360 and 460 ms, $p < .05$ corrected; Figure 6D).

Gamma connectivity between the thalamus, amygdala, and intact V1 predicts behavior

Multiple linear regression was calculated to predict the RTs in response to the stimulation of the intact and blind hemifields based on the high gamma and HFOs power for all ROIs, as well as on

the correlation activity and GC between pairs of ROIs. We observe that both directed (GC) and undirected (correlation) connectivity between subcortical structures via high gamma activity and HFOs significantly correlated with behavior (Table 1). In fact, undirected thalamic and amygdala correlation with the intact V1 significantly correlated with RTs. More precisely, faster RTs were associated with thalamo-striate communication and longer RTs with amygdalo-striate communication. A significant regression equation was found ($F(36,236) = 1.73$, $p = 0.005$, $R2 = 0.252$) (Figure 7) with four variables significantly predicting the RTs (Am-lh ↔ V1-lh (90-120 Hz): $t = 2.06$, $p = .040$, Th-rh ↔ Am-rh (50-90 Hz): $t = 2.09$, $p = .038$, Am-rh ↔ V1-lh (90-120 Hz): $t = 2.36$, $p = .019$, Th-lh → V1-lh (90-120 Hz): $t = 2.57$, $p = 0.011$; Table 1).

Discussion

The aim of this study was to establish the existence of fast subcortical pathways using gamma synchronization involved in negative and positive affective discrimination in the absence of visual awareness. The behavioral and electrophysiological results confirmed a new form of affective blindsight which allowed us to revisit affective unconscious perception using natural scenes.

SJ's Behavior Reflects the Role of Different Mechanisms in Affective-Blindsight

The presentation of natural complex scenes in a 3-alternative forced-choice affective discrimination paradigm allowed us to establish residual affective blindsight abilities in patient SJ. To study SJ's behavior we opted to report the performance as a direct measure of how well SJ was able to discriminate the affective valence of each picture and the RTs as an indirect measure of how conditions modulated behavior. SJ performed above the chance level when all conditions were collapsed and RTs were modulated by awareness, performance, eccentricity, and the affective condition. First, seen stimuli induced faster RTs compared to unseen stimuli showing that attentional capture in the intact hemifield was more salient (Yantis and Hillstrom, 1994). Second, correct responses triggered faster RTs compared to incorrect responses even in the absence of visual awareness (Cowey et al., 2008). We further demonstrated that accurate and inaccurate discrimination depended on separate neural mechanisms which will be discussed in the subsequent connectivity section.

Moreover, for conscious and unconscious perception, RTs showed facilitation for near periphery stimuli favoring the use of global information compared to paracentral stimuli exploiting

local information, which corroborates the rapidity of the peripheral magnocellular system independent of visual awareness (Campana et al., 2016; Maunsell et al., 1999; Tapia and Breitmeyer, 2011). However, seen stimuli triggered more accurate responses for paracentral stimuli compared to near periphery stimuli, suggesting that using local information supported by the parvocellular system is more precise in the presence of visual awareness, while performance was greater for the peripheral system for unseen stimuli (Breitmeyer, 2014). Thus, global information seems to be prioritized in unconscious perception, in terms of precision and rapidity, which could be associated with the koniocellular and magnocellular pathways, respectively. In fact, the koniocellular system could allow color and local information processing showing some similarities with the parvocellular pathway while by-passing V1 (Hendry and Reid, 2000).

One important finding is the superior performance for unseen pleasant pictures compared to neutral and unpleasant stimuli. By using stimuli that do not rely on one psychophysical property as can be the case with emotional faces if not controlled (McFadyen et al., 2017), we confirmed our hypothesis that positive stimuli can be processed in affective-blindsight. However, we did not expect the performance to be better than for unpleasant pictures. So, were pleasant pictures prioritized compared to unpleasant pictures? The answer is that both affective valences seem to use divergent mechanisms in the absence of visual awareness. In fact, facilitation was also found for unpleasant pictures characterized by faster RTs compared to pleasant pictures which corroborate a rapid privileged pathway for negative stimuli. Thus, we explain this discrepancy between performance and RTs by postulating that discrimination of pleasant pictures passes by a slower more precise system independent of V1, which could potentially depend on the koniocellular pathway (Warner et al., 2015), and unpleasant pictures use a fast magnocellular pathway (Méndez-Bértolo et al., 2016; Nicol et al., 2013). The involved mechanisms will be further explained in terms of subcortical top-down and bottom-up pathways as demonstrated by our GC results.

Gamma Power Modulations Indicate Multiple Processes Involved in Perception

In order to identify the spectral and temporal neural mechanisms leading to an understanding of affective-blindsight behavior, we analyzed the oscillatory profile of the high-range frequency activity within the connectome formed by both thalami, amygdalae, and the intact V1 which we assumed played a significant role in perceiving and responding to affective complex natural scenes. First, we confirmed that during the task, an increase in gamma (> 50Hz) was detected in all ROIs.

In fact, modulations of the gamma synchronization over time were observed during the entire time window for both seen and unseen pictures, which indicate the role of gamma during the execution of a perceptual task by reflecting the cognitive load and requirements involved (Tallon-Baudry, 2009). To investigate how gamma fluctuated as a function of perceptual differences, we compared gamma power for seen and unseen pictures.

Between 50 and 90 Hz, an increase in gamma power compared to baseline was observed post-stimulus for both seen and unseen pictures in the intact left V1 with the maintenance of excitatory activity over time for seen stimuli which would be associated with faster and stronger responses in conscious perception (Sedley and Cunningham, 2013) which we assessed with the behavioral results. In fact, gamma synchronization has been reported to correlate with awareness in blindsight (Schurger et al., 2006). Nonetheless, unseen pictures triggered a reversal of activity in both the left V1 and amygdala at around 500 ms which could corroborate previous reports of modulation of attentional allocation mechanisms in the absence of visual awareness (Bauer et al., 2009). The desynchronization could also be due to the use of fewer features and inhibition of unimportant features (Sedley and Cunningham, 2013). While in need of further investigation exploring these hypotheses, post-stimulus synchronization was also observed in HFOs (90-120 Hz) in the intact V1 which indicated the involvement of multiple mechanisms between 200 and 400 ms in perception. The increase between 200 and 270 ms showed no significant differences between conditions and could be related to attentional enhancement (Fiebelkorn et al., 2018; Kastner et al., 2020), sensory processing (Tallon-Baudry, 2009), and working memory (Jensen et al., 2007) prior to conscious perception. However, comparing seen and unseen stimuli, as well as paracentral and near periphery conditions, differences in HFOs power were found between 270 and 425 ms, i.e. larger for seen compared to unseen stimuli between ≈ 275 and 400 ms, larger for seen paracentral compared to seen near periphery pictures between ≈ 250 and 300 ms and larger for unseen paracentral compared to unseen near periphery pictures between ≈ 350 and 425 ms. Considering the timing and specificity of these differences, we postulate that synchronization is increased for stimuli for which involuntary microsaccades were more difficult to inhibit (Yuval-Greenberg et al., 2008), as when a picture is more salient due to conscious perception, i.e. seen vs unseen, or when it is presented at the foveal limit, i.e. paracentral vs near periphery. The timing also demonstrates that involuntary microsaccades are produced earlier for a perceived stimulus compared to an unperceived stimulus. In line with these findings, a greater HFOs

desynchronization for seen paracentral stimuli compared to near periphery stimuli suggests a greater necessity to inhibit saccadic movements in the context of increased attentional cover capture. HFOs differences were also observed in the left thalamus which showed desynchronization for seen stimuli at stimulus onset. We interpret these results in light of previous studies on gamma-band activity (Van Der Werf et al., 2008) and on the primate thalamus (Kunimatsu and Tanaka, 2010), as an explicit inhibition/control of saccades towards the right intact hemifield at stimulus onset.

All of these differences considered, gamma power could reflect attentional allocation, visual saliency, awareness, micro-saccades, and inhibition of saccades following stimulation of the visual system. However, it does not give us a clear indication regarding the neural mechanisms underlying affective-blindsight. In fact, we found that the answers to our questions involved the undirected and directed connectivity between structures that use gamma synchronization to communicate relevant information and guide affective conscious and unconscious perception and behavior.

Subcortical Gamma Communications Are Important Neural Markers of Unconscious Perception

Subcortical correlational activity mediated by gamma oscillations (50-90 Hz and 90-120 Hz) within the connectome greatly contributed to predicting RTs. An important result is the significant correlation found between the left thalamus and left intact V1 specifically for seen stimuli validating the role of gamma (50-120 Hz) in driving thalamo-striate communication in conscious vision which is hypothesized in humans (Dehaene et al., 2003; Mashour et al., 2020) and previously reported in the mouse (McAfee et al., 2018). These results also confirm the thalamocortical role of gamma in consciousness which has been demonstrated in macaques (Redinbaugh et al., 2020). Corroborating the implication of the thalamo-striate pathway, we found that the causal influence mediated by HFOs from the left thalamus to the intact V1 was a significant predictor of SJ's RTs, thus supporting the role of high-frequency oscillations in feedforward processing and its impact on cognition (Van Kerkoerle et al., 2014). Moreover, the activity of the left amygdala significantly correlated with the activity of the intact left V1 in both gamma frequency bands in conscious perception and for HFOs in the absence of visual awareness supporting the implication of the amygdalo-cortical pathway in processing affective scenes (Bocchio et al., 2017).

Significant correlations for both seen and unseen stimuli were also found between the left thalamus and amygdala in the high gamma band and between the right thalamus and amygdala being a significant predictor of SJ's RTs. Activity via HFOs in the right thalamus and amygdala was also significantly correlated. The connectivity between these structures was more important compared to the connectivity between all other ROIs supporting previous reports of greater activity of the right amygdala in processing affective conditions (Hung et al., 2010) notably in the absence of visual awareness (Gainotti, 2012). Electrophysiological studies have likewise shown right lateralization in processing affective stimuli in patients with bilateral cortical blindness (Andino et al., 2009; Burra et al., 2019; Pegna et al., 2005). Increased connectivity between the right thalamus and right amygdala was also reported in fMRI studies for unseen fearful stimuli (Morris et al., 1999; Williams et al., 2006). Nonetheless, these results also confirm previous fMRI reports showing ipsilesional increased communication between the thalamus and the amygdala within the damaged hemisphere (Tamietto et al., 2012) which could be related to compensation mechanisms (Guo et al., 2014; Pedersini et al., 2020). Yet, these results do not provide us with an explanation of how stimuli are accurately processed in the absence of visual awareness or how affective specific information is differentiated. These answers were provided by the temporal dynamics observed in the GC DOI which showed that the thalamo-amygdala pathway specifically driven by HFOs played a significant role in understanding affective-specific and non-affective differences in conscious perception and affective-blindsight. Our results of GC DOI reporting a significant contribution of HFOs in directional thalamic communication provide new insights and perspectives into the human subcortical pathways.

First, we found non-affective specific differences in directionality between correct and incorrect responses for seen and unseen stimuli that were guided by HFOs. For seen pictures, the directed connectivity between the right thalamus and the right amygdala around 200 ms shows bottom-up and top-down subcortical gamma regulations for correct and incorrect responses, respectively. It is usually the case to find gamma oscillations particularly involved in bottom-up mechanisms rather than a top-down activity which has been associated with lower frequency ranges (Michalareas et al., 2016; Richter et al., 2017). Nevertheless, top-down modulations via gamma oscillations have been reported to be involved in affective processing (Carus-Cadavieco et al., 2017; Kajal et al., 2020). Second, the timing of the influences suggests that the difference observed in the accuracy of the behavioral response might be due to differences in visuospatial attention at

the attended location (Fiebelkorn et al., 2018). In fact, a trial where the visual stimulus induced stronger bottom-up modulations resulted in correct responses (Garrido et al., 2012). However, while top-down regulation from the amygdala should increase performance in a task where the location of the stimulus can be predicted (Vuilleumier, 2005), in the context where the timing and location of the stimulus are unpredictable, these top-down modulations could result in incorrect responses. The late influences provide new knowledge on the timing of the human thalamo-amygdala gamma causal directed FC in the presence of conscious perception suggesting that accurate performance is strongly biased by earlier thalamocortical visual processing supporting the role of interactions between the thalamus, cortical areas, and the amygdala in the presence of conscious perception.

Interestingly, when the blind hemifield was stimulated, correct and incorrect responses were associated with similar but faster GC DOI for HFOs between the thalamus and the amygdala. Importantly, this study supports previous results reporting a subcortical pathway that guides the activity of the amygdala independent of the stimulus predictability and affective condition (Garrido et al., 2012) which we show is mediated by fast gamma postulated to have a particular role in the amygdala (Bocchio et al., 2017). Moreover, the GC exploratory analysis showed specifically increased causal connectivity between the right thalamus and the right STS in instances of correct responses confirming the early contribution of the STS in processing social stimuli in affective-blindsight (Andino et al., 2009). The roles of the STS include motion processing (Claeys et al., 2003) even in the absence of motion for stimuli that signal actions (Allison et al., 2000), orientation processing (Bogadhi et al., 2018), spatial awareness within the right hemisphere (Karnath, 2001), social features (Lahnakoski et al., 2012) and natural scenes (Bettencourt and Xu, 2013). This specific thalamo-extrastriate pathway could depend on the koniocellular pathway (Lyon et al., 2010) as proposed in studies of V1-lesions (Schmid et al., 2010) or magnocellular responses and reflect behaviorally relevant information irrespective of conscious perception (de Gelder and Poyo Solanas, 2021) which support our behavioral interpretations. In fact, in individuals with complete cortical blindness, activation of the STS has been shown to contribute to unconscious abilities (Burra et al., 2013; Van den Stock et al., 2014; Striemer et al., 2019). On the other hand, connectivity was inversed for incorrect responses with the right amygdala and STS exerting causal influences on the right thalamus which could be associated with a lack of adequate detection of relevant information (Bogadhi et al., 2021; Corbetta et al., 2008) in context of insufficient thalamic

bottom-up influence. Thus, when the bottom-up signal was strong enough probably due to adequate attentional resources allocated towards the blind hemifield (Dehaene et al., 2006), the thalamus was able to guide the activity of the amygdala 50 ms post-stimulus and influence the STS 100 ms post-stimulus which resulted into correct responses. However, when the stimulus signal received wasn't sufficient, the amygdala and STS influenced the activity of the thalamus under 100 ms to compensate for the lack of thalamic bottom-up projections which led to incorrect responses. Taken together, these temporal dynamics provide novel knowledge about the timing and rapidity of thalamic connectivity which is of particular relevance in understanding the mechanisms involved in triggering performance above chance-level prior to awareness. Hence, these results offer evidence that the thalamus exerts a crucial role on other regions to process non-specific affective unconscious stimuli.

Affective-specific differences were nonetheless revealed by the directed connectivity analysis between the thalamus and amygdala in the contralateral hemifield for seen and unseen pictures. In fact, contralateral subcortical affective specific differences were found around 350 ms for unseen stimuli and 500 ms for seen stimuli, revealing that affective discriminatory information is notably coded within subcortical pathways at late latencies. The timing of these influences suggests (1) that cortical visual and attentional mechanisms are previously recruited before affective-specific discrimination (Andino et al., 2009; Luo et al., 2010) also supported by the reported power increase in the intact V1 around 200 ms and (2) that unconscious affective processing happens earlier than conscious affective perception suggesting a less complex cortical propagation in the absence of visual awareness (Salti et al., 2015). Nevertheless, regardless of awareness, stimulation of each hemifield induced unpleasant and pleasant stimuli to be driven by opposite directionality between the thalamus and the amygdala. In fact, information from unpleasant pictures was mediated by bottom-up gamma propagation from the thalamus to the amygdala. We interpret these results as being part of a system that uses stimuli-relevant information for negative valences resulting in fast RTs, while in contrast, information from pleasant pictures induced top-down gamma propagation from the amygdala to the thalamus highlighting the prioritization of relevant information in positive affective processing (Taylor and Fragopanagos, 2005; Vukelić et al., 2021). Surprisingly, both seen and unseen information were mediated by the same mechanisms that dissociate unpleasant from pleasant stimuli. Therefore, the brain can process effectively affective information in the absence of visual awareness which could explain the

behavioral differences we found between affective conditions and similarities between seen and unseen pictures. These results support our prior interpretations regarding the magnocellular, koniocellular, and parvocellular pathways.

In order to determine whether these neural substrates were involved in the higher order decision-making computation required in a discrimination task with and without visual consciousness, we tried to predict the RTs based on gamma power and directed and undirected FC for both gamma bands extracted from the intact V1, both thalami and amygdalae. The regression results demonstrated the importance of the primary thalamo-striate pathway and the thalamic connectivity with the right and left amygdala in predicting RTs for both conscious and unconscious affective perception. Therefore, while performance differences in GC DOI were mainly found between the right thalamus and amygdala guided by HFOs, RTs were influenced by other interactions within both high gamma frequency bands (50-90 Hz, 90-120 Hz). Hence, the behavior was modulated by the multiple complex neural mechanisms discussed in this paper in different manners.

Importantly, this study proposes that direct causal functional influences guided by HFOs between the human thalamus and the amygdala are driven by bottom-up and top-down processes that diverge in their temporal dynamics in order to code for specific and non-specific affective abilities for seen and unseen stimuli. Taken together, the gamma rhythms showed that subcortical influences were slower for conscious and content-specific activation, whereas fast bottom-up contralateral thalamic connectivity with the amygdala and STS guided general blindsight abilities. Finally, though anticipating human behavior using neural markers is a hard challenge, we were able to partially predict RTs using gamma features extracted from the connectome formed by both thalami, amygdalae, and the intact V1 revealing their importance in visual affective discrimination. Significantly, this paper reveals the role of subcortical gamma influences that contribute to conscious and unconscious affective perception and that modulate and predict behavior.

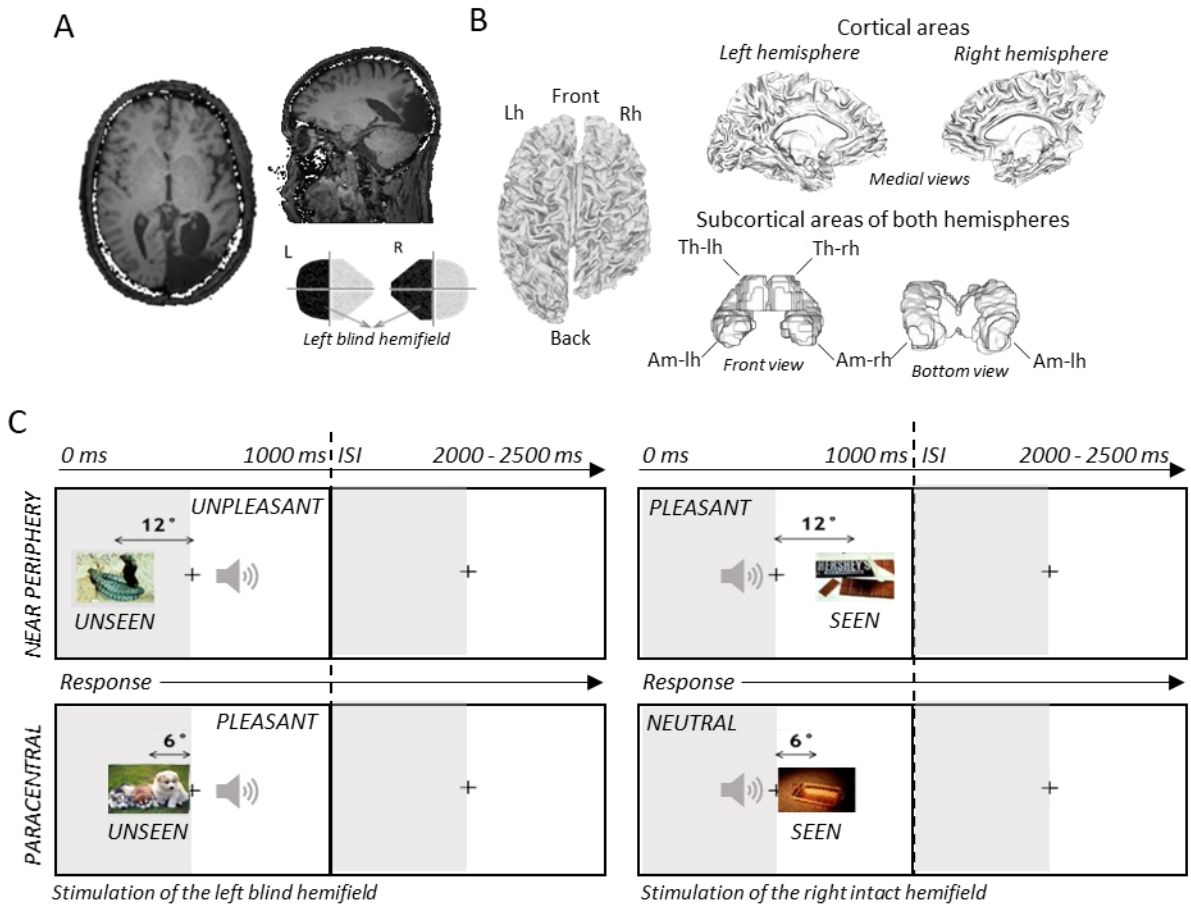

Figure 1. – Affective blindsight for natural scenes was demonstrated in patient SJ.

(A) SJ's MRI shows a surgical removal of the entire right occipital cortex performed to withdraw two epileptic hubs. The resection area extends to the right occipital pole, calcarine sulcus, superior occipital gyrus, precuneus, cuneus, lingual gyrus and the posterior part of the parahippocampal gyrus. A schematic representation of SJ's complete left homonymous hemianopia with no macular sparing is shown. SJ presents a unique form of affective-blindsight for natural complex scenes. (B) Source reconstruction using the T1 weighted MRI of both cortical and subcortical areas including the left thalamus (Th-lh), right thalamus (Th-rh), left and right hippocampus, left amygdala (Am-lh) and right amygdala (Am-rh) in the left hemisphere (Lh) and right hemisphere (Rh). (C) Schematic illustration of the forced-choice paradigm. Pictures from the IAPS were presented for 1000ms either to the intact right hemifield (unseen condition) or to the blind left hemifield (seen condition) centrally at 6° (paracentral) or in the periphery at 12° (near periphery) of eccentricity. An ISI varied between 2000 and 2500 ms. Stimuli were categorized as unpleasant, neutral, and

pleasant. While fixating on the cross at all times, the participant was asked to evaluate the emotional valence as quickly as possible when hearing a 100ms white noise. MAL had to guess the 'correct' answer even when the picture was not perceived. Responses were assessed as correct or incorrect. – Figure 1

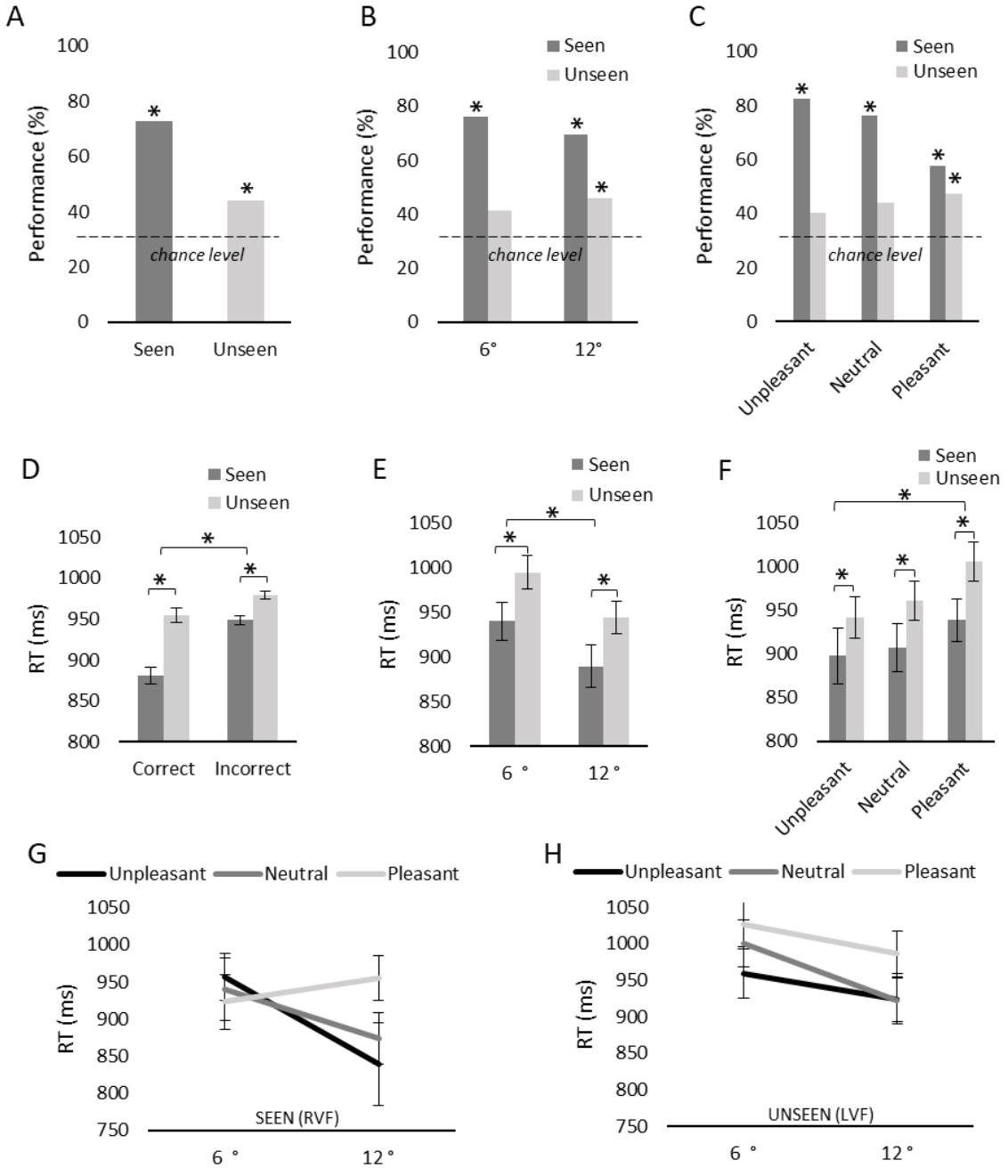

Figure 2. – RTs were modulated by the performance and condition for seen and unseen pictures.

RTs were modulated by the performance and condition for seen and unseen pictures. (A-F) Results associated with pictures presented in the intact hemifield are referred to as seen and illustrated in dark grey while pictures presented in the blind hemifield are referred to as unseen and illustrated in light grey. (A-C) Performance for seen stimuli was greater than for unseen stimuli. To assess the statistical significance, the number of correct responses was compared to a 33.33% chance level (since three response options were available). Asterisks show performance above chance level. (D-H) RTs in ms for seen stimuli were faster than for unseen stimuli. Asterisks show significant differences between hemifields, performance, eccentricity, or affective conditions. (A) Performance scores for seen and unseen stimuli presented in the intact and blind hemifield, respectively. (B) Performance scores for seen and unseen paracentral and near periphery stimuli. (C) Performance scores for seen and unseen unpleasant, neutral and pleasant stimuli. (D) RTs for correct and incorrect responses. Correct responses for seen and unseen stimuli triggered faster RTs compared to incorrect responses. (E) RTs for paracentral (6°) and near periphery (12°) pictures. Seen and unseen near periphery pictures triggered faster RTs compared to paracentral pictures. (F) RTs for unpleasant, neutral, and pleasant pictures. Seen and unseen unpleasant pictures triggered faster RTs compared to pleasant pictures. (G) RTs for seen paracentral and near periphery unpleasant (black), neutral (dark grey), and pleasant (light grey) pictures. (H) RTs for unseen paracentral and near periphery unpleasant (black), neutral (dark grey), and pleasant (light grey) pictures. – Figure 2

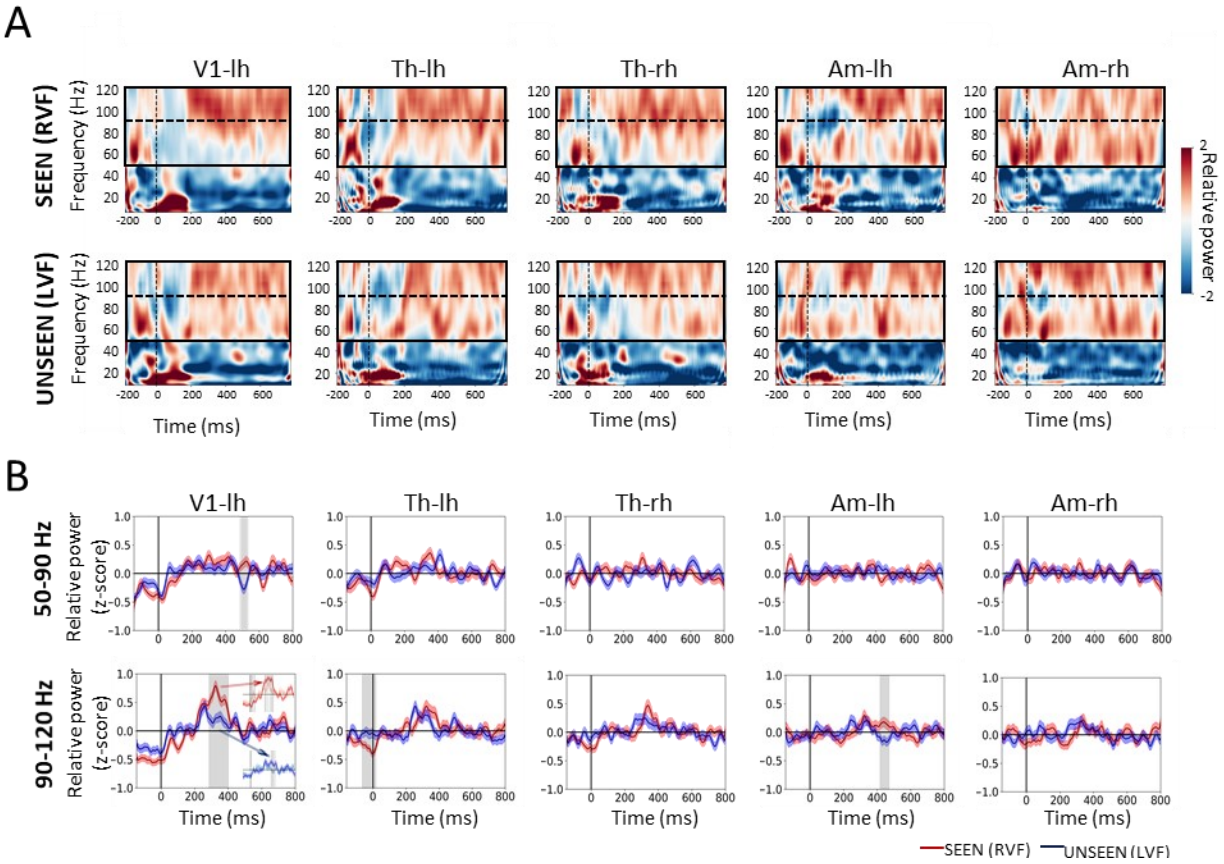

Figure 3. – Gamma power reflected multiple mechanisms involved in perception.

Single-trial analysis of power over time computed from -200 to 800 ms in V1-lh, Th-lh, Th-rh, Am-lh, and Am-rh for seen and unseen pictures presented in the intact and blind hemifields, respectively. (A) Time-frequency maps illustrate relative power modulations over time in z-scores for frequencies between 7 and 120 Hz for each ROI averaged across nodes. Sustained oscillatory synchronization is observed in the high gamma band (50-90 Hz) and for high-frequency oscillations (HFO: 90-120 Hz). (B) Relative power over for seen (red) and unseen (blue) pictures for the high gamma band and HFO for all ROIs. Statistical differences over time between conditions were assessed using cluster-based permutation analysis corrected for multiple comparisons. Significant differences are highlighted in grey. In the 90-120 Hz – V1-lh figure, we observe two temporal power modulations graphs where the above graph represents differences in the intact hemifield between the paracentral (red) and near periphery conditions (pink) and the below graph represents differences in the blind hemifield between the paracentral (blue) and near periphery conditions (light blue). – Figure 3

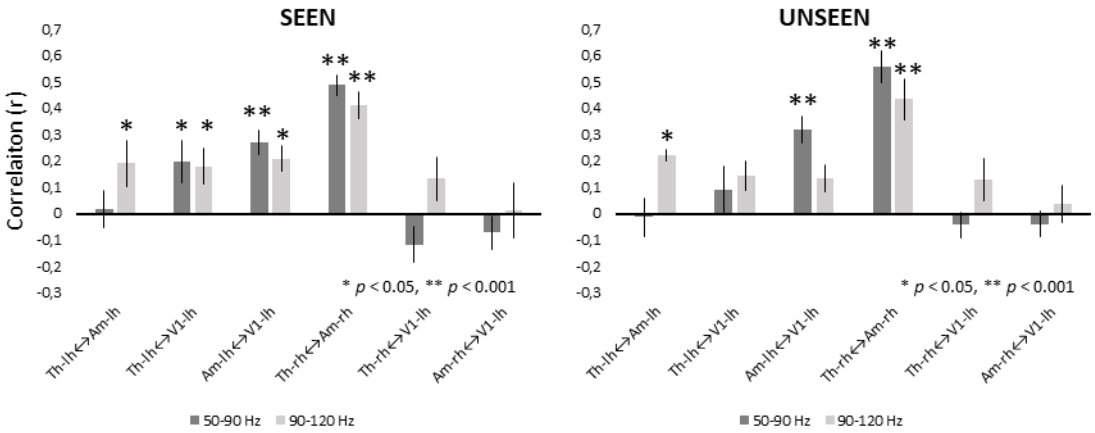

Figure 4. – Correlation between ROIs revealed distinct gamma communication for conscious and unconscious processing.

Pearson coefficient correlation (r) in the high gamma band (50-90 Hz: dark grey) and for HFOs (90-120 Hz: light grey) (A) for seen pictures and (B) for unseen pictures. Asterisks show significant correlation between ROIs (* $p < 0.05$, ** $p < 0.001$). – Figure 4

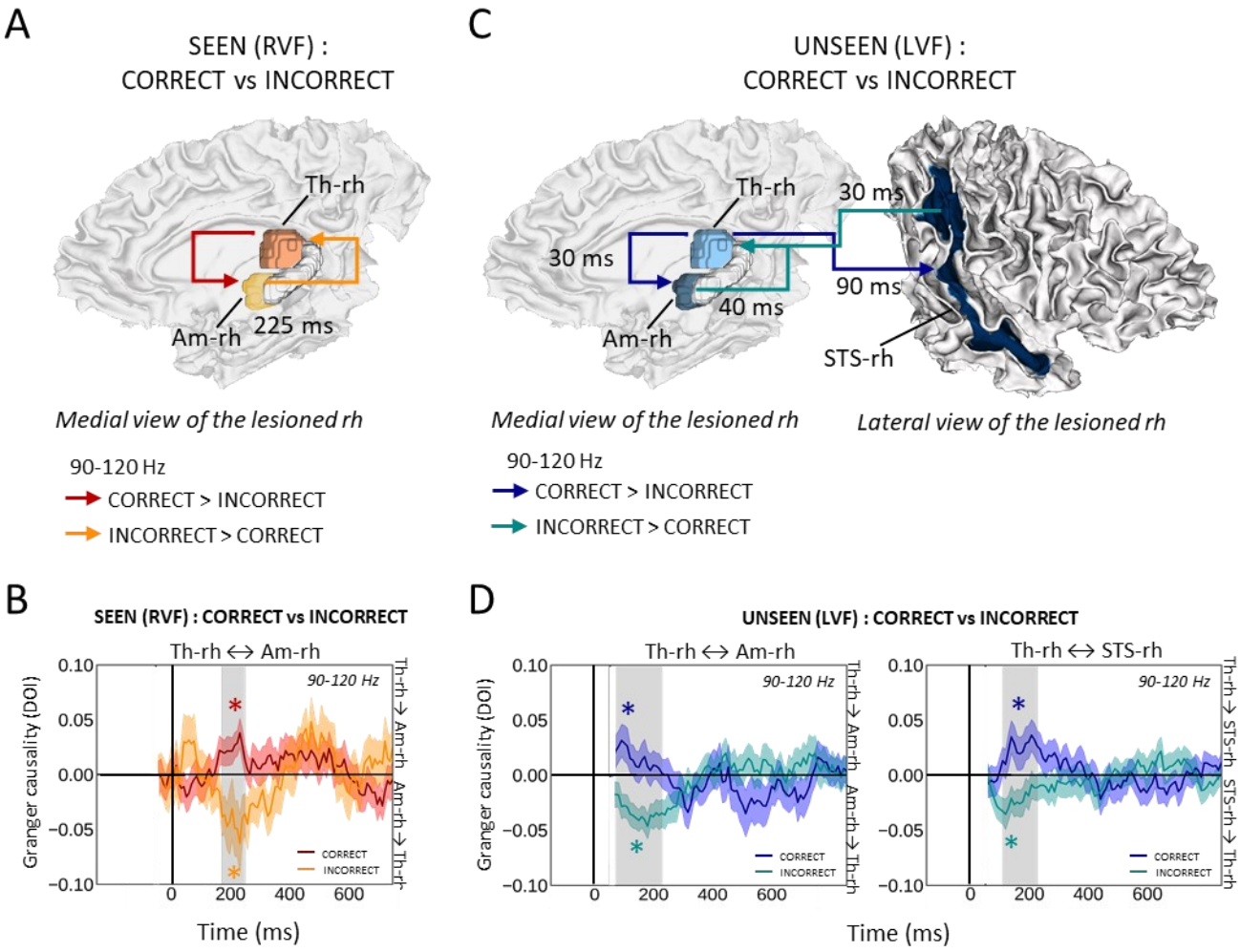

Figure 5. – HFOs guided fast thalamo-amygdala and thalamo-STS communications in unconscious processing.

GC DOI for correct and incorrect differences in conscious and unconscious perception. The dominant directionality in GC between ROIs was computed as the DOI which assessed the net difference between GC measured from the ROI1 to ROI2 and from ROI2 to ROI1. Significant differences over time between correct and incorrect responses in GC DOI were addressed using cluster-based permutation analysis corrected for multiple comparisons. (A) Schematic representation of the direction of the causal functional connectivity found between Th-rh and Am-rh for seen correct (red) and seen incorrect responses (orange). (B) GC DOI over time between Th-rh and Am-rh for seen correct (red) and seen incorrect responses (orange). Significant differences are highlighted in grey. (C) Schematic representation of the direction of the causal functional connectivity found between Th-rh and Am-rh and Th-rh and the right superior temporal sulcus

(STS-rh) for unseen correct (blue) and unseen incorrect responses (green). (D) GC DOI over time between Th-rh and Am-rh, as well as between Th-rh and STS-rh for unseen correct (blue) and unseen incorrect responses (green). Significant differences are highlighted in grey. – Figure 5

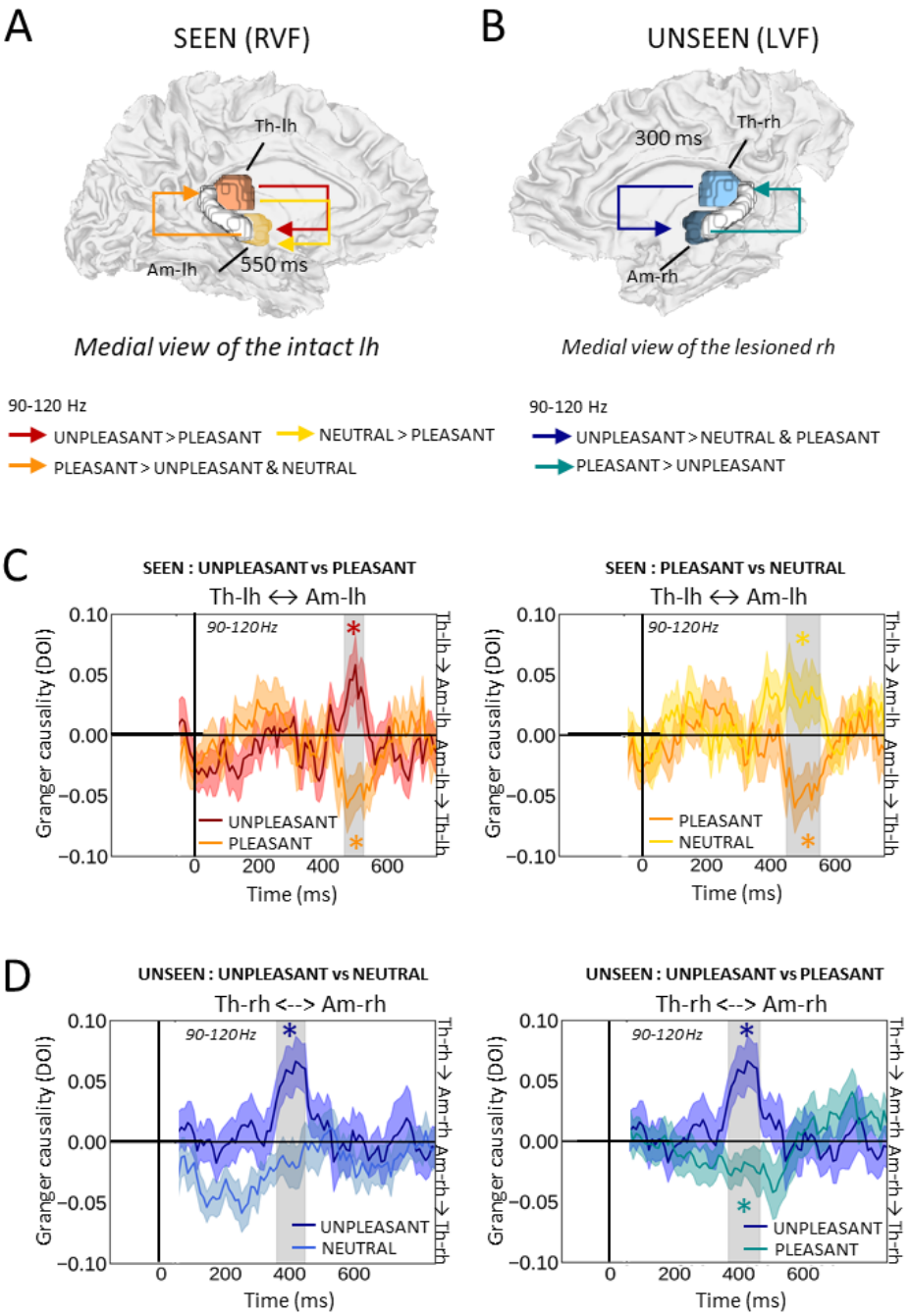

Figure 6. – Unpleasant and pleasant pictures were driven by opposite causal connectivity between the contralateral thalamus and amygdala irrespective of visual awareness

(A) Schematic representation of the GC DOI found between Th-lh and Am-lh for seen unpleasant (red), pleasant pictures (orange), and neutral pictures (yellow). (B) Schematic representation of the GC DOI between Th-rh and Am-rh for unseen unpleasant (blue), pleasant pictures (green), and neutral pictures (light blue). (C) GC DOI over time between Th-lh and Am-lh for seen unpleasant pictures (red), pleasant pictures (orange), and neutral pictures (yellow). Significant differences are highlighted in grey. (D) GC DOI over time between Th-rh and Am-rh for unseen unpleasant pictures (blue), pleasant pictures (green), and neutral pictures (light blue). Significant differences are highlighted in grey. – Figure 6

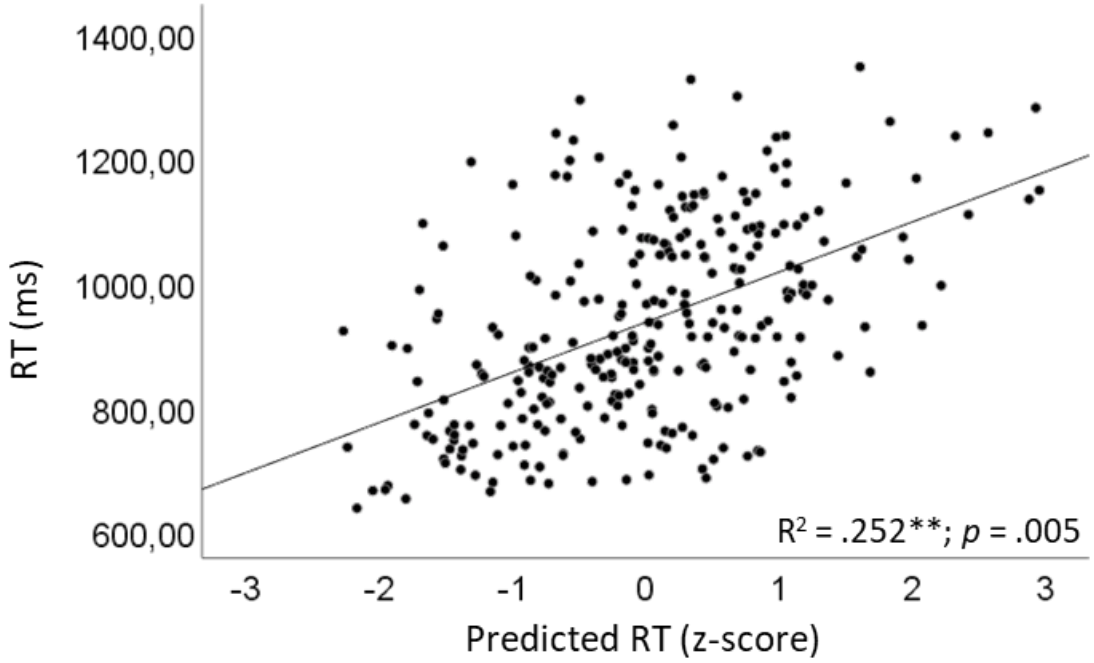

Figure 7. – High gamma power and connectivity features predicted RTs.

Multiple linear regression. A regression equation was calculated to predict the RTs in response to the stimulation of the intact and blind hemifields. There was a collective significant effect between the high gamma and HFOs power, correlations and GC obtained between pairs of ROIs. The graph illustrates the correspondence between the actual RTs (y-axis) and the predicted RTs in z-score (x-axis). – Figure 7

Connectivity measure	ROI	Frequency	B	β	t	*p*	Pearson coefficient	Partial correlation
Correlation between ROIs (undirected connectivity)	Th-lh ↔ Am-lh	50-90Hz	374,44	,172	1.12	.262	-.124*	.073
	Th-lh ↔ V1-lh	50-90Hz	-274.89	-.167	-1.73	.085	-.144*	-.112
	Th-lh ↔ V1-lh	90-120Hz	-290.94	-.116	-0.67	.502	-.138*	-.044
	Am-lh ↔ V1-lh	50-90Hz	240.13	.081	.86	.389	.131*	.056
	Am-lh ↔ V1-lh	90-120Hz	724.81	2.064	2.06	.040*	-.031	.133
	Th-rh ↔ Am-rh	50-90Hz	795.96	.305	2.09	.038*	.286**	.135
	Th-rh ↔ V1-lh	50-90Hz	363.27	.158	1.23	.219	.140*	.080
	Th-rh ↔ V1-lh	90-120Hz	-174.88	-.088	-.79	.431	-.196**	-.051
	Am-rh ↔ V1-lh	90-120Hz	718,05	,404	2.36	. 019*	-.044	.152
GC	Th-lh ← Am-lh	90-120Hz	-230.26	-.042	-.67	.512	-.121*	-.043
	Th-lh → V1-lh	90-120Hz	918.68	.169	2.57	.011*	.163**	.165

Tableau 1. – Independent variables of the regression analysis in predicting RTs (+)

(+) Only variables that significantly correlated with the dependent variable (RT) or significantly contributed to the regression to predict RTs were reported in the table. * $p < 0.05$, ** $p < 0.01$

References

Ajina, S., Pollard, M., and Bridge, H. (2020). The Superior Colliculus and Amygdala Support Evaluation of Face Trait in Blindsight. Front. Neurol. 11.

Allison, T., Puce, A., and McCarthy, G. (2000). Social perception from visual cues: Role of the STS region. Trends Cogn. Sci. 4, 267–278.

Andersen, L.M., Jerbi, K., and Dalal, S.S. (2020). Can EEG and MEG detect signals from the human cerebellum? Neuroimage 215.

Andino, S.L.G., Menendez, R.G. de P., Khateb, A., Landis, T., and Pegna, A.J. (2009). Electrophysiological correlates of affective blindsight. Neuroimage 44, 581–589.

Baizer, J.S., Ungerleider, L.G., and Desimone, R. (1991). Organization of visual inputs to the inferior temporal and posterior parietal cortex in macaques. J. Neurosci. 11, 168–190.

Balderston, N.L., Schultz, D.H., Baillet, S., and Helmstetter, F.J. (2013). How to detect amygdala activity with magnetoencephalography using source imaging. J. Vis. Exp.

Bastin, J., Deman, P., David, O., Gueguen, M., Benis, D., Minotti, L., Hoffman, D., Combrisson, E., Kujala, J., Perrone-Bertolotti, M., et al. (2017). Direct Recordings from Human Anterior Insula Reveal its Leading Role within the Error-Monitoring Network. Cereb. Cortex 27, 1545–1557.

Bauer, F., Cheadle, S.W., Parton, A., Müller, H.J., and Usher, M. (2009). Gamma flicker triggers attentional selection without awareness. Proc. Natl. Acad. Sci. U. S. A. 106, 1666–1671.

Bayle, D.J., Henaff, M.-A., and Krolak-Salmon, P. (2009). Unconsciously perceived fear in peripheral vision alerts the limbic system: a MEG study. PLoS One 4, e8207.

Bayle, D.J., Schoendorff, B., Hénaff, M.-A., and Krolak-Salmon, P. (2011). Emotional facial expression detection in the peripheral visual field. PLoS One 6, e21584.

Bertini, C., Cecere, R., and Làdavas, E. (2013). I am blind, but I "see" fear. Cortex. 49, 985–993.

Bertini, C., Pietrelli, M., Braghittoni, D., and Làdavas, E. (2018). Pulvinar Lesions Disrupt Fear-Related Implicit Visual Processing in Hemianopic Patients. Front. Psychol. 9, 2329.

Bertini, C., Cecere, R., and Làdavas, E. (2019). Unseen fearful faces facilitate visual discrimination in the intact field. Neuropsychologia 128, 58–64.

Bettencourt, K.C., and Xu, Y. (2013). The role of transverse occipital sulcus in scene perception and its relationship to object individuation in inferior intraparietal sulcus. J. Cogn. Neurosci. 25, 1711–1722.

Bocchio, M., Nabavi, S., and Capogna, M. (2017). Synaptic Plasticity, Engrams, and Network Oscillations in Amygdala Circuits for Storage and Retrieval of Emotional Memories. Neuron 94, 731–743.

Bogadhi, A.R., Bollimunta, A., Leopold, D.A., and Krauzlis, R.J. (2018). Brain regions modulated during covert visual attention in the macaque. Sci. Rep. 8.

Bogadhi, A.R., Katz, L.N., Bollimunta, A., Leopold, D.A., and Krauzlis, R.J. (2021). Midbrain activity shapes high-level visual properties in the primate temporal cortex. Neuron 109, 690-699.e5.

Breitmeyer, B.G. (2014). Contributions of magno- and parvocellular channels to conscious and non-conscious vision. Philos. Trans. R. Soc. B Biol. Sci. 369.

Brovelli, A., Chicharro, D., Badier, J.M., Wang, H., and Jirsa, V. (2015). Characterization of cortical networks and corticocortical functional connectivity mediating arbitrary visuomotor mapping. J. Neurosci. 35, 12643–12658.

Burra, N., Hervais-Adelman, A., Kerzel, D., Tamietto, M., de Gelder, B., and Pegna, A.J. (2013). Amygdala activation for eye contact despite complete cortical blindness. J. Neurosci. 33, 10483–10489.

Burra, N., Hervais-Adelman, A., Celeghin, A., de Gelder, B., and Pegna, A.J. (2019). Affective blindsight relies on low spatial frequencies. Neuropsychologia 128, 44–49.

Campana, F., Rebollo, I., Urai, A., Wyart, V., and Tallon-Baudry, C. (2016). Conscious Vision Proceeds from Global to Local Content in Goal-Directed Tasks and Spontaneous Vision. J. Neurosci. 36, 5200–5213.

Carus-Cadavieco, M., Gorbati, M., Ye, L., Bender, F., Van Der Veldt, S., Kosse, C., Börgers, C., Lee, S.Y., Ramakrishnan, C., Hu, Y., et al. (2017). Gamma oscillations organize top-down signaling to hypothalamus and enable food seeking. Nature 542, 232–236.

Chica, A.B., Bartolomeo, P., and Lupiáñez, J. (2013). Two cognitive and neural systems for endogenous and exogenous spatial attention. Behav. Brain Res. 237, 107–123.

Claeys, K.G., Lindsey, D.T., De Schutter, E., and Orban, G.A. (2003). A higher order motion region in human inferior parietal lobule: evidence from fMRI. Neuron 40, 631–642.

Colibazzi, T., Posner, J., Wang, Z., Gorman, D., Gerber, A., Yu, S., Zhu, H., Kangarlu, A., Duan, Y., Russell, J.A., et al. (2010). Neural Systems Subserving Valence and Arousal During the Experience of Induced Emotions. Emotion 10, 377–389.

Combrisson, E., Vallat, R., O'Reilly, C., Jas, M., Pascarella, A., Saive, A.L., Thiery, T., Meunier, D., Altukhov, D., Lajnef, T., et al. (2019). Visbrain: A multi-purpose GPU-accelerated open-source suite for multimodal brain data visualization. Front. Neuroinform. 13.

Corbetta, M., and Shulman, G.L. (2002). Control of goal-directed and stimulus-driven attention in the brain. Nat. Rev. Neurosci. 3, 201–215.

Corbetta, M., Patel, G., and Shulman, G.L. (2008). The Reorienting System of the Human Brain: From Environment to Theory of Mind. Neuron 58, 306–324.

Cornwell, B.R., Carver, F.W., Coppola, R., Johnson, L., Alvarez, R., and Grillon, C. (2008). Evoked amygdala responses to negative faces revealed by adaptive MEG beamformers. Brain Res. 1244, 103–112.

Cowey, A., Alexander, I., and Stoerig, P. (2008). A blindsight conundrum: how to respond when there is no correct response. Neuropsychologia 46, 870–878.

D'Hondt, F., Lassonde, M., Collignon, O., Lepore, F., Honoré, J., and Sequeira, H. (2013). "Emotions guide us": behavioral and MEG correlates. Cortex. 49, 2473–2483.

Dacey, D.M., and Petersen, M.R. (1992). Dendritic field size and morphology of midget and parasol ganglion cells of the human retina. Proc. Natl. Acad. Sci. U. S. A. 89, 9666–9670.

Dalal, S., Jerbi, K., Bertrand, O., Adam, C., Ducorps, A., Schwartz, D., Martinerie, J., Lachaux, J.-P., and Dalal, S.S. (2013). Simultaneous MEG-intracranial EEG: New insights into the ability of MEG to capture oscillatory modulations in the neocortex and the hippocampus. Epilepsy Behav. 10, 1016.

Danckert, J., and Rossetti, Y. (2005). Blindsight in action: what can the different sub-types of blindsight tell us about the control of visually guided actions? Neurosci. Biobehav. Rev. 29, 1035–1046.

Dehaene, S., Sergent, C., and Changeux, J.-P. (2003). A neuronal network model linking subjective reports and objective physiological data during conscious perception. Proc. Natl. Acad. Sci. U. S. A. 100, 8520–8525.

Dehaene, S., Changeux, J.P., Naccache, L., Sackur, J., and Sergent, C. (2006). Conscious, preconscious, and subliminal processing: a testable taxonomy. Trends Cogn. Sci. 10, 204–211.

Dumas, T., Dubal, S., Attal, Y., Chupin, M., Jouvent, R., Morel, S., and George, N. (2013). MEG Evidence for Dynamic Amygdala Modulations by Gaze and Facial Emotions. PLoS One 8.

Fiebelkorn, I.C., Pinsk, M.A., and Kastner, S. (2018). A Dynamic Interplay within the Frontoparietal Network Underlies Rhythmic Spatial Attention. Neuron 99, 842-853.e8.

Fischl, B., Salat, D.H., Busa, E., Albert, M., Dieterich, M., Haselgrove, C., Van Der Kouwe, A., Killiany, R., Kennedy, D., Klaveness, S., et al. (2002). Whole brain segmentation: Automated labeling of neuroanatomical structures in the human brain. Neuron 33, 341–355.

Fischl, B., Van Der Kouwe, A., Destrieux, C., Halgren, E., Ségonne, F., Salat, D.H., Busa, E., Seidman, L.J., Goldstein, J., Kennedy, D., et al. (2004). Automatically Parcellating the Human Cerebral Cortex. Cereb. Cortex.

Fox, D.M., Goodale, M.A., and Bourne, J.A. (2020). The Age-Dependent Neural Substrates of Blindsight. Trends Neurosci. 43, 242–252.

Frank, D.W., and Sabatinelli, D. (2014). Human thalamic and amygdala modulation in emotional scene perception. Brain Res. 1587, 69–76.

Gainotti, G. (2012). Unconscious processing of emotions and the right hemisphere. Neuropsychologia 50, 205–218.

Garrido, M.I. (2012). Brain connectivity: The feel of blindsight. Curr. Biol. 22.

Garrido, M.I., Barnes, G.R., Sahani, M., and Dolan, R.J. (2012). Functional evidence for a dual route to amygdala. Curr. Biol. 22, 129–134.

de Gelder, B., and Poyo Solanas, M. (2021). A computational neuroethology perspective on body and expression perception. Trends Cogn. Sci.

de Gelder, B., Vroomen, J., Pourtois, G., and Weiskrantz, L. (1999). Non-conscious recognition of affect in the absence of striate cortex. Neuroreport 10, 3759–3763.

Goodwin, D. (2014). Homonymous hemianopia: Challenges and solutions. Clin. Ophthalmol. 8, 1919–1927.

Gramfort, A., Luessi, M., Larson, E., Engemann, D.A., Strohmeier, D., Brodbeck, C., Goj, R., Jas, M., Brooks, T., Parkkonen, L., et al. (2013). MEG and EEG data analysis with MNE-Python. Front. Neurosci. 7.

Guo, X., Jin, Z., Feng, X., and Tong, S. (2014). Enhanced effective connectivity in mild occipital stroke patients with hemianopia. IEEE Trans. Neural Syst. Rehabil. Eng. 22, 1210–1217.

Hadid, V., and Lepore, F. (2017). From Cortical Blindness to Conscious Visual Perception: Theories on Neuronal Networks and Visual Training Strategies. Front. Syst. Neurosci. 11, 64.

Hämäläinen, M.S., and Ilmoniemi, R.J. (1994). Interpreting magnetic fields of the brain: minimum norm estimates. Med. Biol. Eng. Comput. 32, 35–42.

Hanlon, F.M., Weisend, M.P., Huang, M., Lee, R.R., Moses, S.N., Paulson, K.M., Thoma, R.J., Miller, G.A., and Cañive, J.M. (2003). A non-invasive method for observing hippocampal function. Neuroreport 14, 1957–1960.

Headley, D.B., and Pare, D. (2013). In sync: gamma oscillations and emotional memory. Front. Behav. Neurosci. 0, 170.

Hendry, S.H., and Reid, R.C. (2000). The koniocellular pathway in primate vision. Annu. Rev. Neurosci. 23, 127–153.

Heywood, C., and Kentridge, R. (2000). Affective blindsight? Trends Cogn. Sci. 4, 125–126.

Hung, Y., Smith, M. Lou, Bayle, D.J., Mills, T., Cheyne, D., and Taylor, M.J. (2010). Unattended emotional faces elicit early lateralized amygdala-frontal and fusiform activations. Neuroimage 50, 727–733.

Jensen, O., Kaiser, J., and Lachaux, J.P. (2007). Human gamma-frequency oscillations associated with attention and memory. Trends Neurosci. 30, 317–324.

Kajal, D.S., Fioravanti, C., Elshahabi, A., Ruiz, S., Sitaram, R., and Braun, C. (2020). Involvement of top-down networks in the perception of facial emotions: A magnetoencephalographic investigation. Neuroimage 222, 117075.

Karnath, H.O. (2001). New insights into the functions of the superior temporal cortex. Nat. Rev. Neurosci. 2, 568–576.

Kastner, S., Fiebelkorn, I.C., and Eradath, M.K. (2020). Dynamic pulvino-cortical interactions in the primate attention network. Curr. Opin. Neurobiol. 65, 10–19.

Van Kerkoerle, T., Self, M.W., Dagnino, B., Gariel-Mathis, M.A., Poort, J., Van Der Togt, C., and Roelfsema, P.R. (2014). Alpha and gamma oscillations characterize feedback and feedforward processing in monkey visual cortex. Proc. Natl. Acad. Sci. U. S. A. 111, 14332–14341.

Kokinous, J., Tavano, A., Kotz, S.A., and Schröger, E. (2017). Perceptual integration of faces and voices depends on the interaction of emotional content and spatial frequency. Biol. Psychol. 123, 155–165.

Koller, K., Rafal, R.D., Platt, A., and Mitchell, N.D. (2019). Orienting toward threat: Contributions of a subcortical pathway transmitting retinal afferents to the amygdala via the superior colliculus and pulvinar. Neuropsychologia 128.

Kunimatsu, J., and Tanaka, M. (2010). Roles of the primate motor thalamus in the generation of antisaccades. J. Neurosci. 30, 5108–5117.

Lahnakoski, J.M., Glerean, E., Salmi, J., Jääskeläinen, I.P., Sams, M., Hari, R., and Nummenmaa, L. (2012). Naturalistic fMRI mapping reveals superior temporal sulcus as the hub for the distributed brain network for social perception. Front. Hum. Neurosci. 6.

LeDoux, J.E. (2000). Emotion circuits in the brain. Annu. Rev. Neurosci. 23, 155–184.

LeDoux, J.E., Michel, M., and Lau, H. (2020). A little history goes a long way toward understanding why we study consciousness the way we do today. Proc. Natl. Acad. Sci. U. S. A. 117, 6976–6984.

Leopold, D.A. (2012). Primary Visual Cortex: Awareness and Blindsight. Annu. Rev. Neurosci. 35, 91–109.

Lithari, C., Moratti, S., and Weisz, N. (2015). Thalamocortical interactions underlying visual fear conditioning in humans. Hum. Brain Mapp. 36, 4592–4603.

Liu, T.-Y., Chen, Y.-S., Hsieh, J.-C., and Chen, L.-F. (2015). Asymmetric engagement of amygdala and its gamma connectivity in early emotional face processing. PLoS One 10, e0115677.

Luo, Q., Holroyd, T., Jones, M., Hendler, T., and Blair, J. (2007). Neural dynamics for facial threat processing as revealed by gamma band synchronization using MEG. Neuroimage 34, 839–847.

Luo, Q., Holroyd, T., Majestic, C., Cheng, X., Schechter, J., and James Blair, R. (2010). Emotional automaticity is a matter of timing. J. Neurosci. 30, 5825–5829.

Lyon, D.C., Nassi, J.J., and Callaway, E.M. (2010). A disynaptic relay from superior colliculus to dorsal stream visual cortex in macaque monkey. Neuron 65, 270–279.

Maris, E., and Oostenveld, R. (2007). Nonparametric statistical testing of EEG- and MEG-data. J. Neurosci. Methods 164, 177–190.

Mashour, G.A., Roelfsema, P., Changeux, J.P., and Dehaene, S. (2020). Conscious Processing and the Global Neuronal Workspace Hypothesis. Neuron 105, 776–798.

Maunsell, J.H., Ghose, G.M., Assad, J.A., McAdams, C.J., Boudreau, C.E., and Noerager, B.D. (1999). Visual response latencies of magnocellular and parvocellular LGN neurons in macaque monkeys. Vis. Neurosci. 16, 1–14.

McAfee, S.S., Liu, Y., Dhamala, M., and Heck, D.H. (2018). Thalamocortical communication in the awake mouse visual system involves phase synchronization and rhythmic spike synchrony at high gamma frequencies. Front. Neurosci. 12.

McFadyen, J., Mermillod, M., Mattingley, J.B., Halász, V., and Garrido, M.I. (2017). A rapid subcortical amygdala route for faces irrespective of spatial frequency and emotion. J. Neurosci. 37, 3864–3874.

McFadyen, J., Mattingley, J.B., and Garrido, M.I. (2019). An afferent white matter pathway from the pulvinar to the amygdala facilitates fear recognition. Elife 8.

McFadyen, J., Dolan, R.J., and Garrido, M.I. (2020). The influence of subcortical shortcuts on disordered sensory and cognitive processing. Nat. Rev. Neurosci. 1–13.

Méndez-Bértolo, C., Moratti, S., Toledano, R., Lopez-Sosa, F., Martínez-Alvarez, R., Mah, Y.H., Vuilleumier, P., Gil-Nagel, A., and Strange, B.A. (2016). A fast pathway for fear in human amygdala. Nat. Neurosci. 19.

Meunier, D., Pascarella, A., Altukhov, D., Jas, M., Combrisson, E., Lajnef, T., Bertrand-Dubois, D., Hadid, V., Alamian, G., Alves, J., et al. (2020). NeuroPycon: An open-source python toolbox for fast multi-modal and reproducible brain connectivity pipelines. Neuroimage 219.

Michalareas, G., Vezoli, J., van Pelt, S., Schoffelen, J.M., Kennedy, H., and Fries, P. (2016). Alpha-Beta and Gamma Rhythms Subserve Feedback and Feedforward Influences among Human Visual Cortical Areas. Neuron 89, 384–397.

Morris, J.S., Öhman, A., and Dolan, R.J. (1999). A subcortical pathway to the right amygdala mediating “unseen” fear. Proc. Natl. Acad. Sci. U. S. A. 96, 1680–1685.

Morris, J.S., DeGelder, B., Weiskrantz, L., and Dolan, R.J. (2001). Differential extrageniculostriate and amygdala responses to presentation of emotional faces in a cortically blind field. Brain 124, 1241–1252.

Mu, E., and Crewther, D. (2020). Occipital Magnocellular VEP Non-linearities Show a Short Latency Interaction Between Contrast and Facial Emotion. Front. Hum. Neurosci. 14.

Nicol, J.R., Perrotta, S., Caliciuri, S., and Wachowiak, M.P. (2013). Emotion-specific modulation of early visual perception. Cogn. Emot. 27, 1478–1485.

Pedersini, C.A., Guardia-Olmos, J., Montala-Flaquer, M., Cardobi, N., Sanchez-Lopez, J., Parisi, G., Savazzi, S., and Marzi, C.A. (2020). Functional interactions in patients with hemianopia: A graph theory-based connectivity study of resting fMRI signal. PLoS One 15.

Pegna, A.J., Khateb, A., Lazeyras, F., and Seghier, M.L. (2005). Discriminating emotional faces without primary visual cortices involves the right amygdala.

Pizzo, F., Roehri, N., Medina Villalon, S., Trébuchon, A., Chen, S., Lagarde, S., Carron, R., Gavaret, M., Giusiano, B., McGonigal, A., et al. (2019). Deep brain activities can be detected with magnetoencephalography. Nat. Commun. 10, 1–13.

Prete, G., Laeng, B., and Tommasi, L. (2016). Modulating adaptation to emotional faces by spatial frequency filtering. Psychol. Res.

Quraan, M.A., Moses, S.N., Hung, Y., Mills, T., and Taylor, M.J. (2011). Detection and localization of hippocampal activity using beamformers with MEG: A detailed investigation using simulations and empirical data. Hum. Brain Mapp. 32, 812–827.

Redinbaugh, M.J., Phillips, J.M., Kambi, N.A., Mohanta, S., Andryk, S., Dooley, G.L., Afrasiabi, M., Raz, A., and Saalmann, Y.B. (2020). Thalamus Modulates Consciousness via Layer-Specific Control of Cortex. Neuron.

Richter, C.G., Thompson, W.H., Bosman, C.A., and Fries, P. (2017). Top-down beta enhances bottom-up gamma. J. Neurosci. 37, 6698–6711.

Ries, A.J., and Hopfinger, J.B. (2011). Magnocellular and parvocellular influences on reflexive attention. Vision Res. 51, 1820–1828.

Rigoulot, S., D'Hondt, F., Defoort-Dhellemmes, S., Despretz, P., Honoré, J., and Sequeira, H. (2011). Fearful faces impact in peripheral vision: Behavioral and neural evidence. Neuropsychologia 49, 2013–2021.

Rohr, M., and Wentura, D. (2014). Spatial frequency filtered images reveal differences between masked and unmasked processing of emotional information. Conscious. Cogn. 29, 141–158.

Roux, F., Wibra, M., Singer, W., Aru, J., and Uhlhaas, P.J. (2013). The phase of thalamic alpha activity modulates cortical gamma-band activity: Evidence from resting-state MEG recordings. J. Neurosci. 33, 17827–17835.

Sahraie, A., Hibbard, P.B., Trevethan, C.T., Ritchie, K.L., and Weiskrantz, L. (2010). Consciousness of the first order in blindsight. Proc. Natl. Acad. Sci. U. S. A. 107, 21217–21222.

Salti, M., Monto, S., Charles, L., King, J.-R., Parkkonen, L., and Dehaene, S. (2015). Distinct cortical codes and temporal dynamics for conscious and unconscious percepts. Elife 4, 1–52.

Schmid, M.C., Mrowka, S.W., Turchi, J., Saunders, R.C., Wilke, M., Peters, A.J., Ye, F.Q., and Leopold, D.A. (2010). Blindsight depends on the lateral geniculate nucleus. Nature 466, 373–377.

Schurger, A., Cowey, A., and Tallon-Baudry, C. (2006). Induced gamma-band oscillations correlate with awareness in hemianopic patient GY. Neuropsychologia 44, 1796–1803.

Sedley, W., and Cunningham, M.O. (2013). Do cortical gamma oscillations promote or suppress perception? An under-asked question with an over-assumed answer. Front. Hum. Neurosci. 7.

Van den Stock, J., Tamietto, M., Zhan, M., Heinecke, A., Hervais-Adelman, A., Legrand, L.B., Pegna, A.J., and de Gelder, B. (2014). Neural correlates of body and face perception following bilateral destruction of the primary visual cortices. Front. Behav. Neurosci. 8.

Striemer, C.L., Whitwell, R.L., and Goodale, M.A. (2019). Affective blindsight in the absence of input from face processing regions in occipital-temporal cortex. Neuropsychologia 128, 50–57.

Tallon-Baudry, C. (2009). The roles of gamma-band oscillatory synchrony in human visual cognition. Front. Biosci. (Landmark Ed. 14, 321–332.

Tamietto, M., Pullens, P., de Gelder, B., Weiskrantz, L., and Goebel, R. (2012). Subcortical connections to human amygdala and changes following destruction of the visual cortex. Curr. Biol. 22, 1449–1455.

Tapia, E., and Breitmeyer, B.G. (2011). Visual consciousness revisited: magnocellular and parvocellular contributions to conscious and nonconscious vision. Psychol. Sci. 22, 934–942.

Taylor, J.G., and Fragopanagos, N.F. (2005). The interaction of attention and emotion. Neural Networks 18, 353–369.

Tran, A., MacLean, M.W., Hadid, V., Lazzouni, L., Nguyen, D.K., Tremblay, J., Dehaes, M., and Lepore, F. (2019). Neuronal mechanisms of motion detection underlying blindsight assessed by functional magnetic resonance imaging (fMRI). Neuropsychologia 128, 187–197.

Urbanski, M., Coubard, O.A., and Bourlon, C. (2014). Visualizing the blind brain: brain imaging of visual field defects from early recovery to rehabilitation techniques. Front. Integr. Neurosci. 8, 74.

Vuilleumier, P. (2005). How brains beware: Neural mechanisms of emotional attention. Trends Cogn. Sci. 9, 585–594.

Vukelić, M., Lingelbach, K., Pollmann, K., and Peissner, M. (2021). Oscillatory eeg signatures of affective processes during interaction with adaptive computer systems. Brain Sci. 11, 1–21.

Ward, R., Danziger, S., and Bamford, S. (2005). Response to visual threat following damage to the pulvinar. Curr. Biol. 15, 571–573.

Warner, C.E., Kwan, W.C., Wright, D., Johnston, L.A., Egan, G.F., and Bourne, J.A. (2015). Preservation of vision by the pulvinar following early-life primary visual cortex lesions. Curr. Biol. 25, 424–434.

Weiskrantz, L. (2004). Roots of blindsight. Prog. Brain Res. 144, 229–241.

Weiskrantz, L., Barbur, J.L., and Sahraie, A. (1995). Parameters affecting conscious versus unconscious visual discrimination with damage to the visual cortex (V1). Proc. Natl. Acad. Sci. U. S. A. 92, 6122–6126.

Van Der Werf, J., Jensen, O., Fries, P., and Medendorp, W.P. (2008). Gamma-band activity in human posterior parietal cortex encodes the motor goal during delayed prosaccades and antisaccades. J. Neurosci. 28, 8397–8405.

Williams, L.M., Das, P., Liddell, B.J., Kemp, A.H., Rennie, C.J., and Gordon, E. (2006). Mode of functional connectivity in amygdala pathways dissociates level of awareness for signals of fear. J. Neurosci. 26, 9264–9271.

Yantis, S., and Hillstrom, A.P. (1994). Stimulus-driven attentional capture: Evidence from equiluminant visual objects. J. Exp. Psychol. Hum. Percept. Perform. 20, 95–107.

Yuval-Greenberg, S., Tomer, O., Keren, A.S., Nelken, I., and Deouell, L.Y. (2008). Transient Induced Gamma-Band Response in EEG as a Manifestation of Miniature Saccades. Neuron 58, 429–441.

Chapter 5:

Article 3: Decoding the Subcortical Neural Mechanisms of Seen and Unseen Affective Perception in Blindsight

Article 3. Decoding the Subcortical Neural Mechanisms of Seen and Unseen Affective Perception in Blindsight

Vanessa Hadid[1,3,8], Annalisa Pascarella[3,4,6], Tarek Lajnef[3,6], Myriam Sehraoui[2,3], Dang Khoa Nguyen[5], Karim Jerbi[2,3,7], Franco Lepore[2,7]

[1]Département de Sciences Biomédicales, Université de Montréal,

[2]Département de Psychologie, Université de Montréal

[3]Computational and Cognitive Neuroscience Lab (CoCo Lab)

[4]Italian National Research Council, Rome, Italy

[5]Service de neurologie, Centre Hospitalier de l'Université de Montréal (CHUM)

[6]Co-second author

[7]Co-last author

[8]Lead contact

Abstract

The case of patient SJ presenting a unique form of affective-blindsight for natural complex scenes suggests the involvement of subcortical pathways in conscious and unconscious perception. However, the underlying cognitive processes remained elusive. Thus, we aimed to probe the cognitive mechanisms following SJ's V1-resection by characterizing and decoding the source time course of visual evoked responses for conscious and unconscious perception using magnetoencephalography, source reconstruction, and machine learning. The results showed that the intact V1 process unseen information through inter-hemispheric transfer, while seen pictures triggered enhanced perceptual maintenance in V1, the thalami, and amygdalae. Moreover, we found that the thalamus extracted unconscious affective-specific information as early as 10 ms post-stimulus for peripheral stimuli which was associated with a fast thalamo-amygdala pathway. Taken together, this study proposes different cognitive and neural processes that support affective conscious and unconscious perception following a V1-lesion.

Introduction

Following a lesion to the primary visual cortex (V1), some patients preserve the ability to process information in their blind hemifield without visual awareness which behavior termed blindsight (Weiskrantz, 2004; Weiskrantz et al., 1995) is thought to be driven by subcortical secondary pathways involving the thalamus and extra-striate regions (Bridge et al., 2008; Ptito and Leh, 2007; Tran et al., 2019). The pulvinar, the biggest structure in the thalamus (Fox et al., 2020), has been thought to rapidly project its activity to the amygdala (Garrido et al., 2012; McFadyen et al., 2020) when blindsight patients accurately process affective content, which neurological conditions is referred as affective-blindsight (de Gelder et al., 1999; Heywood and Kentridge, 2000). To assess the pathways of affective-blindsight, we previously investigated the neural mechanisms in patient SJ who presented a unique form of affective-blindsight for natural complex scenes (Hadid et al., in preparation). We've shown that thalamo-amygdala and extrastriate connectivity characterized non-specific and/or specific affective processing in the absence of visual awareness. Moreover, we've confirmed that communication between the thalamus and the intact V1 was associated with visual consciousness. In order to determine the cognitive processes that could explain these findings, we will now assess the impact of SJ's V1-resection on conscious and unconscious affective perception by decoding the time course of visual evoked responses (VER).

In fact, VER are prevailing cognitive indicators of how differences in perceptual characteristics, attentional load, awareness, and affective content are processed. For instance, an early event-related component evoked as soon as 80 ms in the amygdala thought to be independent of visual consciousness has been found for fearful faces (Bayle et al., 2009; Méndez-Bértolo et al., 2016). The striate cortex has been linked to the early visual component C1 peaking around 90 ms, while the thalamus has been associated with the P50, a subcortical audio-visual component (Starke et al., 2020). Early components, such as P1 and N1, peaking around 100 ms, can reflect extra-striate sensory encoding, lateralization, and early attentional processes (Hillyard and Anllo-Vento, 1998; Klimesch, 2011; Di Russo et al., 2002). On the other hand, later negative components around 200 ms have been associated with attention, awareness, and feedback processing (Koivisto and Grassini, 2016; Pins and Ffytche, 2003; Railo et al., 2015). Moreover, positive potentials after 300 ms, e.g., P3, can reflect multiple higher-order cognitive processes (Patel and Azzam, 2005; Railo et al., 2011; Rutiku et al., 2015) and emotional attentional stimuli capture (Hajcak et al., 2013;

Schönwald and Müller, 2014). As for semantic content and encoding, it has been associated with negativity after 400 ms as the N400 (Taylor and Fragopanagos, 2005). Specifically, VER after 100 ms are postulated to be instigated from extra-striate regions. Thus, any VER in the thalamus, amygdala, or V1 observed after 100 ms is thought to show prior extra-striate cortical processing through top-down feedback (Di Russo et al., 2002, 2008) which we hypothesize to contribute to conscious and unconscious conditions (Koivisto et al., 2010). In fact, studies in neurotypical individuals have suggested that the distinction between unconscious and conscious perception could be mediated by the difference between early and late processing and by the dynamic processes involving bottom-up, recurrent, and top-down activity (Förster et al., 2020; Koivisto et al., 2010; Mashour et al., 2020; Moratti et al., 2011; Rutiku et al., 2016). Nonetheless, the recruitment of such neural mechanisms in blindsight and human subcortical structures is poorly understood, which we will address by employing temporal decoding and generalization (King et al., 2016).

As for now, the electrophysiological literature is divided on whether stimulation of the blind hemifield induces reliable VER (Cecere et al., 2014; Kavcic et al., 2015; Sanchez-Lopez et al., 2017). These controversies can be due to differences in experimental paradigms, lack of source analysis, and heterogeneity between blindsight patients (Hadid and Lepore, 2017). Hence, the aim of this study is to characterize the source time course of subcortical early and late VER in patient SJ in order to decode temporal and spatial signatures of evoked conscious and unconscious activity using magnetoencephalography (MEG). The effects of visual awareness, lateralization and inter-hemispheric transfer, eccentricity and affective condition using natural complex scenes will be tackled.

Experimental Procedures

For all details regarding the following sections: Case study, Procedure, and MEG preprocessing and source reconstruction, please refer to (Hadid et al., in preparation – study 2).

Case study

Blindsight patient SJ, who was 22 years old at the time of this study, has left homonymous hemianopia (HH) with no macular sparing. His cortical blindness resulted from resections at age 15 of the right superior occipital gyrus, cuneus, and lingual gyrus, including a complete V1

resection. In our previous paper, we demonstrated that SJ presented affective-blindsight as he was able to discriminate between affective natural scenes without any visual awareness which abilities weren't yet reported in the literature. In fact, we showed that SJ performed above chance-level to unseen affective information in his left blind hemifield. Reactions times were also modulated by the presented condition as his responses were faster for seen compared to unseen pictures and were faster within both hemifields for correct compared to incorrect responses, near periphery compared to paracentral stimuli, and unpleasant pictures compared to pleasant pictures. We've concluded from the behavioral results that unconscious processing seems to utilize the magnocellular pathway, while conscious processing seems to utilize both magnocellular and parvocellular systems. Specifically, these residual abilities were driven by extra-striate pathways as the surgery resulted in the complete resection of V1. Therefore, SJ's neurological condition offered a unique opportunity to study the neural and cognitive mechanisms of conscious and unconscious affective processing by comparing the activity triggered by stimulation of the intact and blind hemifields.

Experimental design

SJ was tested on a 3-alternative forced-choice affective discrimination paradigm in which unpleasant, neutral, and pleasant natures scenes from the International Affective Picture System (IAPS) were presented. 300 pictures were randomly presented for 1000 ms either in the paracentral or near the periphery i.e., at 6° or 12° of eccentricity from the fixation cross, respectively, of the intact right visual hemifield and blind left visual hemifield. Pictures were presented with an inter-stimulus interval (ISI) that randomly varied between 2000 and 2500 ms. The onset of the picture presentation was accompanied by a white noise of 100 ms which indicated that a response was needed as fast as possible while SJ's fixation had to remain on the cross. All trials associated with saccades to the left or right were removed from further analysis (17 trials were removed on a total of 300 trials). The paradigm required reflexive covert attention which restricted predictions of the picture's position. Thus, attentional processing of the picture was made only after stimulus onset and reorientation of the attentional allocation. When SJ didn't perceive any picture after hearing the noise, he oriented his attention to his left blind hemifield and had to guess the 'correct' answer. Subsequent analyses compared the activity evoked from both hemifields and eccentricities and all affective conditions (Figure 1).

MEG data acquisition

MEG data and eye and heart-related activities were acquired during the affective discrimination task using a 275-channel whole-head MEG system (CTF MEG Int, British Columbia, Canada). The continuous data were recorded with a sampling rate of 1200 Hz. We identified the spatial positions of the fiducial coils and of about 300 scalp points, by means of a 3D digitizer system (Polhemus Isotrack, Polhemus, Colchester, VT, USA), which was subsequently used for the anatomical registration with the anatomical MRI data.

MEG preprocessing and source reconstruction

MEG data preprocessing and source construction were assessed using standard pipelines implemented in the open-source NeuroPycon toolbox (Meunier et al., 2020), and tools from MNE python (Gramfort et al., 2013). First, the data were filtered offline and eye and heart-related artifacts were removed using independent components analysis and visual inspection (17/300 trials). Then, the data was segmented into 283 trials including a baseline period of 200 ms pre-stimulus and post-stimulus period of 800 ms, for a total duration of 1000 ms. The inverse method was subsequently applied to the 283 trials to compute the event-related activity for all cortical and subcortical nodes.

In order to achieve this fine spatio-temporal event-related precision, the inverse solution was conducted by computing (1) the structural segmentation of the patient's T1-weighted MRI images using the lead field matrix with the Boundary Element Method (BEM) and Freesurfer (Fischl et al., 2002), (2) the noise covariance matrix and (3) the weighted Minimum Norm Estimate (wMNE) (Hämäläinen and Ilmoniemi, 1994). Hence, the resulting source reconstruction matrix contained the estimated time series of all mixed source space dipoles for every epoch. The cortical and subcortical source space included 7328 nodes in both hemispheres. For further analysis, we computed the activity in 5 ROIs, including all 58 nodes within the intact calcarine sulcus (V1), 67 nodes in the left thalamus, 56 nodes in the right thalamus, 11 nodes in the left amygdala, and 15 nodes in the right amygdala. The cortical and subcortical MEG activities projected on the brain were visualized using the open-source Visbrain package (Combrisson et al., 2019).

Analysis of visual evoked responses (VER)

The single-trial VER over time for each node were extracted from the source time series. A first analysis was performed where the signal was averaged across nodes within a specific ROI and

computed as z-scores with respect to the baseline over the entire time window of 1000 ms. Thus, the z-transformed scores were calculated for each ROI, i.e., the left calcarine sulcus (V1-lh), the left thalamus (Th-lh), the right thalamus (Th-rh), the left amygdala (Am-lh) and the right amygdala (Am-rh). Cluster-based permutation over time was used to assess differences between conditions.

A second analysis was conducted in which we selected for each cluster of interest one specific time point representing the strongest difference between conditions. The VER for every single node at these specific instants was investigated, i.e., the differences between conditions across nodes (58 nodes for V1-lh, 67 nodes for the Th-lh, 56 nodes for the Th-rh, and 11 nodes for the Am-lh and 15 nodes for the Am-rh). Visual comparisons between conditions were plotted as t-values using a 2-sample t-test showing differences in the signal amplitude associated with either a positive or negative deflection. Statistical comparisons between conditions across nodes were computed using single-trial binary classification.

Finally, to assess the neuronal temporal organization within each ROI, we computed temporal decoding and temporal generalization using the VER across time and nodes as features. This method was used for all comparisons, but only significant comparisons are shown and discussed in the results. Cluster-based permutation, binary classification, temporal decoding, and temporal generalization are described in the statistical assessment section.

Single-trial functional connectivity (FC) analysis between ROIs

We conducted directed functional connectivity (FC) analysis by computing the conditional covariance-based Granger causality (GC) measures using the single-trial VER. The causal FC was performed to assess the temporal causal relation between two regions, X and Y, where X exerts a causal influence on Y. FC results were interpreted as statistical predictions of the future VER of one ROI based on the past VER of another ROI, given the cognitive processes involved. Nonetheless, these interpretations exclude assumptions about structural connectivity.

To assess the GC measures, we computed (1) the total Granger interdependence which had to be superior to 0 informing us about the undirected connectivity between ROIs, and (2) the relations between two ROIs' mutual information and conditional entropies using the directed connectivity based on Brovelli's et al., paper (Brovelli et al., 2015) implemented in the python toolbox FRamework for Information Theoretical analysis of Electrophysiological data and

statistics (Frites). The covariance-based GC measures were assessed among ROI pairs of single-trial gamma activity over time. The time windows duration (T) used for the calculation of the covariance matrices was optimal at 250 times points and the lag was 25 (i.e., 10 % of T). Directed GC measures were computed for each time point and all combinations of ROI pairs, i.e., Th-lh → Am-lh; Th-lh → left V1; Am-lh → V1-lh; Th-rh → Am-rh; Th-rh → left V1; Am-rh → V1-lh; Th-lh ← Am-lh; Th-lh ← left V1; Am-lh ← V1-lh; Th-rh ← Am-rh; Th-rh ← left V1; Am-rh ← V1-lh. Only significant results are reported in the results.

The dominant directionality in GC between pairs of ROIs and conditions was computed using the difference of influence (DOI). The DOI GC was achieved by assessing the net difference between GC measured from ROI 1 to ROI 2 and the GC measured from ROI 2 to ROI 1. Significant differences over time between conditions in DOI among ROI pairs were assessed using cluster-based permutation analysis.

Cluster-based permutation over time

Cluster-based permutation tests corrected for multiple comparisons developed in MNE-python (Gramfort et al., 2013) were used to assess the statistical differences between conditions over time for the VER averaged across nodes and the DOI GC analyses. Clusters were selected based on the temporal adjacency of independent t-tests exceeding an uncorrected p-value of .05. Furthermore, the multiple-comparison problem was addressed, where each cluster was associated with its maximum t-value and then compared to the largest cluster t-value for each permutation under a null distribution of 1000 permutations using shuffled labels. Differences between conditions were considered significant when the maximum t-value at a time point exceeded the maximum cluster-level statistics using a threshold of p-value = .05 corrected for multiple comparisons (Maris and Oostenveld, 2007).

Single-trial classification

In order to decode the activity between two conditions across the nodes of an ROI, we computed the amplitude of the VER at one time point for each condition. These values were used as features of binary classification in a trial-by-trial supervised machine learning (ML) approach using linear discriminant analysis (LDA). The statistical significance of the performance scores for each node within an ROI was computed using a permutation test (n=100) in order to repeat the classification

process n times using shuffled labels which generates a null distribution that allowed us to identify the threshold that needs to be exceeded for a given level of statistical significance (i.e. p-value) (Combrisson and Jerbi, 2015). All significant classification scores for a p-value < .05 were identified when exceeding the chance-level threshold. The chance-level threshold was assessed by addressing the multiple comparisons problem with max-stats correcting across nodes.

Temporal decoding and generalization

In order to determine the specific role of each structure in processing each condition, the temporal neural processes across nodes within each ROI were assessed using temporal decoding and temporal generalization in a multifeatured supervised ML approach across trials (Dehaene & King, 2016; King & Dehaene, 2014) implemented in MNE-python (Gramfort et al., 2013). In fact, multivariate estimators were fitted to the standardized z-score MEG source data (ntrials x nnodes x ntime) to predict the activity between 2 classes (e.g., seen vs. unseen). All time points and nodes within an ROI were given as features to a logistic regression (LR) that was trained using 10-fold cross-validation in which data was divided into 10 folds and in each iteration, the classifier was trained with 9 folds and tested on the remaining one. Thus, temporal decoding performance scores were achieved by fitting the predictive model at each time point and were estimated as the mean area under the curve (AUC) at the same instance on new trials using cross-validation. Significant AUCs were identified using a binomial test corrected for the number of time points and nodes. The corrected threshold associated with a significant p-value was about 62% for seen against unseen (V1-lh: 62.5%, Th-lh: 62.9%, Th-rh: 62.5%, Am-lh: 61.5%, Am-rh: 61.8%), about 68% for central against periphery and correct against incorrect (V1-lh: 68%, Th-lh: 68%, Th-rh: 68%, Am-lh: 68.7%, Am-rh: 65.2%), and about 71% for prediction between affective conditions (V1-lh: 71%, Th-lh: 72%, Th-rh: 71%, Am-lh: 71%, Am-rh: 69%).

The same predictive model was applied to the temporal generalization analysis (Dehaene & King, 2016; King & Dehaene, 2014). However, instead of only testing the model on the same instant across trials, the classifier is first trained on a specific instant and is tested on its ability to generalize on all other time points across trials. In other words, if the same model can predict what happened at a time T and at a time T + 1, we can conclude that the same neuronal mechanisms are used at distinct time instants to classify between conditions. Thus, using the trained classifier at a specific point in time and generalizing its decoding performances at other time points resulted in a

generalization matrix in which AUC scores are organized in a two-dimensional cross-temporal array represented as the training time by the generalization time. The cells in the matrix diagonal correspond to AUC values when classifiers are trained and tested at the same instant, whereas off-diagonal cells represent the AUC values when classifiers are trained and tested at different instants. Specifically, the former characterizes values of temporal decoding and the latter values of temporal generalization.

RESULTS

Our aim was to assess the cognitive mechanisms of conscious and unconscious affective processing by computing the VER in the intact V1, thalami, and amygdalae. In our analyses, we considered the lateralization and eccentricity of the presentation for affective specific and non-specific differences. Thus, we extracted the single-trial VER for each node. Subsequently, we analyzed the results by (1) averaging the temporal activity across all nodes within an ROI to obtain the single-trial activity over time, (2) selecting specific time points within significant clusters to assess the single-trial differences across all nodes, (3) computing the temporal decoding and (4) generalization analyses using all time points and nodes as features, and finally by (5) assessing the dominant directionality in GC between ROIs. We will be describing all the VER waveforms in terms of their onsets, peak latencies, and amplitudes.

VERs in the intact V1 suggest early and late processing for contralateral seen stimuli but only early processing for unseen ipsilateral stimuli through inter-hemispheric transfer

Foremost, looking at the intact V1, VER over time were different between seen (RVF) and unseen (LVF) stimuli almost throughout the whole post-stimulus time window (4 clusters between 0 and 800 ms, $p < .05$ corrected; Figure 2A) which as expected confirmed that the activity recorded in V1 was different between pictures presented in the intact and blind hemifields. More interestingly, not only did seen stimuli trigger a very fast positive P1-N1 complex (P1-N1 between 70 and 160 ms, i.e. duration of 90 ms with a peak at 110 ms and amplitude of 2.18 z-score; t1 = 100 ms; Figure 2A), but unseen stimuli also induced a significant large P1-N1 complex of longer duration in the intact V1 with a peak lag time of 36 milliseconds (P1-N1 between 70 and 251 ms, i.e. duration of 181 ms with a peak at 146 ms and amplitude of 2.14 z-score; t2 = 150 ms; Figure 2A). The duration of P1-N1 will further be discussed in subsequent sections. Focusing on this time window, VER at

100 ms and 150 ms were computed for all nodes within the intact V1. Seen and unseen evoked activity were contrasted revealing 32 nodes with significant increased amplitude for seen stimuli at 100 ms (seen vs unseen: positive t-values between 0 and 8.166149, significant DA values between 57.24 and 71.34 %, $p < .05$ corrected; Figure 2B) and 32 nodes with significant increased amplitude for unseen stimuli at 150 ms (seen vs unseen: negative t-values between -9.229101 and 0, significant DA values between 57.24 and 70.28 %, $p < .05$ corrected; Figure 2B). We also observed N1, P2, and N2 like-waveforms for both seen and unseen stimuli with latent onsets for unseen stimuli which are expected as they were measured in the ipsilateral hemisphere. However, late components, such as the P3 and N400, as well as an additional P2 were only identified for seen stimuli suggesting higher order processing for pictures consciously processed (Table 1).

Temporal generalization results in the intact V1 show sustained differences in neural mechanisms between seen and unseen pictures

In order to understand the early and late neural mechanisms responsible for differentiating between states of visual awareness over the entire window, we computed the temporal decoding and generalization performances using the temporal and spatial features within ROIs. The results showed significant AUC scores as soon as 90 ms in V1 (Figures 2C and 2D). Fitting each estimator of the model at each time point, we observed different non-exclusive processing stages associated with a hybrid model (King, Pescetelli, & Dehaene, 2016) that could explain how V1 distinguishes conscious from unconscious perception. More specifically, the diagonal from 90 to 800 ms suggests dynamic amplitude differences across nodes while data between 140 and 250 ms suggests that seen information reactivates the early stages with reversal of the early processing stages between 150 and 200 ms, corresponding to the P1-N1 complex. At late latencies corresponding to the P3 and N400 latency windows, i.e., between 310 and 800 ms, information was processed according to a maintenance model (King, Pescetelli, & Dehaene, 2016) where differences in amplitude were maintained over time (cluster between 90 and 800 ms and multiple significant time instances in the TG matrix, $0.625 \pm 0.04 <$ sig. AUC $< 0.85 \pm 0.02$; $p < .05$ corrected; Figures 2C and 2D). Importantly, the neural mechanisms underlying the temporal generalization results imply that V1 processes distinctively information from seen and unseen stimuli at different time points throughout the perceptual stages, which underlying cognitive processes will further be debated in the discussion.

It is important to note that these differences resemble the ones observed in previous studies reporting distinctions between seen and unseen pictures (Dehaene and King, 2016), which can't be solely explained by lateralization of the picture presentation. Moreover, subsequent results in the left and right thalami confirm that the generalization results weren't only associated with the side of the picture presentation. Thus, we estimate that the interpretations resulting from the temporal generalization analyses in this paper truly reflect neural mechanisms distinctive of seen and unseen information. Nonetheless, all VER results will be discussed considering the lateralization effects and eccentricity which will be isolated by comparing activities that arise from the same hemifield.

A smaller P1-N1 for paracentral seen pictures suggests rapid processing in V1 for central conscious perception

Comparisons within each hemifield revealed early differences between pictures presented in the paracentral vision (6°) and near periphery (12°) of the intact hemifield (1 cluster between 108 and 191 ms, $p < .05$ corrected; Figure 2E) which confirms that V1 processes information differently depending on the eccentricity but only in the early processing stages. Paracentral stimuli seem to be processed more effectively in V1 (short P1-N1) compared to peripheral pictures or unseen pictures in order to rapidly induce P2s. These differences arise from a significant larger P1-N1 component for near periphery stimuli (6°: N1 starting at 110 and peaking at 160 ms, i.e., a duration of 50 ms and amplitude of 2.01 z-score, 12°: starting at 110 and peaking at 233 ms, i.e., a duration of 123 ms and amplitude of 2.31 z-score; t1 = 150 ms; Figure 2E). The activity at 150 ms was computed for all nodes within the intact V1. The paracentral and near periphery activity were contrasted revealing 31 nodes with significantly increased P1-N1 amplitude for near periphery stimuli (seen paracentral vs near periphery: negative t-values between -10.52 and 0, significant DA values between 59.57 and 84.82 %, $p < .05$ corrected; Figure 2F). Temporal decoding and generalization results suggest that training the model at different time instants allowed to predict the differences between eccentricities at early and late latencies, i.e., between 134 and 194 ms and between 295 and 350 ms. These differences were associated with vertically aligned significant AUC scores in the temporal generalization matrix. Training the model between 134 and 194 ms also resulted in significant predictions between 700 and 800ms ($0.68 \pm 0.05 <$ sig. AUC $< 0.90 \pm$ 01, $p < .05$ corrected; Figures 2G and 2H). Differences between the classical VER measures and the ML analysis suggest that both analyses are complementary and that some information is

probably lost when averaging across nodes which should be taken into consideration in future MEG studies.

By comparing paracentral and near periphery pictures in the blind hemifield, two significant clusters were found (cluster 1 between 150 and 213 ms, cluster 2 between 420 and 566 ms, $p < .05$ corrected; Figure 2I). More specifically, the activity was different across both conditions for P1 around 150 ms (6°: P1 starting at 70 ms and peaking at 138 ms, i.e. duration of 68 ms and amplitude of 2.10 z-score, 12°: starting at 70 ms and peaking at 154 ms, i.e. duration of 84 ms and amplitude of 2.18 z-score; t1 = 150 ms; Figure 2I). Differences were observed in the anterior part of V1-lh showing greater N1 activity in 14 nodes for near periphery stimuli (unseen paracentral vs near periphery: t-values between -2.82 and 1.33, significant DA values between 59.15 and 63.17 %, $p < .05$ corrected; Figure 2J). These differences were highlighted using temporal decoding, but dissociation between eccentricities didn't induce significant generalization results. In fact, significant results were only observed within the diagonal between 175 and 219 ms ($0.625 \pm 0.08 <$ sig. AUC $< 0.78 \pm 0.05$, $p < .05$ corrected; Figures 2K and 2L).

Taken together with the previous VER and ML analyses, results in the intact V1 showed that (1) contralateral seen stimuli were processed rapidly and distinctively from ipsilateral unseen stimuli through differences in multiple perceptual stages, (2) seen pictures triggered late components associated with higher order processing, as the P3 and N400, (3) stimuli in the blind hemifield were processed in the intact ipsilateral V1 despite any visual awareness through inter-hemispheric transfer. This was translated by the peak lag time between the VER onset for seen stimuli and unseen stimuli, while the VER's peak onsets were constant across visual eccentricities within a hemifield, (4) temporal differences between eccentricities were observed for both hemifields but weren't generalized across multiple perceptual stages and (5) stimuli associated with decreased visual perception or qualia requiring longer attentional resources, i.e. unseen stimuli compared to seen stimuli or near periphery compared to paracentral vision, were processed in V1 during a longer period within the P1-N1 latency window.

A stronger N2 in the contralateral thalamus for seen and unseen pictures but stronger late positivity and sustained activity for conscious perception

We postulate to find similar VER-like-components in the subcortical structures as suggested by (Chen et al., 2021). First, in the left thalamus, an audiovisual P50 component was found starting at 27 ms and peaking at 70 ms with no difference between seen and unseen paracentral and near periphery stimuli. These results show that we were able to measure an accurate thalamic audiovisual evoked response triggered by the sound and picture onset (Starke et al., 2020; Talsma et al., 2007). Differences between seen and unseen stimuli were observed at N1 and P2 latency windows which resulted in two significant clusters (cluster 1 between 131 and 191 ms and cluster 2 between 208 and 314 ms, $p < .05$ corrected; Figure 3A). These differences result from the additional late components and the stronger N2 response for seen pictures (Table 1). Investigating these components for each specific node within the left thalamus, we were able to predict if the stimulus was seen or unseen. In fact, at around 150 ms, seen stimuli were associated with P2 predominantly in the anterior part of the left thalamus while unseen stimuli triggered an N1 response around the same instant (seen vs unseen: positive t-values between 0 and 3.99, significant DA values between 56.89 and 61.55 % in 18 nodes, $p < .05$ corrected; Figure 3B). A stronger N2 response was also induced at around 250 ms for seen pictures in the anterior and posterior part of the left thalamus (seen vs unseen: negative t-values between -5.04 and -2.23, significant DA values between 56.54 and 64.80 % in 33 nodes, $p < .05$ corrected; Figure 3B). Using the temporal and spatial features in the ML analysis, we showed that the left thalamus begins to discriminate between seen and unseen stimuli from around 100 ms until 700 ms, and important generalization effects were observed between 430 and 700 ms ($0.625 \pm 0.01 <$ sig. AUC $< 0.72 \pm 0.04$; $p < .05$ corrected; Figures 3C and 3D). These results were comparable to what has been found in the intact V1 showing multiple neural mechanisms involved in conscious and unconscious discrimination, including dynamic amplitude changes, re-entry, and maintenance.

Interestingly, in the right thalamus unseen contralateral information induced a stronger N2 compared to seen pictures, suggesting late processing of information, but no P3 which could be interpreted as a lack of higher order processing. Seen ipsilateral stimuli showed an increased N1 amplitude compared to unseen stimuli in the first cluster across the anterior part of the thalamus. Also, differences of around 450 ms between the N2 in the unseen condition and the P3 in the seen condition resulted in a significant cluster and differences in the posterior part of the thalamus (cluster 1 between 209 and 307 ms and cluster 2 between 348 and 535 ms, $p < .05$ corrected; Figure 3M, seen vs unseen: t-values between -2.93 and 0, significant DA values between 56.89 and

58.76% in 21 nodes and cluster 2 t-values between 1.57 and 5.97, significant DA values between 56.18 and 62.89% in 47 nodes, $p < .05$ corrected; Figure 3N). Results of temporal decoding in the right thalamus were similar to what was found in the left thalamus; however, the generalization effect was less robust, suggesting a dominant role of the left thalamus in decoding conscious (contralateral) from unconscious stimuli (ipsilateral) ($0.625 \pm 0.02 <$ sig. AUC $< 0.75 \pm 0.02$; $p < .05$ corrected; Figures 30 and 3P).

Let's also note that in the right thalamus no P50 was measured which could be due to degeneration of the multisensory neurons in the thalamus. We will further address this question in subsequent sections by demonstrating a P50 specific to unpleasant peripheral pictures in absence of visual awareness.

Eccentricities for both seen and unseen pictures are decoded at early latencies in both thalami

In the left thalamus, discrimination between seen paracentral and near periphery conditions show that P2 was more prominent for paracentral stimuli in parts of the anterior and posterior thalamus (cluster between 120 and 187 ms, $p < .05$ corrected; Figure 3E, seen paracentral vs near periphery: positive t-values between 1.49 and 4.29, significant DA values between 59.57 and 63.83 % in 28 nodes, $p < .05$ corrected; Figure 3F) and that P3 was specific to the paracentral seen condition. On the other hand, for unseen stimuli, the duration and amplitude of N1 were larger for the near periphery condition (96 ms) compared to the paracentral condition (62 ms) in the medial, lateral, and posterior part of the thalamus, suggesting that this negative peak, which was brief for seen stimuli (42 ms) could inversely correlate with the degree of visual processing (cluster between 148 and 187 ms, $p < .05$ corrected; Figure 3I, positive t-values between 1.93 and 4.07, significant DA values between 59.19 and 66.55% in 33 nodes, $p < .05$ corrected; Figure 3J). Significant temporal decoding between eccentricities for seen stimuli is limited to one-time window and induces no generalization effect ($0.68 \pm 0.04 <$ sig. AUC $< 0.74 \pm 0.03$, $p < .05$ corrected; Figures 3G and 3H) while for unseen stimuli no significant discrimination was observed using the multi-feature approach (no sig. AUC, $p < .05$ corrected; Figures 3K and 3L). Finally, no differences in P2 and a lack of N2 and P3 suggest a lack of late components for unseen information in the ipsilateral thalamus (Table 1).

In the right thalamus, P3 was larger for seen periphery stimuli compared to seen paracentral stimuli specifically in the posterior thalamus which was not significant when the signal was

averaged across all thalamic nodes (no significant cluster; Figure 3Q, seen paracentral vs near periphery: t-values between -2.35 and -0.88, significant DA values between 59.15 and 62.06% in 12 nodes; Figure 3R). Considering the previous left thalamic results and the results in the right thalamus, a dissociation between lateralization and eccentricity is revealed with the observable P3. In fact, seen paracentral stimuli induced a contralateral P3 around 356 ms, and seen near periphery stimuli induced an ipsilateral P3 around 459 ms, suggesting that information from both stimuli was processed in late stages via different pathways. For unseen stimuli, as observed in the ipsilateral left thalamus, a larger contralateral N1 was identified in the right thalamus for the peripheral system at around 200 ms, however, this difference wasn't reflected in the node by node decoding scores (cluster between 177 and 283 ms, $p < .05$ corrected; Figure 3I, unseen paracentral vs near periphery: t-values between 0.74 and 2.02, no significant DA with a maximum at 57.46%, $p < .05$ corrected; Figure 3J). Unseen stimuli also triggered a strong contralateral thalamic N2 which was absent in the ipsilateral thalamus. Moreover, temporal decoding results between eccentricities were similar to what was observed in the left thalamus, suggesting a role of the right thalamus in processing ipsilateral conscious information ($0.68 \pm 0.02 <$ sig. AUC $< 0.72 \pm 0.03$, $p < .05$ corrected; Figures 3S and 3T) and no differences were found for contralateral unconscious information (no sig. AUC, $p < .05$ corrected; Figures 3W and 3X).

The main points to consider when resuming the VER in the thalami are that (1) N2 was present in the left thalamus for contralateral seen stimuli at around 200 ms and around 350 ms in the right thalamus for contralateral unseen stimuli, (2) the presence of P3 was observed for seen paracentral stimuli in the contralateral thalamus and for seen near periphery stimuli in the ipsilateral thalamus and (3) differences between eccentricities were observed in the N1 and P2 latency windows for the unseen and seen conditions, respectively.

Activity and generalization differ between the left and right amygdala in processing visual information

In the left amygdala, the seen condition induced larger P1, N1, and P2 components peaking at 126, 213, and 320 ms, respectively, compared to the unseen condition. These larger VERs resulted in latent peaks for perceived stimuli and earlier onsets for unperceived stimuli. Two significant clusters were found in the left amygdala (cluster 1 between 78 and 312 ms and cluster 2 between 425 and 523 ms, $p < .05$ corrected; Figure 4A). Within these clusters we illustrated three time points

that revealed significant differences across nodes (t1 (150ms): t-values between 4.12 and 4.79, significant DA values between 56.89 and 61.41% in 12 nodes, $p < .05$ corrected; t2 (250ms): t-values between -3.18 and -1.67, significant DA values between 56.48 and 56.78% in 4 nodes, $p < .05$ corrected; t3 (450ms): t-values between 2.34 and 3.44, significant DA values between 56.54 and 61.06% in 11 nodes, $p < .05$ corrected; Figure 4B).

In the right amygdala, the seen condition was associated with a larger P1 and more sustained P2. Three significant clusters were observed in the right amygdala (cluster 1 between 100 and 138 ms, cluster 2 between 195 and 326 ms, cluster 3 between 481 and 533 ms, $p < .05$ corrected; Figure 4M) with one selected time point for the classification analysis revealing significant differences across nodes (seen vs unseen: t-values between -2.68 and -2.03, significant DA values between 55.83 and 58.558% in 10 nodes, $p < .05$ corrected; Figure 4N). Successful discrimination between seen and unseen condition started at 151 ms and ended at 500 ms in the left amygdala with reversal of activity around 200 ms ($0.61 \pm 0.02 <$ sig. AUC $< 0.70 \pm 0.02$, $p < .05$ corrected; Figures 4C and 4D). However, the multi-feature analysis showed that decoding in the right amygdala differed from the left amygdala and was more similar to what happens in the thalami and intact V1 with significant temporal decoding starting around 143 ms and generalizing around 400 ms ($0.61 \pm 0.03 <$ sig. AUC $< 0.70 \pm 0.02$, $p < .05$ corrected; Figures 4Q and 4P).

Stronger responses to peripheral stimuli in the unseen condition are observed in both amygdalae

Within the intact hemifield, a larger N1 was induced by the paracentral condition in the left contralateral amygdala (between 130 and 189 ms, $p < .05$ corrected; Figure 4E, t-values between 2.49 and 2.96, significant DA values between 58.16 and 62.06% in 10 nodes, $p < .05$ corrected; Figure 4F), while no difference between eccentricities for the seen condition was observed in the right ipsilateral amygdala. However, using all temporal and spatial features, only the right ipsilateral amygdala showed differences between eccentricities from 145 to 175 ms with no significant temporal generalization. Thus, the classical VER analysis and ML analysis highlighted different mechanisms suggesting the complementarity of both types of analyses (left amygdala, no sig. AUC, $p < .05$ corrected; Figures 4G and 4H, right amygdala, $0.65 \pm 0.04 <$ sig. AUC $< 0.68 \pm 0.02$, $p < .05$ corrected; Figures 4Q and 4P).

Within the blind hemifield, near periphery stimuli compared to paracentral stimuli triggered a larger amplitude of the N1 component in the left ipsilateral amygdala (unseen paracentral vs near periphery: between 134 and 203 ms, $p < .05$ corrected; Figure 4I, t-values between 0.11 and 1.27, no significant DA values; Figure 4J) and a greater P2 in both amygdalae (left amygdala between 257 and 427 ms, right amygdala between 312 and 404 ms, $p < .05$ corrected; Figure 4U, left amygdala - t-values between -3.32 and -3.09, significant DA values between 58.45 and 62.25% in 10 nodes, $p < .05$ corrected; Figure 4V; right amygdala - no significant DA values). Temporal decoding results show significant eccentricities differences in the blind hemifield only in the ipsilateral left amygdala (left amygdala, $0.68 \pm 0.01 <$ sig. AUC $< 0.7 \pm 0.05$, $p < .05$ corrected; Figures 4K and 4L, right amygdala, no sig. AUC, $p < .05$ corrected; Figures 4W and 4X).

Overall, the results in the amygdalae showed that (1) different neural mechanisms in the left and right amygdalae for seen and unseen pictures employing machine learning analysis, (2) P1 was larger for seen paracentral stimuli in the left contralateral amygdala, and (3) N1 and P2 were larger for peripheral unseen stimuli compared to paracentral unseen stimuli in both amygdalae suggesting a magnocellular dominant pathway for unconscious processing which we will further discuss.

Unpleasant pictures trigger an early thalamic response while pleasant pictures induce subcortical magnetic late positive potentials for unconscious peripheral processing

The advantage of the peripheral system in subcortical regions in the absence of visual awareness was moreover observed by showing affective-specific VER and GC for unseen near periphery pictures (Figure 5). First, unpleasant pictures triggered a P50 component in the contralateral right thalamus which wasn't induced by pleasant pictures (unseen near periphery unpleasant: P50 between 10 and 157 ms, i.e., a duration of 147 ms with a peak at 40 ms and amplitude of 1.18 z-score, unseen near periphery pleasant: P50 no significant, unseen near periphery unpleasant vs unseen near periphery pleasant: cluster between 20 and 150 ms, $p < .05$ corrected; Figure 5A). The P50 which we found in the left thalamus for both seen and unseen stimuli notably triggered by the sound, wasn't observed in the right thalamus when all affective and eccentricity conditions were merged, which we interpreted as degeneration of thalamic neurons after striate lesion. However, in the right thalamus, the P50, a component known to be enhanced with audiovisual integration (Talsma et al., 2007), showed an advantage for unpleasant pictures compared to pleasant pictures

in unconscious perception. Later on, we also observe a greater P2 component for unpleasant pictures compared to pleasant pictures for unconscious peripheral processing (unseen near periphery unpleasant: P2 between 200 and 500 ms, i.e. duration of 300 ms with a peak at 310 ms and amplitude of 1.32 z-score, unseen near periphery pleasant: P2 between 180 and 500 ms, i.e. duration of 250 ms with a peak at 328 ms and amplitude of 0.72 z-score, unseen near periphery unpleasant vs unseen near periphery pleasant: cluster between 300 and 410 ms, $p < .05$ corrected; Figure 5B). On the other hand, unseen near periphery pleasant pictures triggered increases in the magnetic late positive potential (mLPP) in the right thalamus compared to neutral pictures (cluster between 400 and 557 ms, $p < .05$ corrected; Figure 5E) and in the left amygdala (cluster between 567 and 688 ms, $p < .05$ corrected; Figure 5F)

The contralateral thalamus and ipsilateral amygdala causally influence each other's activity when processing unconscious peripheral stimuli

After computing the dominant directionality in causal connectivity between all ROIs, we observed significant DOI GC in the right thalamus and left amygdala. In fact, we noted a significant influence from the thalamus to the amygdala involving inter-hemispheric transfer for unpleasant pictures compared to pleasant pictures. On the other hand, activity in the amygdala that arises from the presentation of pleasant pictures causally influenced the activity of the thalamus (unseen near periphery unpleasant: Th-rh --> Am-lh, DOI GC > 0 between 270 and 300 ms and peak value 0.025 ± 0.005, unseen near periphery pleasant: Am-rh --> Th-rh, DOI GC < 0 between 260 and 320 ms and peak value -0.036 ± 0.008, unseen near periphery unpleasant vs unseen near periphery pleasant: cluster between 260 and 300 ms, $p < .05$ corrected; Figure 5C). These results are of clear importance in demonstrating the role of the thalamus and its influence on the amygdala to process affective pictures in the absence of conscious perception via the magnocellular/peripheral system and the importance of computing bidirectionality which show affective-specific differences in favor of unpleasant and pleasant pictures (Figure 5D). Collectively, we show an affective-specific subcortical evoked response for unseen peripheral stimuli supported by a rapid thalamo-amygdala pathway.

DISCUSSION

The aim of this study was to assess the VER at the cortical and subcortical source level that could lead to a better understanding of the cognitive processes that support affective specific and non-specific conscious and unconscious perception when V1 is lesioned. Thus, we used temporal decoding and generalization to predict the evoked activity that arises when SJ's intact and blind hemifields were stimulated with natural affective and neutral scenes.

Unseen pictures are processed in the intact V1 through inter-hemispheric transfer

Stimulating the intact contralateral hemifield yielded the first component in V1 under 100 ms, known as C1 originating from the striate cortex, followed by P1, N1, P2, N2, P3, and N400 triggered by feedback projections from higher-order regions (Railo et al., 2011; Di Russo et al., 2002). Interestingly, C1 wasn't evoked in V1 after stimulation of the blind hemifield, but a reliable P1 was observed. The ipsilateral P1 was longer and shifted in time compared to the contralateral P1 suggesting a strong VER in blindsight through inter-hemispheric transfer and recruitment of extra-striate regions to process information even in the absence of visual awareness (Figure 2A). The longer duration of the P1 component for unseen pictures was also found for peripheral stimuli (which we will discuss later on). In fact, P1 has been shown to be specific to visual selective attention (Hillyard and Anllo-Vento, 1998), to respond to reflexive attentional paradigm (Ries and Hopfinger, 2011) as used in this study, to contralateral and ipsilateral information (Mangun et al., 2001) with expected differences in peak latencies between contralateral and ipsilateral stimulation as observed in typical participants due to inter-hemispheric transfer in the latter case (Di Russo et al., 2002). Thus, we interpret these results in terms of differences in attentional load between unseen/peripheral stimuli and seen/paracentral stimuli (Klimesch, 2011). Moreover, at the source level using decoding, we validated that at around 100 ms the nodes in the intact V1 were greatly activated for seen pictures and were later activated by unseen pictures around 150 ms (Figure 2B) which confirm the processing of unconscious information in the ipsilateral intact V1.

The intact V1 shows differences in late processing for seen and unseen pictures

Classification between a conscious and unconscious percept involved significant decoding accuracy starting at 90 ms and generalization after 400 ms concurring with the P3 and N400 latency window, which generalization wasn't observed for differences in eccentricities within both

hemifields (Figures 2 C, D). The possibility to train the algorithm at 400 ms and predict whether the stimulus was seen or unseen at subsequent time windows suggests reactivation of V1 nodes through rapid re-entrant feedback and maintained activity in V1 that is more important for seen pictures compared to unseen pictures (Dehaene and King, 2016). These late VER differences originating from higher order regions could explain the lack of visual awareness following a V1-lesion (Silvanto, 2015) even when the stimulus in the blind hemifield is able to activate the ipsilateral striate cortex as shown in this case study. Hence, V1 does not seem sufficient to produce visual awareness because its differential activity depends on the ignition of higher-order regions (Baars, 2002; Dehaene and Changeux, 2011; Dehaene et al., 2006) but could be necessary for neuronal recurrent amplification which is more important in conditions of awareness (Aru et al., 2020; Heeger and Zemlianova, 2020; Lamme and Roelfsema, 2000). Adding these results to the observed early desynchronization around 200 ms in the temporal generalization matrix, differences between seen and unseen pictures seem to be induced by a hybrid model (King et al., 2016). Investigating the activity within the thalami furthermore provided insights into these neural mechanisms considering the close link between visual consciousness and the thalamocortical loops (McFadyen et al., 2020).

Activations in the thalamus of the lesioned hemisphere suggest functional reorganization

Classification results also showed significant discrimination between seen and unseen pictures in the thalami. The differences in the left thalamus around 150 ms (Figure 3A) preceded the differences in the right thalamus of the lesioned hemisphere around 200 ms (Figure 3M) but were both after the ones found in the left intact V1 at 100 ms. These first observations shed light on the fact that in both thalami, i.e., contralateral and ipsilateral to the stimulus, we weren't able to dissociate the VER induced by a seen and an unseen picture prior to cortical processing. Thalamic differences associated with visual awareness, thus seem to be contingent on cortical processing (Min, 2010; Sherman, 2016). In fact, seen and unseen pictures induced thalamic VERs that were shifted due to additional positive components for seen pictures (P2 and/or P3). These distinct time courses could reflect the differences in attentional reflexive capture and higher order cognitive processes between seen and unseen pictures as discussed in our previous paper (Hadid et al., in preparation). However, the stronger thalamic N1 found contralaterally to the stimulus presentation for seen and unseen pictures could be used as a marker of contralateral information processing

irrespective of visual awareness. Negativity at the N1 latency window has been associated with visual awareness (Förster et al., 2020), however, the negative component that we found in this study rather seems to indicate the extraction of relevant information from the contralateral hemifield.

As for the early components, a P50 was observed only in the left thalamus suggesting audiovisual processing of the sound cue presented at the onset of the picture (Starke et al., 2020; Talsma et al., 2007), which was almost abolished in the right thalamus. We will further on discuss the P50 in the right thalamus which was in reality induced specifically for unseen peripheral unpleasant pictures. Interestingly, in the thalamus within the intact hemisphere differences were mostly anterior (Figures 3B, F, J) while they were more posterior in the thalamus of the lesioned hemisphere which could suggest functional reorganization of thalamic responses following V1 lesions (Figures 3N, R, V). The posterior part of the thalamus has previously been reported to respond to emotional faces in well-known blindsight patient G.Y. (Morris et al., 2001). In fact, animal studies have shown that the anterior pulvinar within the thalamus is notably driven by V1 projections and posterior parts by projections from the superior colliculus (Bennett et al., 2019; Elorette et al., 2018) which has been hypothesized to play a key role in blindsight (Kinoshita et al., 2019; Tran et al., 2019). Moreover, while in both thalami, temporal prediction of seen and unseen pictures was above chance-level over time (Figures 3C, S), the generalization was stronger in the left thalamus compared to the right thalamus (Figures 3D, T), showing greater recruitment of the contralesional thalamus for seen pictures. Nonetheless, as observed in the intact V1, both thalami showed differences in re-entry feedbacks and perceptual maintenance concurrent to the hybrid model, suggesting the importance of thalamocortical loops in conscious perception even within the lesioned hemisphere.

The left and right amygdalae process information differently

Similar and distinct neural mechanisms were found between both amygdalae. First, an early component around 70 ms was evoked in the left amygdala of the intact hemisphere for seen pictures (Figure 4A) which wasn't observed in the right amygdala of the lesioned hemisphere (Figure 4M). Moreover, shifts in the VER between seen and unseen pictures were triggered by a longer P1-N1 complex for seen pictures in the left amygdala suggesting stronger early responses for contralateral stimuli (Figures 4A, B). In the right amygdala, unseen contralateral pictures triggered a faster and

stronger N1 and P2 while seen ipsilateral pictures triggered a stronger P1 response and a longer P2 (Figures 4M, N). These differences suggest that both seen and unseen pictures are processed by both amygdalae using different cognitive processing integrating emotional attention through top-down mechanisms (Vuilleumier, 2005). In fact, temporal decoding showed significant decoding scores in the left amygdala from 150 to 500 ms (Figure 4C) and generalization throughout this time window which pattern differed from what was found in the intact V1 and both thalami (Figure 4D). On the contrary, the right amygdala showed similar temporal predictions as those found in the intact V1 and thalami suggesting adequate functionality even after a lesion to the right hemisphere (Figures 4O, P), which was not found in previous studies (Bertini et al., 2017, 2019; Cecere et al., 2014) and could explain the reliable VER obtained after stimulation of SJ's blind hemifield. Nonetheless, differences between the left and right amygdalae have been reported in multiple studies, where the left amygdala seems to be specific to emotion content and the right amygdala to unconscious processing (Cornwell et al., 2008; Costafreda et al., 2008; Liu et al., 2015; Morris et al., 1999).

Pictures presented at specific eccentricities reveal different neural processes in V1, the thalamus, and the amygdala for conscious and unconscious perception

To assess whether the VER differences and temporal decoding results were specific to visual awareness, we've compared the responses for paracentral and near peripheral stimuli within each hemifield, isolating the laterality, eccentricity, and awareness effects. We found that seen pictures presented in the periphery triggered stronger P1/P50-N1 complexes compared to paracentral stimuli in the contralateral V1, thalamus, and amygdala (Figures 2E, F, 3E, F, 4E, F). In the intact V1, stimulation of the blind hemifield also triggered a stronger P1-N1 complex a few milliseconds later, once more suggesting inter-hemispheric transfer (Figures 2I, J). The greater early negativity was moreover reported in both thalami (Figures 3I, J, U, V) and ipsilateral left amygdala (Figures 4I, J) showing that even in the absence of visual awareness the central and peripheral systems are differentiated. These results could explain SJ's faster RTs for both seen and unseen pictures presented in the periphery via the recruitment of the magnocellular pathway (Bayle et al., 2011; Calvo et al., 2014). Moreover, presentation in the blind hemifield involved the cortical and subcortical regions within the intact hemisphere showing the importance of compensatory recovery mechanisms following a lesion (Bridge et al., 2008; Georgy et al., 2020; Hadid and Lepore, 2017;

Nakasato et al., 1996). Nonetheless, it is also important to note the recruitment of the contralateral thalamus within the lesioned hemisphere in unconscious processing which we will further discuss in terms of affective-specific differences.

Having said that, seen pictures presented centrally induced P2 responses known for being specific to scene processing (Harel et al., 2016), a P3 associated with higher order processes (Ries and Hopfinger, 2011), and a late negative component in the N400 latency window associated with the semantical encoding of affective content (Taylor and Fragopanagos, 2005) within the intact V1. The P2 response was also stronger for seen paracentral stimuli in the left contralateral thalamus (Figures 3E, F). Moreover, differences between the contralateral and ipsilateral thalami were observed as seen paracentral pictures induced a P3 in the left thalamus (Figures 3E) and seen near periphery pictures induced a P3 in the right thalamus (Figures 3Q) suggesting different roles of the ipsilateral and contralateral thalamus in the visual pathways (Ramachandra et al., 2020). Considering the role of these VERs in task difficulty (Ma et al., 2016; Woods et al., 1992) and the attentional reflexive nature of the task, our results confirm the previous demonstration of the involvement of the macaque thalamus in attentional processing (Fiebelkorn et al., 2018; Kastner et al., 2020) when discriminating between a stimulus presented centrally and peripherally. The amygdalae on the other hand seemed to optimally respond to peripheral pictures with overall larger early negativity (N1) and subsequent positivity (P2) (Figures 4I, J, U) suggesting a bias in the peripheral system (Bayle et al., 2009, 2011).

We interpret the results obtained in the intact V1, thalami, and amygdalae by suggesting that peripheral information is driven by a magnocellular pathway in the early stages, i.e., at the latency of P1, while on the other hand, conscious central presentation recruits the parvocellular pathway at higher-order stages. Using ML, we are able to further understand the neural mechanisms underlying these pathways. In fact, in the intact V1 when pictures are presented in the intact hemifield, significant decoding accuracy was observed under 200 ms (N1 latency window) and between 300 and 400 ms (P2 latency window), suggesting the recruitment of two pathways in discriminating eccentricity under conscious perception, which we attribute to the magnocellular and parvocellular systems, respectively (Figure 2G, H) (Campana et al., 2016; Maunsell et al., 1999; Tapia and Breitmeyer, 2011). These outcomes are very interesting with respect to SJ's behavioral results, where peripheral pictures were associated with faster RTs and central pictures

with more accurate performance (Breitmeyer, 2014). On the other hand, significant decoding accuracy when predicting the eccentricity was observed only at the N1 latency window for unseen pictures suggesting the sole involvement of the magnocellular pathway (Figures 2K, L). In both thalami, significant prediction of the eccentricity was only observed for seen pictures at the N1 latency window(Figure 3G, H, S, T), while an advantage of the ipsilateral amygdala (Liu and Ioannides, 2010) was observed in the temporal decoding performances when discriminating paracentral from near periphery stimuli at the N1 latency in the presence (Figures 4S, T) or absence of visual awareness (Figures 4K, L). Significantly, ML and VER classical approaches provide different conclusions in the comprehension of cognitive processes showing the importance of using both tools in neuroscience. Thus, characterizing the evoked time course using multi-feature ML analysis added complementary information by integrating spatial features as inputs, which contributed to understanding the neural mechanisms underlying the differences between conscious and unconscious perception. Taken together, the intact V1, thalami, and amygdala process information from the central and periphery differently in conditions of awareness and unawareness (Almeida et al., 2015). While all of the above sections contributed to characterizing the neural and cognitive mechanisms that are triggered to predict the activity derived from presenting a picture that is consciously perceived from a picture that is unconsciously perceived, we were further interested in affective-specific differences.

Early evoked responses in the thalamus suggest an advantage of the peripheral unpleasant system in audiovisual integration

We extended the evoked analysis to differences between affective conditions depending on the eccentricity within each hemifield and computed causal FC to assess relations between ROIs for each condition. The first probing result was the presence of a P50 in the right thalamus that was specific to unseen unpleasant peripheral pictures compared to unseen pleasant peripheral pictures (Figure 5A). In fact, when we didn't find any P50 in the right thalamus when combining all conditions for seen and unseen pictures or paracentral and near periphery conditions, we assumed that auditive and more specifically audio-visual responses in the damaged hemisphere were affected by the V1 lesion (Alvarado et al., 2007; Arden et al., 2003; Shimojo and Shams, 2001). Thus, finding a P50 specific to unconscious peripheral unpleasant pictures demonstrate the advantage of this system notably in multisensory integration, i.e., hearing the white noise and

processing specific information presented to the blind hemifield within the contralateral thalamus. To our knowledge, this is the first evidence of a very fast thalamic evoked response specific to unconscious negative processing in the blind hemifield. These results suggest the role of the thalamus in visual attention toward specific emotions (Frank and Sabatinelli, 2014) even in the absence of visual awareness. Thus, conscious and attentional cognitive processes can be dissociated, while being intimately linked.

Bidirectionality of the thalamo-amygdala pathway explains affective-specific differences in unconscious peripheral perception

Moreover, the P50 was followed by an increase of P2 within the left amygdala (Figure 5B) for unpleasant pictures (Tao et al., 2021). Moreover, thalamo-amygdala causal influences were observed using DOI GC around the onset of P2 (Figure 5C) suggesting bottom-up modulations from the thalamus to the amygdala. That said, while previous results showed greater cortical late positive potential (LPP) components to emotional pictures (Schönwald and Müller, 2014), we've demonstrated that pleasant pictures induced greater magnetic LPP (mLPP) which is known to originate from higher-order regions (Moratti et al., 2011) compared to neutral pictures. These differences were found in the right thalamus between 400 and 600 ms (Figure 5E) and in the left amygdala around 600-700 ms (Figure 5F). The temporal relation between the evoked amplitudes was assessed by causal influence from the amygdala to the thalamus for pleasant pictures which showed top-down modulations rather than bottom-up modulations. While we previously identified causal relations in the high-frequency oscillatory domain between the contralateral thalamus and contralateral amygdala in processing non-specific and affective-specific stimulations in SJ's blind hemifield (Hadid et al., in preparation), the VER analysis in this study allowed us to mitigate our previous results by showing the involvement of the ipsilateral amygdala within the intact hemisphere specific to peripheral pictures, which support the role of the left amygdala in processing unseen fearful stimuli (Colibazzi et al., 2010; Troiani et al., 2014). The results regarding the peripheral pleasant pictures also support our previous findings showing that pleasant pictures are associated with a top-down higher-order cognitive system around 300 ms leading to slower RTs and better behavioral responses while unpleasant pictures were processed using the feedforward connectivity around 300 ms (Hadid et al., in preparation). In this paper, we add to previous connectivity results by showing how affective-specific differences associated with the peripheral

system are processed differently within the thalamus and amygdala by measuring the VER. These results support previous postulates of subcortical responses to negative affective valences in the absence of visual awareness (Bayle et al., 2009; Méndez-Bértolo et al., 2016; Ward et al., 2005), but also demonstrate that peripheral pleasant pictures are unconsciously processed using different mechanisms.

In conclusion, we were able to assess the brain mechanisms within the intact V1, thalami, and amygdalae involved in predicting visual awareness, eccentricity for both seen and unseen pictures, and affective valence in unconscious perception. We found that seen and unseen pictures were processed in the intact V1 and subcortical regions by feedback re-entrant activity from extra-striate regions with greater perceptual maintenance over time for conscious visual states. VER showed functional differences in thalamic subregions specific to the distinction between the parvo and magnocellular pathways and the different roles of the left and right amygdala in processing seen and unseen pictures. Subsequently, we showed a thalamic early component (P50) associated with the audio-visual response as soon as 10 ms post-stimulus specific to unpleasant unseen peripheral pictures in the thalamus of the lesioned hemifield which suggested a fast response of the multisensory neurons. This increase in P50 causally increased the P2 component of the left amygdala showing functional connectivity between the thalamus and amygdala for unpleasant peripheral pictures in the absence of visual awareness. On the other hand, the early activity within the amygdala was associated with an increase of the late positive components of the thalamus for pleasant peripheral pictures in the absence of visual awareness. These results shed light on the neural correlates associated with affective-specific differences within the thalamo-amygdala pathway by emphasizing the importance of the bi-directionality of these connections. In conclusion, this study provides new knowledge on the cognitive and neural mechanisms that support conscious and unconscious affective information following a V1-lesion by offering predictive analysis using spatial and temporal precisions in subcortical regions.

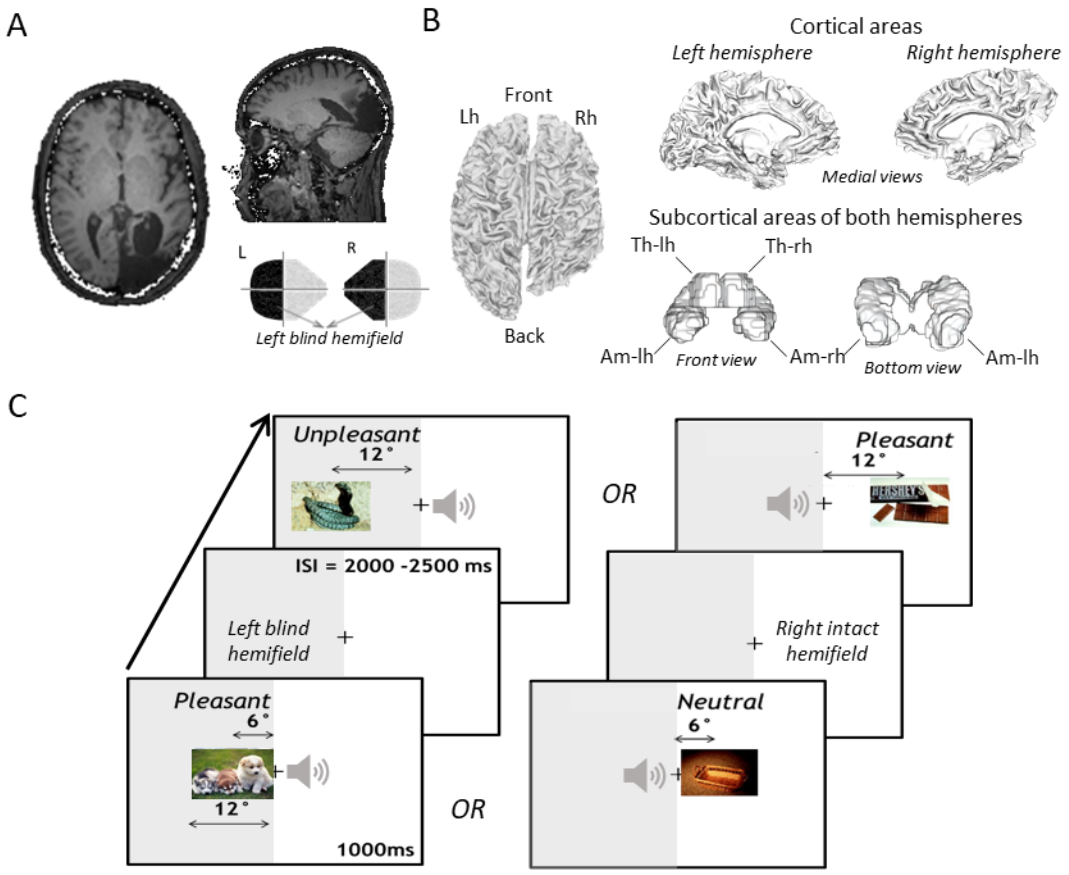

Figure 1. – Patient SJ and methods

(A) A surgical removal of the right occipital cortex was performed on SJ which is shown in the T1-weighted MRI images. The resection area extends to the right superior occipital gyrus, cuneus and lingual gyrus, including a complete V1 resection. Schematic representation of MAL's complete left homonymous hemianopia with no macular sparing. (B) Different views of the source reconstruction show both cortical and subcortical areas, including the left thalamus (Th-lh) and right thalamus (Th-rh), left and right hippocampus and left amygdala (Am-lh) and right amygdala (Am-rh) in the left hemisphere (Lh) and right hemisphere (Rh). (C) Schematic illustration of the forced-choice paradigm. SJ was tested on a 3-alternative forced-choice affective discrimination paradigm in which 300 unpleasant, neutral, and pleasant natures scenes from the IAPS were randomly presented for 1000 ms. Pictures appeared either in the paracentral or near the periphery i.e., at 6° or 12° of eccentricity from the fixation cross, respectively, of the intact right visual hemifield and blind left visual hemifield. An inter-stimulus interval (ISI) randomly varied between

2000 and 2500 ms. White noise at stimulus onset indicated that a response was needed as fast as possible while SJ's fixation had to remain on the cross. When pictures were presented in his blind hemifield, SJ didn't perceive any picture but had to guess the 'correct' answer. – Figure 1

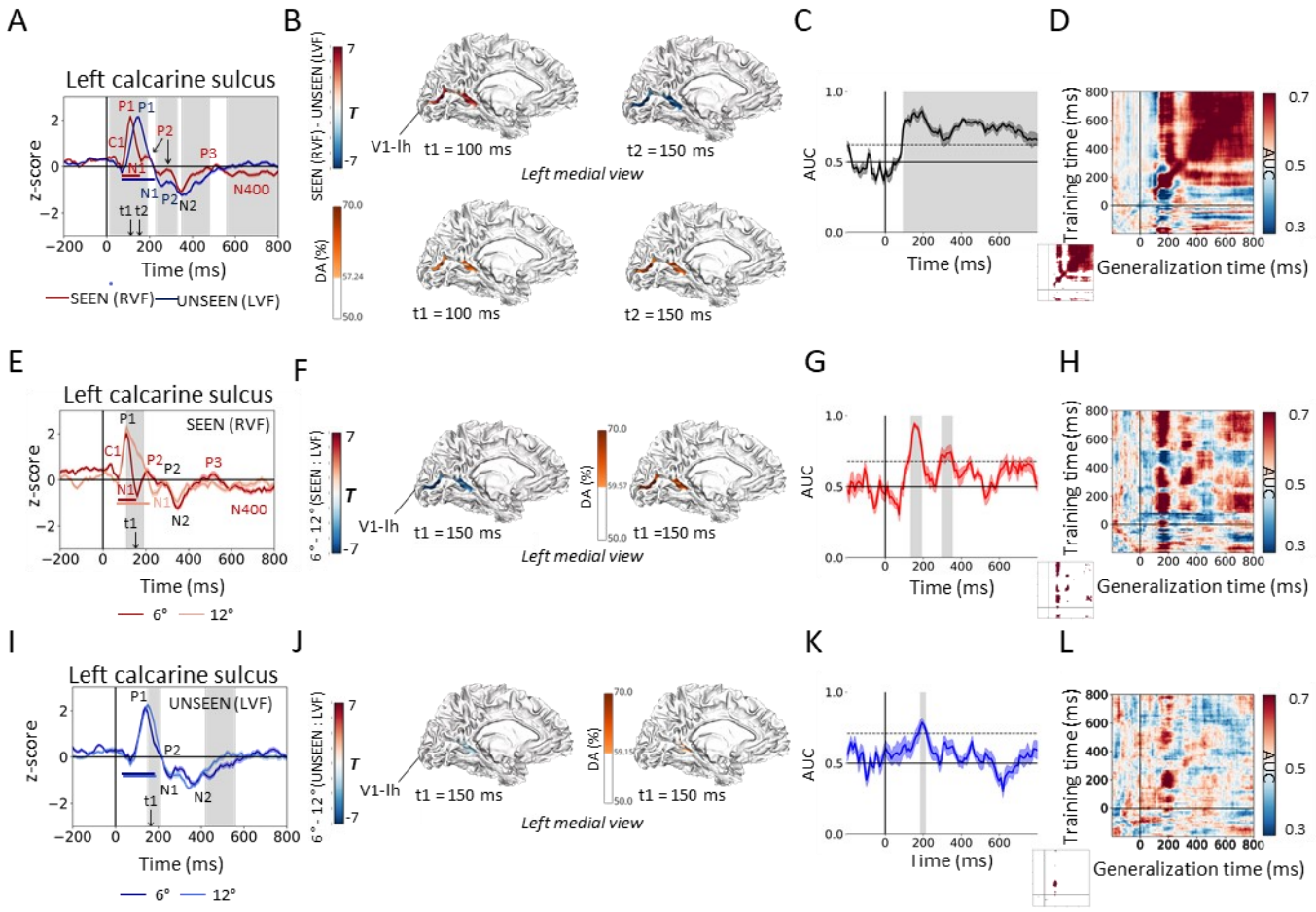

Figure 2. – The intact V1 processes information from the blind hemifield through inter-hemispheric transfer using neural mechanisms that differ from conscious perception.

VER, decoding, temporal decoding, and temporal generalization in single trial analyses revealing activity in the calcarine sulcus (V1-lh). (A-D) Comparisons between seen (red) and unseen (blue) stimuli. (E-H) Comparisons between seen paracentral (red) and seen near periphery (pink) stimuli. (I-L) Comparisons between unseen paracentral (blue) and unseen near periphery (light blue) stimuli. (A,E,I) VER and statistical differences over time between conditions were assessed using cluster-based permutation analysis corrected for multiple comparisons. Significant differences are highlighted in grey. (B,F,J) Differences between conditions for specific time points across all nodes of the intact V1 were illustrated as T-values. Statistical differences corrected for multiple comparisons computed as DA (%) were assessed using ML by decoding conditions across nodes. Only significant nodes are illustrated in the intact V1. (C,G,E) Temporal decoding over time was determined as the AUC using all nodes of the intact V1 as features. Threshold for significance was assessed using Bonferroni corrections. Significant AUCs are highlighted in grey. (D,H,L) Matrices show the results obtained from the temporal generalization analysis measured as the AUC over time using all nodes of the intact V1 as features. Threshold for significance was assessed using Bonferroni correction and significant AUCs are shown in the small matrix at the bottom left of the figure. – Figure 2

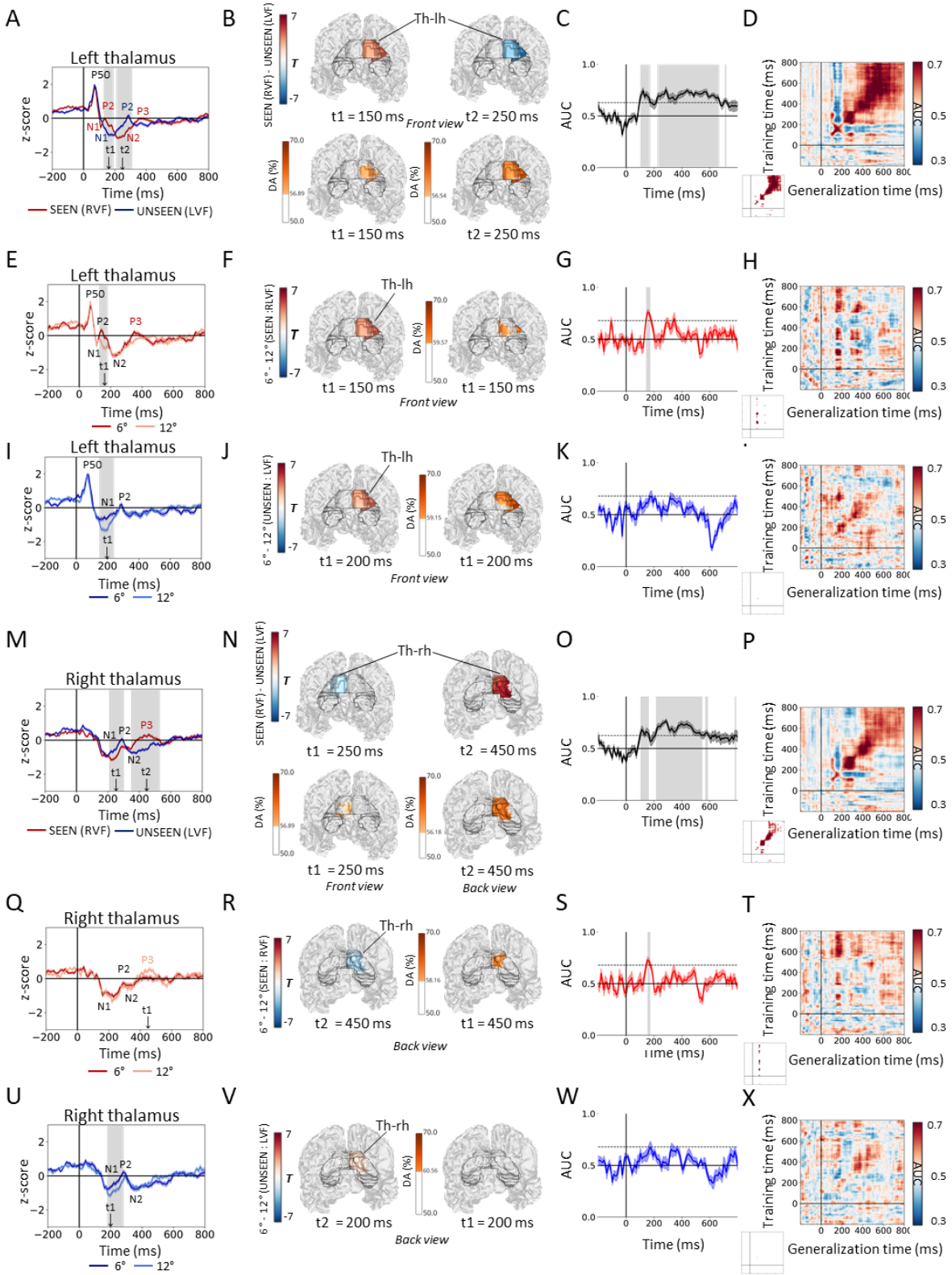

Figure 3. – The thalami play an important role in perceiving conscious and unconscious information.

VER, decoding, temporal decoding, and temporal generalization in single trial analyses reveal activity in the left thalamus (Th-lh) and right thalamus (Th-rh). (A-D) Comparisons between seen (red) and unseen (blue) stimuli in the Th-lh. (E-H) Comparisons between seen paracentral (red) and seen near periphery (pink) stimuli in the Th-lh. (I-L) Comparisons between unseen paracentral (blue) and unseen near periphery (light blue) stimuli in the Th-lh. (M-P) Comparisons between seen (red) and unseen stimuli (blue) in the Th-rh. (Q-T) Comparisons between seen paracentral (red) and seen near periphery (pink) stimuli in the Th-rh. (U-X) Comparisons between unseen paracentral (blue) and unseen near periphery (light blue) in the Th-rh. (A,E,I,M,Q,U) VER and statistical differences over time between conditions were assessed using cluster-based permutation analysis corrected for multiple comparisons. Significant differences are highlighted in grey. (B,F,J,N,R,V) Differences between conditions for specific time points across all nodes of the thalami are illustrated as T-values. Statistical differences corrected for multiple comparisons computed as DA (%) were assessed using ML by decoding conditions across nodes. Only significant nodes are illustrated in the thalami. (C,G,E,O,S,W) Temporal decoding over time was determined as AUC using all nodes of each thalamus as features. Threshold for significance was assessed using Bonferroni corrections. Significant AUCs are highlighted in grey. (D,H,L,P,T,X) Matrices show the results obtained from the temporal generalization analysis measured as the AUC over time using all nodes of each thalamus as features. Threshold for significance was assessed using Bonferroni correction and significant AUCs are shown in the small matrix at the bottom left of the figure. – Figure 3

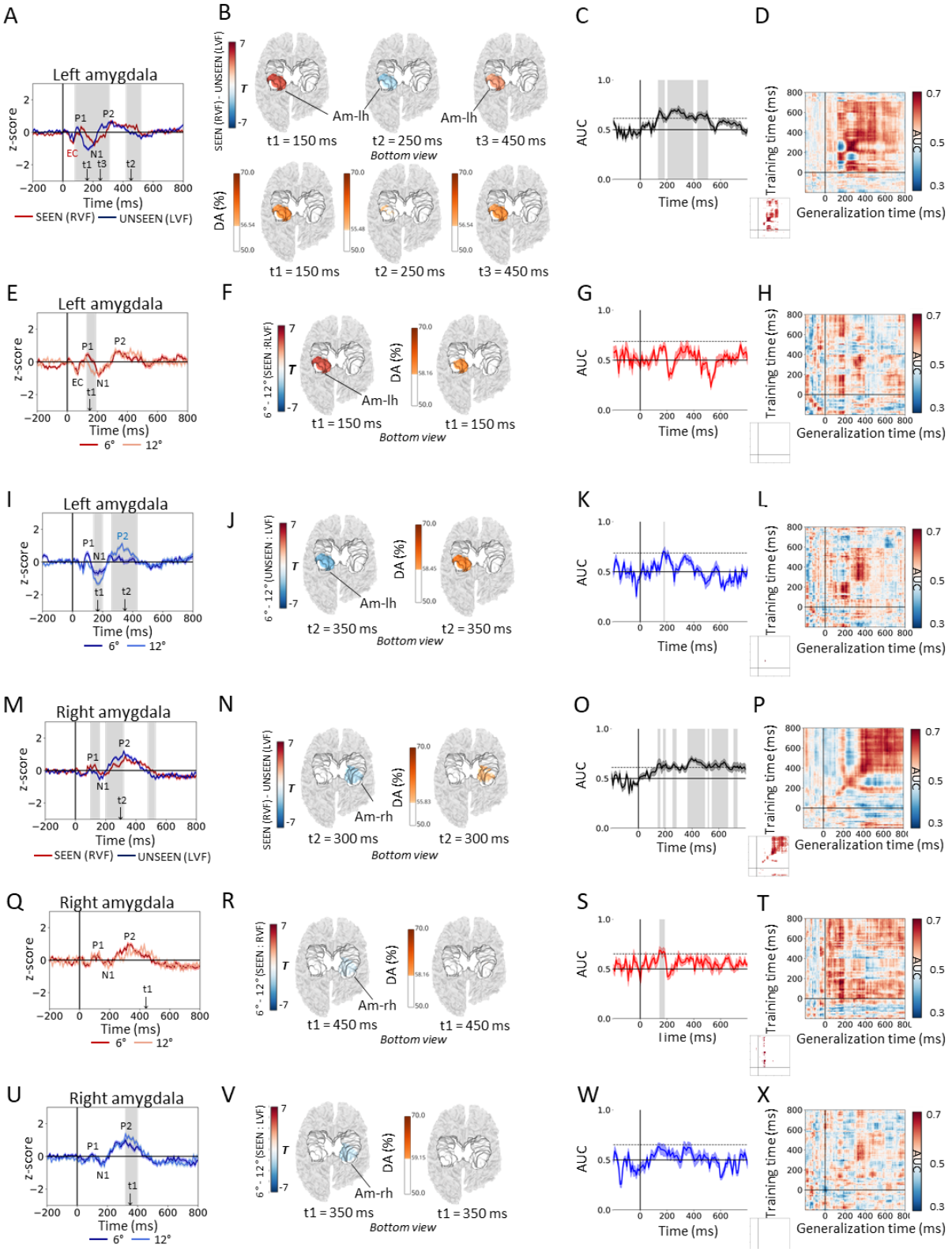

Figure 4. – The left and right amygdala have distinctive roles in processing seen and unseen information.

VER, decoding, temporal decoding, and temporal generalization in single-trial analyses reveal activity in the left amygdala (Am-lh) and right amygdala (Am-rh). (A-D) Comparisons between seen and unseen stimuli in the Am-lh. (E-H) Comparisons between seen paracentral and seen near periphery stimuli in the Am-lh. (I-L) Comparisons between unseen paracentral and unseen near periphery stimuli in the Am-lh. (M-P) Comparisons between seen and unseen stimuli in the Am-rh. (Q-T) Comparisons between seen paracentral and seen near periphery stimuli in the Am-rh. (U-X) Comparisons between unseen paracentral and unseen near periphery stimuli in the Am-rh. (A,E,I,M,Q,U) VER and statistical differences over time between conditions were assessed using cluster-based permutation analysis corrected for multiple comparisons. Significant differences are highlighted in grey. (B,F,J,N,R,V) Differences between conditions for specific time points across all nodes of the amygdalae are illustrated as T-values. Statistical differences corrected for multiple comparisons computed as DA (%) were assessed using ML by decoding conditions across nodes. Only significant nodes are illustrated in the amygdalae. (C,G,E,O,S,W) Temporal decoding over time was determined as the AUC using all nodes of each amygdala as features. Threshold for significance was assessed using Bonferroni corrections. Significant AUCs are highlighted in grey. (D,H,L,P,T,X) Matrices show the results obtained from the temporal generalization analysis measured as the AUC over time using all nodes of each amygdala as features. Threshold for significance was assessed using Bonferroni correction and significant AUCs are shown in the small matrix at the bottom left of the figure. – Figure 4

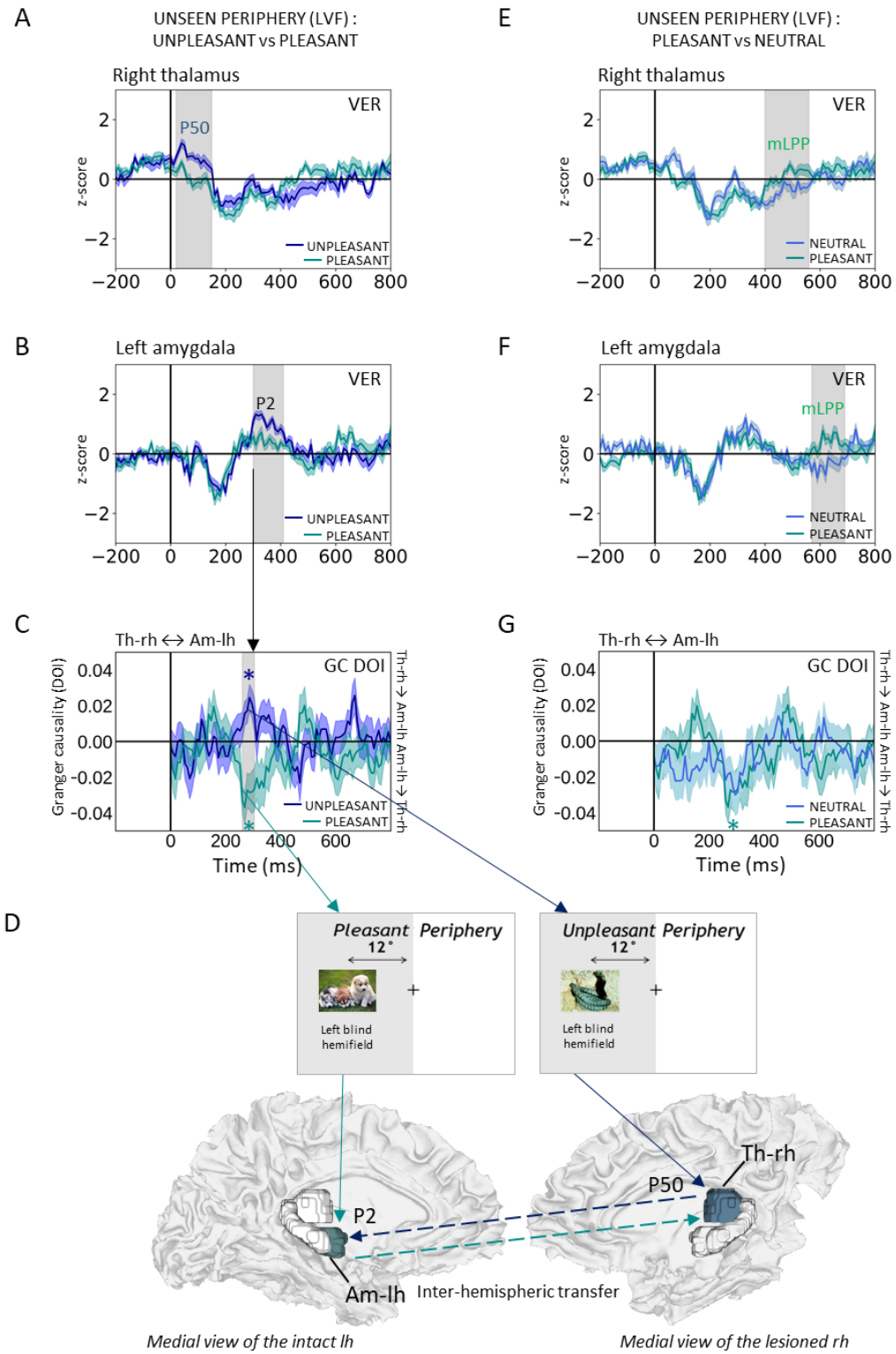

Figure 5. – The thalamus rapidly responds to unpleasant peripheral pictures in the absence of visual awareness and causally drives the activity of the amygdala, while the amygdala influences the activity of the thalamus for pleasant pictures.

Single-trial analysis of VER and GC for unconscious affective-specific differences in the near periphery of the blind hemifield. (A, E) Comparison between unseen near periphery unpleasant pictures (blue), pleasant pictures (green), and neutral pictures (light blue) in the right thalamus. Unpleasant pictures induced a larger P50 compared to pleasant pictures. Pleasant pictures induced a greater magnetic late positivity potential (mLPP) compared to neutral pictures. (B, F) Comparison between unseen near periphery unpleasant pictures (blue), pleasant pictures (green), and neutral pictures (light blue) in the left amygdala. Unpleasant pictures induced a larger P2 compared to pleasant pictures. Pleasant pictures induced an mLPP compared to neutral pictures. (C, G) The dominant directionality in GC between the right thalamus and the left amygdala was computed as the DOI which assessed the net difference between GC measured from the right thalamus (Th-rh) to the left amygdala (Am-lh) and from the left amygdala to the right thalamus. Significant differences over time between conditions in GC DOI were addressed using cluster-based permutation analysis. Around 300 ms, the right thalamus exerted a significant causal influence on the left amygdala for unpleasant pictures, while the left amygdala exerted a significant causal influence on the right thalamus for pleasant pictures. (D) Schematic representation of VER components and the direction of the causal functional connectivity found between the Th-rh and the Am-lh for unseen near periphery unpleasant (blue) and pleasant pictures (green). – Figure 5

Seen (S) *vs* Unseen (U)	EC	EC	P1		N1		P2		N2		P3		N400	
	S	U	*S*	*U*	*S*	*U*	*S*	*U*	*S*	*U*	*S*	*U*	*S*	*U*
Intact V1 (S)	O :10 P :40 D: 60	X	O :70 P :110 D :40	O :70 P :146 D :76	O :110 P :160 D :50	O :146 P :251 D :105	O :160-247 P :183-277 D :23-30	O :251 P :277 D :26	O :277 P :340 D :63	O :277 P :344 D :67	O :340 P :510 D :170	X	O :510 P :591 D :290	X
Left thalamus (S)	O :31 P :70 D: 78	O: 18 P :70 D:140	X	X	O :70 P :112 D :42	O :70 P :163 D :93	O :112 P :132 D :20	O :163 P :280 D :117	O :132 P :215 D :83	X	O :215 P :365 D :150	X	X	X
Right thalamus (U)	X	X	X	X	O :106 P :223 D :117	O :106 P :179 D :73	O :223 P :287 D :64	O :179 P :287 D :111	O :287 P :344 D :57	O :287 P :360 D :73	O :344 P :459 D :115	X	X	X
Left Amygdala (S)	O: 24 P: 70 D: 67	X	O :70 P :126 D :56	O :70 P :92 D :22	O :126 P :213 D :87	O :92 P :166 D :74	O :213 P :320 D :107	O :166 P :261 D :95	X	X	X	X	X	X
Right Amygdala (U)	X	X	O :70 P :102 D :32	O :70 P :94 D :24	O :102 P :166 D :64	O :94 P :162 D :68	O :166 P :334 D :168	O :160 P :318 D :156	X	X	X	X	X	X

S = contralateral to seen; U = contralateral to unseen; grey = significant differences; x = no component

Paracentral (Pc) *vs* Near Periphery (Np)	SEEN													
	EC	EC	P1		N1		P2		N2		P3			
	Pc	*Np*	*Pc*	*Np*	*Pc*	*Np*	*Pc*	*Np*	*Pc*	*Np*	*Pc*	*Np*	*Pc*	*Np*
Intact V1 (C)	O:10 P:40 D:60	X	O :70 P :110 D :40	O :70 P :110 D :40	O :110 P :160 D :50	O :110 P :233 D :123	O :160 P :183 D :23	O :247 P :277 D :30	O :207 P :340 D :133	O :277 P :340 D :63	O :340 P :510 D :170	X	O :520 P :688 D :280	X
Left thalamus (C)	O: 30 P: 70 D: 80	O: 18 P: 70 D: 80	X	X	O :70 P :112 D :42	O :70 P :112 D :42	O :112 P :140 D :28	O :112 P :122 D :10	O :140 P :217 D :77	O :122 P :217 D :95	O :217 P :356 D :139	X	X	X
Right thalamus (I)	X	X	X	X	O :106 P :223 D :117	O :106 P :223 D :117	O :223 P :287 D :64	O :223 P :287 D :64	O :287 P :344 D :57	O :287 P :344 D :57	X	O :344 P :459 D :115	X	X
Left Amygdala (C)	O: 24 P: 70 D: 64	O: 24 P: 60 D: 64	O :70 P :126 D :56	O :70 P :122 D :52	O :126 P :209 D :83	O :122 P :183 D :61	O :209 P :320 D :111	O :183 P :320 D :137	X	X	X	X	X	X
Right Amygdala (I)	X	X	O :70 P :102 D :32	O :70 P :102 D :32	O :102 P :166 D :64	O :102 P :166 D :64	O :166 P :334 D :168	O :166 P :334 D :168	X	X	X	X	X	X

C= contralateral to seen; I = ipsilateral to seen; grey = significant differences; x = no component

Paracentral (Pc) *vs* Near Periphery (Np)	UNSEEN													
	EC	EC	P1		N1		P2		N2		P3			
	Pc	*Np*	*Pc*	*Np*	*Pc*	*Np*	*Pc*	*Np*	*Pc*	*Np*	*Pc*	*Np*	*Pc*	*Np*
Intact V1 (I)	X	X	O :70 P :138 D :68	O :70 P :154 D :84	O :138 P :257 D :119	O :154 P :257 D :103	O :257 P :277 D :20	O :257 P :295 D :38	O :277 P :368 D :91	O :295 P :342 D :47	X	X	X	X
Left thalamus (I)	O: 20 P: 70 D:110	O: 20 P: 70 D:140	X	X	O :70 P :132 D :62	O :70 P :166 D :96	O :132 P :280 D :148	O :166 P :280 D :114	X	X	X	X	X	X
Right thalamus (C)	X	X	X	X	O :106 P :170 D :64	O :106 P :191 D :85	O :170 P :280 D :110	O :191 P :291 D :100	O :280 P :352 D :72	O :291 P :352 D :61	X	X	X	X
Left Amygdala (I)	X	X	O :70 P :92 D :22	O :70 P :92 D :22	O :92 P :166 D :74	O :92 P :166 D :74	X	O :166 P :326 D :160	X	X	X	X	X	X
Right Amygdala (C)	X	X	O :70 P :94 D :24	O :70 P :94 D :24	O :94 P :162 D :68	O :94 P :162 D :68	O :162 P :318 D :156	O :162 P :318 D :156	X	X	X	X	X	X

C= contralateral to unseen; I = ipsilateral to unseen; grey = significant differences; x = no component

Tableau 1. – Onset (O), Peak (P) & Duration (D) of ERF components (*ms*)

References

Almeida, I., Soares, S.C., and Castelo-Branco, M. (2015). The Distinct Role of the Amygdala, Superior Colliculus and Pulvinar in Processing of Central and Peripheral Snakes. PLoS One 10, e0129949.

Alvarado, J.C., Stanford, T.R., Vaughan, J.W., and Stein, B.E. (2007). Cortex mediates multisensory but not unisensory integration in superior colliculus. J. Neurosci. 27, 12775–12786.

Andersen, L.M., Jerbi, K., and Dalal, S.S. (2020). Can EEG and MEG detect signals from the human cerebellum? Neuroimage 215.

Arden, G.B., Wolf, J.E., and Messiter, C. (2003). Electrical activity in visual cortex associated with combined auditory and visual stimulation in temporal sequences known to be associated with a visual illusion. Vision Res. 43, 2469–2478.

Aru, J., Suzuki, M., and Larkum, M.E. (2020). Cellular Mechanisms of Conscious Processing. Trends Cogn. Sci. 24, 814–825.

Baars, B.J. (2002). The conscious access hypothesis: Origins and recent evidence. Trends Cogn. Sci. 6, 47–52.

Bayle, D.J., Henaff, M.-A., and Krolak-Salmon, P. (2009). Unconsciously perceived fear in peripheral vision alerts the limbic system: a MEG study. PLoS One 4, e8207.

Bayle, D.J., Schoendorff, B., Hénaff, M.-A., and Krolak-Salmon, P. (2011). Emotional facial expression detection in the peripheral visual field. PLoS One 6, e21584.

Bennett, C., Gale, S.D., Garrett, M.E., Newton, M.L., Callaway, E.M., Murphy, G.J., and Olsen, S.R. (2019). Higher-Order Thalamic Circuits Channel Parallel Streams of Visual Information in Mice. Neuron 102, 477-492.e5.

Bertini, C., Cecere, R., and Làdavas, E. (2017). Unseen fearful faces facilitate visual discrimination in the intact field. Neuropsychologia.

Bertini, C., Cecere, R., and Làdavas, E. (2019). Unseen fearful faces facilitate visual discrimination in the intact field. Neuropsychologia 128, 58–64.

Breitmeyer, B.G. (2014). Contributions of magno- and parvocellular channels to conscious and non-conscious vision. Philos. Trans. R. Soc. B Biol. Sci. 369.

Bridge, H., Thomas, O., Jbabdi, S., and Cowey, A. (2008). Changes in connectivity after visual cortical brain damage underlie altered visual function. Brain 131, 1433–1444.

Brovelli, A., Chicharro, D., Badier, J.M., Wang, H., and Jirsa, V. (2015). Characterization of cortical networks and corticocortical functional connectivity mediating arbitrary visuomotor mapping. J. Neurosci. 35, 12643–12658.

Calvo, M.G., Beltrán, D., and Fernández-Martín, A. (2014). Processing of facial expressions in peripheral vision: Neurophysiological evidence. Biol. Psychol. 100, 60–70.

Campana, F., Rebollo, I., Urai, A., Wyart, V., and Tallon-Baudry, C. (2016). Conscious Vision Proceeds from Global to Local Content in Goal-Directed Tasks and Spontaneous Vision. J. Neurosci. 36, 5200–5213.

Cecere, R., Bertini, C., Maier, M.E., and Làdavas, E. (2014). Unseen Fearful Faces Influence Face Encoding: Evidence from ERPs in Hemianopic Patients. J. Cogn. Neurosci. 26, 2564–2577.

Chen, Y., Ni, Y., Zhou, J., Zhou, H., Zhong, Q., Li, X., Zhang, J., Ma, Y., and Wei, J. (2021). The Amygdala Responds Rapidly to Flashes Linked to Direct Retinal Innervation: A Flash-evoked Potential Study Across Cortical and Subcortical Visual Pathways. Neurosci. Bull. 1–12.

Colibazzi, T., Posner, J., Wang, Z., Gorman, D., Gerber, A., Yu, S., Zhu, H., Kangarlu, A., Duan, Y., Russell, J.A., et al. (2010). Neural Systems Subserving Valence and Arousal During the Experience of Induced Emotions. Emotion 10, 377–389.

Combrisson, E., and Jerbi, K. (2015). Exceeding chance level by chance: The caveat of theoretical chance levels in brain signal classification and statistical assessment of decoding accuracy. J. Neurosci. Methods 250, 126–136.

Combrisson, E., Vallat, R., O'Reilly, C., Jas, M., Pascarella, A., Saive, A.L., Thiery, T., Meunier, D., Altukhov, D., Lajnef, T., et al. (2019). Visbrain: A multi-purpose GPU-accelerated open-source suite for multimodal brain data visualization. Front. Neuroinform. 13.

Cornwell, B.R., Carver, F.W., Coppola, R., Johnson, L., Alvarez, R., and Grillon, C. (2008). Evoked amygdala responses to negative faces revealed by adaptive MEG beamformers. Brain Res. 1244, 103–112.

Costafreda, S.G., Brammer, M.J., David, A.S., and Fu, C.H.Y. (2008). Predictors of amygdala activation during the processing of emotional stimuli: A meta-analysis of 385 PET and fMRI studies. Brain Res. Rev. 58, 57–70.

Dalal, S., Jerbi, K., Bertrand, O., Adam, C., Ducorps, A., Schwartz, D., Martinerie, J., Lachaux, J.-P., and Dalal, S.S. (2013). Simultaneous MEG-intracranial EEG: New insights into the

ability of MEG to capture oscillatory modulations in the neocortex and the hippocampus. Epilepsy Behav. 10, 1016.

Dehaene, S., and Changeux, J.-P. (2011). Experimental and theoretical approaches to conscious processing. Neuron 70, 200–227.

Dehaene, S., and King, J.R. (2016). Decoding the dynamics of conscious perception: The temporal generalization method. In Research and Perspectives in Neurosciences, (Springer Verlag), pp. 85–97.

Dehaene, S., Changeux, J.P., Naccache, L., Sackur, J., and Sergent, C. (2006). Conscious, preconscious, and subliminal processing: a testable taxonomy. Trends Cogn. Sci. 10, 204–211.

Dumas, T., Dubal, S., Attal, Y., Chupin, M., Jouvent, R., Morel, S., and George, N. (2013). MEG Evidence for Dynamic Amygdala Modulations by Gaze and Facial Emotions. PLoS One 8.

Elorette, C., Forcelli, P.A., Saunders, R.C., and Malkova, L. (2018). Colocalization of tectal inputs with amygdala-projecting neurons in the macaque pulvinar. Front. Neural Circuits 12.

Fiebelkorn, I.C., Pinsk, M.A., and Kastner, S. (2018). A Dynamic Interplay within the Frontoparietal Network Underlies Rhythmic Spatial Attention. Neuron 99, 842-853.e8.

Fischl, B., Salat, D.H., Busa, E., Albert, M., Dieterich, M., Haselgrove, C., Van Der Kouwe, A., Killiany, R., Kennedy, D., Klaveness, S., et al. (2002). Whole brain segmentation: Automated labeling of neuroanatomical structures in the human brain. Neuron 33, 341–355.

Förster, J., Koivisto, M., and Revonsuo, A. (2020). ERP and MEG correlates of visual consciousness: The second decade. Conscious. Cogn. 80.

Fox, D.M., Goodale, M.A., and Bourne, J.A. (2020). The Age-Dependent Neural Substrates of Blindsight. Trends Neurosci. 43, 242–252.

Frank, D.W., and Sabatinelli, D. (2014). Human thalamic and amygdala modulation in emotional scene perception. Brain Res. 1587, 69–76.

Garrido, M.I., Barnes, G.R., Sahani, M., and Dolan, R.J. (2012). Functional evidence for a dual route to amygdala. Curr. Biol. 22, 129–134.

de Gelder, B., Vroomen, J., Pourtois, G., and Weiskrantz, L. (1999). Non-conscious recognition of affect in the absence of striate cortex. Neuroreport 10, 3759–3763.

Georgy, L., Lewis, J.D., Bezgin, G., Diano, M., Celeghin, A., Evans, A.C., Tamietto, M., and Ptito, A. (2020). Changes in peri-calcarine cortical thickness in blindsight. Neuropsychologia 143.

Gramfort, A., Luessi, M., Larson, E., Engemann, D.A., Strohmeier, D., Brodbeck, C., Goj, R., Jas, M., Brooks, T., Parkkonen, L., et al. (2013). MEG and EEG data analysis with MNE-Python. Front. Neurosci. 7.

Hadid, V., and Lepore, F. (2017). From Cortical Blindness to Conscious Visual Perception: Theories on Neuronal Networks and Visual Training Strategies. Front. Syst. Neurosci. 11, 64.

Hajcak, G., MacNamara, A., Foti, D., Ferri, J., and Keil, A. (2013). The dynamic allocation of attention to emotion: Simultaneous and independent evidence from the late positive potential and steady state visual evoked potentials. Biol. Psychol. 92, 447–455.

Hämäläinen, M.S., and Ilmoniemi, R.J. (1994). Interpreting magnetic fields of the brain: minimum norm estimates. Med. Biol. Eng. Comput. 32, 35–42.

Harel, A., Groen, I.I.A., Kravitz, D.J., Deouell, L.Y., and Baker, C.I. (2016). The temporal dynamics of scene processing: A multifaceted EEG investigation. ENeuro 3.

Heeger, D.J., and Zemlianova, K.O. (2020). A recurrent circuit implements normalization, simulating the dynamics of V1 activity. Proc. Natl. Acad. Sci. U. S. A. 117, 22494–22505.

Heywood, C., and Kentridge, R. (2000). Affective blindsight? Trends Cogn. Sci. 4, 125–126.

Hillyard, S.A., and Anllo-Vento, L. (1998). Event-related brain potentials in the study of visual selective attention. Proc. Natl. Acad. Sci. 95, 781–787.

Kastner, S., Fiebelkorn, I.C., and Eradath, M.K. (2020). Dynamic pulvino-cortical interactions in the primate attention network. Curr. Opin. Neurobiol. 65, 10–19.

Kavcic, V., Triplett, R.L., Das, A., Martin, T., and Huxlin, K.R. (2015). Role of inter-hemispheric transfer in generating visual evoked potentials in V1-damaged brain hemispheres. Neuropsychologia 68, 82–93.

King, J.R., and Dehaene, S. (2014). Characterizing the dynamics of mental representations: The temporal generalization method. Trends Cogn. Sci. 18, 203–210.

King, J.R., Pescetelli, N., and Dehaene, S. (2016). Brain Mechanisms Underlying the Brief Maintenance of Seen and Unseen Sensory Information. Neuron 92, 1122–1134.

Kinoshita, M., Kato, R., Isa, K., Kobayashi, K., Kobayashi, K., Onoe, H., and Isa, T. (2019). Dissecting the circuit for blindsight to reveal the critical role of pulvinar and superior colliculus. Nat. Commun. 10.

Klimesch, W. (2011). Evoked alpha and early access to the knowledge system: The P1 inhibition timing hypothesis. Brain Res. 1408, 52–71.

Koivisto, M., and Grassini, S. (2016). Neural processing around 200 ms after stimulus-onset correlates with subjective visual awareness. Neuropsychologia 84, 235–243.

Koivisto, M., Mäntylä, T., and Silvanto, J. (2010). The role of early visual cortex (V1/V2) in conscious and unconscious visual perception. Neuroimage 51, 828–834.

Lamme, V.A.F., and Roelfsema, P.R. (2000). The distinct modes of vision offered by feedforward and recurrent processing. Trends Neurosci. 23, 571–579.

Lithari, C., Moratti, S., and Weisz, N. (2015). Thalamocortical interactions underlying visual fear conditioning in humans. Hum. Brain Mapp. 36, 4592–4603.

Liu, L., and Ioannides, A.A. (2010). Emotion separation is completed early and it depends on visual field presentation. PLoS One 5.

Liu, T.-Y., Chen, Y.-S., Hsieh, J.-C., and Chen, L.-F. (2015). Asymmetric engagement of amygdala and its gamma connectivity in early emotional face processing. PLoS One 10, e0115677.

Luo, Q., Holroyd, T., Jones, M., Hendler, T., and Blair, J. (2007). Neural dynamics for facial threat processing as revealed by gamma band synchronization using MEG. Neuroimage 34, 839–847.

Luo, Q., Holroyd, T., Majestic, C., Cheng, X., Schechter, J., and James Blair, R. (2010). Emotional automaticity is a matter of timing. J. Neurosci. 30, 5825–5829.

Ma, J., Liu, C., and Chen, X. (2016). Emotional Modulation of Conflict Processing in the Affective Domain: Evidence from Event-related Potentials and Event-related Spectral Perturbation Analysis. Sci. Rep. 6.

Mangun, G.R., Hinrichs, H., Scholz, M., Mueller-Gaertner, H.W., Herzog, H., Krause, B.J., Tellman, L., Kemna, L., and Heinze, H.J. (2001). Integrating electrophysiology and neuroimaging of spatial selective attention to simple isolated visual stimuli. In Vision Research, (Vision Res), pp. 1423–1435.

Maris, E., and Oostenveld, R. (2007). Nonparametric statistical testing of EEG- and MEG-data. J. Neurosci. Methods 164, 177–190.

Mashour, G.A., Roelfsema, P., Changeux, J.P., and Dehaene, S. (2020). Conscious Processing and the Global Neuronal Workspace Hypothesis. Neuron 105, 776–798.

Maunsell, J.H., Ghose, G.M., Assad, J.A., McAdams, C.J., Boudreau, C.E., and Noerager, B.D. (1999). Visual response latencies of magnocellular and parvocellular LGN neurons in macaque monkeys. Vis. Neurosci. 16, 1–14.

McFadyen, J., Dolan, R.J., and Garrido, M.I. (2020). The influence of subcortical shortcuts on disordered sensory and cognitive processing. Nat. Rev. Neurosci. 1–13.

Méndez-Bértolo, C., Moratti, S., Toledano, R., Lopez-Sosa, F., Martínez-Alvarez, R., Mah, Y.H., Vuilleumier, P., Gil-Nagel, A., and Strange, B.A. (2016). A fast pathway for fear in human amygdala. Nat. Neurosci. 19.

Meunier, D., Pascarella, A., Altukhov, D., Jas, M., Combrisson, E., Lajnef, T., Bertrand-Dubois, D., Hadid, V., Alamian, G., Alves, J., et al. (2020). NeuroPycon: An open-source python toolbox for fast multi-modal and reproducible brain connectivity pipelines. Neuroimage 219.

Min, B.-K. (2010). A thalamic reticular networking model of consciousness. Theor. Biol. Med. Model. 7, 10.

Moratti, S., Saugar, C., and Strange, B.A. (2011). Prefrontal-occipitoparietal coupling underlies late latency human neuronal responses to emotion. J. Neurosci. 31, 17278–17286.

Morris, J.S., Öhman, A., and Dolan, R.J. (1999). A subcortical pathway to the right amygdala mediating “unseen” fear. Proc. Natl. Acad. Sci. U. S. A. 96, 1680–1685.

Morris, J.S., DeGelder, B., Weiskrantz, L., and Dolan, R.J. (2001). Differential extrageniculostriate and amygdala responses to presentation of emotional faces in a cortically blind field. Brain 124, 1241–1252.

Nakasato, N., Seki, K., Fujita, S., Hatanaka, K., Kawamura, T., Ohtomo, S., Kanno, A., Ikeda, H., and Yoshimoto, T. (1996). Clinical application of visual evoked fields using an MRI-linked whole head MEG system. Front. Med. Biol. Eng. 7, 275–283.

Patel, S.H., and Azzam, P.N. (2005). Characterization of N200 and P300: Selected Studies of the Event-Related Potential. Int. J. Med. Sci. 2, 147.

Pins, D., and Ffytche, D. (2003). The neural correlates of conscious vision. Cereb. Cortex 13, 461–474.

Ptito, A., and Leh, S.E. (2007). Neural substrates of blindsight after hemispherectomy. Neuroscientist 13, 506–518.

Railo, H., Koivisto, M., and Revonsuo, A. (2011). Tracking the processes behind conscious perception: A review of event-related potential correlates of visual consciousness. Conscious. Cogn. 20, 972–983.

Railo, H., Revonsuo, A., and Koivisto, M. (2015). Behavioral and electrophysiological evidence for fast emergence of visual consciousness. Neurosci. Conscious. 2015.

Ramachandra, V., Pawlak, V., Wallace, D.J., and Kerr, J.N.D. (2020). Impact of visual callosal pathway is dependent upon ipsilateral thalamus. Nat. Commun. 11.

Ries, A.J., and Hopfinger, J.B. (2011). Magnocellular and parvocellular influences on reflexive attention. Vision Res. 51, 1820–1828.

Di Russo, F., Martínez, A., Sereno, M.I., Pitzalis, S., and Hillyard, S.A. (2002). Cortical sources of the early components of the visual evoked potential. Hum. Brain Mapp. 15, 95–111.

Di Russo, F., Aprile, T., Spitoni, G., and Spinelli, D. (2008). Impaired visual processing of contralesional stimuli in neglect patients: a visual-evoked potential study. Brain 131, 842–854.

Rutiku, R., Martin, M., Bachmann, T., and Aru, J. (2015). Does the P300 reflect conscious perception or its consequences? Neuroscience 298, 180–189.

Rutiku, R., Aru, J., and Bachmann, T. (2016). General markers of conscious visual perception and their timing. Front. Hum. Neurosci. 10, 23.

Sanchez-Lopez, J., Pedersini, C.A., Di Russo, F., Cardobi, N., Fonte, C., Varalta, V., Prior, M., Smania, N., Savazzi, S., and Marzi, C.A. (2017). Visually evoked responses from the blind field of hemianopic patients. Neuropsychologia.

Schönwald, L.I., and Müller, M.M. (2014). Slow biasing of processing resources in early visual cortex is preceded by emotional cue extraction in emotion-attention competition. Hum. Brain Mapp. 35, 1477–1490.

Sherman, S.M. (2016). Thalamus plays a central role in ongoing cortical functioning. Nat. Neurosci. 19, 533–541.

Shimojo, S., and Shams, L. (2001). Sensory modalities are not separate modalities: Plasticity and interactions. Curr. Opin. Neurobiol. 11, 505–509.

Silvanto, J. (2015). Why is “blindsight” blind? A new perspective on primary visual cortex, recurrent activity and visual awareness. Conscious. Cogn. 32, 15–32.

Starke, J., Ball, F., Heinze, H.-J., and Noesselt, T. (2020). The spatio-temporal profile of multisensory integration. Eur. J. Neurosci. 51, 1210–1223.

Talsma, D., Doty, T.J., and Woldorff, M.G. (2007). Selective attention and audiovisual integration: Is attending to both modalities a prerequisite for early integration? Cereb. Cortex 17, 679–690.

Tao, D., He, Z., Lin, Y., Liu, C., and Tao, Q. (2021). Where does fear originate in the brain? A coordinate-based meta-analysis of explicit and implicit fear processing. Neuroimage 227, 117686.

Tapia, E., and Breitmeyer, B.G. (2011). Visual consciousness revisited: magnocellular and parvocellular contributions to conscious and nonconscious vision. Psychol. Sci. 22, 934–942.

Taylor, J.G., and Fragopanagos, N.F. (2005). The interaction of attention and emotion. Neural Networks 18, 353–369.

Tran, A., MacLean, M.W., Hadid, V., Lazzouni, L., Nguyen, D.K., Tremblay, J., Dehaes, M., and Lepore, F. (2019). Neuronal mechanisms of motion detection underlying blindsight assessed by functional magnetic resonance imaging (fMRI). Neuropsychologia 128, 187–197.

Troiani, V., Price, E.T., and Schultz, R.T. (2014). Unseen fearful faces promote amygdala guidance of attention. Soc. Cogn. Affect. Neurosci. 9, 133–140.

Vuilleumier, P. (2005). How brains beware: Neural mechanisms of emotional attention. Trends Cogn. Sci. 9, 585–594.

Ward, R., Danziger, S., and Bamford, S. (2005). Response to visual threat following damage to the pulvinar. Curr. Biol. 15, 571–573.

Weiskrantz, L. (2004). Roots of blindsight. Prog. Brain Res. 144, 229–241.

Weiskrantz, L., Barbur, J.L., and Sahraie, A. (1995). Parameters affecting conscious versus unconscious visual discrimination with damage to the visual cortex (V1). Proc. Natl. Acad. Sci. U. S. A. 92, 6122–6126.

Woods, D.L., Alho, K., and Algazi, A. (1992). Intermodal selective attention. I. Effects on event-related potentials to lateralized auditory and visual stimuli. Electroencephalogr. Clin. Neurophysiol. 82, 341–355.

Chapter 6

Article 4: The vMMN a Neural Marker for Assessing Automatic Detection of Changes in the Absence of Visual Awareness Independent of Behavior

Article 4. The vMMN a Neural Marker for Assessing Automatic Detection of Changes in the Absence of Visual Awareness Independent of Behavior

Vanesa Hadid[1,3,7], Michèle W. MacLean[2], Annalisa Pascarella[3,4], Tarek Lajnef[3], Marie-Charlotte Higgins[2], Caroline Grand-Maître[2], Dang Khoa Nguyen[5], Karim Jerbi[2,3,6], Franco Lepore[2,6]

[1]Département de Sciences Biomédicales, Université de Montréal,

[2]Département de Psychologie, Université de Montréal

[3]Computational and Cognitive Neuroscience Lab (CoCo Lab)

[4]Italian National Research Council, Rome, Italy

[5]Service de neurologie, CHUM Hôpital Notre-Dame

[6]Co-last author

[7]Lead contact

Abstract

Preserved blindsight abilities in patients with V1-lesions suggest that visual awareness isn't necessary to process information in the blind field. However, the ability to detect unpredicted sudden changes in blindsight has yet to be characterized. We propose to assess such abilities for motion stimuli using the visual mismatch negativity (vMMN) thought to reflect prediction errors in a pre-attentive state. We hypothesize that the neural correlates associated with this mismatch response could potentially be used as a marker of unconscious detection of changes. Therefore, we measured the brain's ability to detect motion changes without participants consciously reporting these changes during EEG recordings. This was possible by using a high load central Stroop task presented simultaneously with a peripheral visual oddball paradigm. The task was performed by neurotypical individuals and patient ML presenting blindsight in her right blind hemifield for motion stimuli. We demonstrated that our paradigm triggered a vMMN, P3a, and synchronization in theta power reflecting a genuine mismatch response and automatic processing in the absence of visual awareness as these components were observed in the neurotypical group and the patient's blind hemifield. Moreover, the prediction errors were seemingly characterized by large-scale functional network modulations in different frequency bands which revealed inequivalent

implications for the left and right hemifields. Interestingly, theta posterior connectivity was stronger in ML's blind hemifield compared to the controls' right hemifield suggesting functional theta enhancement in blindsight. Taken together, our results indicate the potential use of the vMMN as an electrophysiological biomarker to measure unconscious visual processing in neurotypical and blindsight individuals.

Introduction

Detecting sudden changes in the visual field, particularly when they breach environmental expected regularities, is fundamental to effectively responding to relevant or biologically significant stimuli. Blindsight individuals with lesions to the primary visual cortex (V1) causing homonymous hemianopia (HH) can perform above chance-level to biologically significant stimuli, as motion stimuli (Barton and Sharpe, 1997) presented in their blind field, even if they occur in the absence of visual awareness (Sanders et al., 1974; Weiskrantz et al., 1974). However, their ability to automatically detect a deviant change has yet to be established. We propose to assess such abilities for motion stimuli independently of behavior using the visual mismatch negativity (vMMN) as a reliable EEG biomarker thought to reflect automatic unpredicted change detection in a pre-attentive state (Amenedo et al., 2007; Clifford et al., 2010; Lyyra et al., 2012).

The vMMN can be detected as posterior negativity around 200 ms elicited when the presentation of a rare stimulus (i.e., deviant) alters sequential frequent stimuli (i.e., standard) in an oddball sequence (for reviews see Pazo-Alvarez et al., 2003; Qian et al., 2014; Stefanics et al., 2014) caused by a violation of regularities (Fitzgerald and Todd, 2020; Kimura et al., 2010; Kuldkepp et al., 2013; Stefanics et al., 2011; Tales et al., 1999; Yeark et al., 2021). The vMMN can also be characterized by modulations of specific oscillatory responses, notably in the theta (4-7 Hz) and alpha (7-13 Hz) bands (Chen et al., 2020; Hesse et al., 2017; Stothart and Kazanina, 2013; Wei and Gillon-Dowens, 2018; Yan et al., 2017). Such assessments could provide further knowledge on prediction errors associated with the detection of changes that are based on past experience and context, i.e. presentation of a regular sequence of standards, where the system predicts the incoming sensory input (Oxner et al., 2019; Rowe et al., 2020; Stefanics et al., 2016). Therefore, the mismatch between the deviant stimulus and internal representation mirrors the discrepancy between the bottom-up and top-down systems, respectively. While it is still up to debate, both systems have been known to contribute on different network scales to conscious and

unconscious processing (Mashour and Hudetz, 2018) with regard to other higher-order mechanisms such as allocation of attentional resources (Mashour et al., 2020). Nonetheless, the vMMN in the absence of conscious perception has only recently been characterized by oscillatory mismatch responses (Chen et al., 2020) and spatiotemporal network patterns recruiting posterior regions (Rowe et al., 2020). Moreover, in the auditory modality, unconscious detection of unpredicted changes has been assessed by the MMN (King et al., 2013) and by a subsequent fronto-central positivity around 300 ms, i.e. the P3a, independent of attentional reallocation reflecting automatic processing (Muller-Gass et al., 2007). Importantly, the auditory mismatch response in responsive unconscious individuals has been shown to influence the P3a, posterior theta-alpha power, and functional connectivity (Hermann et al., 2020). These mechanisms could be associated with a genuine vMMN that unravels unconscious detection of unpredicted changes. Such demonstration might be used as an alternative or complementary measure of unconscious abilities in blindsight patients and more largely in visual awareness studies to reduce biases induced by subjective measurements (Soto et al., 2019; Tsuchiya et al., 2015).

Thus, the challenge and aim of this study are to assess the local and network neural correlates of a vMMN that is observable in the absence of visual awareness in neurotypical individuals and ML, a patient with a right HH following a complete left V1-lesion known for presenting type II blindsight for motion detection (Tran et al., 2019). We hypothesize the presence of mismatch response independent of visual awareness in the neurotypical group and blindsight patients characterized by (1) posterior negativity around 200 ms, (2) a frontal positivity around 300 ms, (3) posterior theta-alpha power modulations, and (4) changes within a posterior and frontal neural network. To test our predictions, we asked participants to complete a high load central Stroop task requiring focused attention during EEG recordings. With the purpose to induce a mismatch response, we simultaneously presented an unattended peripheral motion oddball paradigm in the left or right hemifield of participants where motion changes weren't consciously reported. Taken together, our results could support the vMMN as an electrophysiological biomarker to measure unconscious visual processing in neurotypical and blindsight individuals.

Methods

Subjects

Twenty neurotypical adults [14 females, age range (mean ± SD 21.65 ± 2.58 y), 16 right-handed] and one HH patient, ML [female, age 28 at the time of the testing, right-handed] participated in the current study. ML has a complete unilateral post-chiasmatic lesion to the left occipital cortex resulting in a contralateral visual loss of her right hemifield with no macular sparing. ML demonstrates Type II blindsight abilities as evaluated by forced-choice motion detection paradigms (Sahraie et al., 2010). A complete description of the patient's history can be found in our previous study (Tran et al., 2019). Except for the patient's blind hemifield, all participants had normal or corrected to normal vision at the time of testing (including the patient's intact visual hemifield). This study was approved by the Comité d'éthique de la recherche du Centre de recherche du Centre hospitalier de l'Université de Montréal (CRCHUM), Montréal, Canada. Participants were asked to provide written and informed consent prior to participation and received financial compensation for their allocated time to this study.

Passive peripheral motion direction oddball design with central Stroop task

Visual stimuli were presented using Presentation® software (Version 18.0, Neurobehavioral Systems, Inc., Berkeley, CA) on a projector screen (195x146cm2) in a darkened anechoic room around 60Lux. Participants were asked to sit 114cm away from the screen (distance maintained with a chinrest) and perform a behavioral high-speeded Stroop Task. Simultaneously, a visual oddball paradigm was presented in their peripheral visual field either in the left or right hemifield to elicit a vMMN. The Stroop Task, which requires a maintained and high level of attention, was presented in central vision to ensure that attention was not drawn to the oddball.

The Stroop task consisted of color words (i.e., red, blue, green, yellow, purple) written in congruent or incongruent ink colors on a black background presented in the middle of the screen for 500 ms with an interstimulus interval (ISI) of 900ms for a total trial duration of 1400ms. Participants were instructed to use their right hand and respond "1" on a numerical keyboard when the word was congruent with the color or "2" if the word was incongruent with the color (e.g. congruent: the word red written in red ink vs. incongruent: the word red written in blue ink). Accuracy rate and reaction times (RTs) were collected for behavioral analyses. There were no instructions regarding the visual oddball presented in the periphery and no details about the nature of the stimuli were provided. We only asked them to ignore anything happening outside their

central vision and ensure that the participant was effectively doing the task for a few minutes with focused attention prior to presenting the peripheral oddball sequence.

The peripheral passive oddball paradigm was designed to induce a strong primitive biological change (Pazo-Alvarez et al., 2004), reduce refractoriness (Kuldkepp et al., 2013; Stefanics et al., 2014b), and a rapid change (short ISI) with respect to the visual sensory memory time span (Astikainen et al., 2008). The peripheral motion stimuli for the oddball paradigm were generated using the random-dot kinematogram (RDK) model (Morrone et al., 2000) and consisted of 150 black moving dots (0.5° in diameter, speed of 12º/sec, lifetime of 150ms), with 100% motion coherence in one direction, presented over a white patch (12°x12°) at 12° of eccentricity in the right or left hemifields. The use of black dots reduced any possibility of refractoriness and luminance indices about the direction of the motion. The oddball paradigm consisted of this stimulus presented in a repetitive sequence, where standard stimuli refer to dots moving in an upward direction for 85% of the trials, and deviant stimuli refer to dots moving downward for 15% of the trials. The duration of each trial of moving dots was 1 second with an ISI of 400ms for a total of 1400 ms which is the equivalent time window as a single trial in the Stroop task, presented simultaneously. The change in motion direction, evoking a potential change in attention, always occurred at the same time as the presentation of a new word, thus excluding the possibility of conscious attention to the periphery within 500 ms. Participants were asked to perform two blocks in total, each lasted 20 minutes and including 800 trials (680 standards and 120 deviants) (Figure 1). At the end of the experiment, participants were asked whether they perceived "something changing in their peripheral vision while performing the Stroop Task", to assess their subjective account of the presentation of the oddball paradigm. However, no participant was able to describe the peripheral stimuli or report conscious perception of changes in motion direction.

Blindsight evaluations

ML's MRI data and visual field evaluations (Figures 2A and 2B) are from our previous study (Tran et al., 2019), where the visual field evaluation was provided by neurologist Dr. Dang Khoa Nguyen and a team of therapists from the Centre Hospitalier de l'Université de Montréal (CHUM). ML's ability to detect motion was demonstrated in our previous study but we further tested her residual abilities using static dots, motion detection, and motion discrimination with the same experimental

apparatus as the one described when performing the Stroop task. The objective was to ensure that we were able to assess a behavioral spectrum of ML's blindsight abilities.

Visual evaluation field

ML first underwent a plot visual evaluation to ensure that she could not see any of the visual stimuli presented in her blind hemifield. She kept her eyes steady on the fixation cross throughout the task, which was ensured with the eye tracker recordings. A grey disk of 2° on a black background was presented for 100 ms with an ISI ranging between 1000 ms and 1500 ms in 165 different positions covering almost every pixel of the screen. No stimulus was presented within a distance of 3º from the fixation point. Each position was presented four times. 165 blank trials were presented to guarantee that ML responded only when the stimulus was perceived or sensed, totaling 825 trials. ML always detected the visual stimuli presented in her normal left hemifield, but never responded to the visual stimulus presented in her right blind hemifield or to the blank trials. This evaluation validated the premise that ML could not see any of the visual stimuli that were presented in her blind right hemifield using the apparatus described in this study.

Pointing task

To validate whether ML was nonetheless able to unconsciously process visual static information in her blind hemifield, we asked her to perform an action towards a target which has been previously shown to assess preserved abilities despite lack of visual awareness (Danckert et al., 2003; Goodale and Milner, 1992). Therefore, ML fixated a white cross at all times and the sound signal, i.e. a white noise of 100 ms, she had to point towards a grey circle of 2º appearing in her blind hemifield during 500 ms even though she couldn't see it as reported by the visual evaluation field. Each trial consisted of a static dot presented on a black background in one of 80 different random positions within her blind hemifield covering the visual field from 3 to 45 º of eccentricity. ML results showed residual unconscious ability as the position where she pointed significantly correlated with the actual position of the target ($R2 = 0,17$; $p < .05$) (Figure 2C).

Spontaneous motion detection

In order to assess ML's spontaneous motion detection abilities, we asked her to fixate the cross throughout the entire task and to signal by pressing either "1" or "2" on a keyboard key if she "felt any sensation" that something static or in motion was presented in her blind hemifield. Each trial

consisted of the presentation of a 12 º white patch holding 150 black dots of 0.5 º presented on a white background at an eccentricity of 12 º which corresponded to the eccentricity and dimension of the motion stimuli described in the peripheral oddball of this study. The dots were either static or they moved upward or downward at a speed of 12 º/sec for 3 seconds. In total 600 trials were presented with 300 static trials and 300 motion trials. ML never responded that she had a feeling of something happening in her blind hemifield for static stimuli, but significantly detected 81% of the motion trials ($X2=120.53$, $p < .001$) confirming her Type II blindsight (Figure 2D). It is important to note that this "sensation" wasn't visual in nature, as ML couldn't describe what triggered or characterized this unconscious feeling.

Forced-choice motion discrimination

Using the same stimuli characteristics as the spontaneous motion detection task, we further examined ML's ability to discriminate between motion directions in a forced-choice task where the response was triggered by a white noise. The instruction was to fixate the cross throughout the entire task and to respond as fast as possible after the auditive signal by pressing "1" if she thought the dots were moving in an upward direction and "2" for a downward direction. However, her performance of 54% wasn't above chance-level ($X2=4.85$, $p = .08$) suggesting that she wasn't able to significantly discriminate between motion directions (Figure 2D). These results are important in terms of interpreting the presence of a vMMN when a task is unable to detect unconscious behavior suggesting its utility as a neural biomarker when a null effect on behavior is observed which is one of the main challenges in blindsight literature (Soto et al., 2019).

Data acquisition: EEG recordings

Electroencephalographic (EEG) activity of the twenty participants was recorded from 32 active electrodes, with a total of 40Ag/AgCl electrode sites and five external electrodes placed according to the international 10-20 system. After equipment breakage, the EEG activity of the eight remaining participants was recorded from 64 active Ag/AgCl electrodes (Biosemi Active Two system) and five external electrodes according to the international 10-10 system. The signal for both systems was re-referenced to the right and left mastoids. Due to differences in electrode

position between the two systems, only 26 common electrodes described in the data analysis section were used for further investigation.

Electrooculography (EOG) activity was recorded from four electrodes to later perform ocular correction on the data. The first two recorded horizontal EOG activity and were placed bilaterally on the zygomatic process of the frontal bone, whereas vertical EOG activity was recorded by placing an electrode above and below the right eye. The impendence was preserved under 5KΩ for all electrodes and verified throughout the entire experiment. The signal was digitized at 1000Hz. The anechoic room served to optimize the signal recording.

Behavioral data analysis

Responses were recorded for the Stroop Task for both correct and incorrect answers to ensure participants successfully completed the task, thus allocating full attention to their central vision. Correct answers refer to answering "1" when the written word and color of the ink were congruent or "2" if the written word and color of the ink were incongruent and vice versa for incorrect answers. Reaction times were collected for each neurotypical participant and we compared the effect of presenting a standard or deviant stimulus in the periphery on the performance and RTs to the Stroop task with t-tests and a significance level of $p < .05$. We also compared ML's intact and blind hemifields. We wanted to confirm that the peripheral task didn't impact the ongoing active task which allowed us to determine that attention was fully allocated to the Stroop task and that participants weren't aware of the ongoing peripheral oddball.

Preprocessing of EEG data

Brain Vision Analyzer 2.1 software (Brain Products GmbH, 2006) was used to achieve cleaning and segmentation of the EEG analyses. The raw data of all participants was filtered using an IIR filter with a low cut-off point of ~0.08Hz, a high cut-off point of 30Hz, and a time constant of 0.1s. Ocular correction using independent component analysis was performed in order to remove components associated with blinks. Finally, an automatic raw data inspection was performed to control for artifacts, such as muscular activity, heart rate, and epochs with amplitudes larger than ±75 μV. An average of 14.4 % of the signal was rejected from the final signal across participants. Standard and deviant stimuli were divided, corrected for their baseline, and averaged. Segmentation was done from -200 ms pre-stimulus to 800 ms post-stimulus, intervals beyond this

range were removed. For further analysis, the data was extracted from Brain Vision Analyzer and converted into MATLAB files.

Event-related potentials (ERPs) analysis

Data from 26 electrodes were investigated (Fp1, Fp2, F7, F3, Fz, F4, F8, FT7, FC3, FCz, FC4, FT8, C3, Cz, C4, TP7, CP3, CPz, CP4, TP8, P3, Pz, P4, O1, Oz, O2). The event-related potentials (ERPs) were assessed for each participant, condition, and hemifield. The vMMN and P3a components associated with the detection of motion changes were calculated by subtracting the deviant's average with the standard's average wave for each subject. The vMMN was marked as a significant negative amplitude within the first time period [150-250ms] and the P3a was marked as a significant positive amplitude within a second subsequent time period (250-350ms). Difference waves (deviant-standard) for all trials were obtained for each participant and hemifield. Statistics on the group were performed across subjects after averaging across trials, while statistics on the patient were achieved across trials. Specifically, statistical t-tests using cluster-based permutations described subsequently were performed to investigate significant differences between standard and deviant stimuli across time (Figures 3A-B) and electrodes (Figure 3C-D).

Power analysis

Relative power for each participant, condition, and hemifield was assessed using a Hilbert transform, implemented in Brainpipe, a python-based toolbox, for five frequency bands, i.e. theta (4-7 Hz), alpha (8-13 Hz), beta (13-30 Hz), low gamma (30-60 Hz) and high gamma (60-90 Hz). Power estimation was computed based on a sliding time window of 250 ms on the signal segment ranging between 200 ms pre-stimulus to 600 ms post-stimulus for each electrode. Baseline normalization was applied by subtracting the power by the baseline average and dividing it by the baseline average. Subsequently, a single-trial relative power value was assigned to each electrode for the standard and deviant conditions, as well as for the difference wave. As described in the ERPs analysis, cluster-based permutations were used to assess power differences between deviant and standard stimuli and were performed across subjects for the group and trials for the patient (Figure 4).

Spectral connectivity analysis

The spectral connectivity analysis allowed us to investigate the relation between the oscillatory phases of different electrodes to assess the long-range functional connections within a specific frequency band. To control for volume conduction and the use of a common reference, we decided to apply the weighted phase lag index (wpli) in order to assess the phase-synchronization between two electrodes (Vinck et al., 2011). This method uses the phase leads and lags in the computation to address the influence of phase delays and an imaginary part to derogate from the volume conduction problem. Thus, the connectivity was assessed in an all-to-all electrode matrix (26*26) for all five frequency bands of interest using the single-trial time series for each participant, condition, and hemifield. The wpli measures for both conditions were subtracted (wpli deviant – wpli standard) to obtain the difference in connectivity between the deviant and the standard conditions (Δwpli) across electrodes. This allowed us to assess the frequency bands contributing to the automatic detection of changes. The analysis was performed through the spectral connectivity pipelines implemented in the open-source NeuroPycon toolbox (Meunier et al., 2020) which calls the wpli function from MNE python (Gramfort et al., 2013). The Δwpli results are shown on circular graphs and square matrices (Figures 5 & 6). Statistical analyses were performed using permutations, max-statistics correction across participants, and the Crawford-Howell t-test comparing the patient to the group.

Statistical analyses

Differences between the deviant and standard conditions across time or electrodes for the ERP and power analyses were assessed using the cluster-based permutation tests corrected for multiple comparisons developed in MNE-python (Gramfort et al., 2013). First, a cluster was identified based on the temporal or spatial adjacency of independent t-tests that surpassed a p-value of .05. To correct over time points or electrodes, 1000 permutations were computed under a null distribution obtained from shuffled labels. The maximum t-value of each cluster was then compared to the largest cluster t-value assessed by permutation using a threshold of p-value < .05 (Maris and Oostenveld, 2007). The same principle was applied when comparing each condition, i.e., deviant and standard, with the null hypothesis. The statistical analysis of the group was performed across participants, while a single-trial approach was used for patient ML.

The Δwpli (wpli deviant – wpli standard) statistical significance was assessed for each electrode by using permutations and max-statistics correction to address the multiple comparison

problem. Therefore, the labels were shuffled 1000 times which created a null distribution (Combrisson and Jerbi, 2015). This distribution provided the threshold of significance which was set at a p-value < .001. All significant Δwpli were consequently identified using max-stats correction across electrodes for a chance-level threshold set to a p-value < .05.

To address the statistical difference between the patient and the neurotypical group in terms of spectral connectivity (Δwpli patient ML - Δwpli neurotypical group), a specific test named the Crawford-Howell t-test was used in case-control comparisons (Crawford and Garthwaite, 2012). In fact, spectral connectivity analysis uses all trials when computing the strength of one connectivity value. Thus, connectivity on one individual can't be assessed unless we compare it to a group and infer statistical differences from the group average. The threshold of significance was set at a p-value < .05.

Results

Accuracy and RTs to the Stroop Task show attentional focus on the central task

Average accuracy and RTs for correct responses to the Stroop Task presented in central vision were standard across all neurotypical participants collapsed for the motion stimuli simultaneously presented in the left and right visual field (i.e., accuracy: 70.86 ± 0.17 %, RTs: 586 ±102 ms). For the blindsight individual, average accuracy and reaction time for correct responses for the Stroop Task were also standard when presented in the left intact visual hemifield (i.e., accuracy: 78.06%, RTs: 517.89 ms) and right blind visual hemifield (i.e., accuracy: 75.6%, RTs: 511.29 ms). Performance and RTs to the Stroop task were not modulated by the presentation of the deviant or standard stimuli in the peripheral visual field for neurotypical participants and the blindsight patient. Thus, there was no interaction between the simultaneous presentations of the Stroop task in the central visual field and the visual oddball in the peripheral visual field. As the Stroop Task is cognitively demanding, accurate performance rates and standard reaction times indicate that participants allocated attention to their central vision, thus not to their peripheral visual field.

The mismatch response in the absence of visual awareness is characterized by vMMN, P3a, and theta power modulations

The first aim of this study was to assess the validity of the peripheral oddball paradigm in inducing a reliable posterior vMMN in both the neurotypical group and the blindsight patient. To do so, the

difference wave resulting from subtracting the standard activity from the deviant activity (deviant minus standard) was computed across all 26 electrodes after stimulation of the left and right hemifields.

The ERP results show a significant occipital vMMN (i.e., O1 and O2 electrodes) for the neurotypical group (N=20) when the oddball was presented to the left hemifield at electrode O1 (cluster between 191 and 240 ms, deviant ERP: peak at 218 ms and amplitude of 1.37 ± 0.67 z-score, standard ERP: peak at 226 ms and amplitude of 2.33 ± 0.74 z-score, deviant-standard: peak at 227 ms and amplitude of -0.98 ± 0.22 z-score, $p < .05$ corrected; Figure 3A) and at electrode O2 (cluster between 225 and 241 ms, deviant ERP: peak at 227 ms and amplitude of 2.5 ± 0.7 z-score, standard ERP: peak at 224 ms and amplitude of 2.14 ± 0.66 z-score, deviant-standard: peak at 227 ms and amplitude of -0.71 ± 0.08 z-score, $p < .05$ corrected; Figure 3A). A significant vMMN was also observed for the right hemifield at electrode O1 (cluster between 190 and 209 ms, deviant: peak at 209 ms and amplitude of 1.13 ± 0.33 z-score, standard: peak at 227 ms and amplitude of 2.05 ± 0.51 z-score, deviant-standard: peak at 227 ms and amplitude of -1.06 ± 0.81 z-score, $p < .05$ corrected; Figure 3A) and electrode O2 (cluster between 156 and 210 ms, deviant: peak at 208 ms and amplitude of 1.19 ± 0.39 z-score, standard: peak at 208 ms and amplitude of 1.90 ± 0.65 z-score, deviant-standard: peak at 208 ms and amplitude of 0.81 ± 0.20 z-score, $p < .05$ corrected; Figure 3A).

Likewise, the occipital negative component around the same time window was observed in the blindsight patient within the intact hemisphere when stimulating her intact left hemifield (cluster between 177 and 191 ms, deviant: peak at 177 ms and amplitude of -5.00 ± 0.40 z-score, standard: peak at 177 ms and amplitude of -2.97 ± 0.03 z-score, deviant-standard: peak at 191 ms and amplitude of -2.62 ± 0.39 z-score, $p < .05$ corrected; Figure 3B). These results confirmed that the paradigm was adequate to induce a vMMN in the absence of visual awareness considering the difficulty of the central task and no conscious report of motion changes in the periphery from any participant. Thus, if our claim is valid, we should also find a similar vMMN when stimulating ML's blind hemifield to unravel blindsight abilities. Such results would also and more importantly suggest the vMMN as a potential neural marker of unconscious detection of changes. This being said, we were able to validate the rationale of our proposal by showing that presenting the oddball to ML's blind right hemifield resulted in occipital negativity in the left hemisphere at O1 (cluster

between 142 and 208 ms, deviant: peak at 189 ms and amplitude of 0.92 ± 0.41 z-score, standard: peak at 180 ms and amplitude of 2.87 ± 0.23 z-score, deviant-standard: peak at 172 ms and amplitude of -2.48 ± 0.63 z-score, $p < .05$ corrected; Figure 3B) and right hemisphere at O2 (cluster between 142 and 208 ms, deviant: peak at 175 ms and amplitude of -7.23 ± 0.35 z-score, standard: peak at 175 ms and amplitude of 5.08 ± 0.02 z-score, deviant-standard: peak at 181 ms and amplitude of -2.53 ± 0.55 z-score, $p < .05$ corrected; Figure 3B). Other significant differences between both conditions were also observed in ML that didn't correspond to the vMMN latency window and could indicate early and late individual specificities, which will not be further discussed in this study.

After validating a reliable vMMN around 200 ms at the occipital electrodes when stimulating both hemifields across participants, intact or blind, we also wanted to assess the spatial configuration of the difference wave. Thus, we looked at the activity at different time windows and showed significant differences between deviant and standard conditions at the vMMN latency window, i.e., between 150 and 250 ms, and at a late positive time window suggesting the presence of a P3a, i.e., between 250 and 350 ms. In fact, the difference wave between 150 and 250 ms for the left hemifield of the neurotypical group was associated with posterior negativity identified by a first significant cluster (cluster formed by O1, Oz, O2, P3, Pz, and P4, with t-values of -3.22, -2.14, -2.46, -3.37, -2.75 and -2.38, respectively, $p < .05$ corrected; Figure 3C) and with a frontal positivity identified by a second significant cluster (cluster formed by FC3, FT7, F7, Fz, F4, F8, Fp1, and Fp2 with t-values of 1.75, 2.16, 4.57, 2.88, 1.72, 4.26, 4.18 and 3.19, respectively, $p < .05$ corrected; Figure 3C). This early frontal positivity was moreover observed in the subsequent time window within one anterior significant cluster (C3, Cz, C4, FT7, FC3, FCz, FC4, FT8, F7, F3, Fz, F4, F8, Fp1, and Fp2 with t-values ranging from 2.84 to 5.97, $p < .05$ corrected; Figure 3D). Stimulation of the right hemifield triggered one significant posterior cluster associated with negativity at the vMMN latency window (cluster formed by O1, Oz, O2, P3, Pz, P4, CP3, CPz, CP4, and TP8 with t-values of -4.08, -4.31, -4.45, -3.71, -3.42, -3.46, -3.24, -3.04, -3.45 and -4.54, respectively, $p < .05$ corrected; Figure 3C) and a significant anterior cluster associated with positivity in the P3a latency window composed of all electrodes, except O1, Oz and O2 with t-values ranging from 1.76 to 3.18 ($p < .05$ corrected; Figure 3C).

In ML, stimulation of her intact left hemifield resulted in two significant clusters between 150 and 200 ms composed of all electrodes except TP7 represented by negativity with t-values ranging from -5.31 to -1.6 ($p < .05$ corrected; Figure 3D). Evoked components from stimulation of the intact hemifield of ML seem to differ from what is observed in controls which could be associated with compensation strategies in response to cortical blindness (Celeghin et al., 2017). On the contrary, stimulation of her right blind hemifield in the same time window resulted in one significant posterior cluster (cluster formed by O1, Oz, O2, P3, Pz, P4, CP3, CPz, CP4, and TP8 with t-values of -4.56, -4.31, -4.45, -3.71, -3.42, -3.46, -3.24, -3.04, -3.45 and -4.54, respectively, $p < .05$ corrected; Figure 3D) which cluster exactly corresponded to the one found in the neurotypical group for the right hemifield. Subsequent frontal positivity was observed for ML's intact hemifield within one frontal cluster (C3, Cz, C4, FT7, FC3, FCz, FC4, FT8, F7, F3, Fz, F4, F8, Fp1, and Fp2 with t-values ranging from 2.65 to 5.68, $p < .05$ corrected; Figure 3D) and for her blind hemifield corresponding to three significant clusters including anterior and posterior regions, notably O1 which corresponds to the lesioned visual cortex (O1, Pz, P4, CPz, CP4, TP8, C3, Cz, C4, FT7, FC3, FCz, FC4, FT8, F7, F3, Fz, F4, F8, Fp1 and Fp2 with t-values ranging from 2.39 to 8.44, $p < .05$ corrected; Figure 3D). Interestingly, the frontal positivity could be associated with automatic processing rather than attentional allocation to the deviant condition presented in the periphery as previously suggested in the auditory modality (Muller-Gass et al., 2007).

We further wanted to assess the role of different frequency bands associated with detecting changes in the absence of visual awareness. Computing evoked oscillatory local power adds an understanding of the role of each frequency band in unconscious change detection. The results showed that the subtraction between the deviant and standard conditions induced significantly increased power activity in the posterior and temporal electrodes specifically within the theta range (4-7 Hz). In fact, theta synchronization was significantly increased in the neurotypical group for the left hemifield (cluster formed by TP7 and C4 with t-values of 6.86 and 1.77, respectively, $p < .05$ corrected; Figure 4A), while similar synchronization in the left temporo-posterior regions was observed for the right hemifield without being statistically significant (Figure 4A). The difference wave also induced synchronization in patient ML when her intact (cluster formed by O1, Oz, and P4 with t-values of 3.32, 2.1, and 3.14, respectively, $p < .05$ corrected; Figure 4B) and blind (cluster formed by TP7, CP3 and CPz with t-values of 3.21, 3.07 and 2.11, respectively, $p < .05$ corrected; Figure 4B) hemifields were stimulated. The increase in theta found in both the group and patient

and within both hemifields was mainly associated with reduced desynchronization in the deviant condition compared to the standard condition.

Spectral connectivity shows specific networks that differ between the side of presentation and between neurotypical individuals and the blindsight patient

Reporting the local event-related neural responses allows us to identify cognitive mechanisms that emerge after processing specific information. However, in order to better comprehend the involvement of the long-range neural networks in the mismatch response, we computed the differential spectral connectivity between the deviant and standard conditions in each frequency band which will be addressed as the Δwpli.

The Δwpli results showed specific differences between frequency bands and hemifields in the neurotypical individuals. In fact, at the group level, we observe that the deviant stimuli presented in the left hemifield induced significant greater synchronization between electrodes in the theta band between the left and right hemispheres of fronto-central regions (F3-CP4, F4-CP3, FT7-F8, FC3-FC4, $p < .05$ corrected; Figure 5A), in the alpha band between Pz and CP4 of the right hemisphere ($p < .05$ corrected; Figure 5A), in the beta band mainly between frontal regions (34 significant connections, $p < .05$ corrected; Figure 5A). We also observe a clear increase of the global connectivity in high-frequency bands compared to lower frequency bands, notably in the low gamma (90 significant connections, $p < .05$ corrected; Figure 5A) and high gamma band (88 significant connections, $p < .05$ corrected; Figure 5A). These differences seem to involve a large network where frontal regions communicate with the rest of the brain. Surprisingly, when the oddball was presented to the right hemifield the important increase of oscillatory communication between regions to the deviant stimulus was greatly reduced. Nonetheless, we found differential connections in the alpha band specific to left frontal electrodes (F7-FT7, $p < .05$ corrected; Figure 5B) and right posterior electrodes (Oz-TP8, $p < .05$ corrected; Figure 5B), in the beta band between fronto-occipital regions (O2-FC3, O2-O1, $p < .05$ corrected; Figure 5B), in the low gamma band (10 significant connections, $p < .05$ corrected; Figure 5B) and high gamma band (17 significant connections, $p < .05$ corrected; Figure 5B) within a fronto-posterior network. The asymmetry when presenting the oddball between the visual fields seems to suggest a greater network involved in detecting changes in the left hemifield.

While statistical analysis of spectral connectivity analysis can't be assessed in one individual, it can be compared to a group to identify if one person statistically differs from the group average. Therefore, we were able to assess whether patient ML processed the deviant stimulus in the same way as the group within her intact and blind hemifields. We only found significant differences in the two frequency bands. The first was found when we compared stimulation of ML's intact hemifield with the left hemifield of the group in the beta band where we noted a decreased connectivity in the lesioned left hemisphere between TP7 and C3 (t-value of -2.06, $p < .05$ corrected; Figure 6A). Thus, it seems that posterior connections after a V1-lesion are less recruited within the lesioned ipsilateral hemisphere when the intact hemifield is stimulated. On the other hand, when the blind hemifield was stimulated, deviant motion presentation induced an increase of theta connectivity in the contralateral lesioned hemisphere between Oz and P3 and Oz and CP3 (t-values of 2.35 and 2.20, respectively, $p < .05$ corrected; Figure 6B).

Discussion

The current study assessed the neural correlates of unconscious automatic change detection caused by a violation of regularities in neurotypical individuals (N=20) and a blindsight patient using EEG. Our results demonstrate the presence of a reliable vMMN when a mismatch response is triggered suggesting that prediction errors are generated even in the absence of visual awareness. We conclude by proposing the vMMN as a potential biomarker for assessing unconscious processing independent of behavior.

Processing of motion changes without visual awareness

We successfully tackled the methodological challenge to ensure that the stimuli presented in the peripheral visual field could not be described or reported by any participant. By using the Stroop Test and increasing the presentation speed to monopolize all attentional resources, no attentional allocation to the periphery is possible to adequately focus and perform the task. We also confirmed that all participants performed the task correctly prior to presenting the oddball within the peripheral system to ensure it did not interfere with the central Stroop task. Thus, we were able to induce motion blindness by utilizing the participants' attention (Sahraie et al., 2001). Nonetheless, the stimuli in the oddball needed to be processed by the participants despite the lack of acknowledged visual awareness. Therefore, we used motion salient stimuli to trigger brain

mechanisms involved in unconscious processing for both blindsight patients with V1-lesions (Barleben et al., 2015; Weiskrantz et al., 1995) and neurotypical adults (Hurme et al., 2019). The motion presented in the peripheral visual field is known to recruit pathways, such as the magnocellular (Baizer et al., 1991; Dacey and Petersen, 1992) and koniocellular (Hendry and Reid, 2000) routes, that can bypass the striate cortex (Hervais-Adelman et al., 2015; Lyon et al., 2010; Schmid et al., 2010) to process information that isn't consciously accessed (Campana et al., 2016; Maunsell et al., 1999; Tapia and Breitmeyer, 2011).

The posterior vMMN shows detection of unpredicted changes

A mismatch response occurs when the prediction and the external stimulus do not concur which mechanism is referred to as prediction errors (Oxner et al., 2019). The prediction error is notably measurable by assessing a reliable vMMN.

Thus, the first aim of this study was to trigger the vMMN that can be identified by posterior negativity around 200 ms which isn't affected by task demands. Our findings reveal that the significant posterior (i.e. occipital) electrophysiological response to the deviant stimulus observed in the neurotypical controls is consistently and reliably present for both left and right hemifield presentation, which demonstrates that the brain processes the deviant stimulus, even in the absence of visual awareness. The temporal structure of our signal confirms results from previous studies with the MMN response elicited 200 ms post deviant stimulus (for reviews see Pazo-Alvarez et al., 2003; Qian et al., 2014; Stefanics et al., 2014b). Stimulus presentation in the left or right hemifield resulted in significant negative activity within both hemispheres (Figures 3A and 3C).

The significant posterior negative component was observed in the blindsight patient's intact right hemisphere when stimulating her intact left hemifield within the same time window as the neurotypical adults. No significant negative component was observed in her lesioned left hemisphere when looking at the signal over time (Figure 3B). However, averaging the evoked response between 150 and 200 ms resulted in generalized negativity across both hemispheres (Figure 3D). Therefore, the evoked components from stimulation of the intact hemifield of ML seem to differ from what is observed in controls which could be associated with an adaptive mechanism or compensatory strategy in response to cortical blindness (Celeghin et al., 2017). Nonetheless, considering the difficulty of the central task combined with no conscious report of motion changes in the periphery from any participant, these results confirm that our design

adequately induced a vMMN in the absence of visual awareness, as we previously reported (Hadid and Lepore, 2017a).

Presenting the oddball to ML's blind right hemifield resulted in a significant posterior (i.e. occipital) negativity in both the left lesioned and right intact hemisphere, suggesting that the lesioned hemisphere can detect motion changes automatically even in the absence of visual awareness (Figure 3B). Frontal negativity was also observed suggesting other possible mechanisms involved in blindsight after a V1 lesion (Figure 3D), which we will further discuss in the spectral connectivity analysis. However, not only did the presence of the vMMN in ML's blind hemifield further elucidate ML's blindsight abilities, but it also suggests that the vMMN could be a potential neural marker of unconscious change detection.

The anterior P3a suggests automatic processing

The current study shows a P3a elicited by a task-irrelevant visual stimulus during a highly difficult Stroop task. A consistent anterior (i.e., frontal) positive component corresponding to the P3a latency window (i.e., between 250-350 ms) was observed following the vMMN in the neurotypical adults for both left and right hemifield presentation. A significant frontal positivity was also observed in ML's intact and lesioned hemisphere when stimulating both intact and blind hemifield. As the amplitude of the MMN response is a determining factor in the generation of the P3a response (Berti et al., 2004; Yago et al., 2001), these results properly align with the MMN responses found in both neurotypical controls and the blindsight patient as described in the previous section.

As attention was strongly focused away from the task-irrelevant visual oddball, our experimental design successfully deactivated the allocation of attention towards the periphery. Although the P3a is commonly associated with attentional orienting (for reviews see Escera et al., 2000; Friedman et al., 2001; Kok, 2001; Polich, 2007), it has been shown to operate without attention (i.e., automatic process) in the auditory modality (Muller-Gass et al., 2007). The P3a could be further defined by distinct sub-components as different experimental conditions elicit the P3a with distinct peak latencies and scalp distributions, which presumably reflect different neural processes and cognitive functions. Escera et al (1998) proposed a minimal division of an early (peaking at 250) and late (peaking at 300ms) P3a sub-component (Escera et al., 1998). Consistent with our findings, in auditory studies, the P3a has been reported to have a stronger amplitude and an anterior scalp distribution when it is associated with task-irrelevant deviants within a task-

relevant sequence (Combs and Polich, 2006; Comerchero and Polich, 1998; Goldstein et al., 2002). Moreover, if the participants' attention were directed to the oddball in the peripheral visual field, the change in motion direction would cause a distraction and potentially interfere with the performance on the central Stroop task, which we did not observe. In contrast, if attention is adequately engaged in the difficult Stroop task, an identical visual stimulus in the peripheral visual field may not prompt an attention switch and, as we observed, would not affect the performance on the Stroop task. Analog to the auditory P3a, the neural processes underlying the visual P3a in our study do not depend on the availability of attentional capacity monopolized in the central visual field and can occur outside the focus of attention. Automatic vs strategic perceptual planning can be dissociated by violating auditory temporal regularities locally or globally across several seconds, respectively, with local violations leading to an early response in the auditory cortex and shown to be independent of attention (Bekinschtein et al., 2009). Our design seemingly induces automatic processing as we presented local temporal novelty in the task-irrelevant stimuli. Thus, the frontal positivity could reflect automatic processing as previously suggested in the auditory modality (Muller-Gass et al., 2007) rather than a component that requires or is modulated by an attentional allocation to the deviant condition presented in the periphery. Moreover, together with the vMMN, the P3a component has been associated with prediction errors (Ylinen et al., 2016) to inform higher visual areas of the violation of predictions. Given the automatic nature of the P3a early subcomponent in our results, it seems predictive coding could facilitate perceptual processing and operate on an unconscious level with no attentional resources necessary.

The role of local theta synchronization in prediction errors

As we computed the power in different frequency band oscillations associated with the difference wave between the deviant and standard stimuli, we found significant synchronization in the theta-band for both neurotypical adults and the blindsight patient. First, these results corroborate with studies showing the MMN in the auditory modality eliciting widespread oscillatory responses in the theta-band frequencies (Choi et al., 2013; Fuentemilla, 2018; Hsiao et al., 2009; Ko et al., 2012). Theta oscillations have namely been associated with a violation of rhythmic (Edalati et al., 2021) or somatosensory expectancies (Zhang et al., 2019) in the context of mismatch negativity experiments as well as with cognitive processes demanding a mental effort, learning, and memory (Chen et al., 2020; Goyal et al., 2020; Zhang et al., 2019). Moreover, given their role in the

underlying network dynamics of the P3 component (Harper et al., 2017), theta-band synchronized oscillatory activity has been assumed to be sensitive to attention-related processing (Hong et al., 2020). Thus, theta power is thought to operate on both lower and higher processing levels across brain regions (Ho et al., 2021). In the context of the mismatch responses, theta oscillations have been shown to underlie auditory prediction-error generation (Recasens et al., 2018) which may reflect a mechanism for updating the sensory representation after a prediction error. The occurrence of theta oscillations with the automatic unpredicted change detection, suggests that the visual system engages in sensory prediction and relies on past perceptual experience and context to anticipate sensory input, even for unconsciously processed stimuli.

Moreover, our results show different patterns of theta-band synchronization, in terms of the localization of the peak theta power, when stimuli were presented in the left or right hemifield suggesting a hemispheric asymmetry for both neurotypical adults and the blindsight patient. Left hemifield presentation for neurotypical controls elicits an increase in theta-band power in temporal and central regions reflecting the difference wave between the deviant and standard stimuli. No significant theta-band modulations were elicited for right hemifield stimuli presentation for neurotypical controls. For the blindsight patient, left hemifield (intact) stimuli presentation elicited an enhancement in posterior theta-band oscillations reflecting the difference wave between the standard and deviant conditions. Right visual field (i.e. blind) presentation elicited an increase in theta-power in temporal and central regions for the deviant minus standard conditions. The observed asymmetry will be addressed and interpreted in the subsequent section as the spectral connectivity allowed us to better understand the neural mechanisms involved in prediction errors.

Large-scale neural networks are involved in prediction errors and hemifield asymmetry

The neural networks involved in unconscious processing recruit seemingly specific frequency bands depending on the state of consciousness and cognitive mechanisms involved (Mashour and Hudetz, 2018). Hence, investigation of the relation between the oscillatory phases of different electrodes is a powerful tool when studying a cognitive mechanism to understand how two long-range regions synchronize together in a specific frequency band. Nonetheless, to our knowledge, spectral connectivity has not yet been characterized in the study of visual automatic detection of change which we aimed to explore.

We addressed the question by computing the phase synchronization associated with the difference in connectivity between the deviant and standard stimuli. The first staggering result appears as a clear left-right asymmetry of the visual fields. In fact, when the left hemifield is stimulated, phase synchronization is enhanced for centro-parietal regions including the motor and somatosensory association cortex. We interpret the connectivity with the motor and pre-motor cortex as having a functional role in coordinating stimulation of the left hemifield when a deviant stimulus tries to recruit automatic processing and the use of the right-hand recruits the left motor cortex (Pool et al., 2014). Thus, while these motor interpretations have to be considered to understand the discrepancy observed between stimulation of the left and right hemifields (significant connections with centro-parietal regions are highlighted in green within the connectivity matrix; Figure 5), we will further analyze the specificities of the spectral connectivity for each frequency band.

Our results showed that for the neurotypical group the deviant condition induced greater synchronization mostly involving frontal areas across all frequency bands and for both hemifields (significant frontal connections are highlighted in pink within the connectivity matrix; Figure 5). The involvement of frontal areas could corroborate the fact that frontal connectivity is essential to learning rules (Johnson et al., 2016). Learning can therefore result in a dynamic system of predictions that recruits large-scale networks involved in prediction errors, such as fronto-posterior interactions, which can be conveyed by gamma oscillations (> 40Hz), and update of the system could be provided by alpha-beta oscillations (< 30Hz) as shown in the primate (Chao et al., 2018). While we can't dissociate the prediction-error and prediction-update signal in our analysis, we showed that connectivity between the frontal and temporal regions is mostly recruited in the gamma bands for both hemifields of the neurotypical individuals and patient ML (significant connections between frontal and posterior regions are highlighted in purple within the connectivity matrix; Figure 5).

Increased frontal theta and gamma connectivity between hemispheres was triggered when the left hemifield was stimulated which could be associated with the early frontal bilateral positivity found in the ERP analysis (Figure 3C) and with the theta power increase (Figure 4A). In fact, it has been shown that theta phase frontal synchronization and increase in P3a amplitude are indicators of effective connectivity in response to a deviant stimulus recruiting the attentional system (Solís-

Vivanco et al., 2021). Consistent with these observations, the relation between gamma synchronization and the late positivity has been linked to higher-order cognitive processes, as post-perceptual processes are required to achieve a task, rather than visual awareness, per se (Pitts et al., 2014). To probe this asymmetric attentional recruitment, a dominance of the left hemifield has been shown in visuospatial perception for stimuli engaging the magnocellular pathway in the absence of visual awareness (Cavézian et al., 2010, 2015; Sanchez-Lopez et al., 2020). Moreover, involvement of posterior connections was also increased for the deviant stimulus possibly showing processing of the visual change in direction (significant posterior connections are highlighted in yellow within the connectivity matrix; Figure 5)

Therefore, considering spectral functional connectivity results and previous interpretations, we propose that the asymmetry between both hemifields is triggered by a greater inhibition of the attentional system towards the oddball and more specifically to the deviant stimulus when the left hemifield is stimulated. Taken together, these observations suggest that deviant stimuli usually automatically recruit attentional resources, however, due to the nature of the task, these attentional allocations need to be inhibited especially when the left hemifield is stimulated (Hadid and Lepore, 2017a). After early inhibition of attentional reallocation, we postulate that the P3a in fronto-central regions within the 250-300 ms time window was associated with automatic processing for stimulation of both hemifields in neurotypical individuals and in ML which can explain the increase in fronto-posterior connectivity in both hemifields. Thus, all of these mechanisms need to be considered when understanding neural networks of prediction errors.

Theta connectivity a neural candidate of unconscious processing as observed in blindsight

Neuroimaging studies typically seek to uncover the neural correlates of conscious visual processing by comparing them to those of unconscious processing (Doerig et al., 2020). Relevant studies have performed connectivity analyses to reveal how modulations of spectral connectivity between different regions (i.e., theta, beta, alpha, or gamma-band power), reflect fluctuations of different states of consciousness (e.g., levels of wakefulness, sleep, disorders of consciousness, anesthesia) (Mashour and Hudetz, 2018; Pal et al., 2020). We intended to contribute to this literature by assessing the spectral connectivity that characterizes blindsight abilities. In other terms, we compared the spectral connectivity associated with prediction errors in the absence of subjective visual awareness reported by neurotypical individuals and spectral connectivity associated with

prediction errors in blindsight. Our aim was to address one central question in the blindsight literature which is whether blindsight is just degraded normal vision set at near-threshold (Azzopardi and Cowey, 1997; Hadid and Lepore, 2017b; Weiskrantz, 2009).

First, we assessed the impact of a V1-lesion on perception within the 'normal' hemifield. Phase synchronization in ML was significantly different compared to the group in the beta and theta bands after stimulation of her intact and blind hemifield, respectively. In fact, stimulation of ML's intact hemifield resulted in decreased beta connectivity within the lesioned left hemisphere between TP7 and C3. Beta oscillations are thought to provide feedback synchronization involved in conscious perception (Bastos et al., 2015; Michalareas et al., 2016) and in detecting local novelty assessed by the presence of the vMMN (El Karoui et al., 2015). Thus, the abnormal connection between the temporo-parietal junction notably involved in motion discrimination and motor regions seems to show that those posterior connections are disconnected within the lesioned hemisphere after a V1-lesion specifically when the intact hemifield is stimulated. These results corroborate previous observations about the cortical reorganization in favor of motion areas in the intact hemisphere (Bridge et al., 2008; Mikellidou et al., 2019) and show that even the intact hemifield of a patient with a V1-lesion is not 'normal'.

To tackle the question about what makes blindsight 'special', we compared the spectral connectivity of the lesioned hemisphere to the right hemifield of neurotypical individuals. We demonstrate that presentation of deviant motion stimuli induced an increase of posterior theta connectivity in the contralateral lesioned hemisphere between Oz and P3 and Oz and CP3. Involvement of this posterior network confirms the results of our previous study on ML showing recruitment of extra-striate dorsal regions for motion processing in blindsight (Tran et al., 2019). More importantly, we suggest that recruitment of such pathways is mediated through theta phase synchronization for the detection of novelty linked to unconsciousness through long-range cortico-cortical functional connectivity (Hermann et al., 2020; Yanagawa et al., 2013) which are known to carry feedforward influences involved in unconscious processing (Bastos et al., 2015). In fact, the theta functional connectivity within posterior regions has been associated with a different state of conscious level (Lee et al., 2019) and has been shown to be increased in patients that preserve a minimally conscious state (Bai et al., 2018; Bourdillon et al., 2020). Thus, theta seems to be

involved in processing information in the absence of conscious clear processing as observed in patient ML preserving Type II blindsight abilities for motion stimuli.

Hence, the comparison between the group and the patient shows for the first time how spectral connectivity is influenced by a lesion and residual visual abilities. Moreover, it is of considerable interest that ML's blind hemifield showed differences when compared to individuals with normal vision despite them being unaware of the oddball. Therefore, it seems that different neural mechanisms are recruited between someone being unable to report a change and someone that can't see the change even when attention is recruited as is the case in blindsight. We, therefore, postulate that blindsight is not like normal near-threshold vision, rather it recruits unconscious mechanisms. Our spectral connectivity results across different frequency bands reveal the role of the different connections between posterior and anterior brain regions reflecting the neural correlates of automatic detection of changes in the absence of visual reported awareness.

We propose the use of the vMMN as a neural biomarker to assess unconscious processing

In summary, the present study assessing the neural correlates of unconscious automatic change detection caused by a violation of regularities demonstrates the reliable and consistent presence of the vMMN in both neurotypical controls and a blindsight individual using EEG. We showed a link between the vMMN, P3a, theta synchronization, and large-scale neural network in prediction errors. This was possible by ensuring no subjective awareness and report of the deviant stimulus in neurotypical individuals and the blindsight patient, by comparing the role of the left and right hemifield with respect to automatic processing, and by comparing lack of visual awareness in normal vision and blindsight. To conclude, this study is of high importance to blindsight research since the vMMN could be used as an electrophysiological biomarker for automatic unpredicted change detection and could lead to advances in understanding the neural correlates of unconscious processing for intact as well as altered vision.

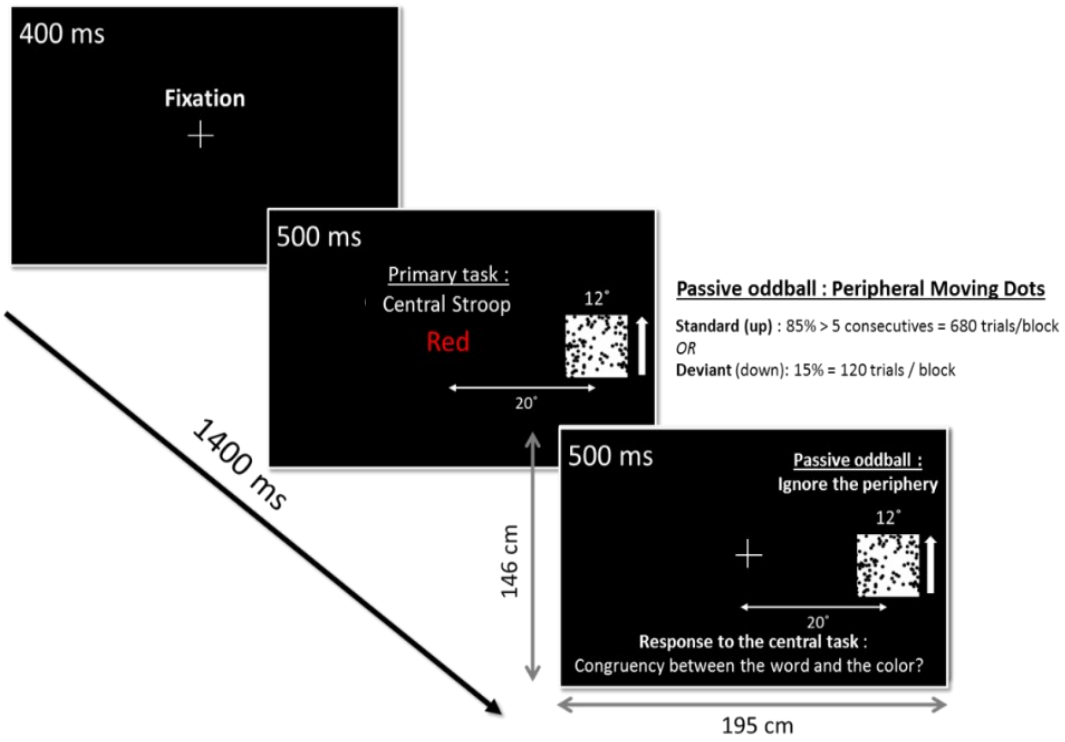

Figure 1. – Stimulus design.

The participant had to fixate a cross presented in the middle of the screen for 400ms. He had to maintain his attention on the central primary tasks corresponding to a Stroop Test where a color word in congruent or incongruent ink color appears on the screen for 500ms. Simultaneously a passive oddball of random moving dots in the periphery at 12˚ appears moving up or downward in a ratio of 85:15 (standard: deviant) for 1 second. Therefore, when the word disappeared the participant had 500 ms to answer correctly to the Stroop test, while the random dots were still moving in the same direction for the same 500ms. After 1400ms, a new trial appeared, with an ISI of 400 ms. At least, 5 consecutive standards preceded a deviant. – Figure 1

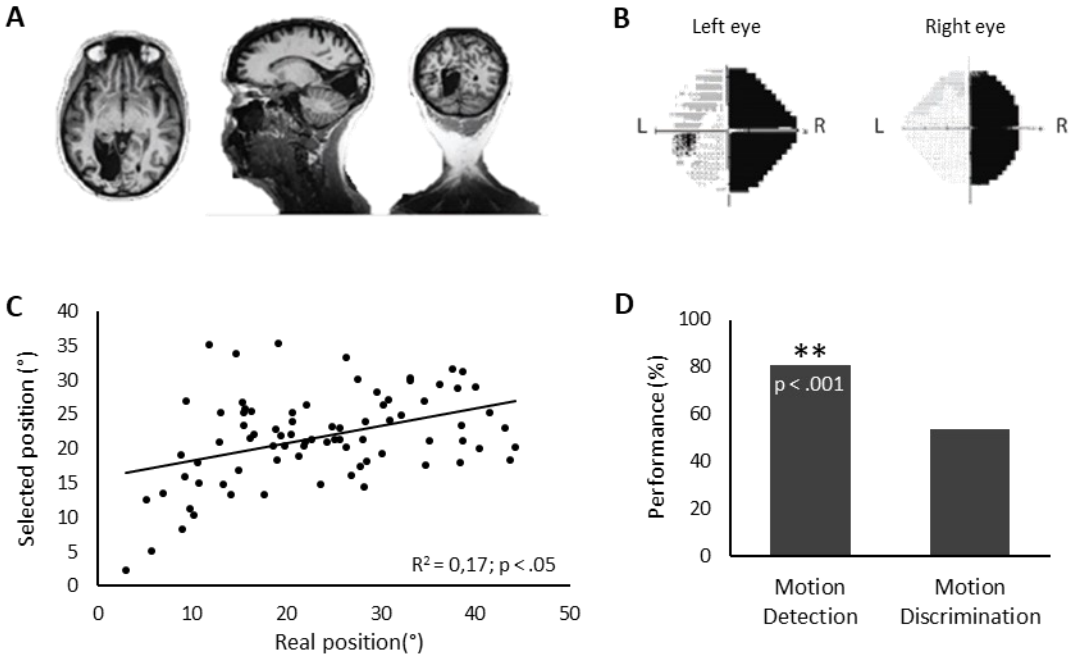

Figure 2. – Blindsight patient ML.

A. T1-weighted anatomical scan with three different slice views of ML's lesion: (a) transverse, (b) sagittal, and (d) coronal slice view showing the primary visual cortex removal in the left hemisphere and the destruction of the primary visual areas. **B.** ML's visual field shows a symmetric loss across both eyes leading to a complete contralateral visual loss in the right visual field. **C.** A pointing task show ML's residual ability to point toward visual dots presented in her blind hemifield. **D.** ML is able to detect unseen motion presented in her blind hemifield but is unable to discriminate between the direction in a forced-choice paradigm. – Figure 2

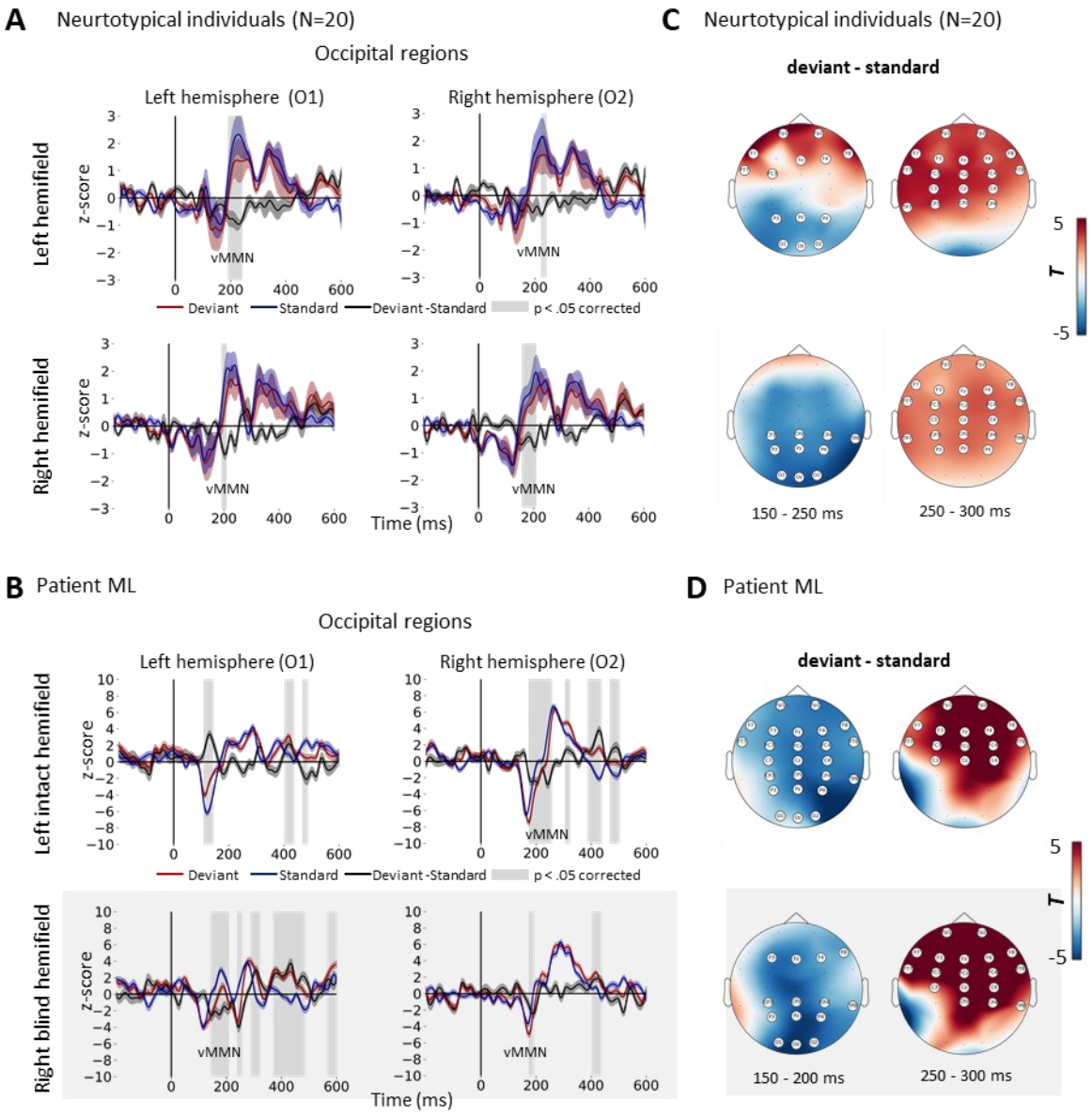

Figure 3. – Event-related potentials (ERPs) obtained from the deviant condition, standard condition and the difference wave (deviant-standard).

(**A-B**) ERPs recorded from occipital regions are illustrated for the left hemisphere (electrode O1) and right hemisphere (electrode O2) after the presentation of the deviant (red) and standard (blue) conditions in the left and right hemifields. Differences over time between the deviant and standard conditions (black) were statistically assessed using cluster-based permutation analysis corrected for multiple comparisons over time. Significant differences are highlighted in grey. (**C-D**) Topographical representation of the difference wave (deviant – standard) is illustrated across electrodes for two times windows (150-250 ms and 250-350 ms). Significant amplitudes were assessed using cluster-based permutation analysis corrected for multiple comparisons over electrodes. White markers show significant electrodes. **A.** ERP results in neurotypical adults. A significant vMMN is observed in both hemispheres after the presentation of the oddball in both hemifields. **B.** ERP results in patient ML. A significant vMMN is observed in the left hemisphere after stimulation of her left intact hemifield and in both hemispheres after stimulation of her blind hemifield. **C.** Difference wave amplitude in neurotypical adults. Visual presentation in the left hemifield induced posterior negativity between 150 and 250 ms and frontal positivity between 150 and 350 ms. Visual presentation in the right hemifield induced global negativity between 150 and 250 ms and frontal positivity between 250 and 350 ms. **D.** Difference wave amplitude in patient ML. Visual presentation in the intact and blind hemifields induced global negativity between 150 and 250 ms and frontal positivity between 250 and 350 ms.- Figure 3

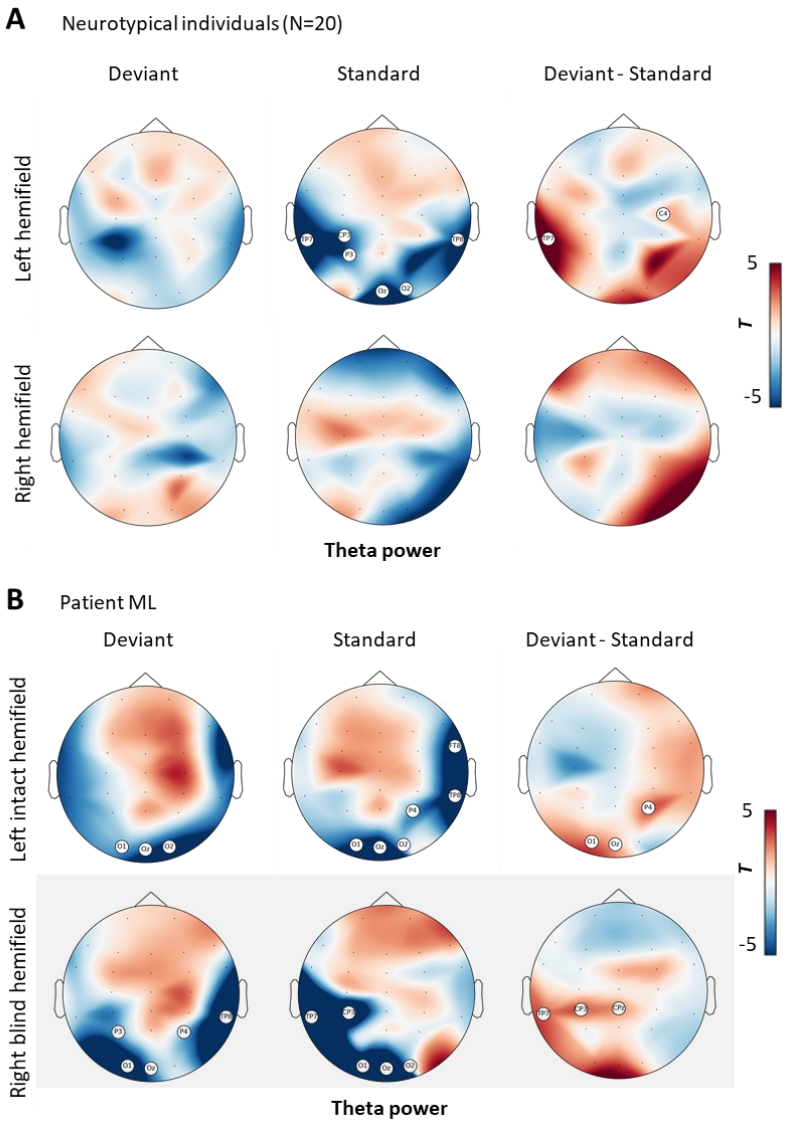

Figure 4. – Power obtained from the deviant condition, standard condition and the difference wave (deviant-standard).

Power modulation is topographically illustrated in the theta band (4-7 Hz). Relative power was assessed using the post-stimulus time window and normalized using the baseline. Significant power modulations were assessed using cluster-based permutation analysis corrected for multiple comparisons over electrodes. White markers show significant electrodes. Deviant stimuli induced significant theta synchronization in posterior regions compared to standard stimuli. **A.** Theta power results in neurotypical adults. **B.** Theta power results in the blindsight patient. – Figure 4

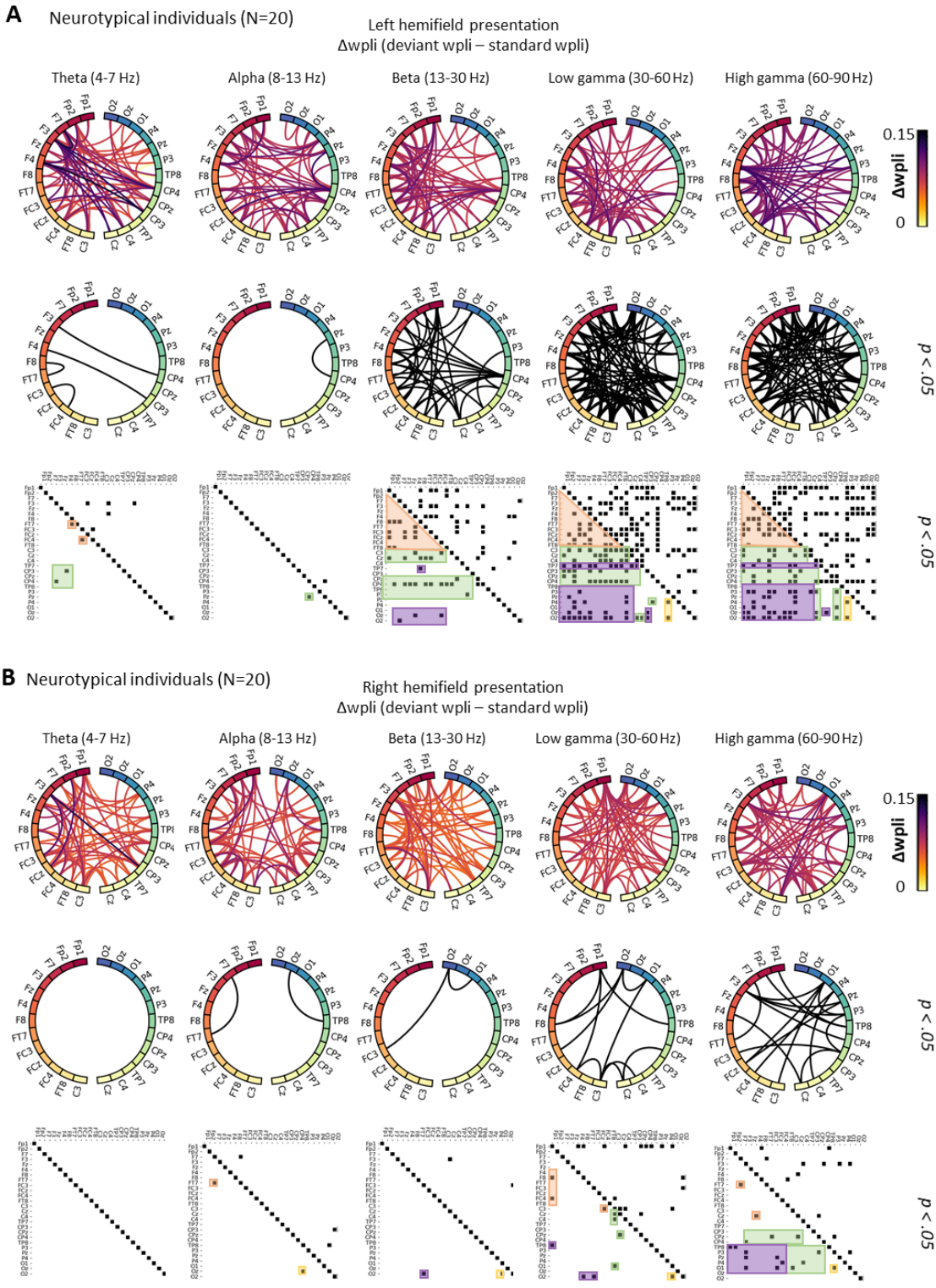

Figure 5. – Spectral connectivity obtained from the difference wave (deviant-standard) for the neurotypical individuals in different frequency bands.

The spectral connectivity for all électrodes was computed using the wpli method for the theta band (4-7 Hz), the alpha band (8-13 Hz), the beta band (13-30 Hz), the low gamma band (30-60 Hz) and the high gamma band (60-90 Hz). Only the 60 most important connections are illustrated in the circular graph. Significant connections ($p < .05$) shown in black were assessed using cluster level inference corrected across all connections and are illustrated in the circular graph and matrix. The significant connections in the matrix are illustrated in different colors depending on the regions involved (frontal: pink, fronto-central: green, fronto-posterior: purple, posterior: yellow). Clear distinctions between frequency bands and between the side of the presentation are observed. A. Spectral connectivity when the peripheral oddball is presented in the left hemifield. B. Spectral connectivity when the peripheral oddball is presented in the right hemifield. – Figure 5

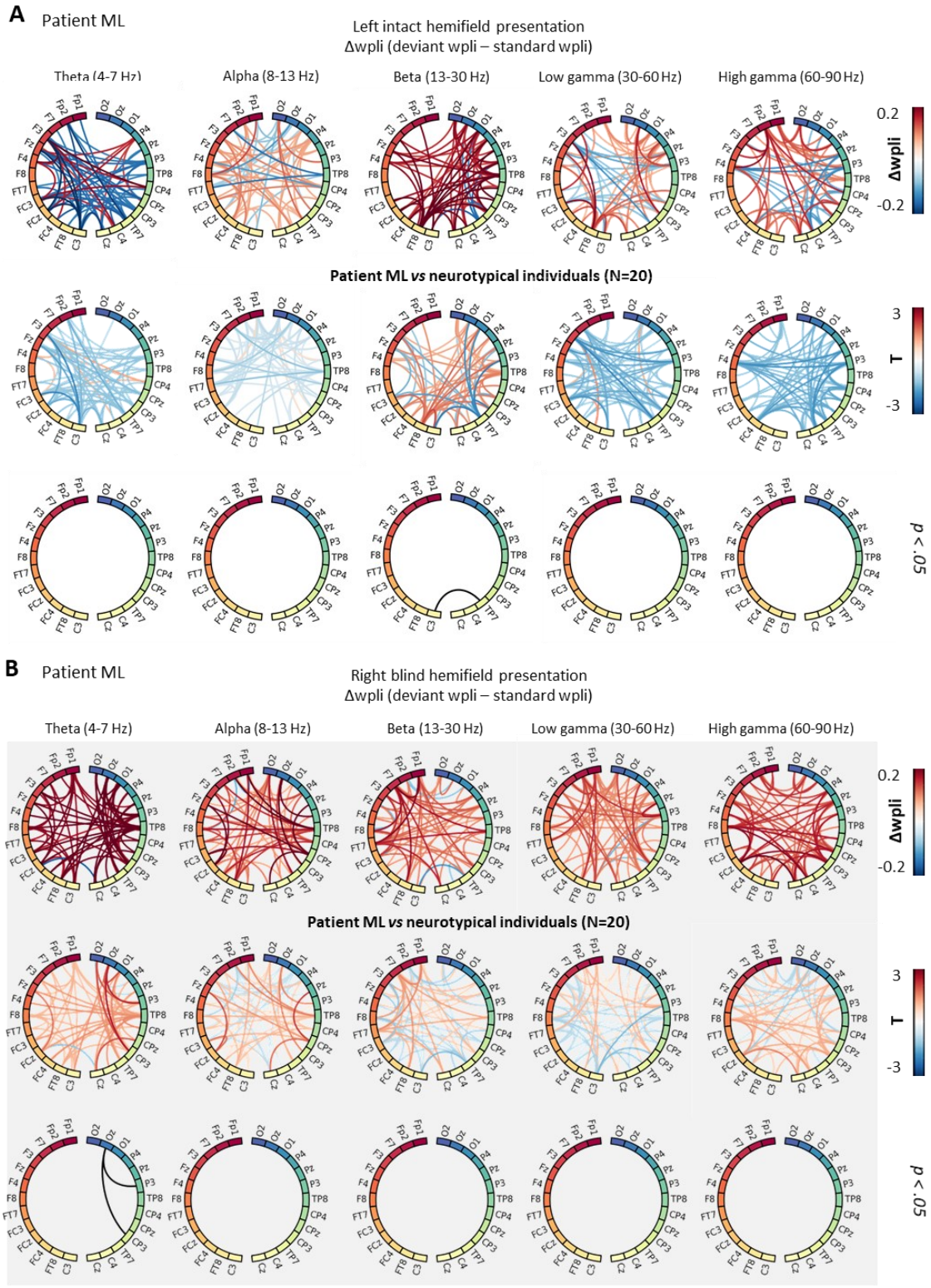

Figure 6. – Differences in spectral connectivity between the neurotypical group and blindsight patient computed from the difference wave (deviant-standard).

The difference in spectral connectivity (patient ML – neurotypical individuals) for all électrodes and frequency bands were computed using the wpli method and illustrated in the left circular graph. Significant differences between the group and patient are illustrated in black on the right circular graph. A. Reduced beta connectivity (13-30 Hz) within the lesioned hemisphere is observed for patient ML compared to the group when her intact left hemifield was stimulated. B. Increased theta connectivity (4-7 Hz) within posterior regions is observed for patient ML compared to the group when her blind right hemifield was stimulated. – Figure 6

References

Amenedo, E., Pazo-Alvarez, P., and Cadaveira, F. (2007). Vertical asymmetries in pre-attentive detection of changes in motion direction. Int. J. Psychophysiol. 64, 184–189.

Astikainen, P., Lillstrang, E., and Ruusuvirta, T. (2008). Visual mismatch negativity for changes in orientation--a sensory memory-dependent response. Eur. J. Neurosci. 28, 2319–2324.

Azzopardi, P., and Cowey, A. (1997). Is blindsight like normal, near-threshold vision? Proc. Natl. Acad. Sci. U. S. A. 94, 14190–14194.

Bai, Y., Xia, X., Wang, Y., Guo, Y., Yang, Y., He, J., and Li, X. (2018). Fronto-parietal coherence response to tDCS modulation in patients with disorders of consciousness. Int. J. Neurosci. 128, 587–594.

Baizer, J.S., Ungerleider, L.G., and Desimone, R. (1991). Organization of visual inputs to the inferior temporal and posterior parietal cortex in macaques. J. Neurosci. 11, 168–190.

Barleben, M., Stoppel, C.M., Kaufmann, J., Merkel, C., Wecke, T., Goertler, M., Heinze, H.-J., Hopf, J.-M., and Schoenfeld, M.A. (2015). Neural correlates of visual motion processing without awareness in patients with striate cortex and pulvinar lesions. Hum. Brain Mapp. 36, 1585–1594.

Barton, J.J., and Sharpe, J.A. (1997). Motion direction discrimination in blind hemifields. Ann. Neurol. 41, 255–264.

Bastos, A.M., Vezoli, J., Bosman, C.A., Schoffelen, J.M., Oostenveld, R., Dowdall, J.R., DeWeerd, P., Kennedy, H., and Fries, P. (2015). Visual areas exert feedforward and feedback influences through distinct frequency channels. Neuron 85, 390–401.

Bekinschtein, T.A., Dehaene, S., Rohaut, B., Tadel, F., Cohen, L., and Naccache, L. (2009). Neural signature of the conscious processing of auditory regularities. Proc. Natl. Acad. Sci. U. S. A. 106, 1672–1677.

Berti, S., Roeber, U., and Schröger, E. (2004). Bottom-up influences on working memory: Behavioral and electrophysiological distraction varies with distractor strength. Exp. Psychol. 51, 249–257.

Bourdillon, P., Hermann, B., Guénot, M., Bastuji, H., Isnard, J., King, J.R., Sitt, J., and Naccache, L. (2020). Brain-scale cortico-cortical functional connectivity in the delta-theta band is a robust signature of conscious states: an intracranial and scalp EEG study. Sci. Rep. 10.

Bridge, H., Thomas, O., Jbabdi, S., and Cowey, A. (2008). Changes in connectivity after visual cortical brain damage underlie altered visual function. Brain 131, 1433–1444.

Campana, F., Rebollo, I., Urai, A., Wyart, V., and Tallon-Baudry, C. (2016). Conscious Vision Proceeds from Global to Local Content in Goal-Directed Tasks and Spontaneous Vision. J. Neurosci. 36, 5200–5213.

Cavézian, C., Gaudry, I., Perez, C., Coubard, O., Doucet, G., Peyrin, C., Marendaz, C., Obadia, M., Gout, O., and Chokron, S. (2010). Specific impairments in visual processing following lesion side in hemianopic patients. Cortex. 46, 1123–1131.

Cavézian, C., Perez, C., Peyrin, C., Gaudry, I., Obadia, M., Gout, O., and Chokron, S. (2015). Hemisphere-dependent ipsilesional deficits in hemianopia: Sightblindness in the "intact" visual field. Cortex. 69, 166–174.

Celeghin, A., Diano, M., De Gelder, B., Weiskrantz, L., Marzi, C.A., and Tamietto, M. (2017). Intact hemisphere and corpus callosum compensate for visuomotor functions after early visual cortex damage. Proc. Natl. Acad. Sci. U. S. A. 114.

Chao, Z.C., Takaura, K., Wang, L., Fujii, N., and Dehaene, S. (2018). Large-Scale Cortical Networks for Hierarchical Prediction and Prediction Error in the Primate Brain. Neuron 100, 1252-1266.e3.

Chen, B., Sun, P., and Fu, S. (2020). Consciousness modulates the automatic change detection of masked emotional faces: Evidence from visual mismatch negativity. Neuropsychologia 144, 107459.

Choi, J.W., Lee, J.K., Ko, D., Lee, G.T., Jung, K.Y., and Kim, K.H. (2013). Fronto-temporal interactions in the theta-band during auditory deviant processing. Neurosci. Lett. 548, 120–125.

Clifford, A., Holmes, A., Davies, I.R.L., and Franklin, A. (2010). Color categories affect pre-attentive color perception. Biol. Psychol. 85, 275–282.

Combrisson, E., and Jerbi, K. (2015). Exceeding chance level by chance: The caveat of theoretical chance levels in brain signal classification and statistical assessment of decoding accuracy. J. Neurosci. Methods 250, 126–136.

Combs, L.A., and Polich, J. (2006). P3a from auditory white noise stimuli. Clin. Neurophysiol. 117, 1106–1112.

Comerchero, M.D., and Polich, J. (1998). P3a, perceptual distinctiveness, and stimulus modality. Cogn. Brain Res. 7, 41–48.

Crawford, J.R., and Garthwaite, P.H. (2012). Single-case research in neuropsychology: A comparison of five forms of t-test for comparing a case to controls. Cortex 48, 1009–1016.

Dacey, D.M., and Petersen, M.R. (1992). Dendritic field size and morphology of midget and parasol ganglion cells of the human retina. Proc. Natl. Acad. Sci. U. S. A. 89, 9666–9670.

Danckert, J., Revol, P., Pisella, L., Krolak-Salmon, P., Vighetto, A., Goodale, M.A., and Rossetti, Y. (2003). Measuring unconscious actions in action-blindsight: exploring the kinematics of pointing movements to targets in the blind field of two patients with cortical hemianopia. Neuropsychologia 41, 1068–1081.

Doerig, A., Schurger, A., and Herzog, M.H. (2020). Hard criteria for empirical theories of consciousness. Cogn. Neurosci. 12, 1–22.

Edalati, M., Mahmoudzadeh, M., Safaie, J., Wallois, F., and Moghimi, S. (2021). Violation of rhythmic expectancies can elicit late frontal gamma activity nested in theta oscillations. Psychophysiology.

Escera, C., Alho, K., Winkler, I., and Näätänen, R. (1998). Neural mechanisms of involuntary attention to acoustic novelty and change. J. Cogn. Neurosci. 10, 590–604.

Escera, C., Alho, K., Schröger, E., and Winkler, I. (2000). Involuntary attention and distractibility as evaluated with event-related brain potentials. Audiol. Neuro-Otology 5, 151–166.

Fitzgerald, K., and Todd, J. (2020). Making Sense of Mismatch Negativity. Front. Psychiatry 11.

Friedman, D., Cycowicz, Y.M., and Gaeta, H. (2001). The novelty P3: An event-related brain potential (ERP) sign of the brain's evaluation of novelty. Neurosci. Biobehav. Rev. 25, 355–373.

Fuentemilla, L. (2018). Memory: Theta Rhythm Couples Periodic Reactivation during Memory Retrieval. Curr. Biol. 28, R1243–R1245.

Goldstein, A., Spencer, K.M., and Donchin, E. (2002). The influence of stimulus deviance and novelty on the P300 and Novelty P3. Psychophysiology 39, 781–790.

Goodale, M.A., and Milner, A.D. (1992). Separate visual pathways for perception and action. Trends Neurosci. 15, 20–25.

Goyal, A., Miller, J., Qasim, S.E., Watrous, A.J., Zhang, H., Stein, J.M., Inman, C.S., Gross, R.E., Willie, J.T., Lega, B., et al. (2020). Functionally distinct high and low theta oscillations in the human hippocampus. Nat. Commun. 11.

Gramfort, A., Luessi, M., Larson, E., Engemann, D.A., Strohmeier, D., Brodbeck, C., Goj, R., Jas, M., Brooks, T., Parkkonen, L., et al. (2013). MEG and EEG data analysis with MNE-Python. Front. Neurosci. 7.

Hadid, V., and Lepore, F. (2017a). Visual mismatch negativity (vMMN): automatic detection change followed by an inhibition of the attentional switch without visual awareness. E. Romero, N. Lepore, J. Brieva, and I. Larrabide, eds. (International Society for Optics and Photonics), p. 101601M.

Hadid, V., and Lepore, F. (2017b). From Cortical Blindness to Conscious Visual Perception: Theories on Neuronal Networks and Visual Training Strategies. Front. Syst. Neurosci. 11, 64.

Harper, J., Malone, S.M., and Iacono, W.G. (2017). Theta- and delta-band EEG network dynamics during a novelty oddball task. Psychophysiology 54, 1590–1605.

Hendry, S.H., and Reid, R.C. (2000). The koniocellular pathway in primate vision. Annu. Rev. Neurosci. 23, 127–153.

Hermann, B., Raimondo, F., Hirsch, L., Huang, Y., Denis-Valente, M., Pérez, P., Engemann, D., Faugeras, F., Weiss, N., Demeret, S., et al. (2020). Combined behavioral and electrophysiological evidence for a direct cortical effect of prefrontal tDCS on disorders of consciousness. Sci. Rep. 10.

Hervais-Adelman, A., Legrand, L.B., Zhan, M., Tamietto, M., de Gelder, B., and Pegna, A.J. (2015). Looming sensitive cortical regions without V1 input: evidence from a patient with bilateral cortical blindness. Front. Integr. Neurosci. 9, 51.

Hesse, P.N., Schmitt, C., Klingenhoefer, S., and Bremmer, F. (2017). Preattentive processing of numerical visual information. Front. Hum. Neurosci. 11.

Ho, H.T., Burr, D.C., Alais, D., and Morrone, M.C. (2021). Propagation and update of auditory perceptual priors through alpha and theta rhythms. Eur. J. Neurosci.

Hong, X., Sun, J., Wang, J., Li, C., and Tong, S. (2020). Attention-related modulation of frontal midline theta oscillations in cingulate cortex during a spatial cueing Go/NoGo task. Int. J. Psychophysiol. 148, 1–12.

Hsiao, F.J., Wu, Z.A., Ho, L.T., and Lin, Y.Y. (2009). Theta oscillation during auditory change detection: An MEG study. Biol. Psychol. 81, 58–66.

Hurme, M., Koivisto, M., Revonsuo, A., and Railo, H. (2019). V1 activity during feedforward and early feedback processing is necessary for both conscious and unconscious motion perception. Neuroimage 185, 313–321.

Johnson, C.M., Peckler, H., Tai, L.H., and Wilbrecht, L. (2016). Rule learning enhances structural plasticity of long-range axons in frontal cortex. Nat. Commun. 7, 1–14.

El Karoui, I., King, J.-R., Sitt, J., Meyniel, F., Van Gaal, S., Hasboun, D., Adam, C., Navarro, V., Baulac, M., Dehaene, S., et al. (2015). Event-Related Potential, Time-frequency, and Functional Connectivity Facets of Local and Global Auditory Novelty Processing: An Intracranial Study in Humans. Cereb. Cortex 25, 4203–4212.

Kimura, M., Schröger, E., Czigler, I., and Ohira, H. (2010). Human visual system automatically encodes sequential regularities of discrete events. J. Cogn. Neurosci. 22, 1124–1139.

King, J.R., Faugeras, F., Gramfort, A., Schurger, A., El Karoui, I., Sitt, J.D., Rohaut, B., Wacongne, C., Labyt, E., Bekinschtein, T., et al. (2013). Single-trial decoding of auditory novelty responses facilitates the detection of residual consciousness. Neuroimage 83, 726–738.

Ko, D., Kwon, S., Lee, G.T., Im, C.H., Kim, K.H., and Jung, K.Y. (2012). Theta oscillation related to the auditory discrimination process in mismatch negativity: Oddball versus control paradigm. J. Clin. Neurol. 8, 35–42.

Kok, A. (2001). On the utility of P3 amplitude as a measure of processing capacity. Psychophysiology 38, 557–577.

Kuldkepp, N., Kreegipuu, K., Raidvee, A., Näätänen, R., and Allik, J. (2013). Unattended and attended visual change detection of motion as indexed by event-related potentials and its behavioral correlates. Front. Hum. Neurosci. 7, 476.

Lee, M., Baird, B., Gosseries, O., Nieminen, J.O., Boly, M., Postle, B.R., Tononi, G., and Lee, S.W. (2019). Connectivity differences between consciousness and unconsciousness in non-rapid eye movement sleep: a TMS–EEG study. Sci. Rep. 9.

Lyon, D.C., Nassi, J.J., and Callaway, E.M. (2010). A disynaptic relay from superior colliculus to dorsal stream visual cortex in macaque monkey. Neuron 65, 270–279.

Lyyra, P., Wikgren, J., Ruusuvirta, T., and Astikainen, P. (2012). Explicit behavioral detection of visual changes develops without their implicit neurophysiological detectability. Front. Hum. Neurosci. 6, 48.

Maris, E., and Oostenveld, R. (2007). Nonparametric statistical testing of EEG- and MEG-data. J. Neurosci. Methods 164, 177–190.

Mashour, G.A., and Hudetz, A.G. (2018). Neural Correlates of Unconsciousness in Large-Scale Brain Networks. Trends Neurosci. 41, 150–160.

Mashour, G.A., Roelfsema, P., Changeux, J.P., and Dehaene, S. (2020). Conscious Processing and the Global Neuronal Workspace Hypothesis. Neuron 105, 776–798.

Maunsell, J.H., Ghose, G.M., Assad, J.A., McAdams, C.J., Boudreau, C.E., and Noerager, B.D. (1999). Visual response latencies of magnocellular and parvocellular LGN neurons in macaque monkeys. Vis. Neurosci. 16, 1–14.

Meunier, D., Pascarella, A., Altukhov, D., Jas, M., Combrisson, E., Lajnef, T., Bertrand-Dubois, D., Hadid, V., Alamian, G., Alves, J., et al. (2020). NeuroPycon: An open-source python toolbox for fast multi-modal and reproducible brain connectivity pipelines. Neuroimage 219.

Michalareas, G., Vezoli, J., van Pelt, S., Schoffelen, J.M., Kennedy, H., and Fries, P. (2016). Alpha-Beta and Gamma Rhythms Subserve Feedback and Feedforward Influences among Human Visual Cortical Areas. Neuron 89, 384–397.

Mikellidou, K., Arrighi, R., Aghakhanyan, G., Tinelli, F., Frijia, F., Crespi, S., De Masi, F., Montanaro, D., and Morrone, M.C. (2019). Plasticity of the human visual brain after an early cortical lesion. Neuropsychologia.

Morrone, M.C., Tosetti, M., Montanaro, D., Fiorentini, A., Cioni, G., and Burr, D.C. (2000). A cortical area that responds specifically to optic flow, revealed by fMRI. Nat. Neurosci. 3, 1322–1328.

Muller-Gass, A., Macdonald, M., Schröger, E., Sculthorpe, L., and Campbell, K. (2007). Evidence for the auditory P3a reflecting an automatic process: elicitation during highly-focused continuous visual attention. Brain Res. 1170, 71–78.

Oxner, M., Rosentreter, E.T., Hayward, W.G., and Corballis, P.M. (2019). Prediction errors in surface segmentation are reflected in the visual mismatch negativity, independently of task and surface features. J. Vis. 19, 9.

Pal, D., Li, D., Dean, J.G., Brito, M.A., Liu, T., Fryzel, A.M., Hudetz, A.G., and Mashour, G.A. (2020). Level of consciousness is dissociable from electroencephalographic measures of cortical connectivity, slow oscillations, and complexity. J. Neurosci. 40, 605–618.

Pazo-Alvarez, P., Cadaveira, F., and Amenedo, E. (2003). MMN in the visual modality: a review. Biol. Psychol. 63, 199–236.

Pazo-Alvarez, P., Amenedo, E., and Cadaveira, F. (2004). Automatic detection of motion direction changes in the human brain. Eur. J. Neurosci. 19, 1978–1986.

Pitts, M.A., Padwal, J., Fennelly, D., Martínez, A., and Hillyard, S.A. (2014). Gamma band activity and the P3 reflect post-perceptual processes, not visual awareness. Neuroimage 101, 337–350.

Polich, J. (2007). Updating P300: An integrative theory of P3a and P3b. Clin. Neurophysiol. 118, 2128–2148.

Pool, E.-M., Rehme, A.K., Fink, G.R., Eickhoff, S.B., and Grefkes, C. (2014). Handedness and effective connectivity of the motor system. Neuroimage 99, 451.

Qian, X., Liu, Y., Xiao, B., Gao, L., Li, S., Dang, L., Si, C., and Zhao, L. (2014). The visual mismatch negativity (vMMN): toward the optimal paradigm. Int. J. Psychophysiol. 93, 311–315.

Recasens, M., Gross, J., and Uhlhaas, P.J. (2018). Low-Frequency Oscillatory Correlates of Auditory Predictive Processing in Cortical-Subcortical Networks: A MEG-Study. Sci. Rep. 8.

Rowe, E.G., Tsuchiya, N., and Garrido, M.I. (2020). Detecting (Un)seen Change: The Neural Underpinnings of (Un)conscious Prediction Errors. Front. Syst. Neurosci. 14.

Sahraie, A., Milders, M., and Niedeggen, M. (2001). Attention induced motion blindness. Vision Res. 41, 1613–1617.

Sahraie, A., Hibbard, P.B., Trevethan, C.T., Ritchie, K.L., and Weiskrantz, L. (2010). Consciousness of the first order in blindsight. Proc. Natl. Acad. Sci. U. S. A. 107, 21217–21222.

Sanchez-Lopez, J., Savazzi, S., Pedersini, C.A., Cardobi, N., and Marzi, C.A. (2020). Neural bases of unconscious orienting of attention in hemianopic patients: Hemispheric differences. Cortex. 127, 269–289.

Sanders, M.D., Warrington, E.K., Marshall, J., and Wieskrantz, L. (1974). “Blindsight”: Vision in a field defect. Lancet 1, 707–708.

Schmid, M.C., Mrowka, S.W., Turchi, J., Saunders, R.C., Wilke, M., Peters, A.J., Ye, F.Q., and Leopold, D.A. (2010). Blindsight depends on the lateral geniculate nucleus. Nature 466, 373–377.

Solís-Vivanco, R., Mondragón-Maya, A., Reyes-Madrigal, F., and de la Fuente-Sandoval, C. (2021). Impairment of novelty-related theta oscillations and P3a in never medicated first-episode psychosis patients. Npj Schizophr. 7.

Soto, D., Sheikh, U.A., and Rosenthal, C.R. (2019). A Novel Framework for Unconscious Processing. Trends Cogn. Sci. 23, 372–376.

Stefanics, G., Kimura, M., and Czigler, I. (2011). Visual mismatch negativity reveals automatic detection of sequential regularity violation. Front. Hum. Neurosci. 5, 46.

Stefanics, G., Kremláček, J., and Czigler, I. (2014a). Visual mismatch negativity: a predictive coding view. Front. Hum. Neurosci. 8, 666.

Stefanics, G., Astikainen, P., and Czigler, I. (2014b). Visual mismatch negativity (vMMN): a prediction error signal in the visual modality. Front. Hum. Neurosci. 8, 1074.

Stefanics, G., Kremláček, J., and Czigler, I. (2016). Mismatch negativity and neural adaptation: Two sides of the same coin. Response: Commentary: Visual mismatch negativity: a predictive coding view. Front. Hum. Neurosci. 10, 13.

Stothart, G., and Kazanina, N. (2013). Oscillatory characteristics of the visual mismatch negativity: what evoked potentials aren’t telling us. Front. Hum. Neurosci. 7, 426.

Tales, A., Newton, P., Troscianko, T., and Butler, S. (1999). Mismatch negativity in the visual modality. Neuroreport 10, 3363–3367.

Tapia, E., and Breitmeyer, B.G. (2011). Visual consciousness revisited: magnocellular and parvocellular contributions to conscious and nonconscious vision. Psychol. Sci. 22, 934–942.

Tran, A., MacLean, M.W., Hadid, V., Lazzouni, L., Nguyen, D.K., Tremblay, J., Dehaes, M., and Lepore, F. (2019). Neuronal mechanisms of motion detection underlying blindsight assessed by functional magnetic resonance imaging (fMRI). Neuropsychologia 128, 187–197.

Tsuchiya, N., Wilke, M., Frässle, S., and Lamme, V.A.F. (2015). No-Report Paradigms: Extracting the True Neural Correlates of Consciousness. Trends Cogn. Sci. 19, 757–770.

Vinck, M., Oostenveld, R., van Wingerden, M., Battaglia, F., and Pennartz, C.M.A. (2011). An improved index of phase-synchronization for electrophysiological data in the presence of volume-conduction, noise and sample-size bias. Neuroimage 55, 1548–1565.

Wei, D., and Gillon-Dowens, M. (2018). Written-Word Concreteness Effects in Non-attend Conditions: Evidence From Mismatch Responses and Cortical Oscillations. Front. Psychol. 9, 2455.

Weiskrantz, L. (2009). Is blindsight just degraded normal vision? Exp. Brain Res. 192, 413–416.

Weiskrantz, L., Warrington, E.K., Sanders, M.D., and Marshall, J. (1974). Visual capacity in the hemianopic field following a restricted occipital ablation. Brain 97, 709–728.

Weiskrantz, L., Barbur, J.L., and Sahraie, A. (1995). Parameters affecting conscious versus unconscious visual discrimination with damage to the visual cortex (V1). Proc. Natl. Acad. Sci. U. S. A. 92, 6122–6126.

Yago, E., Corral, M.J., and Escera, C. (2001). Activation of brain mechanisms of attention switching as a function of auditory frequency change. Neuroreport 12, 4093–4097.

Yan, T., Feng, Y., Liu, T., Wang, L., Mu, N., Dong, X., Liu, Z., Qin, T., Tang, X., and Zhao, L. (2017). Theta oscillations related to orientation recognition in unattended condition: A vMMN study. Front. Behav. Neurosci. 11, 166.

Yanagawa, T., Chao, Z.C., Hasegawa, N., and Fujii, N. (2013). Large-scale information flow in conscious and unconscious states: An ECoG study in monkeys. PLoS One 8.

Yeark, M., Paton, B., and Todd, J. (2021). The influence of variability on mismatch negativity amplitude. Biol. Psychol. 164, 108161.

Ylinen, S., Huuskonen, M., Mikkola, K., Saure, E., Sinkkonen, T., and Paavilainen, P. (2016). Predictive coding of phonological rules in auditory cortex: A mismatch negativity study. Brain Lang. 162, 72–80.

Zhang, Y., Wang, Y., Cai, S., Li, J., Ren, J., Wang, Q., and Huang, L. (2019). EEG Feature Analysis for Detecting the Fluctuation of Consciousness Level during Propofol Anesthesia. In Proceedings of the Annual International Conference of the IEEE Engineering in Medicine and Biology Society, EMBS, (Annu Int Conf IEEE Eng Med Biol Soc), pp. 4525–4528.

Chapter 7

Article 5: A Combined Training Strategy for Visual Rehabilitation in Cortical Blindness: A Step Closer to a Video Game Approach

Article 5. A Combined Training Strategy for Visual Rehabilitation in Cortical Blindness: A Step Closer to a Video Game Approach

Vanessa Hadid[1,3], Karim Jerbi[2,3], Franco Lepore[2]

1Département de Sciences Biomédicales, Université de Montréal,
2Département de Psychologie, Université de Montréal
3Computational and Cognitive Neuroscience Lab (CoCo Lab)

Abstract

Background: One of the major hubs affected by unilateral stroke is the occipital pole leading to cortical blindness (CB) in the contralateral hemifield. CB is a striking health concern; 50 % of stroke survivors present a visual deficit that significantly reduces their quality of life. Even if some recovery is possible within 6 months, neuroplasticity after CB isn't sufficient to allow sight restoration in most of cases and no consensus on visual rehabilitation techniques has been established. However, we postulate that residual altered visual pathways could be triggered by adequate multisensory perceptual video-game, thus generating sufficient neuroplasticity.

Methods: The visual training in this proposal is aimed to target the deficits found in CB as it combines (1) multisensory training that targets several cognitive processes, such as audiovisual facilitation, visual exploration, and audio-motor coordination by ocular movements, and (2) a double paradigm visual restitution training aimed at attentional engagement, multiple dimensions of stimulation and positive reinforcement in a dynamic and motivating environment using the beneficial approaches of video games.

Contributions: Significantly, the use of a combined training strategy using a video game approach for visual rehabilitation could improve vision in patients with CB and provide insights on visual restoration following functional alterations of the primary visual cortex.

1. Background

1.1. Cortical blindness

The occipital pole is one of the primary hubs damaged by unilateral stroke, leading to cortical blindness (CB) in the contralateral hemifield (Goodwin, 2014; Sand et al., 2013). Furthermore, CB, which affects approximately half of all stroke patients, is a severe health problem since it significantly reduces patients' quality of life (Rowe et al., 2019). This condition has a substantial negative impact on quality of life (Perez and Chokron, 2014), as well as the prognosis associated with comorbidity, resulting in a reduction in recovery of other functions (Patel et al., 2000). There is currently no method for inducing function recovery, and in most situations, plasticity is inadequate to allow spontaneous recovery (Duquette & Barrel, 2009). As a result, while vision loss is deemed irreversible, blindsight, or the inability to see while still being able to unconsciously process information in the blind hemifield (Weiskrantz, 1986), may be useful for restoration therapy. In fact, by using specific visual stimulations, we could target the brain mechanisms responsible for residual functions in blindsight (Urbanski et al., 2014) as the unconscious ability to locate random targets (Zihl and Werth, 1984), to identify low spatial frequencies (Sahraie et al., 2010), to detect global movement and to distinguish between coherence (Alexander and Cowey, 2009; Pavan et al., 2011). Multiple recent researchers have tried to achieve restoration by using multisensory stimulation (Grasso et al., 2016) or restitution techniques (Das et al., 2014), and even if some have reached promising results, the proof is missing that CB can be trained to see again. Thus, the aim of this paper is to target residual abilities preserved in the blind field of patients with CB by combining perceptual training (PT) such as multisensory and visual restitution training in a video game approach.

1.2. Perceptual training: Multisensory and restitution strategies

The improvement of sensory and attentional deficits by perceptual training (PT), as the compensation and restitution training, could have a considerable impact on the prognosis following lesions (Latham et al., 2013). Specifically, patients can be trained to make eye movements toward a visual target presented simultaneously with an auditory stimulus inducing multisensory integration, which could improve performance for unseen visual stimulations (Passamonti et al., 2009). In fact, multisensory bottom-up training is hypothesized to activate residual altered visual

pathways without the need for attentional resources or awareness (Ajina et al., 2015) which has been associated with improvements in visual detection and exploration, and quality of life (Bolognini et al., 2005). Reorganization following audio-visual stimulations allows for an increase of the attentional bias towards the blind hemifield (Dundon et al., 2015). Therefore, training of the oculomotor track could allow a potential increase in allocation of attention in the blind hemifield, which is necessary to perception and visual consciousness (Kerkhoff et al., 1992). Although compensation therapies have proven a certain beneficial impact, they are still underused, due to limited clinical evidence of their effectiveness. For this reason, the use of multisensory bottom-up training in association with top-down restitution training could lead to higher chances of improving visual detection, localization, and recognition. Restitution techniques include repeatedly delivering visual stimuli in the blind hemifield in one or more locations until performance exceeds a specific threshold, which increases the difficulty (Saionz et al., 2021). The stimuli used are mainly aimed to target blindsight abilities as motion stimuli and Gabor patches at high contrasts have been shown to induce the best results in terms of improvement of visual functions notably for other types of visual stimuli, i.e. not specific to the blindsight pathway, suggesting transfer in learning (Chokron et al., 2008). Importantly, restitution techniques can target various perceptual processes, such as detection, localization, and discrimination, to improve visual sensitivity (Grunda et al., 2013; Melnick et al., 2016; Pollock et al., 2019). However, because of the amount of training necessary to produce a modest improvement and restricted training sites within the blind hemifield where an effect is reported, restitution training is still inefficient in restoring vision in CB. Thus, we suggest that multisensory saccadic training and restitution techniques can be used in a complementary manner, as the former increases saccadic effectiveness and attentional allocation towards the visual stimulus through multisensory stimulations, and the latter increases visual sensitivity in the blind hemifield. Nonetheless, despite PT training's ability to address deficiencies due to its high specificity, it may be further enhanced by using video games (VGs) more effectively.

1.3. Combining perceptual training and the video game approach

VGs are believed to be less selective to a single stimulus, more motivating, and engaging, allowing for better generalization of cognitive function gains. (Baniqued et al., 2014; Oei and Patterson, 2014; Zhang et al., 2017). Compared with PT, VG simultaneously target several cognitive processes to improve visuospatial performance, motor coordination between the eye and the hand,

the reaction times and allow a more important transfer of learning (Baniqued et al., 2014; Oei and Patterson, 2014; Zhang et al., 2017). More significantly, VGs allow improvements in attention and visuospatial distribution since they require that the player pays attention to several objects simultaneously distributed in the whole visual space. Green and Bavelier (2003, 2006) looked at how action video games affected several attentional tasks and found that they improved visual characteristics including contrast sensitivity and increased perimetry of the central and peripheral visual areas (Green and Bavelier, 2003, 2006a, 2006b). Indeed, action VGs are known to increase sensory, perceptual, and attentional abilities leading to faster information processing (Donohue et al., 2010). The fact that these action VGs involve the pursuit of numerous objects, fast attention shifts, and peripheral vision training generates the perceptual improvement and increase in attentional resources associated with bottom-up processes (Green and Bavelier, 2003, 2006a, 2006b). Furthermore, action VGs improve perceptual sensitivity for low-saliency stimuli in a noisy setting (Whitton et al., 2014) and can have an impact on implicit detection (Pohl et al., 2014). The question we sought to answer is if we can use what we know about blindsight to develop a user-friendly rehabilitation tool with a VG approach, given that our objective is to target the remaining visual abilities in CB.

1.4. Rational

Applying the basics of learning is necessary to establish an effective PT that specifically targets sensory and attentional deficits affected by neurological impairment. A key element to consider in PT is that attention is not required for learning, but potentiates the effects of sensory plasticity, even in the absence of visual awareness (Watanabe et al., 2002). Thus, a method to optimize bottom-up (no attention to the attributes: implicit learning) and top-down systems (attention focused on the visual targets characteristic of learning) would be to use a combination of multisensory stimulations and specific visual stimuli (Kentridge et al., 2004; Schurger et al., 2008; Yoshida et al., 2012). The effect of perceptual training has the disadvantage of being sensitive to perceptual interferences where a change during training prevents the beneficial effect of learning, while effects of the video game are less susceptible to these interferences since the consolidation of learning is stronger and faster (Baniqued et al., 2014; Oei and Patterson, 2014; Zhang et al., 2017). Thus, there is a clear advantage in transforming perceptual learning approaches into a kind of video game, going from highly specific training to global training and ensuring improvements

in contrast threshold and sensitivity function, in the central and peripheral visual areas. Thus, in line with what the literature suggests, the training we propose in the research project combines (1) multisensory training that targets several cognitive processes, such as audiovisual facilitation, visual exploration, and localization, and audio-motor coordination by ocular movements (2) a double paradigm visual restitution training aimed at attentional engagement, multiple dimensions of stimulation and positive reinforcement. We, therefore, intend to target and enhance the neurophysiological mechanisms of blindsight using a dynamic and motivating environment inspired by video games, which will also give the possibility to participants to conduct the training at home and not in a lab.

1.5. Aim and Hypothesis

Our aim was to develop an adaptive take-home multisensory video game to facilitate training for cortically blind patients. By using specific audio-visual training combining ocular compensation and visual restitution strategies within a motivating environment we hypothesize that there will be an improvement in visual performances and awareness in the blind hemifield of HH patients linked to neurophysiological changes after training. In fact, multisensory stimulations combined with visual restitution training could target pre-existing and new neuronal mechanisms to recreate a framework for potential functionality (Hadid and Lepore., 2017). Understanding residual visual abilities and using adequate stimulations, we could induce loops and connections between higher cognitive areas leading to synchronization of neuronal activity and potentially to visual consciousness by lowering the thresholds to access attentional, perceptual, and conscious resources (Deco et al., 2021). The training is actually available and free to use on any computer or android. The link will be sent upon request.

2. Methods

2.1. Goal of the game

The goal of the proposed game is to successfully shoot enemy spaceships while avoiding black holes and meteorite rains during intergalactic trips. The game takes place in space, giving the strong contrast needed for patients to perform adequately in the first levels of the game, knowing that visual acuity is better for high contrast. At the top of the screen, at all times, are displayed four

arrows (left, up, down, right) representing the four directions that need to be discriminated. The patient has a red crosshair to shoot and aim at enemy spaceships. The crosshair will also allow players to select one of the four arrows to indicate the perceived direction of movement of the black holes and meteorite rains to avoid them.

2.2. Configuration

There are 20 levels in total. Each level contains 4 main items that can appear randomly in space: item 1 = enemy spaceship (multisensory integration), item 2 = static black holes (static Gabor patches with a specific spatial frequency oriented vertically or horizontally), item 3 = dynamic black holes (dynamic Gabor patches with a specific temporal frequency moving in one of the four directions) and item 4 = meteorite rains (random moving dots in one of the four directions with a specific coherence). Four items are represented: item 1-multisensory stimulus, item 2-static stimulus, and items 3 and 4- will be motion stimuli. To achieve a level, players need to gain a certain number of points for each item (85% of success) knowing that the multisensory stimulus will appear 400 times in one game and the static and motion stimuli will appear 200 times each. The scoring system includes winning when targets are hit (item 1) or avoided (items 2, 3, and 4) and losing points when targets are missed. Winning and losing will be both associated with a specific sound to give auditory feedback on performance. Each level can be played as many times as required. Difficulty in levels is based on four main parameters: contrast (multisensory stimulus), spatial frequencies (static Gabor patches), temporal frequencies (dynamic Gabor patches), and coherence (moving dots) (for characteristics see Table 1 in annex). Characteristics used in the training are based on results of previous studies done in laboratory settings (Das and Huxlin, 2010; Huxlin, 2008; Huxlin et al., 2009). One game lasts 20 minutes with breaks every 5 minutes. Training is anticipated to last 3 months, with 5 days of training per week and 1 hour per day resulting in a training of 60 hours. All data will be recorded and used to assess the performance and reaction times of each patient throughout the training.

2.3. Procedure composed of two parts

2.3.1. Saccadic multisensory localization (first half of a sequence)

The player is in the center of the galaxy represented by his cursor (crosshair). Enemy vessels can appear anywhere in space. The problem is that these ships are invisible and silent. However, sometimes due to galactic interferences, the ships appear for 100 ms and emit a deafening white

noise of 100ms. The participant will have to initiate an ocular movement to localize the stimulus that will be of a size of 5° (audio-visual spatial and temporal congruency). Therefore, two options are possible: the ship appears in the normal or the blind hemifield covering 40° of eccentricity vertically and 40° horizontally. In both cases, patients will be able to induce an ocular movement toward the target either by using the visual and/or the audio cue explicitly. The important point is that in either case both visual and auditory stimulations are presented congruently inducing multisensory integration, even when this integration is implicit (visual stimulus not consciously seen). When the spaceship appears, it gives the player time to spot the ship just before it disappears. The ocular movement is made after the disappearance of the spaceship knowing that it takes more than 100 ms to initiate a saccade. Therefore, patients need to quickly position the crosshair in an accurate position and shoot at it while it is invisible. If they fail in shooting the spaceship before the second half of the sequence appears, the trial is dismissed. This will allow us to ensure that visual discrimination is always made outside the fixation point.

2.3.2. Visual discrimination (second half of a sequence)

After the spaceship disappears, a static or motion stimulus with a size of 5° in diameter will appear for 400ms to the left or right of the attended position (normal or blind hemifield depending on the lesion) simultaneously with a congruent sound (100ms), used as an auditory cue. As said previously, it takes more than 100 ms to initiate a saccade, and the shooting reaction time is estimated to be around 300 ms, making the operation of saccadic localization and pointing to shoot last for about 400 ms. Therefore, a static or motion stimulus always appears outside the fixation point and falls either in the blind or normal hemifield. This will allow us to evaluate and enhance capacities of orientation or motion direction discrimination in the blind hemifield. We know that blind hemifield training is done within the scotoma edge near the sighted field, therefore items 2, 3, and 4 will be presented within 5° of item 1, when 85% of correct responses for each stimulus are attained, stimulations will appear within 8° of item 1 and then again when 85% of correct responses is achieved, stimuli will appear within 12° of item 1. After succeeding in the last step, patients will pass to the other level.

2.3.3. Data collection

All training data is kept on the computer where the participant is playing the game. Performance for each type of stimulus, as well as reaction times, are measured at all levels. Additional statistics on training duration, global success rate, and level improvement are also collected for future analysis. Preliminary results on a pilot participant as proof of concept showed improvement in performance and reaction times with training time validating the feasibility and learning effect during the game.

Discussion

By training participants during the mentioned proposed timeline, we optimize the chances of improvement in visual performances across levels and of transfer-learning to other tasks hoping to increase the perceptual sensitivity and visuospatial ability driven by plasticity dependent on the experience (Latham et al., 2013; Xiao et al., 2008). In fact, we hypothesize that success in the first levels of the game (1 to 7) will be associated with an increase in performance within the spatiotemporal band in which blindsight is seen. However, if patients can reach level 8 and more, their ability will have grown outside the normal blindsight range, which is associated with specialization of the residual pathways, higher synchronization between multiple regions, and generalization induced by transfer of learning (Das et al., 2014). These new abilities could induce increases in subjective criteria, such as confidence, perceptual awareness, and visual qualia, an increase in performances in a behavioral perspective, as well as an increase in oscillatory and functional changes (Ajina and Kennard, 2012; Bocchio et al., 2017; Grasso et al., 2016; Mueller et al., 2008). Therefore, multisensory training (Làdavas, 2008) combined with the double visual discrimination training using motion and static stimuli (Huxlin et al., 2009) within a video-game approach are expected to improve the ability to detect, discriminate and localize accurately visual stimuli (Baniqued et al., 2014; Oei and Patterson, 2014; Zhang et al., 2017). These strategies are likely to enhance the resources accessible for conscious vision, thus allowing for learning to transfer to other tasks and daily life. In conclusion, the visual training offered in a lucrative form should allow for efficient rehabilitation training by targeting the mechanisms that allow the transfer from a state of blindness to a state of functional perception.

	LEVELS		1	2	3	4	5	6	7	8	9	10	11	12	13	14	15	16	17	18	19	20
ITEM 1*	Multisensory Stimulus	Contrast (%)	100	95	90	85	80	75	70	65	60	55	50	45	40	35	30	25	20	15	10	5
ITEM 2**	Static Gabor Patch	Spatial Frequency (Hz)	0.5	0.6	0.7	0.8	1	1.2	1.5	2	2.5	3	3.5	4	4.5	5	5.5	6	6.5	7	7.5	8
ITEM 3***	Dynamic Gabor Patch	Temporal Frequency (Hz)	20	18	16	14	12	10	9	8	7	6	5	4	3.5	3	2.5	2	1.5	1	0.5	0.2
ITEM 4****	Moving Dots	Coherence (%)	100	95	90	85	80	75	70	65	60	55	50	45	40	35	30	25	20	15	10	5

Tableau 1. – Specifics about the stimuli characteristics for each level

* Item 1: Visual stimulus = Form of a round spaceship of 5° in diameter; luminance will vary in function of the contrast (see below); color = monochrome; duration = 100ms. Auditory stimulus = White noise of 100ms appearing spatially and temporally congruent with the visual stimulus.

** Item 2: Orientation = vertical or horizontal. Gaussian aperture in a 5° in diameter, with σ = 1; 250 ms raised cosine temporal envelope; space-averaged luminance = same as background (0.5 cd/m2); temporal frequency = 0 Hz; duration = 400ms.

*** Item 3: Orientation = vertical when direction of motion = left or right; Orientation = horizontal when direction of motion = up or down; Gaussian aperture in a 5° in diameter, with σ = 1; 250 ms raised cosine temporal envelope; space-averaged luminance = same as background; spatial frequency = 1 Hz; duration = 400ms.

**** Item 4: Circular aperture = 5° in diameter; Density: 2.6 dots/°; Duration of stimulus = 400ms; Size of dots = 0.06°; Speed of dots = 10°/s; lifetime of dots = 200 ms; luminance of the dots = 0.5 cd/m2; direction of motion : left, right, up or down; luminance of the stimulus background = 23cd/m2

References

Ajina, S., and Kennard, C. (2012). Rehabilitation of damage to the visual brain. In Revue Neurologique, pp. 754–761.

Ajina, S., Pestilli, F., Rokem, A., Kennard, C., and Bridge, H. (2015). Human blindsight is mediated by an intact geniculo-extrastriate pathway. Elife 4, e08935.

Alexander, I., and Cowey, A. (2009). The cortical basis of global motion detection in blindsight. Exp. Brain Res. 192, 407–411.

Baniqued, P.L., Kranz, M.B., Voss, M.W., Lee, H., Cosman, J.D., Severson, J., and Kramer, A.F. (2014). Cognitive training with casual video games: points to consider. Front. Psychol. 4, 1010.

Bocchio, M., Nabavi, S., and Capogna, M. (2017). Synaptic Plasticity, Engrams, and Network Oscillations in Amygdala Circuits for Storage and Retrieval of Emotional Memories. Neuron 94, 731–743.

Bolognini, N., Rasi, F., Coccia, M., and Làdavas, E. (2005). Visual search improvement in hemianopic patients after audio-visual stimulation. Brain 128, 2830–2842.

Chokron, S., Perez, C., Obadia, M., Gaudry, I., Laloum, L., and Gout, O. (2008). From blindsight to sight: cognitive rehabilitation of visual field defects. Restor. Neurol. Neurosci. 26, 305–320.

Das, A., and Huxlin, K.R. (2010). New approaches to visual rehabilitation for cortical blindness: outcomes and putative mechanisms. Neuroscientist 16, 374–387.

Das, A., Tadin, D., and Huxlin, K.R. (2014). Beyond blindsight: properties of visual relearning in cortically blind fields. J. Neurosci. 34, 11652–11664.

Deco, G., Vidaurre, D., and Kringelbach, M.L. (2021). Revisiting the global workspace orchestrating the hierarchical organization of the human brain. Nat. Hum. Behav. 2021 54 5, 497–511.

Donohue, S.E., Woldorff, M.G., and Mitroff, S.R. (2010). Video game players show more precise multisensory temporal processing abilities. Atten. Percept. Psychophys. 72, 1120–1129.

Dundon, N.M., Làdavas, E., Maier, M.E., and Bertini, C. (2015). Multisensory stimulation in hemianopic patients boosts orienting responses to the hemianopic field and reduces attentional resources to the intact field. Restor. Neurol. Neurosci. 33, 405–419.

Duquette, J., and Baril, F. (2009). Les interventions de réadaptation visuelle développées à l'intention des personnes ayant une déficience visuelle associée à une condition neurologique. Inst. Nazareth Louis-Braille 15.

Goodwin, D. (2014). Homonymous hemianopia: Challenges and solutions. Clin. Ophthalmol. 8, 1919–1927.

Grasso, P.A., Làdavas, E., and Bertini, C. (2016). Compensatory Recovery after Multisensory Stimulation in Hemianopic Patients: Behavioral and Neurophysiological Components. Front. Syst. Neurosci. 10, 45.

Green, C.S., and Bavelier, D. (2003). Action video game modifies visual selective attention. Nature 423, 534–537.

Green, C.S., and Bavelier, D. (2006a). Effect of action video games on the spatial distribution of visuospatial attention. J. Exp. Psychol. Hum. Percept. Perform. 32, 1465–1478.

Green, C.S., and Bavelier, D. (2006b). Enumeration versus multiple object tracking: the case of action video game players. Cognition 101, 217–245.

Grunda, T., Marsalek, P., and Sykorova, P. (2013). Homonymous hemianopia and related visual defects: Restoration of vision after a stroke. Acta Neurobiol. Exp. (Wars). 73, 237–249.

Hadid, V., and Lepore, F. (2017). From Cortical Blindness to Conscious Visual Perception: Theories on Neuronal Networks and Visual Training Strategies. Front. Syst. Neurosci. 11, 64.

Huxlin, K.R. (2008). Perceptual plasticity in damaged adult visual systems. Vision Res. 48, 2154–2166.

Huxlin, K.R., Martin, T., Kelly, K., Riley, M., Friedman, D.I., Burgin, W.S., and Hayhoe, M. (2009). Perceptual relearning of complex visual motion after V1 damage in humans. J. Neurosci. 29, 3981–3991.

Kentridge, R.W., Heywood, C.A., and Weiskrantz, L. (2004). Spatial attention speeds discrimination without awareness in blindsight. Neuropsychologia 42, 831–835.

Kerkhoff, G., Münßinger, U., Haaf, E., Eberle-Strauss, G., and Stögerer, E. (1992). Rehabilitation of homonymous scotomata in patients with postgeniculate damage of the visual system: saccadic compensation training. Restor. Neurol. Neurosci. 4, 245–254.

Làdavas, E. (2008). Multisensory-based approach to the recovery of unisensory deficit. Ann. N. Y. Acad. Sci. 1124, 98–110.

Latham, A.J., Patston, L.L.M., and Tippett, L.J. (2013). The virtual brain: 30 years of video-game play and cognitive abilities. Front. Psychol. 4, 629.

Melnick, M.D., Tadin, D., and Huxlin, K.R. (2016). Relearning to See in Cortical Blindness. Neurosci. 22, 199–212.

Mueller, I., Gall, C., Kasten, E., and Sabel, B.A. (2008). Long-term learning of visual functions in patients after brain damage. Behav. Brain Res. 191, 32–42.

Oei, A.C., and Patterson, M.D. (2014). Are videogame training gains specific or general? Front. Syst. Neurosci. 8, 54.

Passamonti, C., Bertini, C., and Làdavas, E. (2009). Audio-visual stimulation improves oculomotor patterns in patients with hemianopia. Neuropsychologia 47, 546–555.

Patel, A.T., Duncan, P.W., Lai, S.-M., and Studenski, S. (2000). The relation between impairments and functional outcomes poststroke. Arch. Phys. Med. Rehabil. 81, 1357–1363.

Pavan, A., Alexander, I., Campana, G., and Cowey, A. (2011). Detection of first- and second-order coherent motion in blindsight. Exp. Brain Res. 214, 261–271.

Perez, C., and Chokron, S. (2014). Rehabilitation of homonymous hemianopia: insight into blindsight. Front. Integr. Neurosci. 8, 82.

Pohl, C., Kunde, W., Ganz, T., Conzelmann, A., Pauli, P., and Kiesel, A. (2014). Gaming to see: action video gaming is associated with enhanced processing of masked stimuli. Front. Psychol. 5, 70.

Pollock, A., Hazelton, C., Rowe, F.J., Jonuscheit, S., Kernohan, A., Angilley, J., Henderson, C.A., Langhorne, P., and Campbell, P. (2019). Interventions for visual field defects in people with stroke. Cochrane Database Syst. Rev. 2019.

Rowe, F.J., Hepworth, L.R., Howard, C., Hanna, K.L., Cheyne, C.P., and Currie, J. (2019). High incidence and prevalence of visual problems after acute stroke: An epidemiology study with implications for service delivery. PLoS One 14.

Sahraie, A., Hibbard, P.B., Trevethan, C.T., Ritchie, K.L., and Weiskrantz, L. (2010). Consciousness of the first order in blindsight. Proc. Natl. Acad. Sci. U. S. A. 107, 21217–21222.

Saionz, E.L., Feldon, S.E., and Huxlin, K.R. (2021). Rehabilitation of cortically induced visual field loss. Curr. Opin. Neurol. 34, 67–74.

Sand, K.M., Midelfart, A., Thomassen, L., Melms, A., Wilhelm, H., and Hoff, J.M. (2013). Visual impairment in stroke patients--a review. Acta Neurol. Scand. Suppl. 52–56.

Schurger, A., Cowey, A., Cohen, J.D., Treisman, A., and Tallon-Baudry, C. (2008). Distinct and independent correlates of attention and awareness in a hemianopic patient. Neuropsychologia 46, 2189–2197.

Urbanski, M., Coubard, O.A., and Bourlon, C. (2014). Visualizing the blind brain: brain imaging of visual field defects from early recovery to rehabilitation techniques. Front. Integr. Neurosci. 8, 74.

Watanabe, T., Náñez, J.E., Koyama, S., Mukai, I., Liederman, J., and Sasaki, Y. (2002). Greater plasticity in lower-level than higher-level visual motion processing in a passive perceptual learning task. Nat. Neurosci. 5, 1003–1009.

Weiskrantz, L. (1986). Blindsight : A Case Study and Implications: A Case Study and Implications (Clarendon Press).

Whitton, J.P., Hancock, K.E., and Polley, D.B. (2014). Immersive audiomotor game play enhances neural and perceptual salience of weak signals in noise. Proc. Natl. Acad. Sci. 111, E2606–E2615.

Xiao, L.-Q., Zhang, J.-Y., Wang, R., Klein, S.A., Levi, D.M., and Yu, C. (2008). Complete transfer of perceptual learning across retinal locations enabled by double training. Curr. Biol. 18, 1922–1926.

Yoshida, M., Itti, L., Berg, D.J., Ikeda, T., Kato, R., Takaura, K., White, B.J., Munoz, D.P., and Isa, T. (2012). Residual attention guidance in blindsight monkeys watching complex natural scenes. Curr. Biol. 22, 1429–1434.

Zhang, Y.-X., Tang, D.-L., Moore, D.R., and Amitay, S. (2017). Supramodal Enhancement of Auditory Perceptual and Cognitive Learning by Video Game Playing. Front. Psychol. 8, 1086.

Zihl, J., and Werth, R. (1984). Contributions to the study of "blindsight"--II. The role of specific practice for saccadic localization in patients with postgeniculate visual field defects. Neuropsychologia 22, 13–22.

Chapter 8: General Discussion

8.1. Summary of the Aims and Findings

Views on residual abilities, neural networks, and rehabilitation in blindsight

Study 1: The goal of this research was to put blindsight in the context of an altered global neural workspace so that it may be better understood and targeted during visual rehabilitation. In fact, the unconscious nature of residual abilities after a V1-lesion is still controversial with some claiming that blindsight is just a near-threshold degraded normal vision. To better define the nature of type I and type II blindsight we integrate our understanding of the phenomenon into the context of the global workspace where inefficient bottom-up activations lead to a desynchronized neuronal network impacting perception, attention, and consciousness. By framing blindsight into this altered neuronal network, we propose a new nomenclature to address the observed discrepancies between lesions, behavior, and subjective awareness across patients. We finally propose a combined visual rehabilitation strategy that targets the enhancement of the altered global workspace by activating subcortical extrastriate pathways via bottom-up multisensory and top-down restoration strategies. We thus postulate that such training could improve vision in cortical blindness by targeting both pre-existing and novel brain mechanisms and enhancing neural synchronization.

Evidence of fast thalamo-amygdala and extrastriate pathways: a new case of affective blindsight

Study 2: The purpose of this work was to determine the presence of a rapid subcortical pathway driven by gamma oscillations involved in affective discrimination in the absence of visual awareness. This was achieved by testing a patient presenting blindsight for complex natural affective scenes during a MEG recording. Source reconstruction, power analysis, cluster-based permutation analysis, undirected and causal directed connectivity, and linear regression were computed in order to address our objectives. The causal connectivity mediated by gamma oscillations between the thalamus, amygdala, and STS provided solid evidence that blindsight was first mediated by a fast thalamo-amygdala pathway and subsequently by a fast thalamo-extrastriate pathway providing new insights into the temporal dynamics supporting blindsight. Moreover, the behavioral and MEG findings supported different subcortical pathways guided by high-frequency rhythms involved in conscious and unconscious processing. Significantly, the study re-examines affective unconscious perception under a new scope.

Insights on the early vs. late debate of visual consciousness: a new case of affective blindsight

Study 3: The goal of this paper was to examine the striate and subcortical evoked responses in order to gain a better comprehension of the temporal cognitive mechanisms involved in affective blindsight and conscious perception. The analysis was done on the MEG data recorded while patient SJ performed the forced-choice affective discrimination task utilizing affective complex natural scenes described in study 2. Source reconstruction, evoked analysis, cluster-based permutation analysis, decoding across nodes, temporal decoding and generalization as well as directed causal connectivity were computed in order to consider effects of visibility, lateralization, eccentricity, and affective valence. The results showed that temporal information of seen and unseen pictures was coded at early and late latencies through different mechanisms in V1, the thalamus, and the amygdala, as visual awareness was coded through greater maintained activity at late stages. However, subcortical and striate evoked differences in eccentricity for seen and unseen information was decoded only in early time windows and not maintained over time. Finally, affective specific differences for unconscious peripheral perception were reflected by subcortical early and late differences in evoked responses and by the direction of the flow of information showing the role of subcortical neural signatures in affective blindsight. The subcortical implications seem to indicate the existence of an unconscious route processing affective information that is engaged when conscious access is inhibited.

Using the vMMN to address the discussion on the nature of blindsight and its objective measure

Study 4: The goal of this study was to address the use of the vMMN in unconscious processing by assessing the brain mechanisms involved in automatic change detection induced by a violation of regularities. The aim was achieved by testing neurotypical individuals (N=20) and a blindsight patient in a demanding central task while an unattended oddball paradigm was presented in the periphery. The oddball consisted of the presentation of motion stimuli moving in two directions where one direction was shown on 85% of the trials, i.e. standard condition, and the other 15%, i.e. deviant condition. Detection of the deviant stimuli resulted in significant vMMN, P3a, theta synchronization, and large-scale neural networks in both neurotypical individuals and the blindsight patient suggesting the involvement of automatic processing and prediction errors.

Furthermore, differences in spectral connectivity revealed a significant theta increase in posterior regions for the blindsight patient compared to the neurotypical group suggesting unconscious processing that differs from near-threshold vision. Significantly, this study could be critical to blindsight research as the vMMN could be utilized as an objective electrophysiological biomarker for automatic unpredicted change detection independent of behavior. Such assessment could lead to new insights into the neurological underpinnings of unconscious processing in both intact and impaired vision.

Training residual abilities of patients with CB in a dynamic environment: a methods paper

Study 5: The goal of this methods paper was to propose a multisensory-restitution video game training that could be played at home to help individuals with CB enhance their visual abilities within the blind hemifield using a dynamic environment and providing feedback on performance for motivation. We predict that by using specific audio-visual training that combines ocular compensation and visual restitution strategies in a motivating environment, visual performances, and awareness in the blind hemifield of HH patients will improve and induce neurophysiological changes after training. In fact, multimodal stimulations coupled with visual restoration training might construct a foundation for prospective functioning by targeting pre-existing and novel neural processes.

8.2. Theoretical, Methodological, and Empirical Contributions

A proposed framework for blindsight

This section summarizes the contributions provided by the first study: article 1, **chapter 3**.

A terminology to differentiate residual abilities

CB can be caused by different neurophysiological disorders affecting the extent and location of V1 lesions making each patient unique (Sand et al., 2013). Interestingly, some patients preserve blindsight abilities in their blind hemifield assessed by behavioral measures reported in the literature. The open question of why only some patients preserve residual abilities leads to two

main debates. The first one is about the way blindsight is assessed, i.e. instead of using behavioral and subjective measures not adapted to each patient why not use no-report paradigms or objective measures of blindsight as proposed for neurotypical individuals (Soto et al., 2019; Tsuchiya et al., 2015) and the other is about the nature of blindsight, i.e. is it an unconscious vision or degraded near-threshold vision (Azzopardi and Cowey, 1997; Weiskrantz, 2009)? To better address both debates, we first have to understand the subjective nature of blindsight which is categorized into type I blindsight and type II blindsight. Type I blindsight refers to residual visual abilities in the blind hemifield that are not accompanied by any subjective sensation (Lau and Passingham, 2006). On the other hand, patients with type II blindsight report a sense that something is happening in their blind hemifield in response to certain stimuli, raising the question of whether these feelings are 'non-visual' or visual in origin, raising the debate on whether blindsight should be classified as unconscious vision or degraded vision. Unconscious vision is described as the processing of information that is deprived of its qualitative visual nature and is mediated through secondary subcortical visual pathways (Weiskrantz, 2009). Degraded vision can refer to near-threshold normal vision or abnormal vision. Degraded near-threshold normal vision is defined by accuracy above-chance level, a perception that is accompanied by visual qualia and visual information that passes through the primary visual pathway. The rationale supporting the hypothesis of a degraded near-threshold normal vision is mainly associated with the existence of spared V1 islands which would allow information to be processed through the geniculo-striate pathway (Morland et al., 2004). For this reason, case reports are essential to assess the neural correlates of blindsight and unconscious processing as patients usually have delimited or complete resection of their striate cortex as described in this thesis' research (studies 2 to 4). On the other hand, degraded abnormal vision refers to accuracy above-chance level, a perception that is accompanied by visual qualia and visual information that passes through secondary subcortical visual pathways (Mazzi et al., 2016). The difference between unconscious vision and degraded abnormal vision is harder to tackle. One way to do so is to test patients that, under any circumstances, do not report any sensation in their blind hemifield or where subjective assessments do not correlate with neurophysiological assessments which was the case of the patient described in studies 2 and 3. Another way to do so is to test a patient that reports a subjective sense of something happening in his blind hemifield, i.e. type II blindsight, but assess his blindsight through a no-report paradigm independent of behavior which was the aim of study 4. Taken together, we argue that in order to better understand blindsight,

we must examine it through the lens of a certain framework, namely the global neural workspace (Baars, 1988) that provides a perspective on conscious and unconscious visual perception through a neural network (Dehaene et al., 1998) which explains why we used connectivity analysis in studies 2, 3, and 4 to better understand the neural underpinnings of blindsight.

A neuronal framework of altered global workspace to comprehend the nature of blindsight

The global workspace of Baars (1988), adapted by Dehaene, Kerszberg & Changeux (1998), support that in order to reach a state of visual consciousness five processors need to work in synchronization (Baars, 1988; Dehaene et al., 1998) where bottom-up and top-down modulations interact through feedforward and feedback projections, respectively (Dehaene et al., 2006). Specifically, interactions between the perceptual (sensory system), attentional (access system), memory (encoding system), and evaluative (self-processing system) processors are achieved in order to access visual consciousness (global workspace or consciousness) and induce behavior that can be measured. Conscious processors can more specifically be enhanced by interactions between fronto-parietal and prefrontal networks and visual areas (Dehaene et al., 2003; Lee et al., 2019; Quentin et al., 2015; Schutter and van Honk, 2004). Therefore, we address the incapacity of blindsight patients to access visual consciousness as a lack of global availability due to ineffective looping and propagation across systems that are altered, notably the perceptual system, i.e. bottom-up/feedforward propagation and the attentional system, i.e. top-down/feedback propagation (Silvanto, 2015). Nonetheless, the observed and measured residual abilities in blindsight, which based on the global neuronal workspace are unconscious in nature, could be supported by local activations of the perceptual and attentional systems activated by secondary subcortical alternative visual pathways, such as the thalamo-extra-striate pathways (Ajina et al., 2015), investigated in studies 2 and 4, and the thalamo-amygdala pathway (Morris et al., 2001), investigated in studies 2 and 3. The lack of long-range connectivity and synchronization (Melloni et al., 2007) between the different systems and networks that can be tested by measuring brain rhythms could suppress visual qualia as observed in type I blindsight. However, the presence of local activity mediated by alternative pathways could explain performance above chance-level. However, we propose that type II blindsight can also be explained in terms of unconscious processing as it is possible that local activity is insufficient to propagate and reach the threshold of global availability for visual

qualia but that recurrent processing within regions notably, within the 'conscious space', is sufficient to induce a sense of 'awareness'. Therefore, considering this rationale it would be possible to enhance local and global synchronization using visual rehabilitation strategies targeting bottom-up and top-down matter perceptual and attentional systems, respectively. In other terms, we propose to use training that can stimulate secondary visual pathways to get from (1) a state of 'no awareness' to (2) a state of 'awareness' independent of the nature of this awareness and finally (3) to a state of visual awareness.

A combined rehabilitation strategy

Here we propose a theoretical frame for combining multisensory training using saccades and visual restitution training using motion stimuli. The description and proof of concept of both types of training were described in chapter 1 and will be further discussed in the methodological contributions section as in study 5 we proposed a dynamic way to integrate both types of training into a video game approach. Thus, we propose to train the bottom-up system using multisensory stimulations to facilitate the enhancement of the top-down system and lower its threshold, as we know that attention is necessary though not sufficient for conscious perception (Kentridge et al., 2004; Schurger et al., 2008; Yoshida et al., 2012). Thus, by stimulating the perceptual system stronger connections could be formed with the attentional network. This attentional network can be moreover strengthened using visual restitution training with motion stimuli which can in return create stronger connections with the perceptual network in order to enhance perception. As discussed in chapter 1, both types of training stimulate the subcortical pathways involved in blindsight but use different pathways to do so. Therefore, by simultaneously enhancing the activity at both gates, i.e. the perceptual and attentional processors, through different directions, i.e. feedforward and feedback connectivity, we could increase the availability of information through large-scale connectivity guided by brain rhythms aiming to improve conscious visual perception as a result (Deco et al., 2021). Thus, the objective of this first study was to provide the groundwork for the conceptualization of all the other studies presented in this thesis as we used these notions to assess the neural substrates of blindsight and designed a rehabilitation strategy.

Fast subcortical pathways for blindsight under the scope of gamma oscillations

This section summarizes the contributions provided by the second study: article 2, **chapter 4**.

Behavioral assessment of a new case report of affective blindsight

The case of patient SJ is new to the literature as we are the first to report his exceptional ability to unconsciously discriminate between complex natural affective scenes. To our knowledge, he is the first patient with affective blindsight able to discriminate between such complex features. Moreover, he has no spared V1 islands in his right hemisphere resulting in a complete left HH with no macular sparing and no visual awareness whatsoever. Thus, any residual ability couldn't derive from spared striate functionality, suggesting the involvement of an extra-striate unconscious pathway which we demonstrated in this study.

The behavioral assessment on a 3-alternative forced-choice affective discrimination task showed that SJ was able to discriminate between affective scenes when they were presented in his blind hemifield. As expected, SJ accuracy was significantly better in his intact hemifield compared to the blind hemifield, and reaction times (RTs) were faster. However, we showed that he performed above chance level, and more importantly that his RTs were modulated by the performance, i.e. correct or incorrect, the eccentricity, i.e. paracentral (6°) or near periphery (12°), and the affective condition, i.e. unpleasant, neutral or pleasant, despite a complete lack of visual awareness. These results suggest that we can measure blindsight abilities without the bias from subjective reports. One unexpected finding was that performance in the blind hemifield was better for pleasant pictures than for unpleasant pictures, demonstrating SJ's ability to identify pleasant pictures. Nonetheless, his RTs were faster for unpleasant pictures. Considering both the performance and RTs, we hypothesized and later demonstrated by causal connectivity that pleasant and unpleasant pictures are driven by distinct neural pathways. Overall, differences in RTs across conditions were very similar between the intact and the blind hemifield, as faster RTs were found for correct responses, near the periphery and in unpleasant conditions. However, when looking at the interaction between the conditions, we observe that for conscious perception, there is an advantage for pleasant paracentral stimuli while the advantage for unpleasant pictures was more specifically found in the near periphery. In contrast, in the blind hemifield, the advantage for near periphery was found for both unpleasant and pleasant pictures. These results corroborate the

advantage of the peripheral magnocellular system that is faster for negative stimuli in processing emotional pictures (Campana et al., 2016; Maunsell et al., 1999; Tapia and Breitmeyer, 2011).

Insights on the neural dynamics of visual perception

The thalamo-striate pathway known to drive visual perception as the LGN within the thalamus projects its activity in V1 is hypothesized to communicate through synchronization of gamma rhythms (Dehaene et al., 2003; Mashour et al., 2020). These thalamic gamma modulations have previously been investigated in the animal (McAfee et al., 2018; Redinbaugh et al., 2020), but haven't been associated with visual consciousness in humans. In chapter 4, we provide evidence that the contralateral thalamus and V1 gamma rhythms were significantly correlated when the intact hemifield was stimulated, which wasn't the case when pictures were presented in the blind hemifield. This rhythmic correlation when causally assessed showed that the bottom-up activity projected from the thalamus to V1 was a significant predictor of SJ's RTs, demonstrating the role of this pathway in conscious visual perception (Van Kerkoerle et al., 2014). Moreover, we found that gamma activity of the contralateral amygdala and V1 were significantly correlated with conscious perception suggesting a role of the amygdalo-cortical pathway ('the long conscious pathway') in affective discrimination (Bocchio et al., 2017).

A closer look into blindsight as gamma influences from the thalamus to the amygdala and extrastriate regions drives correct discrimination

One of the most probing results in this study is the difference in the directionality of the subcortical causal influences when comparing correct and incorrect performances for unseen stimuli presented within the blind hemifield. In fact, at stimulus onset, we were able to identify and distinguish a signal that would lead to an accurate performance from a signal that would induce an incorrect answer by looking at the causal directionality between the contralateral thalamus and the amygdala. We hypothesize that the pulvinar within the thalamic structure was involved in these projections through a magnocellular pathway as connections between both structures have been evidenced (Day-Brown et al., 2010; McFadyen et al., 2017, 2019). This bidirectional communication bypassing V1 triggered as soon as 50 ms was found to be independent of the stimulus predictability and affective condition. In fact, the presentation of a picture was randomly presented in the left or

right hemifield whit no prior cue on the timing of the presentation or location. Moreover, the inverse connectivity between correct and incorrect responses was not associated with the emotional content as it was found for unpleasant, neutral, and pleasant pictures providing insights into the debate of whether the fast-thalamo amygdala pathway mediating unconscious processing is only specific to negative stimuli (Garrido et al., 2012).

The contralateral thalamus also rapidly sent its projection via gamma rhythms causally influencing the contralateral STS and bypassing V1 around 100 ms leading to a correct response. The difference in latency observed between projections from the thalamus to the amygdala and the STS suggests that accurate discrimination is first mediated by subcortical communication and then by subcortical-cortical communication. The STS previously reported as being involved in correct responses (Andino et al., 2009) measured in affective (Burra et al., 2013; Van den Stock et al., 2014; Striemer et al., 2019) is known for its multiple roles in brain mechanisms crucial when processing a natural complex affective scene (Allison et al., 2000; Bettencourt and Xu, 2013; Bogadhi et al., 2018; Claeys et al., 2003; Karnath, 2001; Lahnakoski et al., 2012). This thalamic extra-striate pathway also independent of the affective condition could either be supported by the LGN through a koniocellular pathway (Schmid et al., 2010) or by the pulvinar through a magnocellular pathway (de Gelder and Poyo Solanas, 2021). This subcortical pathway mediating information that will be adequately discriminated was specific to stimulation of the blind hemifield as the thalamo-STS causal connectivity wasn't associated with accuracy for stimulation of the intact hemifield.

On the contrary, incorrect responses were associated with causal influences exerted from the contralateral amygdala and STS on the contralateral thalamus. We hypothesize that the lack of blindsight abilities, i.e. performance below chance-level without visual awareness, could mainly be associated with insufficient bottom-up causal connectivity between the thalamus and other structures (Dehaene et al., 2006) due to incapacity in detecting relevant information (Bogadhi et al., 2021; Corbetta et al., 2008). The inverse connectivity could indicate a top-down mechanism associated with uncertainty, trying to compensate and 'guess' the correct answer which was also observed between the thalamus and amygdala for seen stimuli in later latencies suggesting prior cortical involvement (D'Hondt et al., 2013). Importantly, the early timing observed specifically in

the case of blindsight suggests rapid thalamo-amygdala and thalamo-extra-striate pathways that could predict unconscious behavior. In fact, SJ's RTs were predicted using the subcortical connectivity mediated by gamma rhythms which confirm the involvement of thalamic high-frequency modulations in perception.

Seen and unseen unpleasant and pleasant pictures are differentiated by the direction of the connectivity between the thalamus and amygdala at late latencies

The literature is dominated by the view that unconscious negative information is specifically mediated by a fast thalamo-amygdala pathway that bypasses V1 (Anderson et al., 2003; LeDoux, 2000; Ward et al., 2005). However, our paper did not provide any evidence of such early specificity for unpleasant pictures when connectivity was assessed through high gamma oscillations (*refer to* study 3, chapter5 for specific evoked differences associated with the unpleasant system). As we previously mentioned the fast thalamo-amygdala connectivity for unsee pictures was observed irrespective of an affective condition. Nonetheless, we found that the directionality of causal influences between the thalamus and amygdala differed between unpleasant and pleasant pictures after 300 ms for unseen pictures and around 500 ms for seen stimuli, suggesting for both conscious and unconscious perception that cortical areas were previously involved (Boucher et al., 2015; Codispoti et al., 2006; Vuilleumier, 2005; Vukelić et al., 2021; Del Zotto et al., 2013) as well as attentional processing (Andino et al., 2009; Luo et al., 2010). This difference in timing between unconscious and conscious percept is very interesting regarding how much higher order processing was required to discriminate between affective conditions. Thus, putting these results into the perspective of the global neuronal workspace it seems that unconscious affective perception requires less complex cortical propagation and synchronization (Salti et al., 2015a). As to why unpleasant and pleasant conditions are mediated through opposite directions, we hypothesize that negative valences are mediated through a bottom-up propagation resulting in faster RTs as observed in the behavioral assessment, while pleasant pictures mainly induce top-down propagation resulting in better extraction of the information as assessed by SJ's performance (Taylor and Fragopanagos, 2005; Vukelić et al., 2021). Interestingly, the same interpretations can be done for the intact hemifield, where seen affective information displayed the same subcortical directionality in causal connectivity.

Summary

Significantly, this study provides evidence that fast thalamo-amygdala and thalamo-extra-striate pathways subserve the ability to identify complex scenes without visual awareness after a V1 lesion. Specifically, within an early latency range, we assessed that subcortical communications preceded the subcortico-cortical interactions providing insights into the temporal and spectral dynamics involved in both pathways. Affective-specific differences on the other hand seem to involve late bottom-up and top-down mechanisms between the thalamus and amygdala which we hypothesize is provided by cortico-subcortical communication. These influences are observed at earlier stages for unconscious processing suggesting less complex cortical propagation and synchronization compared to conscious perception of affective scenes.

Early and late processing in blindsight as investigated in V1 and subcortical structures

This section summarizes the contributions provided by the third study: article 3, **chapter 5**.

Early positive components in the intact V1 show processing of conscious and unconscious information at the early stages

The goal of this work was to examine the visual evoked responses at the cortical and subcortical source levels to gain a better understanding of the temporal profile that supports the conscious and unconscious perception of affective complex natural scenes when V1 is lesioned. Thus, we employed temporal decoding and generalization to predict the evoked activity that occurs when affective and neutral scenes are presented to SJ's intact and blind hemifields whose affective abilities were reported in study 2.

Differences between the contralateral and ipsilateral hemifields were first identified at stimulus onset where seen information triggered a C1 component. The C1 component originates from the striate cortex and shows direct processing of the information through the geniculo-striate pathway (Railo et al., 2011; Di Russo et al., 2002). While this striate evoked response was not

found for unseen pictures, some studies have suggested the involvement of the intact hemisphere in processing information from the blind hemifield which could support blindsight abilities (Celeghin et al., 2015; Chaumillon et al., 2018s; Goebel et al., 2001; Tamietto and de Gelder, 2008) and more specifically within the intact V1 (Georgy et al., 2020). Our findings showed that at around 100 ms a positive component, i.e. P1, for seen contralateral pictures was elicited across the nodes within V1 showing early sensory processing of perceived stimuli (Mangun et al., 2001). Interestingly, the positive early component was observed around 150 ms in V1 for unseen ipsilateral pictures after interhemispheric transfer. There was clear recruitment of V1 in order to process unconscious information at early stages. Subsequent components such as the N1, P2, and N2 were also been elicited in both conscious and unconscious processing with differences in time latencies due to interhemispheric transfer (Di Russo et al., 2002). All of these evoked components found in V1 which we know originate from extrastriate and higher-order regions show that even in the absence of visual awareness information is processed through feedback projections (Railo et al., 2011; Di Russo et al., 2002). However, pictures presented in the blind hemifield didn't evoke any late components, i.e. the P3 and N400, as opposed to seen pictures which indicated that higher order processing in V1 was only mediated by conscious perception (Dehaene et al., 2003a; Salti et al., 2012).

When comparing eccentricity, i.e. paracentral vs near periphery, within hemifields, we observe that the evoked response in V1 differed between eccentricity at the P1 and N1 time range, therefore at an early time window. Moreover, V1 is also able to discriminate between eccentricities when pictures were presented in the blind hemifield, nonetheless, these differences were elicited at the N2 time range where N2 was greater for paracentral pictures. We interpret these results as a faster attentional allocation to the contralateral intact hemifield compared to the ipsilateral blind hemifield (Hillyard and Anllo-Vento, 1998; Patel and Azzam, 2005; Schindler et al., 2018; Xu et al., 2016).

Decoding of seen and unseen pictures is first initiated in cortical areas and then in subcortical structures

As we assessed the evoked differences and decoding accuracies, the differences between seen and unseen pictures in the thalamus were found around 70 ms, while they started at stimulus onset in V1. Thus, thalamic differences were subsequent to those found in V1 suggesting that cortical processing was able to decode information from seen and unseen pictures before subcortical differentiation (Cecere et al., 2013). The differences between seen and unseen pictures in the amygdala were decoded prior to those in the thalamus but subsequent to the ones in V1, suggesting that cortical decoding between conscious and unconscious processing happens prior to subcortical decoding. These findings agree with the notion that consciousness emerges from the cortex which interacts with subcortical structures (John, 2002; Schutter and van Honk, 2004; Zeman, 2004).

Evoked responses in subcortical structures reveal different mechanisms for the central and peripheral system

An early visual negative component referred to as N1 was found to be modulated by the side of the presentation and by the eccentricity at which a picture was presented within each hemifield (Hillyard and Anllo-Vento, 1998; Klimesch, 2011; Di Russo et al., 2002). These differences were observed in the thalamus and amygdala for seen pictures and unseen pictures contributing to the literature on human evoked responses (Koivisto et al., 2010). In fact, N1 was larger for seen and unseen pictures presented in the near periphery compared to pictures presented in the paracentral visual hemifield suggesting this early negative component is modulated by a magnocellular pathway. On the other hand, the thalamic P2 was larger for paracentral seen pictures compared to near periphery seen pictures suggesting its role within the parvocellular pathway for conscious perception as observed in studies on P3 (Patel and Azzam, 2005; Railo et al., 2011; Rutiku et al., 2015). The evoked responses in the subcortical regions can be summed up as follows: N1 for seen and unseen: periphery > central, P1/P2 for seen: central > periphery, P2 for unseen: periphery > central.

Similarly, differences between eccentricity for seen pictures were also found in the contralateral amygdala at early stages corresponding to the P1-N1 latency window, where P1 was larger for paracentral stimuli and N1 for near periphery stimuli. Therefore, P1/P2 could reflect the use of the parvocellular pathway for seen pictures while N1 appears to reflect characteristics of the

magnocellular pathway for seen and unseen pictures (Campana et al., 2016; Maunsell et al., 1999; Tapia and Breitmeyer, 2011). On the other hand, P2 in the left amygdala reflected the processing of peripheral unconscious information, which as we will discuss later on, was specific to affective processing. Therefore, a clear advantage of the magnocellular for peripheral stimuli in subcortical structures in unconscious perception is evidenced in this study. Differences in asymmetry between the left and right hemifields and hemispheres are discussed in the study as we suggest that multiple factors contributed to these modulations.

Late higher-order processing differs for seen and unseen pictures in V1 and subcortical structures: insights from the temporal decoding and generalization analyses

The temporal decoding and generalization analysis was computed with a multi-feature ML approach using the source information, i.e. nodes, within each structure as well as the temporal dynamics as features. These results showed that decoding between seen and unseen information starts very early on, around 90 ms, in the intact V1 and is rapidly observed in the thalamus and amygdala in both hemispheres. Looking at the temporal generalization results, training the classifier around 400 ms, i.e. at the P3 latency, showed significant decoding accuracy at subsequent time windows until 800 ms for V1, the thalamus, and the amygdala (specific differences are discussed in the paper). These results suggest that information is dynamically maintained across multiples stages including modulation in amplitude and re-entrant feedback activations (Aru et al., 2020; Heeger and Zemlianova, 2020; Lamme and Roelfsema, 2000) from higher order regions through a global workspace (Baars, 2002; Dehaene and Changeux, 2011; Dehaene et al., 2006). Based on these results and the fact that accurate decoding performance maintained over time wasn't obtained for other specific differences, i.e. eccentricity or affective valence, decoding seen and unseen information involves complex dynamics specific to visibility (Dehaene and King, 2016). Therefore, we can hypothesize that the lack of re-entrant activity at late time windows for unseen pictures could be linked to the absence of visual awareness (Silvanto, 2015). While we can't take a firm position, these results provide insights into the early vs late debate as we show that (1) decoding information from seen and unseen starts very early on through the coding of dynamic amplitude and (2) generalization of learning occurs only at a late time window where information is maintained until 800 ms.

Distinct temporal mechanisms for unpleasant and pleasant pictures as revealed by the evoked subcortical responses

The earliest evoked response found in the thalamus was a positive component peaking at 70 ms referred to as the P50 which is associated with multisensory integration of the bimodal thalamic neurons (Starke et al., 2020). Let's reiterate that in the paradigm when a picture was presented in the hemifield, white noise was simultaneously presented to trigger a forced-choice response from SJ as he wasn't aware of when a picture was presented to his blind hemifield. An important P50 was observed in the thalamus for both seen and unseen pictures and further analysis didn't reveal any difference between conditions. In the right thalamus, as we observed the differences between hemifields or eccentricity no probing P50 was elicited for any condition which we interpreted as functional degeneration at the level of the thalamus, and more importantly in the LGN (Alvarado et al., 2007; Arden et al., 2003; Shimojo and Shams, 2001). However, when we further investigated the interaction between the affective condition and eccentricity, we observed a significant P50 in the right thalamus specific to unpleasant peripheral pictures presented in the contralateral blind hemifield suggesting the involvement of the magnocellular pathway. Therefore, to our knowledge, our findings demonstrate for the first time the advantage of the unconscious peripheral fast thalamic pathway specific to a negative emotion presented in the blind hemifield of a blindsight patient.

As we previously mentioned, a stronger significant P2 response was evoked for peripheral pictures in the left amygdala compared to central pictures suggesting the dominance of the peripheral system in subcortical areas for unseen information. This advantage was translated by faster RTs for stimuli presented in the periphery as reported in study 2. When looking at the interaction between the eccentricity and affective condition, we found that unseen unpleasant pictures presented in the periphery triggered a greater P2 in the left amygdala compared to the pleasant condition (Tao et al., 2021) which could also explain faster RTs for the unpleasant condition (Bayle et al., 2011; Calvo et al., 2014). Taken together, the subcortical evoked analysis showed an advantage for the peripheral system specific to unpleasant pictures in the absence of visual awareness (Bayle et al., 2009; Méndez-Bértolo et al., 2016; Ward et al., 2005) which as we were able to demonstrate was specific to blindsight abilities.

On the other hand, a late advantage for unseen pleasant pictures was found in the thalamus between 400 and 600 ms and amygdala around 600-700 ms compared to neutral pictures. This difference was translated by a greater evoked magnetic late positive potential associated with affective discrimination (Schönwald and Müller, 2014) which we know originate from higher-order cortical regions (Moratti et al., 2011). Combined with SJ's behavioral performance showing an advantage in accurate responses for pleasant pictures, we postulate that pleasant pictures in blindsight are processed through a distinct mechanism that seems to involve a koniocellular pathway rather than a magnocellular pathway privileging the extraction of relevant information rather than a quick response (Campana et al., 2016; Maunsell et al., 1999; Tapia and Breitmeyer, 2011).

Temporal-directed thalamo-amygdala connectivity supports affective differences in blindsight

Finally, we aimed to assess the role of the thalamo-amygdala communications in processing affective scenes which resulted in demonstrating a bidirectional interaction between both structures that coded for the affective valence. In fact, corroborating the results described in study 3 while also reporting the effect of eccentricity, we showed that unpleasant information from the peripheral system passes from the thalamus to the amygdala at around 300 ms, while pleasant from the peripheral system passes from the amygdala to the thalamus in the same time window. The flow of information through a bottom-up and top-down system coding for affective specific differences solidifies the previous behavioral and empirical findings as assessed by study 2.

Summary

Importantly, this study reveals the temporal signature of subcortical and striate evoked responses in blindsight providing some insights into the early and late debate of consciousness. We first showed that information from the blind hemifield is transferred to the intact V1 at the early stages. Within this early time window information extracted from seen and unseen pictures are first decoded in V1 and are subsequently and rapidly decoded by subcortical structures. followed. Thus, the coding of visual consciousness seems to be first translated into a cortical response prior to

subcortical coding. Cortical and subcortical early evoked responses also code for differences in visual qualia between central and peripheral pictures irrespective of visual awareness. On the other hand, ML analysis showed that signatures of seen and unseen information were maintained over time only through late higher-order processing in V1 and subcortical structures. By refining the analysis to assess affective-specific differences, we showed that unpleasant information from the periphery in the unseen condition was extracted at very early stages by the thalamus and at late stages in the amygdala, while an advantage for pleasant information was found at late stages within the subcortical structures. These affective differences were translated into inverse causal connectivity between the thalamus and amygdala demonstrating that information circulates in a different direction to discriminate between the affective condition in blindsight.

Probing the neural dynamics of the vMMN to address the debate on evaluating unconscious processing independent of behavior

This section summarizes the contributions provided by the fourth study: article 4, **chapter 6**.

A reliable vMMN can be measured in the absence of visual awareness independent of behavior

The purpose of this work was to assess a neural biomarker of unconscious processing independent of behavior. To accomplish this goal, we decided to: (1) use a well-known evoked component as the vMMN which is highly favorable to be elicited in the absence of visual awareness (Rowe et al., 2020), and (2) by assessing the neural substrates of the vMMN a posterior negative component elicited around 200 ms (Pazo-Alvarez et al., 2003; Qian et al., 2014; Stefanics et al., 2014b) in neurotypical individuals and in a blindsight patient (ML) where the experimental task obviated the need for subjective visual awareness.

First, ML residual abilities were assessed for motion stimuli as she presented type II blindsight. In fact, when testing her in behavioral tasks where her attention was allocated to her blind hemifield, she was significantly able to detect motion stimuli without perceiving them, even though she 'felt' that something was happening. Interestingly, she claimed that this sensation wasn't describable as it wasn't a visual feeling' (Tran et al., 2019). However, when testing her on a discrimination motion task, her performance was at chance-level. Thus, we hypothesized that if

we were able to measure a reliable vMMN in her blind hemifield as a consequence of motion direction changes, therefore the assessed brain mechanisms were independent of visual awareness and behavior. Such a neural biomarker could therefore be used as a complementary or alternative measure of blindsight which would mitigate previous debate on the nature of blindsight and could lead to better identification of patients with residual abilities.

With this purpose in mind, we presented a sequence of motion stimuli in the peripheral system while participants were engaged in doing the Stroop test a high demanding task (Hadid and Lepore, 2017a). In fact, by showing a regular sequence of standard motion stimuli, the brain learns and creates an internal representation of predictions (Johnson et al., 2016). However, when we alter this prediction by inserting a deviant stimulus, the external and internal representations enter a state of mismatch resulting in prediction errors measured by the vMMN (Oxner et al., 2019). As neurotypical participants and ML didn't report any subjective visual awareness of the oddball peripheral sequence, we then tested our hypothesize that the vMMN is measurable in the absence of visual awareness by computing the difference between the deviant evoked response and the standard evoked response (deviant – standard) for both neurotypical individuals and the blindsight patient, ML. The results showed reliable posterior negativity around 200 ms across both hemispheres for the neurotypical individuals and ML when the stimulus was presented in both hemifields, demonstrating automatic detection of changes, thus validating that our methodological design elicited a vMMN in the absence of visual awareness.

The anterior P3a conveys the automatic processing of detection of changes

The evoked activity across electrodes showed a frontal positivity across both hemispheres when the difference was averaged between 250 and 300 ms for both hemifields and neurotypical individuals and the blindsight patient. As no allocation of attention was possible towards the periphery during the execution of the Stroop task, the attentional switch was inhibited. Therefore, the P3a that can often be attributed to attentional orienting (Escera et al., 2000; Friedman et al., 2001; Kok, 2001; Polich, 2007) is also a neural indicator of automatic processing in the auditory modality (Muller-Gass et al., 2007). In fact, it has been shown that the amplitude of the P3a is stronger for task-irrelevant changes when participants performed a task-relevant sequence (Combs

and Polich, 2006; Comerchero and Polich, 1998; Goldstein et al., 2002). Another reason supporting our interpretation of the observed anterior positivity representing automatic processing is that the given oddball exploited local violations of regularities rather than global temporal novelty which has been shown to be independent of attention (Bekinschtein et al., 2009). Moreover, considering that it is extremely unlikely that ML oriented any attention to her blind hemifield while doing the Stroop task and the fact that the P3a was observed when her blind hemifield was stimulated, it strengthens our case that we were able to measure automatic processing of information. These results suggest that the prediction error system consists of a posterior negative component followed by an anterior positive component (Ylinen et al., 2016).

Theta synchronization as an indicator of prediction errors

The presentation of a deviant stimulation systematically induced greater posterior and temporal theta synchronization compared to the standard condition for the neurotypical participants and ML. Theta oscillations have been shown to be involved in multiple higher-order cognitive processes, such as learning and memory (Chen et al., 2020; Goyal et al., 2020; Zhang et al., 2019), which could be both used in prediction errors in (Edalati et al., 2021; Recasens et al., 2018). The relation between the theta band and P3a suggests intertwingling of lower, i.e. bottom-up and higher, i.e. top-down, systems in predicting errors under automatic processing and updating the sensory representation (Harper et al., 2017; Ho et al., 2021; Hong et al., 2020). Therefore, the automatic unpredicted change detection seems to be associated with theta oscillations using sensory prediction, even for subconsciously processed inputs.

Frontal and posterior spectral connectivity suggest large-scale networks in prediction errors

Brain networks involved in unconscious processing employ seemingly particular frequency ranges (Mashour and Hudetz, 2018), however, the spectral networks involved in the vMMN have yet to be investigated. Therefore, this study provides a first insight into the neural dynamics involved in large-scale networks when automatic detection of motion changes occurs in the absence of visual awareness. The differences across frequency bands and hemifields in the neural networks showed (1) interaction between neural mechanisms associated with the motor response and the side of the

presentation (Pool et al., 2014), and (2) asymmetry between hemifields in relation to an inhibition of attentional allocation recruiting theta and gamma oscillations which dynamics are discussed with respect to the P3a (Cavézian et al., 2010, 2015; Sanchez-Lopez et al., 2020; Solís-Vivanco et al., 2021). These results highlight that various mechanisms are recruited and need to be carefully considered when interpreting the neural dynamics associated with the mismatch response as they are thoroughly discussed in study 4. Importantly, with regards to the prediction error system, the spectral connectivity analysis revealed large-scale cortico-cortical interactions mainly involving frontal regions through phase synchronization of oscillatory rhythms from 7 to 90 Hz. Interestingly, a distinct neural signature can be observed across frequency bands each potentially contributing to updating the system of prediction. In fact, results on the primate showed that fronto-posterior interactions associated with prediction errors are mediated by gamma oscillations while the update of the system of prediction is guided by alpha-beta oscillations (Chao et al., 2018).

Enhancement of posterior theta connectivity could reflect a neural signature of blindsight

We calculated the difference in spectral connectivity across different frequency bands between the neurotypical group and the blindsight patient to see if the brain processes of unconscious processing in neurotypical persons and blindsight patients were supported by the same neural network. By doing so, we targeted an important topic in the blindsight literature: is blindsight just degraded normal vision set at near-threshold (Azzopardi and Cowey, 1997; Hadid and Lepore, 2017b; Weiskrantz, 2009)?

To begin with, we looked at how a V1-lesion affected perception in the intact hemifield. After stimulation of her intact hemifield, phase synchronization in the beta band was significantly reduced compared to the neurotypical group. In fact, a beta desynchronized network of the temporo-parietal connections potentially involved in motion processing was observed in the lesioned left hemisphere. In light of the above, a V1 lesion could disrupt posterior connections in the lesioned hemisphere, causing them to disengage when the intact hemifield is stimulated, notably in the automatic detection of changes. Considering the role of feedback synchronization guided by beta oscillations on conscious perception (Bastos et al., 2015; Michalareas et al., 2016) and local novelty detection (El Karoui et al., 2015), we hypothesize that stimulation of the intact

hemifield reduces feedback connectivity within the lesioned hemisphere conform to the hypothesis of cortical remodeling in the intact hemisphere (Bridge et al., 2008; Mikellidou et al., 2019).

Subsequently, we addressed the question of the nature of blindsight by comparing ML's residual abilities within the blind hemifield with neurotypical people's absence of visual awareness. Interestingly, we observed an enhanced theta synchronization between occipito-parietal regions within the lesioned hemisphere. These results not only support our prior findings that stimulation of ML's blind hemifield recruits extra-striate areas for motion processing in the lesioned hemisphere (Tran et al., 2019), but they add valuable information on the dynamic interactions between these structures by showing a posterior network that synchronizes through slow oscillations. Moreover, theta cortico-cortical synchronization has been suggested to be a signature of novelty detection in the auditory modality for different states of consciousness across posterior regions (Lee et al., 2019) and when patients are in a minimally conscious state (Bai et al., 2018; Bourdillon et al., 2020). We could therefore extrapolate these results in the visual modality and hypothesize that residual abilities could be assessed by theta synchronization for a mismatch response. In fact, theta synchronization has also been linked to unconscious processing in the visual modality (Hermann et al., 2020; Yanagawa et al., 2013). Importantly, it appears that distinct brain processes are recruited between a lack of subjective visual awareness and blindsight. As a result, we propose that blindsight is unconscious in nature as it is not like conventional near-threshold vision.

Summary

In conclusion, the current investigation examining the neural correlates of unconscious automatic change detection showed that both neurotypical individuals and ML were able to detect the changes in motion direction without being aware of these changes. This was assessed by the presence of a reliable posterior vMMN which was followed by a frontal P3a confirming the detection of change and the automatic aspect of this detection, respectively. Furthermore, confirming the role of theta oscillations in prediction error generation in the auditory modality, we showed significant theta synchronization for the deviant motion stimulus. The prediction error system seems to involve a large-scale network across different frequency bands with an emphasis on the role of high-frequency oscillations. Nonetheless, ML theta posterior connectivity significantly differed from

the neurotypical individuals as increased synchronization was observed suggesting that blindsight is different from near-threshold vision. Thus, we interpret these modulations as potential neural correlates of unconscious processing. Importantly, this study sheds new light on the neurological substrates supporting unconscious processing providing a new framework for assessing blindsight abilities independent of behavior.

Proposing a rehabilitation strategy using a video game approach to enhance visual residual abilities in cortical blindness

This section discusses the potential contributions provided by the fifth study: article 5, **chapter 7**.

Brief description of the training's storyline

Study 5 is a methodological paper describing a training that was developed in a video game approach and that is ready to be used by participants and patients with CB on any computer. All configuration details are described in the study. Here's a quick rundown of the game's description: The goal of the proposed game is to successfully shoot enemy spaceships while avoiding black holes and meteorite rains during intergalactic travels. The game takes place in space, providing the high contrast essential for patients to do well in the early levels of the game, understanding that high contrast improves visual acuity. At all times, four arrows (left, up, down, and right) will be shown at the top of the screen, indicating the four directions that must be distinguished. A red crosshair will be used by the patient to fire and aim at hostile spacecraft. The stimuli's characteristics are based on the findings of prior laboratory investigations (Das and Huxlin, 2010; Huxlin, 2008; Huxlin et al., 2009)**.** The recommended training is anticipated to take 3 months, with one hour One game lasts 20 minutes with breaks every 5 minutes. Training is anticipated to last 3 months, with 5 days of training per week and 1 hour per day resulting in a training of 60 hours. All data will be recorded and used to assess the performance and reaction times of each patient throughout the training.

The benefits and drawbacks of perceptual training

Thus, even though we utilize the benefices of video games, which we will discuss later on, the rehabilitation strategy we propose in this study is based on principles of perceptual training (PT) (Latham et al., 2013) and combines (1) a multisensory training that targets several cognitive processes, such as audiovisual facilitation, visual exploration, and localization, and audio-motor coordination via saccades (Bolognini et al., 2005), and (2) a visual restitution training with a dual paradigm and feedback on performance using motion stimuli, spatial and temporal Gabor patches which stimulated the hemifield at different locations (Das et al., 2014). The key to the feedback technique is to use a dual-paradigm recognized in perceptual learning to elicit a generalization of learning (Xiao et al., 2008). By dual paradigm, we refer here to learning that is both stimulus property and stimulus feature specific and learning that is not stimulus attribute specific, e.g., target position. While we previously discussed the neurophysiological rationale for using both types of training, this part will explain why we suggest a methodological approach based on video game research to improve visual residual abilities.

The improvement of sensorimotor and attentional deficits by PT may have a significant influence on the prognosis following neurological lesions, particularly following visual cortex lesions that cause contralateral cortical blindness (Latham et al., 2013). The use of learning principles is required for the establishment of an effective PT capable of specifically targeting sensorimotor and attentional deficits caused by a neurological injury (Oei and Patterson, 2015; Sabel et al., 2011; Saionz et al., 2020). One critical element to consider in PT is that while attention is not required for learning, it does have the capacity for sensory plasticity, even in the absence of visual awareness (Watanabe et al., 2002). As we theoretically proposed previously, the PT in our rehabilitation strategy should aim to enhance bottom-up and top-down synchronization through a global workspace network by using a combination of bottom-up multisensory and top-down visual restitution training. Although the high specificity of the PT, in terms of the attributes and stimuli characteristics, allows for better targeting of deficits and makes this technique indispensable in rehabilitation (Matteo et al., 2016; Poggel et al., 2004; Saionz et al., 2020), this advantage also comes at the expense of a lack of transfer, which can be compensated for by combining the PT with a video game (VG) approach. The latter is known for being less specific, more motivating, and entertaining, allowing for a greater generalization of improvements at the level of various cognitive processes (Baniqued et al., 2014; Oei and Patterson, 2014; Zhang et al., 2017). Therefore,

while PT can precisely target the deficits observed in CB, an approach combining PT and VG as proposed in this study might help enhance visual rehabilitation in CB on a large neuronal scale by targeting multiple cognitive mechanisms. To support this assertion, we will emphasize the directing lines that show the benefits that VG may offer to our rehabilitation plan.

The contribution of video games

Green and Bavelier's work (Green and Bavelier, 2003, 2006a, 2006b) has focused on the impact of action VG on a variety of attentional tests (tests of flanking and enumeration), on attentional distribution in the visual space (UFOV, attentional blink) and on the ability to follow multiple objects at the same time. They have demonstrated, via their various paradigms, an improvement in the perception of visual sensory attributes such as contrast sensitivity, as well as an increase in the perimetry of central and peripheral visual fields. Indeed, combined strategies are known to improve sensory, perceptual, and attentional abilities, resulting in faster information processing. The perceptual improvement associated with bottom-up processes and the expansion of attentional resources is caused by the fact that these action VG need the pursuit of many objects, fast attentional switches, and peripheral vision training (Green and Bavelier, 2003, 2006a, 2006b). By integrating and covering these processes that are critical in perceptual learning in the training we proposed in study 5 of this thesis, we hope to potentiate the effect of rehabilitation in CB. Furthermore, action VG provides benefits related to the improvement of multisensory perception (Donohue et al., 2010) as exploited by the training in our proposed training and allows for an increase in perceptual sensitivity for low-salience stimuli in a noisy environment (Whitton et al., 2014). It is worth noting at this point that better implicit detection has been demonstrated among VG players in a priming task in which masked animal pictures were presented for 20 ms after a congruent or incongruent image (Pohl et al., 2014). Interestingly, the collaboration of newer strategies combining a cognitive and video game approach appears to be promising because it improves perceptual speed which correlates with the white matter in the hippocampus (Ray et al., 2017), and facilitates the effect of perceptual learning by increasing the connectivity of higher-level hierarchies, and this, early in the training process (Kim et al., 2015).

Summary

In summary, the effect of perceptual training has the disadvantage of being sensitive to perceptual interferences, where a change during training prevents the beneficial effect of learning, whereas VG players are less sensitive to these interferences since learning is more strongly and quickly consolidated (Berard et al., 2015). As a result, there is a clear advantage to transforming perceptual learning approaches into video games, in order to transition from highly specific training to more general training and ensure improvements in contrast sensitivity, central and peripheral visual acuity, and contrast threshold (Deveau et al., 2014). Thus, by proposing this new methodological approach based on video game research to improve visual residual abilities, we hope for reinforcement of cognitive processes, especially motivational, by directing attention to high specific stimuli and using a feedback system.

8.3. Implications, Limitations, and Future Directions

Implications

This thesis framed the debates around blindsight and addressed them with methodological advances and novel methods in order to characterize the underlying neural mechanisms of blindsight at both small and large scales. The investigation of patients with V1 lesions presenting unique residual abilities in their blind hemifields made such an endeavor possible. While underestimated in the ‘era of big data, the study of case reports paired with new methodological standards is essential for comprehending particular challenges since they provide direct access to a specific mechanism, such as unconsciousness. In the first chapter of this thesis and first study, we raised multiple points on our understanding of blindsight. We proposed to comprehend the existence of unconscious abilities following a V1 lesion by integrating the phenomenology of blindsight into an altered global workspace where local processing was still possible but large-scale global availability was disrupted by an unsynchronized neural network responsible for higher order mechanisms. As we argue, such understanding could have a considerable impact on clinical rehabilitation and the quality of life of patients living with CB. In fact, we propose a novel approach for visual rehabilitation to target and potentiate neural mechanisms at both the local and global

scale which is theoretically explained in **study 1** and methodologically documented in **study 5**. In other words, we argue that understanding the neural mechanisms of blindsight is critical for theories of consciousness and unconsciousness, as well as therapeutic treatments. In reality, the consciousness literature seeks to extract the brain correlates of consciousness by contrasting them with the neural correlates of unconsciousness (Mashour and Hudetz, 2018; Melloni et al., 2021; Sohn, 2019), but it is frequently met with dependencies and biases in the behavioral evaluation of what is seen and what is unseen (Peters et al., 2017; Soto et al., 2019; Tsuchiya et al., 2015). Grasping unconsciousness can also be challenging in patients with CB since only a few appear to have residual abilities, which is why we propose employing an objective assessment of unconscious abilities that might eventually be used to determine the optimal rehabilitation strategy for each patient. We, therefore, lay the concerns surrounding the behavioral and objective assessments of blindsight, its subcortical neural pathways, and its temporal dynamics.

To address these points, this Ph.D. work presented three empirical studies (**studies 2**, **3,** and **4**) reporting the cases of patients SJ with type I blindsight for affective natural complex scenes and ML with type II blindsight for motion stimuli. The two studies on SJ had the advantage of using new standards in MEG analysis in order to probe the neural substrates supporting his unique abilities. The study investigating ML's neural mechanisms using EEG had the advantage to include a group of neurotypical individuals to assess the validity of a neural biomarker of unconscious processing in normal and altered vision. As a result of these procedures, we were able to address certain open debates in the blindsight literature. In fact, **study 2** addressed the question of the existence and characteristics of a fast thalamo-amygdala pathway in affective blindsight by studying causal connectivity under the scope of gamma oscillations. **Study 3** provided new inputs into the early vs. late debate on consciousness by assessing the subcortical neural mechanisms in affective blindsight using the evoked responses, temporal generalization analysis, and causal connectivity. Finally, by analyzing the neural substrates of the vMMN and establishing its validity as a neural biomarker of unconscious processing, **study 4** could have a direct influence on how we may identify blindsight in a patient independent of behavior and therefore use targeted rehabilitation. Insightfully, the empirical findings provided a fresh understanding of the brain mechanisms sustaining residual abilities following a V1 injury. To understand the thorough implications of our studies, we will now clarify how the testing of unique blindsight patients and

the application of methodological breakthroughs in electrophysiology enabled us to revisit some notions and answer our specific questions.

Studies 2 and **3** provided the opportunity to test a new case of affective blindsight assessed in patient SJ who suffered from a left complete HH with no macular sparing following a complete resection of his right striate cortex leaving him with no visual awareness. SJ presented the unique ability to discriminate affective natural scenes which were impressive considering the complexity of these scenes and is, to our knowledge, the first reported patient to have such exceptional residual abilities (Celeghin et al., 2015, 2017). Our results were solidified by the differences in RTs across conditions showing real processing of affective scenes. Thus, the study of patient SJ has a clear impact on the affective blindsight literature as we were able to identify the subcortical neural substrates that supported his behavior. The source reconstruction methods of SJ's MEG data used in the second and third studies allowed us to extract the temporal and spectral activity across time within deep structures providing our research with very rich data of high temporal, spatial and spectral precision (Meunier et al., 2020). Using this complex signal across trials, we tackled a single-trial analysis approach using causal connectivity and machine learning as the research on the subcortical temporal dynamics involved in unconsciousness is scarce.

In fact, we computed the single trial causal connectivity as well as the difference in the directionality of the influences between conditions (Bastin et al., 2017). This analysis showed that fast thalamo-amygdala and thalamo-extra-striate pathways subserve the ability to accurately identify complex scenes without visual awareness after a V1 lesion. Interestingly, these fast unconscious thalamic pathways guided by high-frequency oscillations were not specific to an affective condition but rather to the unconscious aspect of the processing shedding light on the hypothesis of a fast 'low road' between the human thalamus and the amygdala that is only specific to negative emotions (Liu et al., 2015; Luo et al., 2007; Morris et al., 1999). Nonetheless, the evoked analysis in **study 3** notably provided insights into the advantage of negative stimuli as the thalamus quickly responded to unpleasant peripheral pictures presented in the blind hemifield. Therefore, the evoked response and connectivity analysis should be used conjointly as it provides different information. Moreover, we found that at a later time window the affective information is transmitted by the direction of the causal connectivity between the thalamus and amygdala. Thus,

unpleasant and pleasant information travel using the same path, yet in opposite directions. This distinction was interpreted as explaining the better performance for pleasant unseen pictures and faster RTs for unpleasant unseen pictures. In fact, all of these connectivity features were predictive of SJ's behavior as assessed by linear regression, which demonstration was lacking in the literature. Predicting behavior could be of great interest when trying to objectively evaluate blindsight abilities in concert with behavioral and subjective assessments. Therefore, the present work provides considerable insights not only for the blindsight literature but also for the comprehension of human thalamic connectivity involved in unconscious perception.

Predictive analyses using classical statistics are of great use, however, machine learning approaches can extract additional and complementary information within the complexity of the neural data (De Lucia and Tzovara, 2015; Savage, 2019). For instance, in **study 3**, we used a multi-feature machine learning approach where the temporal information across all trials recorded from each node within a region was given to the predictive model in order to recognize, at each instant, a specific pattern. We furthermore tested the performance of the classifier trained at a specific point in time on subsequent instants to assess whether the information in the future could be predicted from past information (Dehaene & King, 2016; King & Dehaene, 2014). This approach used to identify the neural correlates of conscious and unconscious perception in neurotypical individuals (King et al., 2016; Sergent and Dehaene, 2004; Sohn, 2019; Soto et al., 2019) could bring new insights into the blindsight literature. In fact, the predictive model could identify a conscious and unconscious process without the need to assess behavior, and thus could be suggested as an objective measure of residual abilities. Therefore, using this approach combined with source reconstruction, the algorithm was able to extract the temporal signature for seen and unseen information confirming its potential implication in the assessment of blindsight in patients with CB. Specifically, the prediction model was applied to data from the thalamus and amygdala, demonstrating that conscious and unconscious perception is mediated by distinct subcortical mechanisms. These results combined with a classical approach to assess evoked responses provided some insights into the early and late debate of consciousness by showing that seen information is more strongly maintained in time even in subcortical structures.

While the work on SJ exploited his rare abilities and assessed the underlying neural correlates to comprehend affective blindsight, the majority of patients with CB tested on behavioral paradigms do not exhibit any sign of residual abilities in their blind field. In **study 4**, we had the opportunity to test blindsight patient ML whose residual abilities we previously reported is able to detect motion (Tran et al., 2019) but is unable to discriminate between motion directions as assessed by a classical forced-choice paradigm. Nonetheless, it is reasonable to believe that ML preserved unconscious abilities for discriminating motion changes that our experimental design failed to assess. This hypothesis laid the groundwork for using changes in motion direction in a protocol designed to induce a vMMN. In fact, the vMMN, an electrophysiological component independent of behavior that can be measured when the brain automatically detects an unexpected change in a passive oddball, has been recently linked with unconscious processing in neurotypical subjects (Chen et al., 2020). One difficulty with such a claim is ensuring that the stimuli are not seen by the participants which were tested in this work on a neurotypical group and ML using a new paradigm. Thus, we successfully addressed this methodological challenge as we measured a reliable vMMN without any subjective report by both the neurotypical group and ML demonstrating that the brain detected the shift in motion direction unconsciously. These findings are significant as they imply the value of the vMMN as a neural biomarker of unconscious processing independent of behavior. Therefore, this study could have a direct implication for the development of an experimental and clinical tool to assess unconscious processing for intact and altered vision.

In fact, the objective neurophysiological measure of unconscious processing in patients with CB could be used prior to and after visual rehabilitation training in order to assess the subsequent neural changes. Importantly, from a clinical point of view, lesions of V1 are very frequent and unfortunately significantly reduce the quality of life of patients living with CB. Hence, determining a method to evaluate their unconscious abilities and target an optimal rehabilitation strategy is critical. To that end, **study 5** offers a novel video-game-based training that combines multisensory compensation training (Huxlin et al., 2009) and visual restitution training (Làdavas, 2008) in a dynamic and compelling environment in order to enhance neural systems that facilitate unconscious processing. We expect that by doing so, we can achieve improved synchronization across neural networks, which would improve perception and perhaps restore vision in the blind region. Taken as a whole, this thesis advocates for the use of methodological advances to

understand and target the neurophysiological substrates underlying blindsight, which might allow future studies to build efficient therapeutic tools and multimodal rehabilitation trainings.

Limitations

To improve future empirical studies and clinical trials, it is necessary to identify the limitations of this thesis so that they may be taken into consideration in future studies. One of the general limitations is that blindsight was framed within the global workspace hypothesis, but as previously stated, various theories might account for unconscious and conscious processing, leading to several debates in the consciousness literature. Our decision to focus largely on the global workplace theory, which prompted the rationale for **study 1**, was meant to facilitate comprehension by employing a consistent framework throughout this dissertation. However, the 'conscious problem' has generated multiple streams of research. The neural correlates of consciousness and unconsciousness could be comprehended not only through a global neuronal workspace (Baars, 1988, 2002; Dehaene and Changeux, 2011; Dehaene et al., 1998) but also through local activation of sensory areas (Boly et al., 2017; Koch et al., 2016). Other explanations include integration of the experience and structure (Tononi et al., 2016) and neuronal recurrent amplification (Aru et al., 2020; Heeger and Zemlianova, 2020; Lamme and Roelfsema, 2000), while others support an integrative view (Brown et al., 2019). This integrative viewpoint is appealing considering that consciousness is complex in nature (Doerig et al., 2020; Melloni et al., 2021). In fact, it may emerge from numerous neural processes that appear at first look contradictory but that are in reality complementary, as it was suggested by the findings of our empirical investigations. As a result, in future designs, we should stress a coherent integrative approach to framing blindsight.

Another limitation that should be considered in our doctorate work was that we only reported on the cases of two patients. This was due to the fact that we had strict criteria for selecting individuals since we knew we wanted to exploit new approaches and needed robust blindsight models which are very rare. Indeed, our patient selection criteria were notably (1) the nature and extent of the lesion as we aimed for patients with a complete resection of V1 resulting in a HH with no macular sparing, and (2) the presence of exceptional unconscious abilities. Nonetheless, interpreting results from these case studies could be limited in terms of interpretation and generalization to other patients or regarding unconscious processing in neurotypical individuals.

One example is the behavioral and neural differences that can be found between patients with left and right lesions (Bertini et al., 2019; Cecere et al., 2013). As a result, future research should incorporate both single-subject and group analyses to better understand the impact of specific lesions on the neural pathways sustaining residual abilities and the benefits obtained from visual rehabilitation.

Specific methodological limitations can also be identified throughout this work. For instance, in **studies 2** and **3**, a subjective assessment after each trial by using the perceptual scale of awareness (Mazzi et al., 2016; Overgaard et al., 2008) discussed in study 1 would have provided either (1) a subjective dimension to the analysis or (2) a clear assessment that SJ didn't preserve any subjective awareness as we hypothesized in the study. In fact, prior to the task we tested SJ on multiple trials and asked him to tell us whether he had any feeling of something happening in his blind hemifield. His answer was always negative which allowed us to perform the protocol without a subjective assessment after each trial as it would have significantly increased the number of trials required and the duration of the task. In the same order of idea, it would have been useful to have increased the number of trials for each condition in the experiment as it would have given us statistical leverage. Moreover, as discussed in **study 2**, pictures presented in paracentral vision within one hemifield potentially triggered involuntary microsaccades suggested by the power analysis (Yuval-Greenberg et al., 2008). However, the performance in his blind hemifield revealed that these microsaccades didn't lead to better or faster discrimination for paracentral pictures compared to peripheral pictures. Therefore, we were confident that the paracentral pictures in his blind hemifield were not perceived.

In **study 3**, we focused on decoding seen and unseen pictures presented in the left and right hemifields which required taking into consideration the laterality of the presentation as well as the difference in awareness between both hemifields when interpreting our results. Besides, the intact hemifield of SJ may be different from what is observed in neurotypical individuals which hypothesis could be investigated by comparing the findings with a group study (Guo et al., 2014; Mikellidou et al., 2019). Therefore, we controlled for both variables by comparing the results between eccentricities within the left and right hemifields for conscious and unconscious processing, respectively. Fortunately enough, our findings regarding seen and unseen processes were comparable to other studies reporting evoked responses (Bodis-Wollner et al., 1992; Kavcic

et al., 2015; Klimesch, 2011; Di Russo et al., 2002) and temporal generalization results (Dehaene and King, 2016; King et al., 2016; Salti et al., 2015b; Soto et al., 2019). The analysis within hemifields and similarity with previous reports allowed us to identify and distinguish the effect of laterality of the presentation and awareness for further interpretations. Finally, some might argue that MEG and source reconstruction do not provide the spatial resolution to assess activity in subcortical structures, however, there is significant evidence that MEG can be used to evaluate activity in subcortical structures, including the thalamus (Lithari et al., 2015; Liu et al., 2015; Luo et al., 2007; Roux et al., 2013) and the amygdala (Balderston et al., 2013; Bayle et al., 2009; Cornwell et al., 2008; Dumas et al., 2013; Luo et al., 2010; Pizzo et al., 2019).

The main limitation in **study 4** concerns the striking difference in the spectral profile of the vMMN when comparing the left and right hemifields of the neurotypical group which was attributed to a motor and attentional effect. In fact, the connections revealed increased connectivity between motor areas and other regions when the left hemifield was stimulated as participants were asked to use their contralateral hand, i.e. right hand, to perform the task (Pool et al., 2014). Therefore, there was a considerable bias linked to the use of the right hand which should be controlled in further studies by having participants use their right and left hand in distinct experimental blocks. After further investigations, we also associated this asymmetry with differences in attentional recruitment between the left and right hemifields where attentional recruitment seems to be prioritized within the left hemifield (Müller et al., 1998). In fact, a dominance of the left hemifield has been shown in visuospatial perception in the absence of visual awareness (Cavézian et al., 2010, 2015; Chokron et al., 2019; Fayel et al., 2014; Sanchez-Lopez et al., 2020). These observations emphasize the importance to have an additional task that can allow contrasting the attentional recruitment within both hemifields from the vMMN.

Finally, **study 5** provided the methodology for a potential rehabilitation strategy combining two well-known rehabilitation strategies, i.e. compensation (Huxlin et al., 2009) and restitution (Làdavas, 2008), into a video game to enhance perceptual abilities (Whitton et al., 2014). Moving forward, the proposed training must be validated on a group of neurotypical people and CB patients to determine its practicality, efficiency, needed length, effect on transfer learning, and motivating component. Furthermore, the game as it is presently designed is extremely minimal and has to be enhanced in terms of design. Nonetheless, these genuine basic elements will allow us to determine

how each training feature influences behavior in order to understand how to optimize the game, which may then lead to investing in enhancing the aesthetics and user experience, providing a home-based video game restoration training for CB. While the drawbacks of a possible video game for visual rehabilitation include the inability to control for variables as effectively as in a laboratory setting, it'll have a greater clinical impact as it will be more accessible, engaging, motivating, and will offer a flexible environment (Deveau et al., 2014).

Future Directions

We hope that the studies presented in this thesis highlight the relevance of case reports and lead the way to the development of systematic clinical protocols targeted for patients with CB that could potentially be offered in the subacute phase, i.e. six months post-lesion, while plasticity is optimal (Saionz et al., 2020). In order to offer a targeted intervention, one future direction that can be taken as a result of this Ph.D. work should be aimed at improving the video game and assessing its efficiency in sight restoration. In other words, will it be possible to enhance visual consciousness within the blind field of a patient with CB using a video game? Providing an answer to such a question requires the need to understand the neural substrates supporting consciousness and unconsciousness. Therefore, we propose to combine both the empirical work on consciousness and the establishment of clinical interventions by building a predictive model that can identify the neural substrates that best predict sight restoration to target these mechanisms and optimize visual rehabilitation. As we identified some neural substrates of blindsight in our studies, we suggest that the model include behavioral and single-trial electrophysiological measures with high temporal resolution extracted at the source level, such as the evoked responses, power, causal and spectral connectivity, and the vMMN. Anatomical and functional magnetic resonance imaging assessments should also be integrated into the model for higher spatial resolution. Specifically, each extracted information could be concatenated into a vector in order to perform multi-feature machine learning analyses and identify the best predictors of sight restoration. In other words, a breakthrough needs to be made and future blindsight research should converge a translational work by taking a multimodal approach that combines empirical and clinical dimensions while leveraging advances in machine learning. Such an achievement will promote comprehension of visual consciousness and optimization of visual rehabilitation strategies within a single framework.

Moreover, to conserve the richness and complexity of the data recorded from each patient, we advise future studies to combine the usual group study with the single-subject approach and compare the results between each patient within the scope of the same research. Importantly, patients with delimited lesions or stroke and patients with or without blindsight are needed to understand the impact of lesion extent, age of onset, and blindness duration on visual recovery, which might lead to better prognostic. Other avenues to sight restoration include the potential use of neuromodulation (Alber et al., 2017; Gall et al., 2015; Plow et al., 2011) and pharmacological interventions (Gratton et al., 2017) combined with visual rehabilitation.

8.4. Conclusion

This Ph.D. work is framed around an empirical and clinical perspective aiming to contribute to blindsight research by demonstrating the significance of using novel methods at both poles. In fact, the main objective was to shed light on the importance of assessing the neurophysiological correlates of unconscious processing by bringing a new degree of integration between empirical findings and therapeutic goals. Thus, through empirical electrophysiological observations using advanced or novel methods, we addressed open debates on conscious and unconscious perception by bringing insights into the neural correlates and biomarkers of blindsight. Clinically, this thesis might set new benchmarks for assessing residual skills, addressing underlying brain processes, and designing more specific and efficient multimodal rehabilitation strategies combining perceptual training and video game principles. Significantly, the studies presented in this work are intended to be part of a lineage of research that has contributed to blindsight research via their discoveries on case reports as they have profoundly inspired the rationale of this thesis.

Références Bibliographiques

Ajina, S., and Bridge, H. (2017). Blindsight and Unconscious Vision: What They Teach Us about the Human Visual System. Neuroscientist 23.

Ajina, S., and Bridge, H. (2019). Subcortical pathways to extrastriate visual cortex underlie residual vision following bilateral damage to V1. Neuropsychologia 128.

Ajina, S., Kennard, C., Rees, G., and Bridge, H. (2014). Motion area V5/MT+ response to global motion in the absence of V1 resembles early visual cortex. Brain 1–15.

Ajina, S., Pestilli, F., Rokem, A., Kennard, C., and Bridge, H. (2015). Human blindsight is mediated by an intact geniculo-extrastriate pathway. Elife 4, e08935.

Alber, R., Moser, H., Gall, C., and Sabel, B.A. (2017). Combined Transcranial Direct Current Stimulation and Vision Restoration Training in Subacute Stroke Rehabilitation: A Pilot Study. PM&R.

Alexander, I., and Cowey, A. (2009). The cortical basis of global motion detection in blindsight. Exp. Brain Res. 192, 407–411.

Allison, T., Puce, A., and McCarthy, G. (2000). Social perception from visual cues: Role of the STS region. Trends Cogn. Sci. 4, 267–278.

Alvarado, J.C., Stanford, T.R., Vaughan, J.W., and Stein, B.E. (2007). Cortex mediates multisensory but not unisensory integration in superior colliculus. J. Neurosci. 27, 12775–12786.

Alvarado, J.C., Rowland, B.A., Stanford, T.R., and Stein, B.E. (2008). A neural network model of multisensory integration also accounts for unisensory integration in superior colliculus. Brain Res. 1242, 13–23.

Anderson, A.K., Christoff, K., Panitz, D., De Rosa, E., and Gabrieli, J.D.E. (2003). Neural correlates of the automatic processing of threat facial signals. J. Neurosci. 23, 5627–5633.

Andino, S.L.G., Menendez, R.G. de P., Khateb, A., Landis, T., and Pegna, A.J. (2009). Electrophysiological correlates of affective blindsight. Neuroimage 44, 581–589.

Arcaro, M.J., Pinsk, M.A., and Kastner, S. (2015). The Anatomical and Functional Organization of the Human Visual Pulvinar. J. Neurosci. 35, 9848–9871.

Arden, G.B., Wolf, J.E., and Messiter, C. (2003). Electrical activity in visual cortex associated with combined auditory and visual stimulation in temporal sequences known to be associated with a visual illusion. Vision Res. 43, 2469–2478.

Aru, J., and Bachmann, T. (2009). Occipital EEG correlates of conscious awareness when subjective target shine-through and effective visual masking are compared: Bifocal early increase in gamma power and speed-up of P1. Brain Res. 1271, 60–73.

Aru, J., Suzuki, M., and Larkum, M.E. (2020). Cellular Mechanisms of Conscious Processing. Trends Cogn. Sci. 24, 814–825.

Azzopardi, P., and Cowey, A. (1997). Is blindsight like normal, near-threshold vision? Proc. Natl. Acad. Sci. U. S. A. 94, 14190–14194.

Baars, B.J. (1988). A cognitive theory of consciousness.

Baars, B.J. (2002). The conscious access hypothesis: Origins and recent evidence. Trends Cogn. Sci. 6, 47–52.

Baars, B.J., Franklin, S., and Ramsoy, T.Z. (2013). Global workspace dynamics: cortical "binding and propagation" enables conscious contents. Front. Psychol. 4, 200.

Babiloni, C., Marzano, N., Soricelli, A., Cordone, S., Millàn-Calenti, J.C., Del Percio, C., and Bujàn, A. (2016). Cortical neural synchronization underlies primary visual consciousness of qualia: Evidence from event-related potentials. Front. Hum. Neurosci. 10.

Bai, Y., Xia, X., Wang, Y., Guo, Y., Yang, Y., He, J., and Li, X. (2018). Fronto-parietal coherence response to tDCS modulation in patients with disorders of consciousness. Int. J. Neurosci. 128, 587–594.

Balderston, N.L., Schultz, D.H., Baillet, S., and Helmstetter, F.J. (2013). How to detect amygdala activity with magnetoencephalography using source imaging. J. Vis. Exp.

Baniqued, P.L., Kranz, M.B., Voss, M.W., Lee, H., Cosman, J.D., Severson, J., and Kramer, A.F. (2014). Cognitive training with casual video games: points to consider. Front. Psychol. 4, 1010.

Bastin, J., Deman, P., David, O., Gueguen, M., Benis, D., Minotti, L., Hoffman, D., Combrisson, E., Kujala, J., Perrone-Bertolotti, M., et al. (2017). Direct Recordings from Human Anterior Insula Reveal its Leading Role within the Error-Monitoring Network. Cereb. Cortex 27, 1545–1557.

Bastos, A.M., Vezoli, J., Bosman, C.A., Schoffelen, J.M., Oostenveld, R., Dowdall, J.R., DeWeerd, P., Kennedy, H., and Fries, P. (2015). Visual areas exert feedforward and feedback influences through distinct frequency channels. Neuron 85, 390–401.

Bayle, D.J., Henaff, M.-A., and Krolak-Salmon, P. (2009). Unconsciously perceived fear in peripheral vision alerts the limbic system: a MEG study. PLoS One 4, e8207.

Bayle, D.J., Schoendorff, B., Hénaff, M.-A., and Krolak-Salmon, P. (2011). Emotional facial expression detection in the peripheral visual field. PLoS One 6, e21584.

Bekinschtein, T.A., Dehaene, S., Rohaut, B., Tadel, F., Cohen, L., and Naccache, L. (2009). Neural signature of the conscious processing of auditory regularities. Proc. Natl. Acad. Sci. U. S. A. 106, 1672–1677.

Bell, A.H., Meredith, M.A., Van Opstal, A.J., and Munoz, D.P. (2005). Crossmodal integration in the primate superior colliculus underlying the preparation and initiation of saccadic eye movements. J. Neurophysiol. 93, 3659–3673.

Berard, A. V., Cain, M.S., Watanabe, T., and Sasaki, Y. (2015). Frequent Video Game Players Resist Perceptual Interference. PLoS One 10, e0120011.

Bertini, C., Cecere, R., and Làdavas, E. (2013). I am blind, but I "see" fear. Cortex 49, 985–993.

Bertini, C., Cecere, R., and Làdavas, E. (2017). Unseen fearful faces facilitate visual discrimination in the intact field. Neuropsychologia.

Bertini, C., Cecere, R., and Làdavas, E. (2019). Unseen fearful faces facilitate visual discrimination in the intact field. Neuropsychologia 128, 58–64.

Bettencourt, K.C., and Xu, Y. (2013). The role of transverse occipital sulcus in scene perception and its relationship to object individuation in inferior intraparietal sulcus. J. Cogn. Neurosci. 25, 1711–1722.

Bocchio, M., Nabavi, S., and Capogna, M. (2017). Synaptic Plasticity, Engrams, and Network Oscillations in Amygdala Circuits for Storage and Retrieval of Emotional Memories. Neuron 94, 731–743.

Bodis-Wollner, I., Brannan, J.R., Nicoll, J., Frkovic, S., and Mylin, L.H. (1992). A short latency cortical component of the foveal VEP is revealed by hemifield stimulation. Electroencephalogr. Clin. Neurophysiol. 84, 201–208.

Bogadhi, A.R., Bollimunta, A., Leopold, D.A., and Krauzlis, R.J. (2018). Brain regions modulated during covert visual attention in the macaque. Sci. Rep. 8.

Bogadhi, A.R., Katz, L.N., Bollimunta, A., Leopold, D.A., and Krauzlis, R.J. (2021). Midbrain activity shapes high-level visual properties in the primate temporal cortex. Neuron 109, 690-699.e5.

Bolognini, N., Rasi, F., Coccia, M., and Làdavas, E. (2005). Visual search improvement in hemianopic patients after audio-visual stimulation. Brain 128, 2830–2842.

Boly, M., Massimini, M., Tsuchiya, N., Postle, B.R., Koch, C., and Tononi, G. (2017). Are the neural correlates of consciousness in the front or in the back of the cerebral cortex? Clinical and neuroimaging evidence. J. Neurosci. 37, 9603–9613.

Boucher, O., D'Hondt, F., Tremblay, J., Lepore, F., Lassonde, M., Vannasing, P., Bouthillier, A., and Nguyen, D.K. (2015). Spatiotemporal dynamics of affective picture processing revealed by intracranial high-gamma modulations. Hum. Brain Mapp. 36, 16–28.

Bourdillon, P., Hermann, B., Guénot, M., Bastuji, H., Isnard, J., King, J.R., Sitt, J., and Naccache, L. (2020). Brain-scale cortico-cortical functional connectivity in the delta-theta band is a robust signature of conscious states: an intracranial and scalp EEG study. Sci. Rep. 10.

Bourne, J.A., and Morrone, M.C. (2017). Plasticity of Visual Pathways and Function in the Developing Brain: Is the Pulvinar a Crucial Player? Front. Syst. Neurosci. 11, 3.

Bouwmeester, L., Heutink, J., and Lucas, C. (2007). The effect of visual training for patients with visual field defects due to brain damage: a systematic review. J. Neurol. Neurosurg. Psychiatry 78, 555–564.

Breitmeyer, B.G. (2014). Contributions of magno- and parvocellular channels to conscious and non-conscious vision. Philos. Trans. R. Soc. B Biol. Sci. 369.

Brent, P.J., Kennard, C., and Ruddock, K.H. (1994). Residual colour vision in a human hemianope: spectral responses and colour discrimination. Proc. Biol. Sci. 256, 219–225.

Bridge, H., Thomas, O., Jbabdi, S., and Cowey, A. (2008). Changes in connectivity after visual cortical brain damage underlie altered visual function. Brain 131, 1433–1444.

Bridge, H., Leopold, D.A., and Bourne, J.A. (2016). Adaptive Pulvinar Circuitry Supports Visual Cognition. Trends Cogn. Sci. 20, 146–157.

Brogaard, B. (2011). Are there unconscious perceptual processes? Conscious. Cogn. 20, 449–463.

Brown, L.E., Kroliczak, G., Demonet, J.-F., and Goodale, M.A. (2008). A hand in blindsight: hand placement near target improves size perception in the blind visual field. Neuropsychologia 46, 786–802.

Brown, R., Lau, H., and LeDoux, J.E. (2019). Understanding the Higher-Order Approach to Consciousness. Trends Cogn. Sci. 23, 754–768.

Burra, N., Hervais-Adelman, A., Kerzel, D., Tamietto, M., de Gelder, B., and Pegna, A.J. (2013). Amygdala activation for eye contact despite complete cortical blindness. J. Neurosci. 33, 10483–10489.

Burra, N., Kerzel, D., de Gelder, B., and Pegna, A.J. (2014). Lack of automatic attentional orienting by gaze cues following a bilateral loss of visual cortex. Neuropsychologia 58, 75–80.

Burra, N., Hervais-Adelman, A., Celeghin, A., de Gelder, B., and Pegna, A.J. (2019). Affective blindsight relies on low spatial frequencies. Neuropsychologia 128, 44–49.

Calvert, G.A., Hansen, P.C., Iversen, S.D., and Brammer, M.J. (2001). Detection of audio-visual integration sites in humans by application of electrophysiological criteria to the BOLD effect. Neuroimage 14, 427–438.

Calvo, M.G., Beltrán, D., and Fernández-Martín, A. (2014). Processing of facial expressions in peripheral vision: Neurophysiological evidence. Biol. Psychol. 100, 60–70.

Campana, F., Rebollo, I., Urai, A., Wyart, V., and Tallon-Baudry, C. (2016). Conscious Vision Proceeds from Global to Local Content in Goal-Directed Tasks and Spontaneous Vision. J. Neurosci. 36, 5200–5213.

Cavanaugh, M.R., Barbot, A., Carrasco, M., and Huxlin, K.R. (2019). Feature-based attention potentiates recovery of fine direction discrimination in cortically blind patients. Neuropsychologia 128.

Cavézian, C., Gaudry, I., Perez, C., Coubard, O., Doucet, G., Peyrin, C., Marendaz, C., Obadia, M., Gout, O., and Chokron, S. (2010). Specific impairments in visual processing following lesion side in hemianopic patients. Cortex. 46, 1123–1131.

Cavézian, C., Perez, C., Peyrin, C., Gaudry, I., Obadia, M., Gout, O., and Chokron, S. (2015). Hemisphere-dependent ipsilesional deficits in hemianopia: Sightblindness in the “intact” visual field. Cortex. 69, 166–174.

Cecere, R., Bertini, C., and Ladavas, E. (2013). Differential Contribution of Cortical and Subcortical Visual Pathways to the Implicit Processing of Emotional Faces: A tDCS Study. J. Neurosci. 33, 6469–6475.

Cecere, R., Bertini, C., Maier, M.E., and Làdavas, E. (2014). Unseen fearful faces influence face encoding: Evidence from ERPs in hemianopic patients. J. Cogn. Neurosci. 26, 2564–2577.

Celeghin, A., Barabas, M., Mancini, F., Bendini, M., Pedrotti, E., Prior, M., Cantagallo, A., Savazzi, S., and Marzi, C.A. (2015a). Speeded manual responses to unseen visual stimuli in hemianopic patients: what kind of blindsight? Conscious. Cogn. 32, 6–14.

Celeghin, A., de Gelder, B., and Tamietto, M. (2015b). From affective blindsight to emotional consciousness. Conscious. Cogn. 36, 414–425.

Celeghin, A., Diano, M., Bagnis, A., Viola, M., and Tamietto, M. (2017). Basic Emotions in Human Neuroscience: Neuroimaging and Beyond. Front. Psychol. 8, 1432.

Chao, Z.C., Takaura, K., Wang, L., Fujii, N., and Dehaene, S. (2018). Large-Scale Cortical Networks for Hierarchical Prediction and Prediction Error in the Primate Brain. Neuron 100, 1252-1266.e3.

Chaumillon, R., Blouin, J., and Guillaume, A. (2018). Interhemispheric Transfer Time Asymmetry of Visual Information Depends on Eye Dominance: An Electrophysiological Study. Front. Neurosci. 12, 72.

Chen, B., Sun, P., and Fu, S. (2020). Consciousness modulates the automatic change detection of masked emotional faces: Evidence from visual mismatch negativity. Neuropsychologia 144, 107459.

Chokron, S., Perez, C., Obadia, M., Gaudry, I., Laloum, L., and Gout, O. (2008). From blindsight to sight: cognitive rehabilitation of visual field defects. Restor. Neurol. Neurosci. 26, 305–320.

Chokron, S., Peyrin, C., and Perez, C. (2019). Ipsilesional deficit of selective attention in left homonymous hemianopia and left unilateral spatial neglect. Neuropsychologia 128.

Claeys, K.G., Lindsey, D.T., De Schutter, E., and Orban, G.A. (2003). A higher order motion region in human inferior parietal lobule: evidence from fMRI. Neuron 40, 631–642.

Codispoti, M., Ferrari, V., De Cesarei, A., and Cardinale, R. (2006). Implicit and explicit categorization of natural scenes. In Progress in Brain Research, pp. 53–65.

Combs, L.A., and Polich, J. (2006). P3a from auditory white noise stimuli. Clin. Neurophysiol. 117, 1106–1112.

Comerchero, M.D., and Polich, J. (1998). P3a, perceptual distinctiveness, and stimulus modality. Cogn. Brain Res. 7, 41–48.

Corbetta, M., Patel, G., and Shulman, G.L. (2008). The Reorienting System of the Human Brain: From Environment to Theory of Mind. Neuron 58, 306–324.

Corneil, B.D., Van Wanrooij, M., Munoz, D.P., and Van Opstal, A.J. (2002). Auditory-visual interactions subserving goal-directed saccades in a complex scene. J. Neurophysiol. 88, 438–454.

Cornwell, B.R., Carver, F.W., Coppola, R., Johnson, L., Alvarez, R., and Grillon, C. (2008). Evoked amygdala responses to negative faces revealed by adaptive MEG beamformers. Brain Res. 1244, 103–112.

D'Hondt, F., Lassonde, M., Collignon, O., Lepore, F., Honoré, J., and Sequeira, H. (2013). "Emotions Guide Us": Behavioral and MEG correlates. Cortex 49, 2473–2483.

Danckert, J., and Goodale, M. a. (2000). Blindsight: A conscious route to unconscious vision. Curr. Biol. 10, R64–R67.

Danckert, J., and Rossetti, Y. (2005). Blindsight in action: what can the different sub-types of blindsight tell us about the control of visually guided actions? Neurosci. Biobehav. Rev. 29, 1035–1046.

Danckert, J., Revol, P., Pisella, L., Krolak-Salmon, P., Vighetto, A., Goodale, M.A., and Rossetti, Y. (2003). Measuring unconscious actions in action-blindsight: exploring the kinematics of pointing movements to targets in the blind field of two patients with cortical hemianopia. Neuropsychologia 41, 1068–1081.

Das, A., and Huxlin, K.R. (2010). New approaches to visual rehabilitation for cortical blindness: outcomes and putative mechanisms. Neuroscientist 16, 374–387.

Das, A., Tadin, D., and Huxlin, K.R. (2014). Beyond blindsight: properties of visual relearning in cortically blind fields. J. Neurosci. 34, 11652–11664.

Day-Brown, J.D., Wei, H., Chomsung, R.D., Petry, H.M., and Bickford, M.E. (2010). Pulvinar projections to the striatum and amygdala in the tree shrew. Front. Neuroanat. 4, 143.

Deco, G., Vidaurre, D., and Kringelbach, M.L. (2021). Revisiting the global workspace orchestrating the hierarchical organization of the human brain. Nat. Hum. Behav. 2021 54 5, 497–511.

Dehaene, S., and Changeux, J.-P. (2011). Experimental and theoretical approaches to conscious processing. Neuron 70, 200–227.

Dehaene, S., and Changeux, J.P. (2005). Ongoing spontaneous activity controls access to consciousness: A neuronal model for inattentional blindness. PLoS Biol. 3, 0910–0927.

Dehaene, S., and King, J.R. (2016). Decoding the dynamics of conscious perception: The temporal generalization method. In Research and Perspectives in Neurosciences, (Springer Verlag), pp. 85–97.

Dehaene, S., Kerszberg, M., and Changeux, J.P. (1998). A neuronal model of a global workspace in effortful cognitive tasks. Proc. Natl. Acad. Sci. U. S. A. 95, 14529–14534.

Dehaene, S., Sergent, C., and Changeux, J.-P. (2003a). A neuronal network model linking subjective reports and objective physiological data during conscious perception. Proc. Natl. Acad. Sci. U. S. A. 100, 8520–8525.

Dehaene, S., Sergent, C., and Changeux, J.P. (2003b). A neuronal network model linking subjective reports and objective physiological data during conscious perception. Proc. Natl. Acad. Sci. U. S. A. 100, 8520–8525.

Dehaene, S., Changeux, J.P., Naccache, L., Sackur, J., and Sergent, C. (2006). Conscious, preconscious, and subliminal processing: a testable taxonomy. Trends Cogn. Sci. 10, 204–211.

Deveau, J., Lovcik, G., and Seitz, A.R. (2014). Broad-based visual benefits from training with an integrated perceptual-learning video game. Vision Res. 99, 134–140.

Doerig, A., Schurger, A., and Herzog, M.H. (2020). Hard criteria for empirical theories of consciousness. Cogn. Neurosci. 12, 1–22.

Doesburg, S.M., Green, J.J., McDonald, J.J., and Ward, L.M. (2009). Rhythms of consciousness: binocular rivalry reveals large-scale oscillatory network dynamics mediating visual perception. PLoS One 4, e6142.

Donohue, S.E., Woldorff, M.G., and Mitroff, S.R. (2010). Video game players show more precise multisensory temporal processing abilities. Atten. Percept. Psychophys. 72, 1120–1129.

Doubell, T.P., Skaliora, I., Baron, J., and King, A.J. (2003). Functional connectivity between the superficial and deeper layers of the superior colliculus: an anatomical substrate for sensorimotor integration. J. Neurosci. 23, 6596–6607.

Dumas, T., Dubal, S., Attal, Y., Chupin, M., Jouvent, R., Morel, S., and George, N. (2013). MEG Evidence for Dynamic Amygdala Modulations by Gaze and Facial Emotions. PLoS One 8.

Dundon, N.M., Làdavas, E., Maier, M.E., and Bertini, C. (2015). Multisensory stimulation in hemianopic patients boosts orienting responses to the hemianopic field and reduces attentional resources to the intact field. Restor. Neurol. Neurosci. 33, 405–419.

Duquette, J., and Baril, F. (2009). Les interventions de réadaptation visuelle développées à l'intention des personnes ayant une déficience visuelle associée à une condition neurologique. Inst. Nazareth Louis-Braille 15.

Edalati, M., Mahmoudzadeh, M., Safaie, J., Wallois, F., and Moghimi, S. (2021). Violation of rhythmic expectancies can elicit late frontal gamma activity nested in theta oscillations. Psychophysiology.

Engel, A.K., and Singer, W. (2001). Temporal binding and the neural correlates of sensory awareness. Trends Cogn. Sci. 5, 16–25.

Escera, C., Alho, K., Schröger, E., and Winkler, I. (2000). Involuntary attention and distractibility as evaluated with event-related brain potentials. Audiol. Neuro-Otology 5, 151–166.

Fayel, A., Chokron, S., Cavézian, C., Vergilino-Perez, D., Lemoine, C., and Doré-Mazars, K. (2014). Characteristics of contralesional and ipsilesional saccades in hemianopic patients. Exp. Brain Res. 232, 903–917.

Fiebelkorn, I.C., Pinsk, M.A., and Kastner, S. (2018). A Dynamic Interplay within the Frontoparietal Network Underlies Rhythmic Spatial Attention. Neuron 99, 842-853.e8.

Fitzgerald, K., and Todd, J. (2020). Making Sense of Mismatch Negativity. Front. Psychiatry 11.

Förster, J., Koivisto, M., and Revonsuo, A. (2020). ERP and MEG correlates of visual consciousness: The second decade. Conscious. Cogn. 80.

Fox, D.M., Goodale, M.A., and Bourne, J.A. (2020). The Age-Dependent Neural Substrates of Blindsight. Trends Neurosci. 43, 242–252.

Friedman, D., Cycowicz, Y.M., and Gaeta, H. (2001). The novelty P3: An event-related brain potential (ERP) sign of the brain's evaluation of novelty. Neurosci. Biobehav. Rev. 25, 355–373.

Gall, C., Silvennoinen, K., Granata, G., de Rossi, F., Vecchio, F., Brösel, D., Bola, M., Sailer, M., Waleszczyk, W.J., Rossini, P.M., et al. (2015). Non-invasive electric current stimulation for restoration of vision after unilateral occipital stroke. Contemp. Clin. Trials 43, 231–236.

Gallotto, S., Sack, A.T., Schuhmann, T., and de Graaf, T.A. (2017). Oscillatory Correlates of Visual Consciousness. Front. Psychol. 8, 1147.

Garrido, M.I., Barnes, G.R., Sahani, M., and Dolan, R.J. (2012). Functional evidence for a dual route to amygdala. Curr. Biol. 22, 129–134.

de Gelder, B., and Poyo Solanas, M. (2021). A computational neuroethology perspective on body and expression perception. Trends Cogn. Sci.

de Gelder, B., Vroomen, J., Pourtois, G., and Weiskrantz, L. (1999). Non-conscious recognition of affect in the absence of striate cortex. Neuroreport 10, 3759–3763.

Georgy, L., Lewis, J.D., Bezgin, G., Diano, M., Celeghin, A., Evans, A.C., Tamietto, M., and Ptito, A. (2020). Changes in peri-calcarine cortical thickness in blindsight. Neuropsychologia 143.

Gingras, G., Rowland, B.A., and Stein, B.E. (2009). The differing impact of multisensory and unisensory integration on behavior. J. Neurosci. 29, 4897–4902.

Goebel, R., Muckli, L., Zanella, F.E., Singer, W., and Stoerig, P. (2001). Sustained extrastriate cortical activation without visual awareness revealed by fMRI studies of hemianopic patients. In Vision Research, pp. 1459–1474.

Goldstein, A., Spencer, K.M., and Donchin, E. (2002). The influence of stimulus deviance and novelty on the P300 and Novelty P3. Psychophysiology 39, 781–790.

Goodwin, D. (2014). Homonymous hemianopia: Challenges and solutions. Clin. Ophthalmol. 8, 1919–1927.

Goyal, A., Miller, J., Qasim, S.E., Watrous, A.J., Zhang, H., Stein, J.M., Inman, C.S., Gross, R.E., Willie, J.T., Lega, B., et al. (2020). Functionally distinct high and low theta oscillations in the human hippocampus. Nat. Commun. 11.

Grasso, P.A., Làdavas, E., and Bertini, C. (2016). Compensatory Recovery after Multisensory Stimulation in Hemianopic Patients: Behavioral and Neurophysiological Components. Front. Syst. Neurosci. 10, 45.

Gratton, C., Yousef, S., Aarts, E., Wallace, D.L., D'Esposito, M., and Silver, M.A. (2017). Cholinergic, But Not Dopaminergic or Noradrenergic, Enhancement Sharpens Visual Spatial Perception in Humans. J. Neurosci. 37, 4405–4415.

Green, C.S., and Bavelier, D. (2003). Action video game modifies visual selective attention. Nature 423, 534–537.

Green, C.S., and Bavelier, D. (2006a). Effect of action video games on the spatial distribution of visuospatial attention. J. Exp. Psychol. Hum. Percept. Perform. 32, 1465–1478.

Green, C.S., and Bavelier, D. (2006b). Enumeration versus multiple object tracking: the case of action video game players. Cognition 101, 217–245.

Guo, X., Jin, Z., Feng, X., and Tong, S. (2014). Enhanced effective connectivity in mild occipital stroke patients with hemianopia. IEEE Trans. Neural Syst. Rehabil. Eng. 22, 1210–1217.

Hadid, V., and Lepore, F. (2017a). Visual mismatch negativity (vMMN): automatic detection change followed by an inhibition of the attentional switch without visual awareness. E. Romero, N. Lepore, J. Brieva, and I. Larrabide, eds. (International Society for Optics and Photonics), p. 101601M.

Hadid, V., and Lepore, F. (2017b). From Cortical Blindness to Conscious Visual Perception: Theories on Neuronal Networks and Visual Training Strategies. Front. Syst. Neurosci. 11, 64.

Harper, J., Malone, S.M., and Iacono, W.G. (2017). Theta- and delta-band EEG network dynamics during a novelty oddball task. Psychophysiology 54, 1590–1605.

Heeger, D.J., and Zemlianova, K.O. (2020). A recurrent circuit implements normalization, simulating the dynamics of V1 activity. Proc. Natl. Acad. Sci. U. S. A. 117, 22494–22505.

Hermann, B., Raimondo, F., Hirsch, L., Huang, Y., Denis-Valente, M., Pérez, P., Engemann, D., Faugeras, F., Weiss, N., Demeret, S., et al. (2020). Combined behavioral and electrophysiological evidence for a direct cortical effect of prefrontal tDCS on disorders of consciousness. Sci. Rep. 10.

Hervais-Adelman, A., Legrand, L.B., Zhan, M., Tamietto, M., de Gelder, B., and Pegna, A.J. (2015). Looming sensitive cortical regions without V1 input: evidence from a patient with bilateral cortical blindness. Front. Integr. Neurosci. 9, 51.

Hillyard, S.A., and Anllo-Vento, L. (1998). Event-related brain potentials in the study of visual selective attention. Proc. Natl. Acad. Sci. 95, 781–787.

Ho, H.T., Burr, D.C., Alais, D., and Morrone, M.C. (2021). Propagation and update of auditory perceptual priors through alpha and theta rhythms. Eur. J. Neurosci.

Höller, Y., Bergmann, J., Kronbichler, M., Crone, J.S., Schmid, E.V., Golaszewski, S., and Ladurner, G. (2011). Preserved oscillatory response but lack of mismatch negativity in patients with disorders of consciousness. Clin. Neurophysiol. 122, 1744–1754.

Hong, X., Sun, J., Wang, J., Li, C., and Tong, S. (2020). Attention-related modulation of frontal midline theta oscillations in cingulate cortex during a spatial cueing Go/NoGo task. Int. J. Psychophysiol. 148, 1–12.

Hung, Y., Smith, M. Lou, Bayle, D.J., Mills, T., Cheyne, D., and Taylor, M.J. (2010). Unattended emotional faces elicit early lateralized amygdala-frontal and fusiform activations. Neuroimage 50, 727–733.

Hurme, M., Koivisto, M., Revonsuo, A., and Railo, H. (2017). Early processing in primary visual cortex is necessary for conscious and unconscious vision while late processing is necessary only for conscious vision in neurologically healthy humans. Neuroimage 150, 230–238.

Hurme, M., Koivisto, M., Revonsuo, A., and Railo, H. (2019). V1 activity during feedforward and early feedback processing is necessary for both conscious and unconscious motion perception. Neuroimage 185.

Huxlin, K.R. (2008). Perceptual plasticity in damaged adult visual systems. Vision Res. 48, 2154–2166.

Huxlin, K.R., Martin, T., Kelly, K., Riley, M., Friedman, D.I., Burgin, W.S., and Hayhoe, M. (2009). Perceptual relearning of complex visual motion after V1 damage in humans. J. Neurosci. 29, 3981–3991.

Jiang, H., Stein, B.E., and McHaffie, J.G. (2015). Multisensory training reverses midbrain lesion-induced changes and ameliorates haemianopia. Nat. Commun. 6, 7263.

John, E.R. (2002). The neurophysics of consciousness. Brain Res. Rev. 39, 1–28.

Johnson, C.M., Peckler, H., Tai, L.H., and Wilbrecht, L. (2016). Rule learning enhances structural plasticity of long-range axons in frontal cortex. Nat. Commun. 7, 1–14.

Karnath, H.O. (2001). New insights into the functions of the superior temporal cortex. Nat. Rev. Neurosci. 2, 568–576.

El Karoui, I., King, J.-R., Sitt, J., Meyniel, F., Van Gaal, S., Hasboun, D., Adam, C., Navarro, V., Baulac, M., Dehaene, S., et al. (2015). Event-Related Potential, Time-frequency, and Functional Connectivity Facets of Local and Global Auditory Novelty Processing: An Intracranial Study in Humans. Cereb. Cortex 25, 4203–4212.

Kasten, E., Guenther, T., and Sabel, B.A. (2008). Inverse stimuli in perimetric performance reveal larger visual field defects: implications for vision restoration. Restor. Neurol. Neurosci. 26, 355–364.

Kato, R., Takaura, K., Ikeda, T., Yoshida, M., and Isa, T. (2011). Contribution of the retino-tectal pathway to visually guided saccades after lesion of the primary visual cortex in monkeys. Eur. J. Neurosci. 33, 1952–1960.

Kavcic, V., Triplett, R.L., Das, A., Martin, T., and Huxlin, K.R. (2015). Role of inter-hemispheric transfer in generating visual evoked potentials in V1-damaged brain hemispheres. Neuropsychologia 68, 82–93.

Kentridge, R.W., Heywood, C.A., and Weiskrantz, L. (1999). Effects of temporal cueing on residual visual discrimination in blindsight. Neuropsychologia 37, 479–483.

Kentridge, R.W., Heywood, C.A., and Weiskrantz, L. (2004). Spatial attention speeds discrimination without awareness in blindsight. Neuropsychologia 42, 831–835.

Kerkhoff, G., Münßinger, U., Haaf, E., Eberle-Strauss, G., and Stögerer, E. (1992). Rehabilitation of homonymous scotomata in patients with postgeniculate damage of the visual system: saccadic compensation training. Restor. Neurol. Neurosci. 4, 245–254.

Van Kerkoerle, T., Self, M.W., Dagnino, B., Gariel-Mathis, M.A., Poort, J., Van Der Togt, C., and Roelfsema, P.R. (2014). Alpha and gamma oscillations characterize feedback and feedforward processing in monkey visual cortex. Proc. Natl. Acad. Sci. U. S. A. 111, 14332–14341.

Kiebel, S.J., Garrido, M.I., Moran, R., Chen, C.-C., and Friston, K.J. (2009). Dynamic causal modeling for EEG and MEG. Hum. Brain Mapp. 30, 1866–1876.

Kim, R.S., Seitz, A.R., and Shams, L. (2008). Benefits of Stimulus Congruency for Multisensory Facilitation of Visual Learning. PLoS One 3, e1532.

Kim, Y.-H., Kang, D.-W., Kim, D., Kim, H.-J., Sasaki, Y., and Watanabe, T. (2015). Real-Time Strategy Video Game Experience and Visual Perceptual Learning. J. Neurosci. 35, 10485–10492.

King, J.R., and Dehaene, S. (2014). Characterizing the dynamics of mental representations: The temporal generalization method. Trends Cogn. Sci. 18, 203–210.

King, J.R., Pescetelli, N., and Dehaene, S. (2016). Brain Mechanisms Underlying the Brief Maintenance of Seen and Unseen Sensory Information. Neuron 92, 1122–1134.

Kinoshita, M., Kato, R., Isa, K., Kobayashi, K., Kobayashi, K., Onoe, H., and Isa, T. (2019). Dissecting the circuit for blindsight to reveal the critical role of pulvinar and superior colliculus. Nat. Commun. 10.

Klimesch, W. (2011). Evoked alpha and early access to the knowledge system: The P1 inhibition timing hypothesis. Brain Res. 1408, 52–71.

Knotts, J.D., Odegaard, B., and Lau, H. (2018). Neuroscience: The Key to Consciousness May Not Be under the Streetlight. Curr. Biol. 28, R749–R752.

Koch, C., Massimini, M., Boly, M., and Tononi, G. (2016). Neural correlates of consciousness: Progress and problems. Nat. Rev. Neurosci. 17, 307–321.

Koivisto, M., and Grassini, S. (2016). Neural processing around 200 ms after stimulus-onset correlates with subjective visual awareness. Neuropsychologia 84, 235–243.

Koivisto, M., Mäntylä, T., and Silvanto, J. (2010). The role of early visual cortex (V1/V2) in conscious and unconscious visual perception. Neuroimage 51, 828–834.

Kok, A. (2001). On the utility of P3 amplitude as a measure of processing capacity. Psychophysiology 38, 557–577.

Koller, K., Rafal, R.D., Platt, A., and Mitchell, N.D. (2019). Orienting toward threat: Contributions of a subcortical pathway transmitting retinal afferents to the amygdala via the superior colliculus and pulvinar. Neuropsychologia 128.

Kranczioch, C., Debener, S., Maye, A., and Engel, A.K. (2007). Temporal dynamics of access to consciousness in the attentional blink. Neuroimage 37, 947–955.

Làdavas, E. (2008). Multisensory-based approach to the recovery of unisensory deficit. Ann. N. Y. Acad. Sci. 1124, 98–110.

Lahnakoski, J.M., Glerean, E., Salmi, J., Jääskeläinen, I.P., Sams, M., Hari, R., and Nummenmaa, L. (2012). Naturalistic fMRI mapping reveals superior temporal sulcus as the hub for the distributed brain network for social perception. Front. Hum. Neurosci. 6.

Lamme, V.A.F. (2018). Challenges for theories of consciousness: Seeing or knowing, the missing ingredient and how to deal with panpsychism. Philos. Trans. R. Soc. B Biol. Sci. 373.

Lamme, V.A.F., and Roelfsema, P.R. (2000). The distinct modes of vision offered by feedforward and recurrent processing. Trends Neurosci. 23, 571–579.

Latham, A.J., Patston, L.L.M., and Tippett, L.J. (2013). The virtual brain: 30 years of video-game play and cognitive abilities. Front. Psychol. 4, 629.

Lau, H.C., and Passingham, R.E. (2006). Relative blindsight in normal observers and the neural correlate of visual consciousness. Proc. Natl. Acad. Sci. U. S. A. 103, 18763–18768.

LeDoux, J.E. (2000). Emotion circuits in the brain. Annu. Rev. Neurosci. 23, 155–184.

Lee, C., Rohrer, W.H., and Sparks, D.L. (1988). Population coding of saccadic eye movements by neurons in the superior colliculus. Nature 332, 357–360.

Lee, M., Baird, B., Gosseries, O., Nieminen, J.O., Boly, M., Postle, B.R., Tononi, G., and Lee, S.W. (2019). Connectivity differences between consciousness and unconsciousness in non-rapid eye movement sleep: a TMS–EEG study. Sci. Rep. 9.

Leh, S.E., Johansen-Berg, H., and Ptito, A. (2006). Unconscious vision: new insights into the neuronal correlate of blindsight using diffusion tractography. Brain 129, 1822–1832.

Leo, F., Bolognini, N., Passamonti, C., Stein, B.E., and Làdavas, E. (2008). Cross-modal localization in hemianopia: new insights on multisensory integration. Brain 131, 855–865.

Leopold, D.A. (2012). Primary visual cortex: awareness and blindsight. Annu. Rev. Neurosci. 35, 91–109.

Lithari, C., Moratti, S., and Weisz, N. (2015). Thalamocortical interactions underlying visual fear conditioning in humans. Hum. Brain Mapp. 36, 4592–4603.

Liu, S., Yu, Q., Tse, P.U., and Cavanagh, P. (2019). Neural Correlates of the Conscious Perception of Visual Location Lie Outside Visual Cortex. Curr. Biol.

Liu, T.-Y., Chen, Y.-S., Hsieh, J.-C., and Chen, L.-F. (2015). Asymmetric engagement of amygdala and its gamma connectivity in early emotional face processing. PLoS One 10, e0115677.

Lou, H.C., Changeux, J.P., and Rosenstand, A. (2017). Towards a cognitive neuroscience of self-awareness. Neurosci. Biobehav. Rev. 83, 765–773.

De Lucia, M., and Tzovara, A. (2015). Decoding auditory EEG responses in healthy and clinical populations: A comparative study. J. Neurosci. Methods 250, 106–113.

Luo, Q., Holroyd, T., Jones, M., Hendler, T., and Blair, J. (2007). Neural dynamics for facial threat processing as revealed by gamma band synchronization using MEG. Neuroimage 34, 839–847.

Luo, Q., Holroyd, T., Majestic, C., Cheng, X., Schechter, J., and James Blair, R. (2010). Emotional automaticity is a matter of timing. J. Neurosci. 30, 5825–5829.

Lyon, D.C., Nassi, J.J., and Callaway, E.M. (2010). A disynaptic relay from superior colliculus to dorsal stream visual cortex in macaque monkey. Neuron 65, 270–279.

Maior, R.S., Hori, E., Tomaz, C., Ono, T., and Nishijo, H. (2010). The monkey pulvinar neurons differentially respond to emotional expressions of human faces. Behav. Brain Res. 215, 129–135.

Mangun, G.R., Hinrichs, H., Scholz, M., Mueller-Gaertner, H.W., Herzog, H., Krause, B.J., Tellman, L., Kemna, L., and Heinze, H.J. (2001). Integrating electrophysiology and

neuroimaging of spatial selective attention to simple isolated visual stimuli. In Vision Research, (Vision Res), pp. 1423–1435.

Mashour, G.A., and Hudetz, A.G. (2018). Neural Correlates of Unconsciousness in Large-Scale Brain Networks. Trends Neurosci. 41, 150–160.

Mashour, G.A., Roelfsema, P., Changeux, J.P., and Dehaene, S. (2020). Conscious Processing and the Global Neuronal Workspace Hypothesis. Neuron 105, 776–798.

Matteo, B.M., Viganò, B., Cerri, C.G., and Perin, C. (2016). Visual field restorative rehabilitation after brain injury. J. Vis. 16, 11.

Maunsell, J.H., Ghose, G.M., Assad, J.A., McAdams, C.J., Boudreau, C.E., and Noerager, B.D. (1999). Visual response latencies of magnocellular and parvocellular LGN neurons in macaque monkeys. Vis. Neurosci. 16, 1–14.

Mazzi, C., Bagattini, C., and Savazzi, S. (2016). Blind-Sight vs. Degraded-Sight: Different Measures Tell a Different Story. Front. Psychol. 7, 901.

McAfee, S.S., Liu, Y., Dhamala, M., and Heck, D.H. (2018). Thalamocortical communication in the awake mouse visual system involves phase synchronization and rhythmic spike synchrony at high gamma frequencies. Front. Neurosci. 12.

McFadyen, J., Mermillod, M., Mattingley, J.B., Halász, V., and Garrido, M.I. (2017). A rapid subcortical amygdala route for faces irrespective of spatial frequency and emotion. J. Neurosci. 37, 3864–3874.

McFadyen, J., Mattingley, J.B., and Garrido, M.I. (2019). An afferent white matter pathway from the pulvinar to the amygdala facilitates fear recognition. Elife 8.

McFadyen, J., Dolan, R.J., and Garrido, M.I. (2020). The influence of subcortical shortcuts on disordered sensory and cognitive processing. Nat. Rev. Neurosci. 1–13.

Melloni, L., Molina, C., Pena, M., Torres, D., Singer, W., and Rodriguez, E. (2007). Synchronization of neural activity across cortical areas correlates with conscious perception. J. Neurosci. 27, 2858–2865.

Melloni, L., Mudrik, L., Pitts, M., and Koch, C. (2021). Making the hard problem of consciousness easier. Science (80-.). 372, 911–912.

Méndez-Bértolo, C., Moratti, S., Toledano, R., Lopez-Sosa, F., Martínez-Alvarez, R., Mah, Y.H., Vuilleumier, P., Gil-Nagel, A., and Strange, B.A. (2016). A fast pathway for fear in human amygdala. Nat. Neurosci. 19.

Meunier, D., Pascarella, A., Altukhov, D., Jas, M., Combrisson, E., Lajnef, T., Bertrand-Dubois, D., Hadid, V., Alamian, G., Alves, J., et al. (2020). NeuroPycon: An open-source python toolbox for fast multi-modal and reproducible brain connectivity pipelines. Neuroimage 219.

Michalareas, G., Vezoli, J., van Pelt, S., Schoffelen, J.M., Kennedy, H., and Fries, P. (2016). Alpha-Beta and Gamma Rhythms Subserve Feedback and Feedforward Influences among Human Visual Cortical Areas. Neuron 89, 384–397.

Mikellidou, K., Arrighi, R., Aghakhanyan, G., Tinelli, F., Frijia, F., Crespi, S., De Masi, F., Montanaro, D., and Morrone, M.C. (2019). Plasticity of the human visual brain after an early cortical lesion. Neuropsychologia.

Min, B.-K. (2010). A thalamic reticular networking model of consciousness. Theor. Biol. Med. Model. 7, 10.

Moratti, S., Saugar, C., and Strange, B.A. (2011). Prefrontal-occipitoparietal coupling underlies late latency human neuronal responses to emotion. J. Neurosci. 31, 17278–17286.

Morland, A.B., Lê, S., Carroll, E., Hoffmann, M.B., and Pambakian, A. (2004). The role of spared calcarine cortex and lateral occipital cortex in the responses of human hemianopes to visual motion. J. Cogn. Neurosci. 16, 204–218.

Morris, J.S., Öhman, A., and Dolan, R.J. (1999). A subcortical pathway to the right amygdala mediating “unseen” fear. Proc. Natl. Acad. Sci. U. S. A. 96, 1680–1685.

Morris, J.S., DeGelder, B., Weiskrantz, L., and Dolan, R.J. (2001). Differential extrageniculostriate and amygdala responses to presentation of emotional faces in a cortically blind field. Brain 124, 1241–1252.

Muller-Gass, A., Macdonald, M., Schröger, E., Sculthorpe, L., and Campbell, K. (2007). Evidence for the auditory P3a reflecting an automatic process: elicitation during highly-focused continuous visual attention. Brain Res. 1170, 71–78.

Müller, M.M., Picton, T.W., Valdes-Sosa, P., Riera, J., Teder-Sälejärvi, W.A., and Hillyard, S.A. (1998). Effects of spatial selective attention on the steady-state visual evoked potential in the 20–28 Hz range. Cogn. Brain Res. 6, 249–261.

Oei, A.C., and Patterson, M.D. (2014). Are videogame training gains specific or general? Front. Syst. Neurosci. 8, 54.

Oei, A.C., and Patterson, M.D. (2015). Enhancing perceptual and attentional skills requires common demands between the action video games and transfer tasks. Front. Psychol. 6, 113.

Overgaard, M., and Grünbaum, T. (2011). Consciousness and modality: on the possible preserved visual consciousness in blindsight subjects. Conscious. Cogn. 20, 1855–1859.

Overgaard, M., Fehl, K., Mouridsen, K., Bergholt, B., and Cleeremans, A. (2008). Seeing without Seeing? Degraded Conscious Vision in a Blindsight Patient. PLoS One 3, e3028.

Oxner, M., Rosentreter, E.T., Hayward, W.G., and Corballis, P.M. (2019). Prediction errors in surface segmentation are reflected in the visual mismatch negativity, independently of task and surface features. J. Vis. 19, 9.

Pal, D., Li, D., Dean, J.G., Brito, M.A., Liu, T., Fryzel, A.M., Hudetz, A.G., and Mashour, G.A. (2020). Level of consciousness is dissociable from electroencephalographic measures of cortical connectivity, slow oscillations, and complexity. J. Neurosci. 40, 605–618.

Panagiotaropoulos, T.I., Deco, G., Kapoor, V., and Logothetis, N.K. (2012). Neuronal Discharges and Gamma Oscillations Explicitly Reflect Visual Consciousness in the Lateral Prefrontal Cortex. Neuron 74, 924–935.

Passamonti, C., Bertini, C., and Làdavas, E. (2009). Audio-visual stimulation improves oculomotor patterns in patients with hemianopia. Neuropsychologia 47, 546–555.

Patel, S.H., and Azzam, P.N. (2005). Characterization of N200 and P300: Selected Studies of the Event-Related Potential. Int. J. Med. Sci. 2, 147.

Patel, A.T., Duncan, P.W., Lai, S.-M., and Studenski, S. (2000). The relation between impairments and functional outcomes poststroke. Arch. Phys. Med. Rehabil. 81, 1357–1363.

Pavan, A., Alexander, I., Campana, G., and Cowey, A. (2011). Detection of first- and second-order coherent motion in blindsight. Exp. Brain Res. 214, 261–271.

Pazo-Alvarez, P., Cadaveira, F., and Amenedo, E. (2003). MMN in the visual modality: a review. Biol. Psychol. 63, 199–236.

Pegna, A.J., Khateb, A., Lazeyras, F., and Seghier, M.L. (2005). Discriminating emotional faces without primary visual cortices involves the right amygdala. Nat. Neurosci. 8, 24–25.

Perez, C., and Chokron, S. (2014). Rehabilitation of homonymous hemianopia: insight into blindsight. Front. Integr. Neurosci. 8, 82.

Perrault, T.J., Stein, B.E., and Rowland, B.A. (2011). Non-stationarity in multisensory neurons in the superior colliculus. Front. Psychol. 2, 144.

Persaud, N., Davidson, M., Maniscalco, B., Mobbs, D., Passingham, R.E., Cowey, A., and Lau, H. (2011). Awareness-related activity in prefrontal and parietal cortices in blindsight reflects more than superior visual performance. Neuroimage 58, 605–611.

Peters, M.A.K., Kentridge, R.W., Phillips, I., and Block, N. (2017). Does unconscious perception really exist? Continuing the ASSC20 debate. Neurosci. Conscious. 2017.

Phillips, I. (2020). Blindsight Is Qualitatively Degraded Conscious Vision. Psychol. Rev.

Pins, D., and Ffytche, D. (2003). The neural correlates of conscious vision. Cereb. Cortex 13, 461–474.

Pizzo, F., Roehri, N., Medina Villalon, S., Trébuchon, A., Chen, S., Lagarde, S., Carron, R., Gavaret, M., Giusiano, B., McGonigal, A., et al. (2019). Deep brain activities can be detected with magnetoencephalography. Nat. Commun. 10, 1–13.

Plow, E.B., Obretenova, S.N., Halko, M.A., Kenkel, S., Jackson, M. Lou, Pascual-Leone, A., and Merabet, L.B. (2011). Combining visual rehabilitative training and noninvasive brain stimulation to enhance visual function in patients with hemianopia: a comparative case study. PM R 3, 825–835.

Poggel, D.A., Kasten, E., and Sabel, B.A. (2004). Attentional cueing improves vision restoration therapy in patients with visual field defects. Neurology 63, 2069–2076.

Pohl, C., Kunde, W., Ganz, T., Conzelmann, A., Pauli, P., and Kiesel, A. (2014). Gaming to see: action video gaming is associated with enhanced processing of masked stimuli. Front. Psychol. 5, 70.

Polich, J. (2007). Updating P300: An integrative theory of P3a and P3b. Clin. Neurophysiol. 118, 2128–2148.

Pollock, A., Hazelton, C., Henderson, C.A., Angilley, J., Dhillon, B., Langhorne, P., Livingstone, K., Munro, F.A., Orr, H., Rowe, F.J., et al. (2011). Interventions for visual field defects in patients with stroke. Cochrane Database Syst. Rev. CD008388.

Pool, E.-M., Rehme, A.K., Fink, G.R., Eickhoff, S.B., and Grefkes, C. (2014). Handedness and effective connectivity of the motor system. Neuroimage 99, 451.

Qian, X., Liu, Y., Xiao, B., Gao, L., Li, S., Dang, L., Si, C., and Zhao, L. (2014). The visual mismatch negativity (vMMN): toward the optimal paradigm. Int. J. Psychophysiol. 93, 311–315.

Quentin, R., Chanes, L., Vernet, M., and Valero-Cabré, A. (2015a). Fronto-Parietal Anatomical Connections Influence the Modulation of Conscious Visual Perception by High-Beta Frontal Oscillatory Activity. Cereb. Cortex 25, 2095–2101.

Quentin, R., Chanes, L., Vernet, M., and Valero-Cabré, A. (2015b). Fronto-Parietal Anatomical Connections Influence the Modulation of Conscious Visual Perception by High-Beta Frontal Oscillatory Activity. Cereb. Cortex 25, 2095–2101.

Railo, H., Koivisto, M., and Revonsuo, A. (2011). Tracking the processes behind conscious perception: A review of event-related potential correlates of visual consciousness. Conscious. Cogn. 20, 972–983.

Railo, H., Revonsuo, A., and Koivisto, M. (2015). Behavioral and electrophysiological evidence for fast emergence of visual consciousness. Neurosci. Conscious. 2015.

Ray, N.R., O'Connell, M.A., Nashiro, K., Smith, E.T., Qin, S., and Basak, C. (2017). Evaluating the relationship between white matter integrity, cognition, and varieties of video game learning. Restor. Neurol. Neurosci. 35, 437–456.

Recasens, M., Gross, J., and Uhlhaas, P.J. (2018). Low-Frequency Oscillatory Correlates of Auditory Predictive Processing in Cortical-Subcortical Networks: A MEG-Study. Sci. Rep. 8.

Redinbaugh, M.J., Phillips, J.M., Kambi, N.A., Mohanta, S., Andryk, S., Dooley, G.L., Afrasiabi, M., Raz, A., and Saalmann, Y.B. (2020). Thalamus Modulates Consciousness via Layer-Specific Control of Cortex. Neuron.

Rigoulot, S., D'Hondt, F., Defoort-Dhellemmes, S., Despretz, P., Honoré, J., and Sequeira, H. (2011). Fearful faces impact in peripheral vision: Behavioral and neural evidence. Neuropsychologia 49, 2013–2021.

Rohr, M., and Wentura, D. (2014). Spatial frequency filtered images reveal differences between masked and unmasked processing of emotional information. Conscious. Cogn. 29, 141–158.

Roth, T., Sokolov, A.N., Messias, A., Roth, P., Weller, M., and Trauzettel-Klosinski, S. (2009). Comparing explorative saccade and flicker training in hemianopia: A randomized controlled study. Neurology 72, 324–331.

Roux, F., Wibra, M., Singer, W., Aru, J., and Uhlhaas, P.J. (2013). The phase of thalamic alpha activity modulates cortical gamma-band activity: Evidence from resting-state MEG recordings. J. Neurosci. 33, 17827–17835.

Rowe, E.G., Tsuchiya, N., and Garrido, M.I. (2020). Detecting (Un)seen Change: The Neural Underpinnings of (Un)conscious Prediction Errors. Front. Syst. Neurosci. 14.

Rowe, F.J., Hepworth, L.R., Howard, C., Hanna, K.L., Cheyne, C.P., and Currie, J. (2019). High incidence and prevalence of visual problems after acute stroke: An epidemiology study with implications for service delivery. PLoS One 14.

Di Russo, F., Martínez, A., Sereno, M.I., Pitzalis, S., and Hillyard, S.A. (2002). Cortical sources of the early components of the visual evoked potential. Hum. Brain Mapp. 15, 95–111.

Rutiku, R., Martin, M., Bachmann, T., and Aru, J. (2015). Does the P300 reflect conscious perception or its consequences? Neuroscience 298, 180–189.

Rutiku, R., Aru, J., and Bachmann, T. (2016). General markers of conscious visual perception and their timing. Front. Hum. Neurosci. 10, 23.

Sabel, B.A., Henrich-Noack, P., Fedorov, A., and Gall, C. (2011). Vision restoration after brain and retina damage: the "residual vision activation theory". Prog. Brain Res. 192, 199–262.

Sahraie, A., Trevethan, C.T., MacLeod, M.J., Murray, A.D., Olson, J.A., and Weiskrantz, L. (2006). Increased sensitivity after repeated stimulation of residual spatial channels in blindsight. Proc. Natl. Acad. Sci. U. S. A. 103, 14971–14976.

Sahraie, A., Trevethan, C.T., Macleod, M.-J., Weiskrantz, L., and Hunt, A.R. (2013). The continuum of detection and awareness of visual stimuli within the blindfield: from blindsight to the sighted-sight. Invest. Ophthalmol. Vis. Sci. 54, 3579–3585.

Saionz, E.L., Tadin, D., Melnick, M.D., and Huxlin, K.R. (2020). Functional preservation and enhanced capacity for visual restoration in subacute occipital stroke. Brain 143, 1857–1872.

Saionz, E.L., Feldon, S.E., and Huxlin, K.R. (2021). Rehabilitation of cortically induced visual field loss. Curr. Opin. Neurol. 34, 67–74.

Salti, M., Bar-Haim, Y., and Lamy, D. (2012). The P3 component of the ERP reflects conscious perception, not confidence. Conscious. Cogn. 21, 961–968.

Salti, M., Monto, S., Charles, L., King, J.-R., Parkkonen, L., and Dehaene, S. (2015). Distinct cortical codes and temporal dynamics for conscious and unconscious percepts. Elife 4, 1–52.

Sanchez-Lopez, J., Savazzi, S., Pedersini, C.A., Cardobi, N., and Marzi, C.A. (2020). Neural bases of unconscious orienting of attention in hemianopic patients: Hemispheric differences. Cortex. 127, 269–289.

Sand, K.M., Midelfart, A., Thomassen, L., Melms, A., Wilhelm, H., and Hoff, J.M. (2013). Visual impairment in stroke patients--a review. Acta Neurol. Scand. Suppl. 52–56.

Savage, N. (2019). How AI and neuroscience drive each other forwards. Nature 571, S15–S17.

Schindler, S., Schettino, A., and Pourtois, G. (2018). Electrophysiological correlates of the interplay between low-level visual features and emotional content during word reading. Sci. Rep. 8.

Schmid, M.C., and Maier, A. (2015). To see or not to see - thalamo-cortical networks during blindsight and perceptual suppression. Prog. Neurobiol. 126, 36–48.

Schmid, M.C., Mrowka, S.W., Turchi, J., Saunders, R.C., Wilke, M., Peters, A.J., Ye, F.Q., and Leopold, D.A. (2010). Blindsight depends on the lateral geniculate nucleus. Nature 466, 373–377.

Schönwald, L.I., and Müller, M.M. (2014). Slow biasing of processing resources in early visual cortex is preceded by emotional cue extraction in emotion-attention competition. Hum. Brain Mapp. 35, 1477–1490.

Schurger, A., Cowey, A., Cohen, J.D., Treisman, A., and Tallon-Baudry, C. (2008). Distinct and independent correlates of attention and awareness in a hemianopic patient. Neuropsychologia 46, 2189–2197.

Schutter, D.J.L.G., and van Honk, J. (2004). Extending the global workspace theory to emotion: phenomenality without access. Conscious. Cogn. 13, 539–549.

Seitz, A.R., Kim, R., and Shams, L. (2006). Sound Facilitates Visual Learning. Curr. Biol. 16, 1422–1427.

Sergent, C., and Dehaene, S. (2004). Neural processes underlying conscious perception: experimental findings and a global neuronal workspace framework. J. Physiol. Paris 98, 374–384.

Shimojo, S., and Shams, L. (2001). Sensory modalities are not separate modalities: Plasticity and interactions. Curr. Opin. Neurobiol. 11, 505–509.

Silvanto, J. (2015). Why is "blindsight" blind? A new perspective on primary visual cortex, recurrent activity and visual awareness. Conscious. Cogn. 32, 15–32.

Silvanto, J., Walsh, V., and Cowey, A. (2009). Abnormal functional connectivity between ipsilesional V5/MT+ and contralesional striate cortex (V1) in blindsight. Exp. Brain Res. 193, 645–650.

Sincich, L.C., Park, K.F., Wohlgemuth, M.J., and Horton, J.C. (2004). Bypassing V1: a direct geniculate input to area MT. Nat. Neurosci. 7, 1123–1128.

Sohn, E. (2019). Decoding the neuroscience of consciousness. Nature.

Solís-Vivanco, R., Mondragón-Maya, A., Reyes-Madrigal, F., and de la Fuente-Sandoval, C. (2021). Impairment of novelty-related theta oscillations and P3a in never medicated first-episode psychosis patients. Npj Schizophr. 7.

Song, I., and Keil, A. (2013). Affective engagement and subsequent visual processing: Effects of contrast and spatial frequency. Emotion 13, 748–757.

Soto, D., Sheikh, U.A., and Rosenthal, C.R. (2019). A Novel Framework for Unconscious Processing. Trends Cogn. Sci. 23, 372–376.

Starke, J., Ball, F., Heinze, H.-J., and Noesselt, T. (2020). The spatio-temporal profile of multisensory integration. Eur. J. Neurosci. 51, 1210–1223.

Stefanics, G., Kremláček, J., and Czigler, I. (2014a). Visual mismatch negativity: a predictive coding view. Front. Hum. Neurosci. 8, 666.

Stefanics, G., Astikainen, P., and Czigler, I. (2014b). Visual mismatch negativity (vMMN): a prediction error signal in the visual modality. Front. Hum. Neurosci. 8, 1074.

Stefanics, G., Kremláček, J., and Czigler, I. (2016). Mismatch negativity and neural adaptation: Two sides of the same coin. Response: Commentary: Visual mismatch negativity: a predictive coding view. Front. Hum. Neurosci. 10, 13.

Van den Stock, J., Tamietto, M., Zhan, M., Heinecke, A., Hervais-Adelman, A., Legrand, L.B., Pegna, A.J., and de Gelder, B. (2014). Neural correlates of body and face perception following bilateral destruction of the primary visual cortices. Front. Behav. Neurosci. 8.

Stoerig, P., and Cowey, A. (1995). Visual perception and phenomenal consciousness. Behav. Brain Res. 71, 147–156.

Striemer, C.L., Whitwell, R.L., and Goodale, M.A. (2019). Affective blindsight in the absence of input from face processing regions in occipital-temporal cortex. Neuropsychologia 128, 50–57.

Swienton, D.J., and Thomas, A.G. (2014). The visual pathway--functional anatomy and pathology. Semin. Ultrasound. CT. MR 35, 487–503.

Tamietto, M., and de Gelder, B. (2008). Affective blindsight in the intact brain: neural interhemispheric summation for unseen fearful expressions. Neuropsychologia 46, 820–828.

Tamietto, M., and Morrone, M.C. (2016). Visual Plasticity: Blindsight Bridges Anatomy and Function in the Visual System. Curr. Biol. 26, R70–R73.

Tamietto, M., Castelli, L., Vighetti, S., Perozzo, P., Geminiani, G., Weiskrantz, L., and de Gelder, B. (2009). Unseen facial and bodily expressions trigger fast emotional reactions. Proc. Natl. Acad. Sci. U. S. A. 106, 17661–17666.

Tamietto, M., Cauda, F., Corazzini, L.L., Savazzi, S., Marzi, C.A., Goebel, R., Weiskrantz, L., and de Gelder, B. (2010). Collicular vision guides nonconscious behavior. J. Cogn. Neurosci. 22, 888–902.

Tao, D., He, Z., Lin, Y., Liu, C., and Tao, Q. (2021). Where does fear originate in the brain? A coordinate-based meta-analysis of explicit and implicit fear processing. Neuroimage 227, 117686.

Tapia, E., and Breitmeyer, B.G. (2011). Visual consciousness revisited: magnocellular and parvocellular contributions to conscious and nonconscious vision. Psychol. Sci. 22, 934–942.

Taylor, J.G., and Fragopanagos, N.F. (2005). The interaction of attention and emotion. Neural Networks 18, 353–369.

Tipura, E., Pegna, A.J., de Gelder, B., and Renaud, O. (2017). Visual stimuli modulate frontal oscillatory rhythms in a cortically blind patient: Evidence for top-down visual processing. Clin. Neurophysiol. 128, 770–779.

Tong, F. (2003). Cognitive neuroscience: Primary visual cortex and visual awareness. Nat. Rev. Neurosci. 4, 219–229.

Tononi, G., Boly, M., Massimini, M., and Koch, C. (2016). Integrated information theory: From consciousness to its physical substrate. Nat. Rev. Neurosci. 17, 450–461.

Tran, A., MacLean, M.W., Hadid, V., Lazzouni, L., Nguyen, D.K., Tremblay, J., Dehaes, M., and Lepore, F. (2019). Neuronal mechanisms of motion detection underlying blindsight assessed by functional magnetic resonance imaging (fMRI). Neuropsychologia 128, 187–197.

Troiani, V., Price, E.T., and Schultz, R.T. (2014). Unseen fearful faces promote amygdala guidance of attention. Soc. Cogn. Affect. Neurosci. 9, 133–140.

Tsuchiya, N., Wilke, M., Frässle, S., and Lamme, V.A.F. (2015). No-Report Paradigms: Extracting the True Neural Correlates of Consciousness. Trends Cogn. Sci. 19, 757–770.

Urbanski, M., Coubard, O.A., and Bourlon, C. (2014). Visualizing the blind brain: brain imaging of visual field defects from early recovery to rehabilitation techniques. Front. Integr. Neurosci. 8, 74.

Vakalopoulos, C. (2005). A theory of blindsight--the anatomy of the unconscious: a proposal for the koniocellular projections and intralaminar thalamus. Med. Hypotheses 65, 1183–1190.

Vernet, M., Stengel, C., Quentin, R., Amengual, J.L., and Valero-Cabré, A. (2019a). Entrainment of local synchrony reveals a causal role for high-beta right frontal oscillations in human visual consciousness. Sci. Rep. 9, 14510.

Vernet, M., Japee, S., Lokey, S., Ahmed, S., Zachariou, V., and Ungerleider, L.G. (2019b). Endogenous visuospatial attention increases visual awareness independent of visual discrimination sensitivity. Neuropsychologia 128, 297–304.

Villeneuve, M.Y., Kupers, R., Gjedde, A., Ptito, M., and Casanova, C. (2005). Pattern-motion selectivity in the human pulvinar. Neuroimage 28, 474–480.

van Vugt, B., Dagnino, B., Vartak, D., Safaai, H., Panzeri, S., Dehaene, S., and Roelfsema, P.R. (2018). The threshold for conscious report: Signal loss and response bias in visual and frontal cortex. Science 360, 537–542.

Vuilleumier, P. (2005). How brains beware: Neural mechanisms of emotional attention. Trends Cogn. Sci. 9, 585–594.

Vuilleumier, P., Sagiv, N., Hazeltine, E., Poldrack, R.A., Swick, D., Rafal, R.D., and Gabrieli, J.D. (2001). Neural fate of seen and unseen faces in visuospatial neglect: a combined event-related functional MRI and event-related potential study. Proc. Natl. Acad. Sci. U. S. A. 98, 3495–3500.

Vukelić, M., Lingelbach, K., Pollmann, K., and Peissner, M. (2021). Oscillatory eeg signatures of affective processes during interaction with adaptive computer systems. Brain Sci. 11, 1–21.

Ward, R., Danziger, S., and Bamford, S. (2005). Response to visual threat following damage to the pulvinar. Curr. Biol. 15, 571–573.

Warner, C.E., Goldshmit, Y., and Bourne, J.A. (2010). Retinal afferents synapse with relay cells targeting the middle temporal area in the pulvinar and lateral geniculate nuclei. Front. Neuroanat. 4, 8.

Warner, C.E., Kwan, W.C., Wright, D., Johnston, L.A., Egan, G.F., and Bourne, J.A. (2015). Preservation of vision by the pulvinar following early-life primary visual cortex lesions. Curr. Biol. 25, 424–434.

Watanabe, T., Náñez, J.E., Koyama, S., Mukai, I., Liederman, J., and Sasaki, Y. (2002). Greater plasticity in lower-level than higher-level visual motion processing in a passive perceptual learning task. Nat. Neurosci. 5, 1003–1009.

Weiskrantz, L. (1986). Blindsight : A Case Study and Implications: A Case Study and Implications (Clarendon Press).

Weiskrantz, L. (2009). Is blindsight just degraded normal vision? Exp. Brain Res. 192, 413–416.

Weiskrantz, L., Warrington, E.K., Sanders, M.D., and Marshall, J. (1974). Visual capacity in the hemianopic field following a restricted occipital ablation. Brain 97, 709–728.

Whitton, J.P., Hancock, K.E., and Polley, D.B. (2014). Immersive audiomotor game play enhances neural and perceptual salience of weak signals in noise. Proc. Natl. Acad. Sci. 111, E2606–E2615.

Wiens, S. (2006). Subliminal emotion perception in brain imaging: findings, issues, and recommendations. Prog. Brain Res. 156, 105–121.

Xiao, L.-Q., Zhang, J.-Y., Wang, R., Klein, S.A., Levi, D.M., and Yu, C. (2008). Complete transfer of perceptual learning across retinal locations enabled by double training. Curr. Biol. 18, 1922–1926.

Xu, M., Wang, Y., Nakanishi, M., Wang, Y.-T., Qi, H., Jung, T.-P., and Ming, D. (2016). Fast detection of covert visuospatial attention using hybrid N2pc and SSVEP features. J. Neural Eng. 13, 066003.

Yanagawa, T., Chao, Z.C., Hasegawa, N., and Fujii, N. (2013). Large-scale information flow in conscious and unconscious states: An ECoG study in monkeys. PLoS One 8.

Yeark, M., Paton, B., and Todd, J. (2021). The influence of variability on mismatch negativity amplitude. Biol. Psychol. 164, 108161.

Ylinen, S., Huuskonen, M., Mikkola, K., Saure, E., Sinkkonen, T., and Paavilainen, P. (2016). Predictive coding of phonological rules in auditory cortex: A mismatch negativity study. Brain Lang. 162, 72–80.

Yoshida, M., Itti, L., Berg, D.J., Ikeda, T., Kato, R., Takaura, K., White, B.J., Munoz, D.P., and Isa, T. (2012). Residual attention guidance in blindsight monkeys watching complex natural scenes. Curr. Biol. 22, 1429–1434.

Yuval-Greenberg, S., Tomer, O., Keren, A.S., Nelken, I., and Deouell, L.Y. (2008). Transient Induced Gamma-Band Response in EEG as a Manifestation of Miniature Saccades. Neuron 58, 429–441.

Zeman, A. (2004). Theories of visual awareness. Prog. Brain Res. 144, 321–329.

Zhang, Y.-X., Tang, D.-L., Moore, D.R., and Amitay, S. (2017). Supramodal Enhancement of Auditory Perceptual and Cognitive Learning by Video Game Playing. Front. Psychol. 8, 1086.

Zhang, Y., Wang, Y., Cai, S., Li, J., Ren, J., Wang, Q., and Huang, L. (2019). EEG Feature Analysis for Detecting the Fluctuation of Consciousness Level during Propofol Anesthesia. In Proceedings of the Annual International Conference of the IEEE Engineering in Medicine and Biology Society, EMBS, (Annu Int Conf IEEE Eng Med Biol Soc), pp. 4525–4528.

Del Zotto, M., Deiber, M.P., Legrand, L.B., De Gelder, B., and Pegna, A.J. (2013). Emotional expressions modulate low α and β oscillations in a cortically blind patient. Int. J. Psychophysiol. 90, 358–362.